Universitat de les Illes Balears

Facultat de Ciències

Departament de Biologia

# Role of the regulation of cell lipid composition and membrane structure in the antitumor effect of 2-hydroxyoleic acid

PhD Thesis

**Maria Laura Martin**

**Mallorca, 2011**

Supervisors:

**Gwendolyn Barceló-Coblijn and Pablo Escribá**

Nosaltres, Gwendolyn Barceló-Coblijn, Professor Associada de la Facultat de Ciències de la Universitat de les Illes Balears, i Pablo Escribá, Catedràtic de la Facultat de Ciències de la Universitat de les Illes Balears

CERTIFIQUEM:

Que el present treball titulat “Role of the regulation of cell lipid composition and membrane structure in the antitumor effect of 2-hydroxyoleic acid”, presentat per Maria Laura Martin per optar al TÍTOL univesitari oficial de DOCTOR per la Universitat de les Illes Balears dins del programa de doctorat en Biotecnología, Genética y Biología Celular, s’ha realitzat sota la nostra direcció al Departament de Biologia de la Facultat de Ciències de la Universitat de las Illes Balears.

Revisat el present treball, autoritzem la seva presentació per que pugui ésser jutjada pel tribunal corresponent.

Palma de Mallorca, 19 de Julio de 2011

| Director | Director | Autor |
| --- | --- | --- |
| Dr Gwendolyn Barceló-Coblijn | Prof. Pablo Escribá | Maria Laura Martin |

*“All good research begins with wishful thinking before scientific discipline converts it into controlled interventions that address `How does this happen?' and `What is the consequence of this happening?' In the end, we affirm a superiority of controlled interventions over associative evidence for choosing the best story to tell future generations.”* William E. M. Lands, 2000. Stories about acyl chains.

# Acknowledgements/Agradecimientos

Esta tesis fue realizada en el Departamento de Biología de la Universitat de les Illes Balears y financiada con una beca otorgada por la Conselleria d'Educació, Cultura i Universitats.

En primer lugar, quisiera agradecer a mis directores de tesis. Al Profesor Pablo Escribá por darme la oportunidad de trabajar en su grupo y realizar esta tesis, por la libertad que nos brindó para trabajar y por su interés en el plano personal. A la Dra. Gwendolyn Barceló-Coblijn por haber aceptado dirigirme la tesis y así, introducirme en el fantástico mundo de los lípidos y por todas sus enseñanzas.

Además quisiera agradecer al Profesor Xavier Busquets, por sus innumerables consejos durante la tesis, incluyendo su frase célebre KISS, "*Keep it simple and stupid*".

Quisiera agradecer a todos mis compañeros de laboratorio que durante más o menos tiempo me acompañaron por este camino: Maria Antonia, Amaia, Joana, Dani, Francis, Mónica, Vicky, Silvia, Rafa, David, Maitane, Laia, Victor C, Andrea, Margalida y Victor V. Gracias por ayudarme y enseñarme tantas veces a lo largo de estos años. En especial quisiera agradecer a dos personas en quienes encontré dos amigas: Maria Antonia y Amaia. Y a Joana, que aunque nos conocimos hace poco, te ganaste nuestra amistad y condimentaste nuestras vidas ¡Gracias por estar chicas!

Me gustaría agradecer también al Profesor José Manuel García-Verdugo y Mario Soriano-Navarro por su colaboración con la microscopía electrónica. A la Dra. Gemma Fabriàs por analizarnos tan amablemente las muestras de radiactividad (cuando no teníamos ninguna opción en nuestra universidad) y al Dr. Amadeu Llebaria por enviarnos tan gentilmente muestras del inhibidor D609. Al Dr. Oliver Vögler por facilitarnos tan amablemente muestras de algunos de los ácidos grasos modificados. A la Dra. Silvia Terés y la futura Dra. Mónica Higuera por su trabajo con los ratones. Y a la Dra. Francisca Guardiola-Serrano por su colaboración con la citometría de flujo.

I would like to thank Dr. Rodrigo de Almeida and his group, Joaquim, Francisco, André M. and André B., for their hospitality during my stay in Lisbon and especially Rodrigo for the analysis of the biophysical properties of membranes and for introducing me to the complex world of biophysics so important to biology. Muito Obrigado!

I would also like to thank Prof. Gerd Schmitz and Dr. Gerhard Liebisch for the lipidomics analysis; and Dr. Anja Lüth and Burhard Kleuser for the HPLC analysis.

Me gustaría agradecer al Dr Sergio Rodriguez Cuenca por su invalorable asesoramiento sobre RNA de interferencia y RT-PCR.

A mi familia de Argentina, a mi mamá, mi papá y mi hermana que me apoyaron siempre incondicionalmente desde el otro lado del charco. A mi familia de Marbella, que me trataron siempre como a otra hija. A mis amigos de Argentina, que a pesar de las distancias, están siempre presentes. Y a las que son nuestras segundas familias en Mallorca, la de S'Esgleieta, la de Ctra. de Valldemossa y la de Sa Cabaneta ¡Gracias por adoptarme! Y a la pastelería/rotisería del Pelado, que con esos desayunos y pizzas le levantan el ánimo a cualquiera.

Finalmente quisiera dedicarte esta tesis a vos, Adri, porque estamos construyendo un camino juntos y como siempre, y en particular en esta parte del camino, me brindaste todo tu apoyo y estuviste siempre a mi lado ¡Gracias por todo!

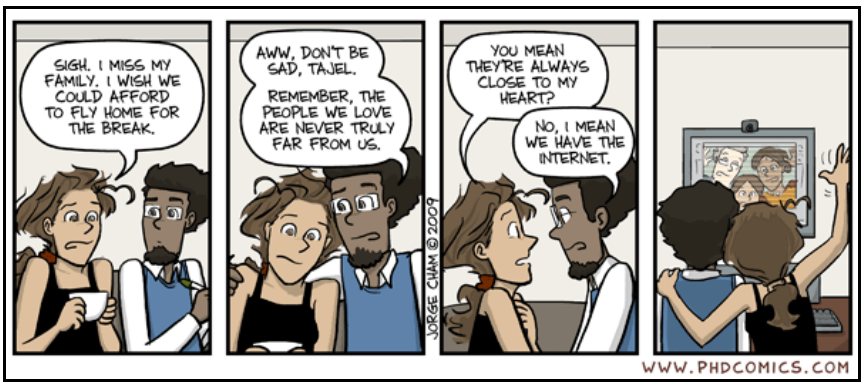


**Piled Higher & Deeper** ***by Jorge Cham***

# Contents

# Abbreviations

| | |
|---|---|
| **2OHOA** | 2-hydroxyoleic acid |
| **ACC** | Acetyl-CoA carboxylase |
| **ACL** | ATP citrate lyase |
| **ADRP** | Adipose differentiation-related protein |
| **AGPAT** | Acyl-CoA:1-acylglycerol-sn-3-phosphate acyltransferase |
| **Akt** | Protein kinase B |
| **BSA** | Bovine serum albumin |
| **C1P** | Ceramide-1-phosphate |
| **CDK** | Cyclin-dependent kinases |
| **CDP** | Cytidine diphospho |
| **CEPT** | Diacylglycerol choline/ethanolamine phosphostransferase |
| **Cer** | Ceramide |
| **CerS** | Ceramide synthase |
| **Cho/Chol** | Cholesterol |
| **CL** | Cardiolipin |
| **CoA** | Coenzime A |
| **CPT** | Diacylglycerol choline phosphostransferase |
| **CCT** | CTP:phosphocholine cytidylyltransferase α |
| **DAG** | Diacylglycerol |
| **DGAT** | Acyl-CoA:diacylglycerol acyltransferase |
| **DHA** | Docosahexanoic acid |
| **dhCer** | Dihydroceramide |
| **DHFR** | Dihydrofolate reductase |
| **DPH** | Diphenyl-hexatriene |
| **dhSM** | Dihydrosphingomyelin |
| **dhSph** | Dihydrosphingosine/sphinganine |
| **EGFR** | Epidermal growth factor receptor |
| **ER** | Endoplasmic reticulum |
| **FAS** | Fatty-acid synthase |
| **FasR** | Fas ligand receptor |
| **FFA** | Free fatty acids |
| **GalCer** | Galactosylceramide |
| **GlcCer** | Glucosylceramide |
| **GPAT** | Glycerol-3-phosphate acyltransferase |
| **GSLs** | Glycosphingolipids |

| | |
|---|---|
| **HPLC** | High performance liquid chromatography |
| **HPTLC** | High performance TLC |
| **LacCer** | Lactosylceramide |
| **LDs** | Lipid droplets |
| $l_d$ | Liquid disordered |
| $l_o$ | Liquid ordered |
| **LPA** | Lysophosphatidic acid |
| **LPC** | Lysophosphatidylcholine |
| **LUVs** | Large unilamellar vesicles |
| **MAG** | Monoacylglycerol |
| **MLVs** | Multilamellar vesicles |
| **MM** | Model membranes |
| **MS** | Mass spectrometry |
| **MUFAs** | Monounsaturated fatty acids |
| **NBD** | N-[2-hydroxy-1-(hydroxymethyl)-3-heptadecenyl]-6-[(7-nitro-2,1,3-benzoxadiazol-4-yl)amino] |
| **NBD-C6-Cer** | NBD-C6-ceramide |
| **NBD-C6-GlcCer** | NBD-C6- glucosylceramide |
| **NBD-C6-PC** | NBD-C6-phosphatidylcholine |
| **NDD-C6-PE** | NBD-C6- phosphatidylethanolamine |
| **NBD-C6-SM** | NBD-C6-sphingomyelin |
| **OA** | Oleic acid |
| **PA** | Phosphatidic acid |
| **PC** | Glycerophosphocholine |
| **PE** | Glycerophosphoethanolamine |
| **PEMT** | Phosphatidylethanolamine N-methyltransferase |
| **PG** | Glycerophosphoglycerol |
| **PI** | Glycerophosphoinositol |
| **PI(3,5)P2** | Glycerophosphoinositol-(4,5)-bisphosphate |
| **PI(4,5)P2** | Glycerophosphoinositol-(4,5)-bisphosphate |
| **PI3P** | Glycerophosphoinositol-(3,4,5)-trisphosphate |
| **PI3K** | Phosphatidylinositol 3-kinase |
| **PI4P** | Glycerophosphoinositol-4-phosphate |
| **PKC** | Protein kinase C |
| **PLA2** | Phospholipase A2 |
| **PLC** | Phospholipase C |
| **POPC** | Palmitoyloleoylphosphatidylcholine |
| **POPE** | Palmitoyloleoylphosphatidylethanolamine |
| **pRb** | Retinoblastoma protein |
| **PS** | Glycerophosphoserine |
| **PSM** | Palmitoylsphingomyelin |

| | |
|---|---|
| **PSS** | Phosphatidylserine synthase |
| **PTEN** | Phosphatase and tensin homology |
| **PUFAs** | Polyunsaturated fatty acids |
| **S1P** | Sphingosine-1-phosphate |
| **SCD1** | Stearoyl-coa desaturase-1 |
| **SFA** | Saturated fatty acids |
| **siRNA** | Small interference RNA |
| **SM** | Sphingomyelin |
| **SMase** | Sphingomyelinase |
| **SMS** | Sphingomyelin synthase |
| $s_o$ | Solid ordered (gel) |
| **Sph** | Sphingosine |
| **SPT** | Serine-palmitoyl transferase |
| **TAG** | Triacylglycerol |
| **TLC** | Thin Layer Chromatography |
| $T_m$ | Transition temperature |
| ***t*-Pna** | *trans*-parinaric acid. |

# Resumen

La mayoría de los fármacos utilizados actualmente en terapias humanas interactúan con proteínas, modificando su actividad y la de proteínas reguladas por ellas, produciendo cambios en la fisiología celular que revierten el proceso patológico. Sin embargo, los eventos de señalización celular, pueden verse afectados también por modificaciones de la composición lipídica de la membrana plasmática y su estructura. Tal participación en las funciones celulares, indica que los lípidos de membrana podrían constituir dianas de fármacos cuyo efecto estaría asociado a la modulación de la composición y las propiedades fisicoquímicas de membrana. El ácido 2-hidroxioleico (2OHOA) es un fármaco antitumoral diseñado para regular la estructura y composición de los lípidos de membrana y la función de importantes proteínas de membrana. Como se ha demostrado en diferentes líneas de células tumorales, su mecanismo de acción involucra la inhibición de la proliferación celular, induciendo apoptosis o parada del ciclo celular seguida de diferenciación y autofagia. El objetivo principal de este trabajo fue estudiar cómo el 2OHOA modula la composición lipídica y la estructura de membrana en las células tumorales.

Con el fin de estudiar el efecto del 2OHOA sobre la composición lipídica de la membrana, se analizaron los lípidos en células U118 de glioma humano tratadas con 2OHOA (200µM, 72 h), mediante cromatografía en capa fina (TLC). Se observó que el 2OHOA indujo profundas alteraciones en el contenido de fosfolípidos, aumentando 4,6 veces el contenido de esfingomielina (SM), principalmente en la membrana plasmática, y disminuyendo el contenido de fosfatidiletanolamina (PE) y de fosfatidilcolina (PC), 57 y 30%, respectivamente. Este efecto fue específico contra las células cancerosas, ya que el tratamiento no afectó la composición lipídica de las células no tumorales MRC-5 de fibroblastos humanos. En este contexto, se observó que los niveles basales de SM de las células cancerosas eran aproximadamente la mitad que las células no tumorales; y que el aumento de SM inducido por el 2OHOA en las células cancerosas alcanzó niveles similares a los encontrados en las células no tumorales MRC-5. El aumento de SM se debió a una activación rápida y específica de las SM sintasas (SMS). Cabe destacar que la inhibición farmacológica de la SMS con el inhibidor D609 disminuyó la capacidad del 2OHOA de inducir parada de ciclo celular. Como consecuencia de la activación sostenida de la SMS, todo el metabolismo de los esfingolípidos se vio afectado. Así, el análisis del contenido de esfingolípidos por espectrometría de masas de las células tumorales tratadas con 2OHOA, reveló la acumulación de esfingosina, dihidroesfingosina y de esfingolípidos que contenían ácido palmítico (C16-ceramida, C16-dihidroSM y C16-glucosilceramida). Cabe destacar que la esfingosina se genera

principalmente por la vía de reciclaje, mientras que la dihidroesfingosina se origina por la síntesis *de novo* de los esfingolípidos. Estos resultados confirmaron por tanto la desregulación del metabolismo esfingolipídico tras el tratamiento con 2OHOA, tanto por la activación de la síntesis *de novo* como de la vía de reciclaje. En concordancia con estos resultados, se observó un aumento del número de lisosomas, que son vesículas ácidas donde tiene lugar la vía de reciclaje; y la activación de la serin-palmitoil transferasa (SPT) que es la primera enzima de la síntesis *de novo*.

Por otra parte, se analizó el efecto del 2OHOA sobre la composición de ácidos grasos de las células tumorales mediante cromatografía de gases. Los cambios más notorios fueron la disminución de ácido oleico (40-60%) y el aumento de ácido esteárico (60-90%). Estos cambios se relacionaron con la inhibición de la estearoil-CoA desaturasa (SCD1), que se considera como una nueva diana en la terapia contra el cáncer. Por otra parte, el análisis por espectrometría de masas mostró la incorporación de 2OHOA en distintas clases de lípidos (aprox. un 15% del total de ácidos grasos). Por último, el análisis de los lípidos neutros mediante TLC, mostró un aumento de diacilglicerol (DAG), ácidos grasos libres (FFA) y triacilglicerol (TAG). La acumulación de éstos últimos se relacionó con un aumento de vesículas lipídicas (LDs).

Finalmente, se evaluó el impacto de todos estos cambios sobre las propiedades biofísicas de membrana mediante espectroscopia de fluorescencia. Para ello, se prepararon liposomas reconstituidos a partir de extractos lipídicos de células U118 control y tratadas. Se observó que el tratamiento con 2OHOA indujo un aumento de la rigidez y compactación de los dominios ordenados, debido básicamente al aumento en el contenido de SM, mientras que disminuyó el orden global de la membrana, probablemente a casusa de los cambios que el tratamiento induce en la composición de ácidos grasos.

Todas estas modificaciones inducidas por el 2OHOA, tanto en la composición como en la estructura de las membranas, explicarían las alteraciones observadas en la localización de proteínas implicadas en apoptosis celular (receptor Fas) y diferenciación (Ras). Teniendo en cuenta los resultados de este estudio, proponemos que niveles bajos de SM podrían ser críticos para el proceso de transformación tumorigénica; y que la regulación de la actividad de SMS en las células tumorales es un evento crítico en el mecanismo antitumoral del 2OHOA. Esta regulación explicaría además la capacidad de este compuesto para inducir parada del ciclo celular, diferenciación celular y autofagia o apoptosis en las células cancerosas. Debido a que el 2OHOA es un fármaco potente y específico para combatir los tumores, sin efectos secundarios a dosis terapéuticas, los datos mostrados aquí, no sólo presentan el primer activador de la SMS conocido, sino que también definen una diana molecular novedosa para el diseño de nuevos fármacos contra el cáncer.

# Abstract

Most drugs currently used for human therapy interact with proteins, altering their activity and that of downstream proteins, producing changes in the cell physiology that reverse the pathological process. However, it is known that changes in membrane lipid composition alter membrane structure, protein-membrane interactions and cell signaling. The participation of membrane lipids in cellular activities indicates that they might constitute targets for drugs whose pharmacological effects would be associated with the modulation of the composition and physicochemical properties of membranes. 2-Hydroxyoleic acid (2OHOA) is a potent antitumor drug that was designed to regulate membrane lipid composition and structure and the function of important membrane proteins. As it was shown in different tumor cell lines, its mechanism of action involves impairment of cell proliferation. Thus, the main goal of this work was to study how 2OHOA modulates the membrane lipid composition and structure of tumor cells.

To address this question, we analyzed membrane lipids from human glioma U118 cells exposed to 2OHOA (200 µM, 72 h), by thin layer chromatography (TLC). In this context, 2OHOA induced dramatic alterations in phospholipid content, increasing sphingomyelin (SM) mass 4.6-fold, mainly at the plasma membrane, and decreasing phosphatidyl-ethanolamine (PE) and phosphatidylcholine (PC) mass, 57 and 30%, respectively. This effect was specific against cancer cells as it did not affect non-tumor MRC-5 cells. In this context, human cancer cells have markedly lower basal levels of SM than non-tumor cells and 2OHOA strongly augmented SM content, restoring the levels found in MRC-5 cells. The increased SM mass was due to a rapid and highly specific activation of SM synthases (SMS). Importantly, pharmacological inhibition of SMS by D609 diminished 2OHOA capability to induce the cell cycle arrest. As a consequence of the sustained activation of SMS, the whole sphingolipid metabolism was affected. Thus, the analysis by mass spectrometry showed the accumulation of sphingosine, dihydrosphingosine and palmitic acid-containing sphingolipids (C16-ceramide, C16-dihydroSM and C16- glucosylceramide) after treatment with 2OHOA. It is worth to point out that sphingosine is mainly generated by the salvage pathway, while dihydrosphingosine is originated by the *de novo* synthesis of sphingolipids. Therefore, these results confirmed the deregulation of the sphingolipid metabolism induced by 2OHOA, both by the activation of the *de novo* synthesis and the salvage pathway. Accordingly, 2OHOA induced the accumulation of lysosomes, acidic vesicles where the salvage pathway occurs; and the activation of the serin-palmitoyl transferase (SPT), the first enzyme of the *de novo* synthesis.

We also analyzed the effect of 2OHOA on fatty acid composition of tumor cells by gas chromatography. The most notorious changes were the decrease in oleic acid (40-60%) and the increase in stearic acid (60-90%). These changes were linked to the inhibition of stearoyl-CoA desaturase (SCD1), an emerging target in cancer therapy. In addition, mass spectrometry analysis showed the incorporation of 2OHOA into different lipid classes (ca. 15% of total fatty acids). Finally, the analysis of the neutral lipid fraction by TLC showed an increase in diacylglycerol (DAG), free fatty acids (FFA) and triacylglycerol (TAG), with the ensuing formation of lipid droplets (LDs).

Then, the impact of all these changes on membrane biophysical properties was evaluated by fluorescence spectroscopy. Thus, the study of the biophysical properties of reconstituted liposomes from control and treated cells lipid extracts, showed that 2OHOA induced an increased packing of the ordered domains, due to the substantial increase in SM content, while the global order of the membrane decreased, probably due to the global changes in fatty acid composition.

These modifications would account for the observed alteration in the localization of proteins involved in cell apoptosis (Fas receptor) or differentiation (Ras) induced by 2OHOA. Therefore, we propose that the regulation of SMS activity in tumor cells is a critical upstream event in 2OHOA antitumor mechanism and it also explains the ability of this compound to trigger cell cycle arrest, cell differentiation and autophagy or apoptosis in cancer cells. In addition, low SM levels would be associated with the tumorigenic transformation that produces cancer cells. Because 2OHOA is a potent and specific drug to combat tumors, with no side effects at therapeutic doses, the data presented not only introduce the first known activator of SMS but also, define a novel molecular target for the design of new drugs against cancer.

# 1 Introduction

## 1.1 Cell membranes

Biological membranes are composed of lipids, proteins and carbohydrates which together form hydrophobic barriers that limit the distribution of aqueous macromolecules and metabolites (Figure 1-1; Alberts, 1994; Tamm, 2005). Cells are bounded and defined by membranes, which have additional functions, such as segregation and protection from the environment, compartmentalization of functions, energy production, storage, protein synthesis and secretion, phagocytosis, movement and cell-cell interactions. In addition, eukaryotic cells contain ordered structures, called organelles, to organize and carry out complex processes and to enable distinct reactions that require a hydrophobic environment or specific molecular features not found in the cytosol. The level and complexity of compartmentalization varies among organisms and among mammalian cells (Fagone, 2009; van Meer *et al.*, 2008).

The versatility of biological membranes depends on their different lipid and protein composition, which dictate the membranes structure and biophysical properties. The functions of membranes require a certain fluid plasticity which is accomplished through alteration in lipid composition determined through regulation of *de novo* synthesis at designated cellular sites, selective distribution or trafficking to new sites, and by localized remodeling reactions. All these processes are highly regulated and therefore they allow cells the maintenance of a very diverse lipid composition, not only among different organisms, but also among different compartments within the same cells and between the two leaflets of the same membrane (Fagone, 2009).

## 1.2 Membrane proteins

Membrane proteins can be classified into integral and peripheral on the basis of the nature of the membrane–protein interactions (Figure 1-1; Lodish, 2008). Integral membrane proteins, also called transmembrane proteins, contain one or more hydrophobic regions that transverse the membrane bilayer and therefore these proteins become intimately exposed to membrane lipids. Such exposure results in a variety of lipid–protein interactions that are relevant to the membrane protein activity. Most transmembrane proteins are thought to extend across the bilayer as a single α helix or as multiple α helices (Escribá *et al.*, 2008). For example, the epidermal growth factor

receptor (EGFR) is a tyrosine kinase receptor that consists of an extracellular portion that binds polypeptide ligands, a transmembrane helix, and a cytoplasmic portion that possesses tyrosine kinase catalytic activity (Hubbard & Till, 2000). Recently, it was demonstrated that the ganglioside GM3 but no other related lipids strongly inhibited the autophosphorylation of the EGFR kinase domain, in liposomes with compositions that allow the separation of coexisting liquid domains (Coskun *et al.*, 2011).

Peripheral membrane proteins reversibly bind to membranes through their lipid co/post-translational modifications (a fatty acid chain or isoprenyl group), or specific amino acid regions that provide the appropriate context for electrostatic and/or hydrophobic interactions. These non-permanent membrane proteins are generally soluble and do not fold and assemble into membranes in a constitutive way, but they develop the ability to insert and/or translocate onto membranes under specific conditions, thereby remaining membrane bound, or returning promptly to the aqueous medium where they belong (Escribá *et al.*, 2008). Non-permanent membrane proteins may be classified either according to the reversibility of the membrane contact, or to the nature (strength) of their interaction with the host membrane (Goñi, 2002). This class of proteins is relevant in the context of signal transduction and cellular physiology because they can propagate messages from the plasma membrane to intracellular membranous or aqueous compartments (Escribá *et al.*, 1995; Vance & Vance, 1996). In this regard, small GTPases exhibit continuous dynamic interactions with the internal leaflet of the plasma membrane by specific lipid modifications and/or polybasic clusters. For example, all Ras proteins contain a C-terminal motif that undergoes posttranslational prenylation by the stable linkage of a farnesyl moiety. Some members of the Ras family also contain one (N-Ras) or two (H-Ras) palmitoyl moieties or a six-lysine polybasic cluster (K-Ras) that interacts electrostatically with negatively-charged phospholipids (Eisenberg & Henis, 2008). Prenylation alone excludes proteins from raft-like domains, while dual acylation (S-palmitoyl and/or N-myristoyl residues) leads to association with raft domains. However, when activated, Ras proteins are predominantly non-raft residents (Niv *et al.*, 2002; Prior *et al.*, 2003).

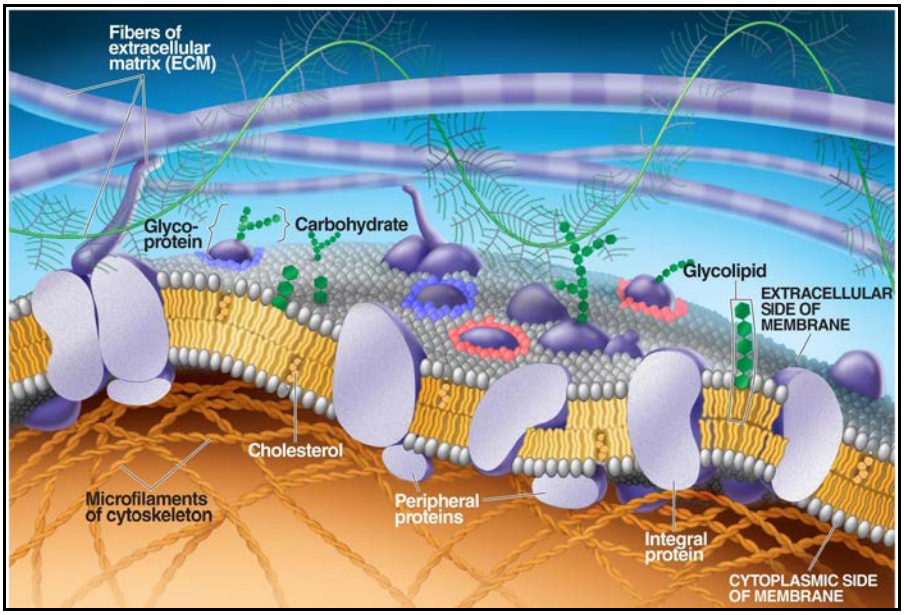


**Figure 1-1. Schematic illustration of a biomembrane.**
The diagram depicts the membrane lipid asymmetry as well as microdomains enriched in particular lipids and those induced by membrane proteins. It also shows how various classes of proteins associate with the lipid bilayer. Further from the membrane are membrane associated proteins including the cytoskeleton and the extracellular matrix (Pearson Education, 2008).

## 1.3 Membrane lipids

### 1.3.1 Lipid repertoire in nature

Eukaryotic cells invest substantial resources in generating thousands of different lipids (van Meer *et al.*, 2008). The lipidome of a particular cell is constituted by the myriad of lipid species present in it. An extraordinary structural variety exists within each class so that hundreds of individual lipid species and tens of thousands of subspecies exist within each cell (Futerman & Hannun, 2004). Thus, the first goal of lipidomics analyses is to define and quantify all of these lipid molecular species in a cell (Dennis, 2009; Han, 2007). Secondly, lipidomics seeks a comprehensive understanding of the influence of all lipids on a biological system with respect to cell signaling, membrane architecture, transcriptional and translational modulation, cell-cell and cell-protein interactions, and response to environmental changes over time. Recent advances

in soft-ionization mass spectrometry, combined with established separation techniques, have allowed the rapid and sensitive detection of a variety of lipid species with minimal sample preparation (Watson, 2006).

LIPID Metabolites And Pathways Strategy (LIPID MAPS, www.lipidmaps.org) is a multi-institutional effort created in 2003 to identify and quantify, using a systems biology approach and sophisticated mass spectrometers, all major — and many minor — lipid species in mammalian cells, as well as to quantify the changes in these species in response to perturbation. The ultimate goal of their research is a better understanding of lipid metabolism and the active role that lipids play in diabetes, stroke, cancer, arthritis, Alzheimer's disease and other diseases in which lipids may have a relevant role, to facilitate the development of more effective treatments.

The LIPID MAPS Initiative in conjunction with the International Committee for the Classification and Nomenclature of Lipids have developed a "Comprehensive Classification System for Lipids", published in 2005, that have defined eight categories of lipids and numerous classes and subclasses to allow the description of lipid molecular species. The major categories of lipids present in mammals are: fatty acyls, glycerolipids, glycerophospholipids, sphingolipids, sterol lipids, and prenol lipids (Figure 1-2; Fahy *et al.*, 2005; Fahy *et al.*, 2009).

The fatty acyl structure represents the major lipid building block of complex lipids and therefore is one of the most fundamental categories of biological lipids. However, only traces of free fatty acids are present in free form in tissues and cells. The fatty acyl group is characterized by a repeating series of methylene groups that are esterified to the backbone structure of the complex lipids through ester or amide bonds and provides hydrophobic character to this category of lipids. The fatty acids differ from each other with respect to their hydrocarbon chain length ($C_4$-$C_{36}$), the degree of unsaturation (number of double bonds), which also governs their physical properties and of the lipid that contains them, and the substitution at one or more methyl groups (Table 1-1; Prasad, 1996). The hydrocarbon chain of the fatty acid may contain one (monounsaturated) or more (polyunsaturated) double bonds. The configuration of the double bond is mostly *cis*- which provides a rigid kink of 30° in the hydrocarbon chain, whereas the *trans*- configuration results in an extended chain structure.

Glycerolipids essentially encompass all glycerol-containing lipids. It is purposely a separate category because of their abundance and importance as membrane constituents, metabolic fuels, and signaling molecules. The glycerolipid category includes mono-, di- and tri-substituted glycerols (MAG, DAG and TAG, respectively), the most well-known being the fatty acid esters of glycerol (acylglycerols), but also include alkyl and 1*Z* -alkenyl variants (Coleman & Lee, 2004). TAG formation occurs

as an energy storage and lipid-neutralizing mechanism in response to fatty acid accumulation within the cell. When this is the case, three fatty acids and one glycerol molecule are bound together to form TAG, which, along with cholesterol, are stored in lipid droplets (LDs).

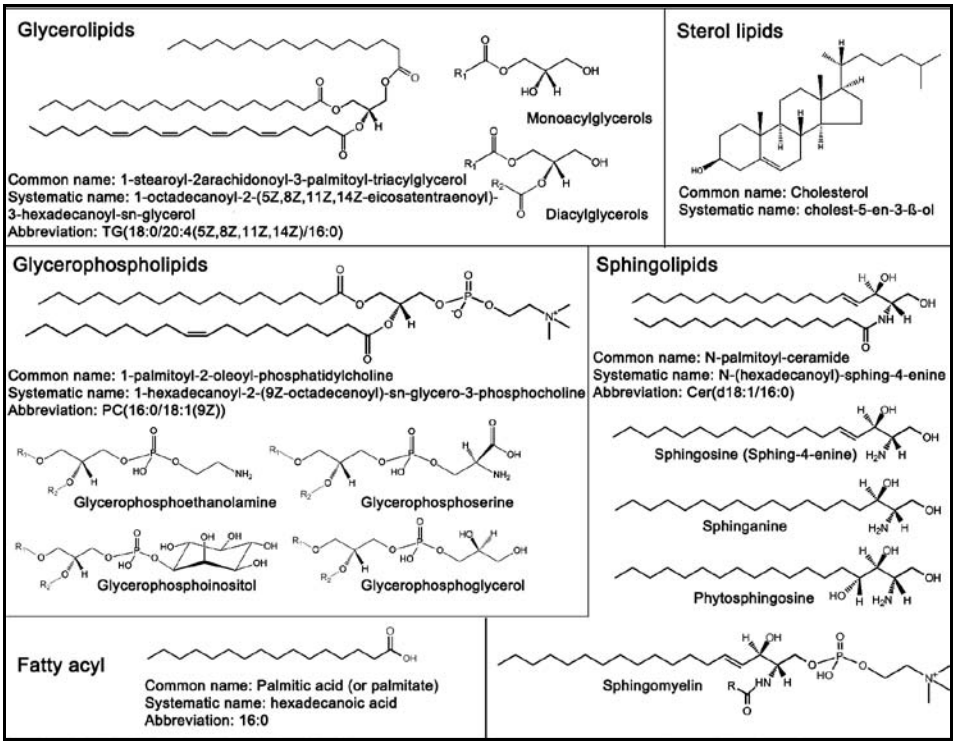


**Figure 1-2. Summary of the structural diversity of the most common lipid species (Sud *et al.*, 2006).**

Glycerophospholipids (also called phospholipids) are ubiquitous in nature and are key components of the lipid bilayer of cells. Phospholipids may be subdivided into distinct classes based on the nature of the polar "head group" at the *sn*-3 position of the glycerol backbone in eukaryotes and eubacteria or the *sn*-1 position in the case of archaebacteria (Pereto *et al.*, 2004). Phospholipids include: glycerophosphocholine (PC), glycerophosphoethanolamine (PE), glycerophosphoserine (PS), glycerophospho-inositol (PI), glycerophosphoglycerol (PG), phosphatidic acid (PA; Fahy *et al.*, 2009).

Cardiolipin (CL) is a glycerolphospho-glycerophosphoglycerol, where a third glycerol unit is typically acylated at the *sn*-1' and *sn*-2' positions to create a pseudosymmetrical molecule. In addition, plasmalogens are vinyl-ether linked at the *sn*-1-position of glycerophospholipids and contribute almost 18% to the total lipid mass in humans (Fagone, 2009). Lysophospholipids, such as lysophosphatidylcholine (LPC), are produced when phospholipase A2 (PLA2) catalyzes the hydrolysis of the fatty acyl ester bond at the *sn*-2 position of glycerophospholipids. LPC has been implicated in several types of cell death, as an effector in the lipoapoptosis of hepatocytes (Han *et al.*, 2008).

Sphingolipids are a complex family of compounds that share a common structural feature, a sphingoid base backbone that is synthesized *de novo* from serine and a long chain fatty acyl-CoA, and then converted into ceramides (Cer), phosphosphingolipids, glycosphingolipids (GSLs), and other species (Chapter 2). The major sphingolipids in mammalian cells are sphingomyelin (SM) and GSLs, which contain mono-, di- or oligosaccharides based on glucosylceramide (GlcCer) and sometimes galactosylceramide (GalCer). Gangliosides are GSLs with terminal sialic acids (Vance & Vance, 1996). Besides playing structural roles in cellular membranes, some metabolites including Cer, ceramide-1-phosphate (C1P), sphingosine (Sph) and sphingosine-1-phosphate (S1P), have drawn attention as bioactive signaling molecules involved in regulation of cell growth, differentiation, senescence, and apoptosis (Bartke & Hannun, 2009).

Sterol lipids are the main non-polar lipids of cell membranes: cholesterol predominates in mammals whereas ergosterol predominates in yeast and phytosterol in plants. Cholesterol itself and isoprenoid intermediates in cholesterol synthesis are biosynthetic precursors of steroid hormones, bile acids, lipid-soluble vitamins, and numerous other bioactive molecules (Lodish, 2008). As it will be explained later, cholesterol is critical for membrane fluidity regulation. These lipids share a common biosynthetic pathway with prenol lipids via the polymerization of dimethylallyl pyrophosphate/isopentenyl pyrophosphate but have obvious differences in terms of their eventual structure and function (Watson, 2006).

**Table 1-1. Some common fatty acids.**

| Systematic name | Common name | Carbon Skeleton | Structure |
|---|---|---|---|
| **Saturated** | | | |
| n-Dodecanoic acid | Lauric acid | 12:0 | $CH_3(CH_2)_{10}COOH$ |
| n-Tetradecanoic acid | Myristic acid | 14:0 | $CH_3(CH_2)_{12}COOH$ |
| n-Hexadecanoic acid | Palmitic acid (PA) | 16:0 | $CH_3(CH_2)_{14}COOH$ |
| n-Octadecanoic acid | Stearic acid (SA) | 18:0 | $CH_3(CH_2)_{16}COOH$ |
| n-Eicosanoic acid | Arachidic acid | 20:0 | $CH_3(CH_2)_{18}COOH$ |
| n-Docosanoic acid | Behenic acid | 22:0 | $CH_3(CH_2)_{20}COOH$ |
| n-Tetracosanoic acid | Lignoceric acid | 24:0 | $CH_3(CH_2)_{22}COOH$ |
| **Unsaturated** | | | |
| cis-9-Hexadecenoic acid | Palmitoleic acid | 16:1(Δ9) | $CH_3(CH_2)_5CH=CH(CH_2)_7COOH$ |
| cis-9-Octadecenoic acid | Oleic acid (OA) | 18:1(Δ9) | $CH_3(CH_2)_7CH=CH(CH_2)_7COOH$ |
| cis-,cis-9,12-Octadecadienoic acid | Linoleic acid (LA) | 18:2(Δ9,12) | $CH_3(CH_2)_4CH=CHCH_2CH=CH(CH_2)_7COOH$ |
| cis-,cis-,cis-9,12,15-Octadecatrienoic acid | α-Linolenic acid (ALA) | 18:3(Δ9,12,15) | $CH_3CH_2CH=CHCH_2CH=CHCH_2CH=CH(CH_2)_7COOH$ |
| cis-,cis-,cis-6,9,12-Octadecatrienoic acid | γ-Linolenic acid (GLA) | 18:3(Δ6,9,12) | $CH_3(CH_2)_4CH=CHCH_2CH=CHCH_2CH=CH(CH_2)_4COOH$ |
| cis-,cis-,cis-,cis-5,8,11,14-Icosatetraenoic acid | Arachidonic acid (ARA) | 20:4(Δ5,8,11,14) | $CH_3(CH_2)_4CH=CHCH_2CH=CHCH_2CH=CHCH_2CH=CH(CH_2)_3COOH$ |
| cis-,cis-,cis-,cis-,cis-5,8,11,14,17-Eicosapentaenoic acid | Eicosapentaenoic acid (EPA) | 20:5(Δ5,8,11,14,17) | $CH_3CH_2CH=CHCH_2CH=CHCH_2CH=CHCH_2CH=CHCH_2CH=CH(CH_2)_3COOH$ |
| cis-,cis-,cis-,cis-,cis-4,7,10,13,16,19-Docosahexaenoic acid | Docosahexaenoic acid (DHA) | 22:6(Δ4,7,10,13,16,19) | $CH_3CH_2CH=CHCH_2CH=CHCH_2CH=CHCH_2CH=CHCH_2CH=CHCH_2CH=CH(CH_2)_2COOH$ |

(Adapted from Lehninger *et al.*, 2005; Prasad, 1996).

### 1.3.2 Lipid functions

Lipids fulfill three general functions: (i) they serve as an efficient source of energy; (ii) they form cell membranes that contain bipolar lipids such as glycerophospholipids and sphingolipids; and (iii) they serve as messengers during cellular signal transduction (van Meer *et al.*, 2008). An additional function, related to membrane lipid organization, has been proposed (Escribá *et al.*, 2008; Escribá *et al.*, 1997; Escribá *et al.*, 1995). Lipids by themselves can induce the organization of membrane lipids into microdomains with different structure that act as spatial/temporal platforms that control the interaction of cell signaling proteins and tune the type and extent of messages propagated into the cells. This function of membranes will be addressed later in the present work.

First, because of their relatively reduced state, lipids are used for energy storage in LDs, which are cytosolic organelles present in all cell types, consisting of a hydrophobic core of TAG and cholesteryl esters, surrounded by a monolayer of phospholipids and cholesterol with associated proteins. *De novo* formation of LDs is tightly connected to the endoplasmic reticulum (ER) but the molecular mechanism involved in this process remains unsolved (Digel *et al.*, 2010; Walther & Farese, 2009). LDs are considered storage organelles for energy generation and membrane-building blocks (fatty acids and sterols), although new roles in protein storage and sorting have been proposed recently (Welte, 2007). In the last years, LDs have been recognized as highly relevant for widespread and serious human diseases like diabetes type II, hepatosteatosis and atherosclerosis (Digel *et al.*, 2010).

Second, cell membranes are formed by polar lipids, mainly organized in bilayer structures with a hydrophobic and a hydrophilic region. The propensity of the hydrophobic moieties to self-associate (entropically driven by water), and the tendency of the hydrophilic moieties to interact with aqueous environments and with each other, constitute the physical basis of the spontaneous formation of membranes. This fundamental principle of amphipathic lipids is a chemical property that possibly enabled the first cells to segregate their internal constituents from the external environment. This same principle is recapitulated within the cell to produce discrete organelles (van Meer *et al.*, 2008).

Finally, lipids can act as first and second messengers in signal transduction and molecular recognition processes. These include Cer, C1P, Sph and S1P, which are potent messenger molecules involved in the regulation of cell growth and apoptosis; DAG and inositol phosphate derivatives (PIPs) are involved in calcium-mediated activation of protein kinase C and other phenomena; prostaglandins are one type of

fatty-acid derived eicosanoid involved in inflammation and immunity; and steroid hormones such as estrogen, testosterone and cortisol, which modulate a wide range of functions such as reproduction, metabolism and blood pressure (The LIPID MAPS– Nature Lipidomics Gateway, www.lipidmaps.org).

### 1.3.3 Membrane lipid structure

The fluid mosaic model of the structure of cell membranes proposed by Singer and Nicolson (1972), implied an homogeneous lateral distribution of the bulk of lipids. This model proved to be a very useful hypothesis in explaining many, but certainly not all, phenomena taking place in biological membranes. However, new experimental data has allowed the extension of the model, showing additional structural and functional aspects of membrane organization (Vereb *et al.*, 2003). Therefore, according to the extended model, the mosaic is configured not only by different proteins on membranes, but also by (i) the different protein and lipid composition of outer and inner leaflets of the plasma membrane, (ii) regions enriched in certain protein and lipid species, and (iii) local (domain-restricted) membrane functions provided by the discrete localization of membrane proteins and lipids and by the lipid polymorphism (Figure 1-1; Escribá *et al.*, 1997).

Hence, one essential feature of membranes is the asymmetric distribution of lipids and proteins both laterally and between the two bilayer leaflets. Whereas the plasma, Golgi, and endosomal membranes display an asymmetric lipid distribution; in the ER, where most lipids are synthesized, lipids are symmetrically distributed between the two leaflets. In the plasma membrane, for example, choline-containing lipids such as PC and SM, as well as GSLs are enriched in the non-cytosolic (external leaflet and luminal side), whereas PS and PE are enriched in the cytosolic leaflet. Minor lipids such as PI and PA are predominantly in the cytosolic leaflet, where they participate in cell signaling (Figure 1-3; Devaux & Morris, 2004). Maintaining the differences in lipid composition between organelles and between the two leaflets of individual organelle membranes requires selectivity and directionality, which are provided by various transport mechanisms. In this regard, membrane lipids may be subject to two kinds of movement: flip–flop across the membrane from one to another monolayer and diffusion out of the membrane into the aqueous phase, followed by insertion into another membrane (Holthuis & Levine, 2005). Within the same membrane, lipids are transported to or segregated into one of the two leaflets of the membrane by virtue of their chemical structure or by the action of enzymes called flippases, whose function is to favor (energy-independent, mainly in the ER) or force the movement (energy-

dependent, mainly at the plasma membrane) of specific lipids between the two leaflets of the membrane (van Meer *et al.*, 2008). Some lipids are transported by vesicular pathways, as in the case of SM that cannot flip and travels in the luminal leaflet of the vesicles. The asymmetric distribution of lipids has important functional consequences. For example, when exposed on the cell surface, PS acts as susceptibility signal for phagocytosis and as a propagation signal in blood coagulation. The loss of transmembrane lipid asymmetry and the concomitant exposure of PS to the external milieu also occurs upon induction of programmed cell death (apoptosis; Fadok *et al.*, 1992).

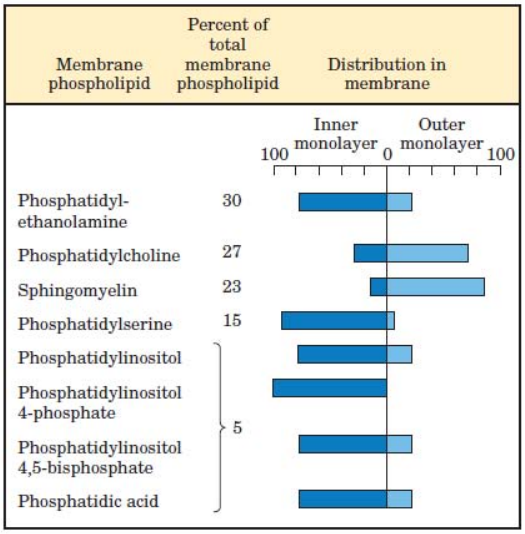


**Figure 1-3. Asymmetric distribution of glycerophospholipids between the inner and outer monolayers of erythrocyte plasma membrane (Lehninger *et al.*, 2005).**

The lateral asymmetry is achieved by lateral diffusion in the two-dimensional plane of the membrane and the subsequent differentiation of membrane regions (basal, lateral, apical) and specialized membrane microdomains such as lipid rafts, caveolae, coated pits, synaptosomes, etc. (Escribá, 2006; Lingwood & Simons, 2010). Within such domains there is not only an enrichment of particular lipids and proteins, but their rotational movement may be different from that of molecules in other domains. In this

regard, fluidity is one of the most important biophysical properties of membrane lipids and together with the cross-sectional area, electric charge, surface packing, molecular weight and nonlamellar-phase propensity, contribute to the curvature stress in biomembranes (Escribá, 2006). Membrane fluidity depends on the phase behavior of the lipids, which are not covalently bound in membranes but rather interact dynamically to form transient arrangements whose stability can vary. Biological membrane lipids can exist in multiple possible phase states (Figure 1-4). All lamellar states are the most relevant to cell biomembranes, where lipids can adopt fluid and solid phases, which are characterized by a different spatial arrangement and motional freedom of each lipid with respect to its neighbors (Figure 1-4B; van Meer *et al.*, 2008). The fluidity of individual lipid molecules changes with the temperature. This response is known as the phase behavior of the bilayer. At a given temperature a lipid bilayer can exist in either a liquid or a solid phase. All lipids have a characteristic melting temperature ($T_m$) at which they undergo a transition from the gel to liquid phase and this temperature is affected by the acyl-chain length and unsaturation degree. Non-bilayer lipid phases, such as hexagonal and cubic phases (not shown), may relate to transient biomembrane events, such as membrane fusion, fission and pore formation.

The fluid lamellar phase called liquid disordered ($l_d$), is currently acknowledged as the structure found in most membrane regions. In $l_d$ structures, the hydrocarbon chains that form the membrane core, exhibit a high level of mobility as illustrated in Figure 1-4B (Escribá, 2006). Under different conditions, lipids can organize into more ordered bilayers, such as the solid ordered ($s_o$) or gel structure. As indicated above, the degree of fatty acyl chains saturation influences the physical properties of the compound that contains them. Thus, SM contains long, saturated (or *trans*-unsaturated) hydrocarbon chains, with high $T_m$, so that SM-rich mixtures tend to form these $s_o$ phases. However, biomembrane glycerophospholipids contain mainly *cis*-unsaturated hydrocarbon chains, with low $T_m$, thus they are abundant in liquid phases. Within the membrane glycerophospholipids, PC self-organizes spontaneously as a planar bilayer, less tightly than SM, in which each PC has a nearly cylindrical molecular geometry, with the lipidic tails facing each other and the polar headgroups interfacing with the aqueous phase (Vance & Vance, 1996). In the liquid-ordered ($l_o$) phase, the acyl chains of lipids are extended and tightly packed as in the gel phase, but they have a higher degree of lateral mobility. Generally, the $l_o$ phase represents lipid rafts in model membranes, since lipid rafts segregate from the rest of the membrane, forming defined domains. Sterols by themselves do not form bilayer phases, but together with a bilayer-forming lipid, they can organize into $l_o$ phases, regulating their fluidity (Castro *et al.*, 2009). However, not all sterols have the ability to induce the formation of $l_o$ phases or lipid rafts. While cholesterol is responsible for the $l_o$ domain formation in mammals and

ergosterol in yeast, some other sterols such as zymosterol do not form $l_o$ domains (Megha *et al.*, 2006). Membrane rafts are defined as small (10-200 nm), heterogeneous, highly dynamic, sterol- and sphingolipid enriched domains that compartmentalize cellular processes. Small rafts can sometimes be stabilized to form larger platforms through protein-protein and protein-lipid interactions (Lingwood & Simons, 2010; Pike, 2006).

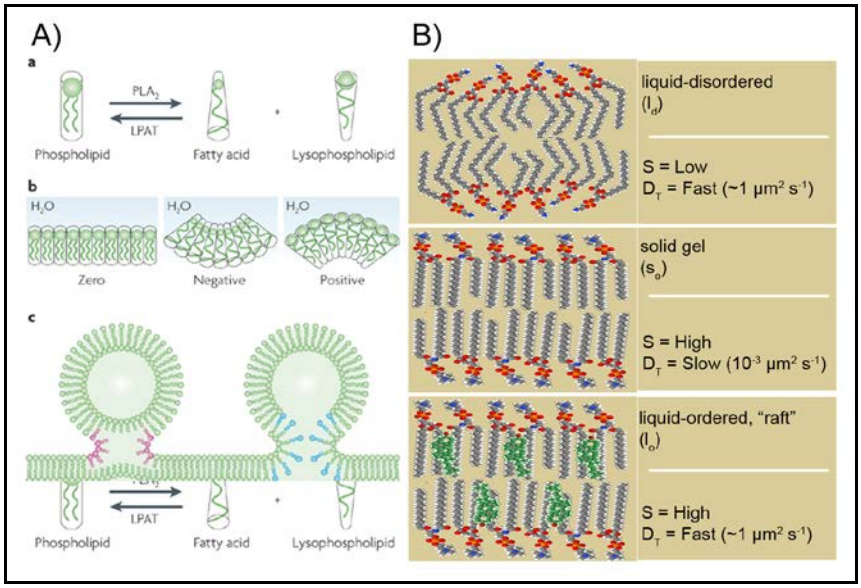


**Figure 1-4. Membrane lipid structure.**
Examples of lipid shapes and their influence on membrane structure. (A) (a) and (b) GPs in which the polar head group and the fatty acid chains have similar sizes adopt a cylindrical shape in membranes (solid circles symbolize the polar head groups; wavy lines represent the fatty-acid chains). Lipids with a small polar head have a molecular shape that resembles a truncated cone. They induce a negative curvature strain, favoring the reorganization of membranes into inverted micelles and $H_{II}$ phases in general. Lipids with a bulky polar head and only one acyl chain have a molecular shape similar to an inverted cone and induce a positive curvature strain in membranes ($H_I$ phases). PLA2, phospholipase A2; LPAT, lysophospholipid acyl transferases. c) The two steps of membrane fusion: left, during stalk formation, two adjoining membranes merge their outer leaflets producing a negatively curved monolayer region (red) that is facilitated by cone-shaped lipids; right, widening of the stalk generates a fusion pore that is lined by a positively curved monolayer region (blue). (B) Lipid phases in membranes. All membrane phase behaviors that have been observed are characteristic of the corresponding lipids. S, the order parameter of a segment of acyl chain; and $D_T$, the translational diffusion coefficient (Adapted from Escribá, 2006; Piomelli *et al.*, 2007; van Meer *et al.*, 2008).

Non-lamellar prone glycerophospholipids add versatility to lipid structures. Lipid curvature stress controls the organization of lipids into different types of hexagonal phases ($H_I$ and $H_{II}$; Figure 1-4A). Lipids with a small polar headgroup, such as PE, have a molecular shape that resembles a truncated cone. These lipids induce a negative curvature strain, which favors the reorganization of membranes into inverted micelles ($H_{II}$ phases). The inclusion of PE in PC bilayers imposes a curvature stress onto the membrane, which is used for budding, fission and fusion (Piomelli *et al.*, 2007). Non-bilayer lipids like PE and CL may also be used to accommodate membrane proteins, which may stabilize the bilayers, and modulate their activities. Lipids with a bulky polar head and only one acyl chain (e.g. lysophospholipids) have a molecular shape that is similar to an inverted cone and induce a positive curvature strain in membranes. In this case, they favor the formation of tubular ($H_I$) or spherical micelles. In this context, lipid hydrolases, such as PLA2 convert phospholipids into conical (fatty acid) and inverted conical (lysophospholipid) products, whereas fatty acid transferases such as lysophospholipid acyl transferases catalyze the opposite reaction.

### 1.3.4 Lipid metabolism

The ER and Golgi apparatus together constitute the endomembrane compartment in the cytoplasm of eukaryotic cells, where not only lipids but also membrane-bound proteins and secretory proteins are synthesized (Fagone, 2009). The ER produces the bulk of the structural glycerophospholipids, such as PC, PE, PI, PS and PA; as well as cholesterol, Cer (which is the precursor for complex sphingolipids) and significant levels of TAG and cholesteryl esters (Figure 1-5; van Meer *et al.*, 2008).

For the biosynthesis of glycerolipids, glycerophospholipids and cholesterol esters, fatty acids first need to be activated as acyl-coenzyme A (CoA), produced by one of several long-chain or very-long-chain acyl-CoA synthases (Coleman *et al.*, 2002; Kornberg & Pricer, 1953). Then, acyl-CoA can be used as donors, to form glycerolipids and glycerophospholipids by a *de novo* pathway (Kennedy pathway) or be modified by a remodeling pathway (Lands' cycle) to generate membrane asymmetry and diversity. This remodeling pathway involves the rapid turnover of the *sn*-2-acyl moiety of glycerophospholipids by the concerted and coordinated actions of PLA2 and lysophospholipid acyltransferases (Lands, 2000; Shimizu *et al.*, 2006). It is worth to mention that saturated fatty acids (SFA) are usually esterified at the *sn*-1-position, whereas unsaturated acyl groups are esterified at the *sn*-2-position (Shindou & Shimizu, 2009).

In the *de novo* pathway, 1-acyl-sn-glycerol-3-phosphate (lysophosphatidate, LPA) is first formed from glycerol 3-phosphate by the glycerol-3-phosphate acyltransferase (GPAT), which attaches a fatty acyl moiety to the *sn*-1 position (Figure 1-6; Coleman & Lee, 2004; Shindou & Shimizu, 2009). Next, LPA is converted to PA by the acyl-CoA:1-acylglycerol-*sn*-3-phosphate acyltransferase (AGPAT, also called lysophosphatidate acyltransferase or LPAAT), which attaches a fatty acyl moiety to the *sn*-2 position. GPAT and AGPAT activities are associated with the ER and the mitochondria (Athenstaedt & Daum, 1999). In the ER, PA is metabolized into two types of glycerol derivatives. By the phosphatidic acid phosphatase enzymes (PAP), PA is dephosphorylated to yield DAG, which is then converted to TAG, PC and PE. The other glycerol derivative is cytidine diphospho-DAG (CDP-DAG), which is transformed into the acidic phospholipids PI, PG and CL (Heacock & Agranoff, 1997). The GPAT and AGPAT association with the mitochondria indicates that these activities provide the PA precursor (CDP-DAG) for the synthesis of PG and CL located at the same site. CL is present only in the mitochondria, where it is absolutely required for energy production, and its synthesis is restricted to the inner mitochondrial membrane (Schlame *et al.*, 2000). Approximately 45% of the phospholipid in mitochondria (mostly PE, PA and CL) is autonomously synthesized by the organelle (Fagone, 2009; van Meer *et al.*, 2008). In turn, PA can be synthesized from DAG by diacylglycerol kinase, which is believed to generate a PA as a signaling molecule rather than a precursor for TAG biosynthesis (Martelli *et al.*, 2002).

PC is the most abundant glycerophospholipid species in mammalian cells, (~50% of glycerophospholipid mass), and it is synthesized in the ER and Golgi apparatus (Figure 1-5). Two biosynthetic pathways are available for PC synthesis and are located in different endomembrane domains. The Kennedy pathway is the predominant route to PC in most cells, and the final step is catalyzed either by the bifunctional diacylglycerol choline/ethanolamine phosphostransferase (CEPT), which is located in the ER, or alternatively by the diacylglycerol choline phosphostransferase (CPT), which is located in the Golgi apparatus (Henneberry *et al.*, 2002; Vance *et al.*, 1997). Both the CEPT and the CPT use DAG and CDP-choline to form PC. The rate-limiting step for PC synthesis is catalyzed by the amphitropic CTP:phosphocholine cytidylyltransferase α (CCT), which is found in the nucleus in most cell types, immediately upstream of CEPT and CPT, and it translocates from a soluble nuclear location to the nuclear membrane in response to activators of the CDP-choline pathway (Henneberry *et al.*, 2002). Phosphatidylethanolamine N-methyltransferase (PEMT) converts PE to PC and is associated with mitochondria-associated membranes. PEMT is generally considered to be a liver-specific enzyme although there is PE methylation activity (1% or less of that recovered from rat liver microsomes) in various other cells

and tissues (Vance & Ridgway, 1988). PE is the second most abundant glycerophospholipid species (~25% of glycerophospholipid mass), and its *de novo* synthesis can be catalyzed by CEPT using CDP-ethanolamine, located in the ER. PE can also arise from head-group exchange with PS in the ER as mediated by phosphatidylserine synthase 2 (PSS2) or in the mitochondria by PS decarboxylation, mediated by phosphatidylserine decarboxylase.

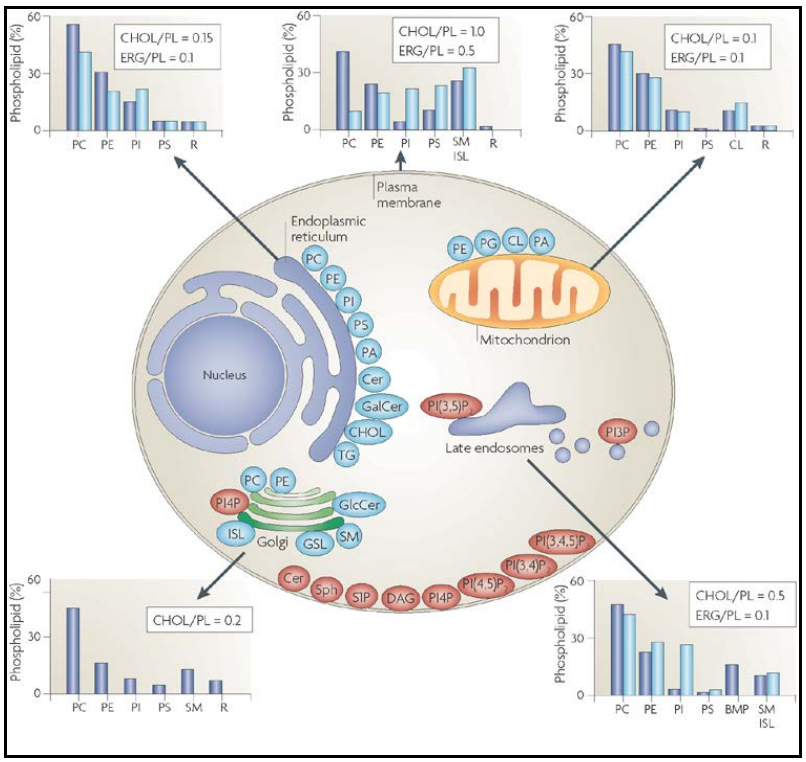


**Figure 1-5. Lipid synthesis and steady-state composition of cell membranes.**
The lipid composition of different membranes varies throughout the cell. Lipid composition data (shown in graphs) are expressed as a percentage of the total glycerophospholipid in mammals (blue) and yeast (light blue). The molar ratio of cholesterol and ergosterol to glycerophospholipid is also included. The figure shows the site of synthesis of the major glycerophospholipids (blue) and lipids that are involved in signaling and organelle recognition pathways (red). It should be appreciated that the levels of signaling and recognition lipids are significantly below 1% of the total glycerophospholipid, except for Cer (van Meer *et al.*, 2008).

By contrast with PC and PE, PS is synthesized in the ER or the Golgi apparatus through head-group exchange of already-made PC and PE as catalyzed by PSS1 and PSS2, respectively (Vance, 2008). PI is also synthesized in the ER by the CDP-diacylglycerol-inositol 3-phosphatidyltransferase, and its conversion into highly phosphorylated forms, which play critical roles in signaling and membrane vesicle trafficking, occurs outside the ER (Antonsson, 1997). Phosphoinositides identify endocytic membranes and allow them to recruit proteins from the cytosol that are involved in this process. A dedicated system of kinases and phosphatases produces and hydrolyses specific phosphoinositides, including phosphatidylinositol-(4,5)-bisphosphate ($PI(4,5)P_2$) in the plasma membrane, phosphatidylinositol-trisphosphate (PI3P) on early endosomes, phosphatidylinositol-(3,5)-bisphosphate ($PI(3,5)P_2$) on late endosomes and PI4P on the (trans)-Golgi network (Di Paolo & De Camilli, 2006). Plasmalogen synthesis occurs in peroxisomes. Among plasmalogens, plasmenylethanolamine is the most abundant and it is also the precursor of plasmenylcholine (Fagone, 2009).

TAGs are also synthesized in the ER and in the plasma membrane either by the Kennedy pathway or the MAG pathway (Yen *et al.*, 2008). While the glycerol phosphate pathway is present in most cells, the MAG pathway is found in specific cell types, such as enterocytes, hepatocytes, and adipocytes, where it may participate in the reesterification of hydrolyzed TAG. In the final reaction of both pathways, a fatty acyl-CoA and DAG are covalently bound to form TAG. This reaction is catalyzed by acyl-CoA:diacylglycerol acyltransferase (DGAT) enzymes (Weiss *et al.*, 1960). Newly synthesized TAGs are thought to be released into the associated lipid bilayer, where they are channeled into cytosolic LDs or, in cells that secrete TAG, to nascent lipoproteins. TAGs are the main energy store and, through a lipase-catalyzed reaction, can be reconverted to DAG as a precursor for the synthesis of complex lipids (Coleman & Lee, 2004). DAG can also act as a substrate for DAG lipases that hydrolyze the fatty acid in position 1 or 2, generating MAG. DAG lipases are also strongly linked to signaling functions. For example, in platelets, in response to thrombin their combined action with phospholipase C (PLC) facilitates the release of arachidonic acid, an intermediate in thromboxane and prostaglandin synthesis (Smith *et al.*, 1991).

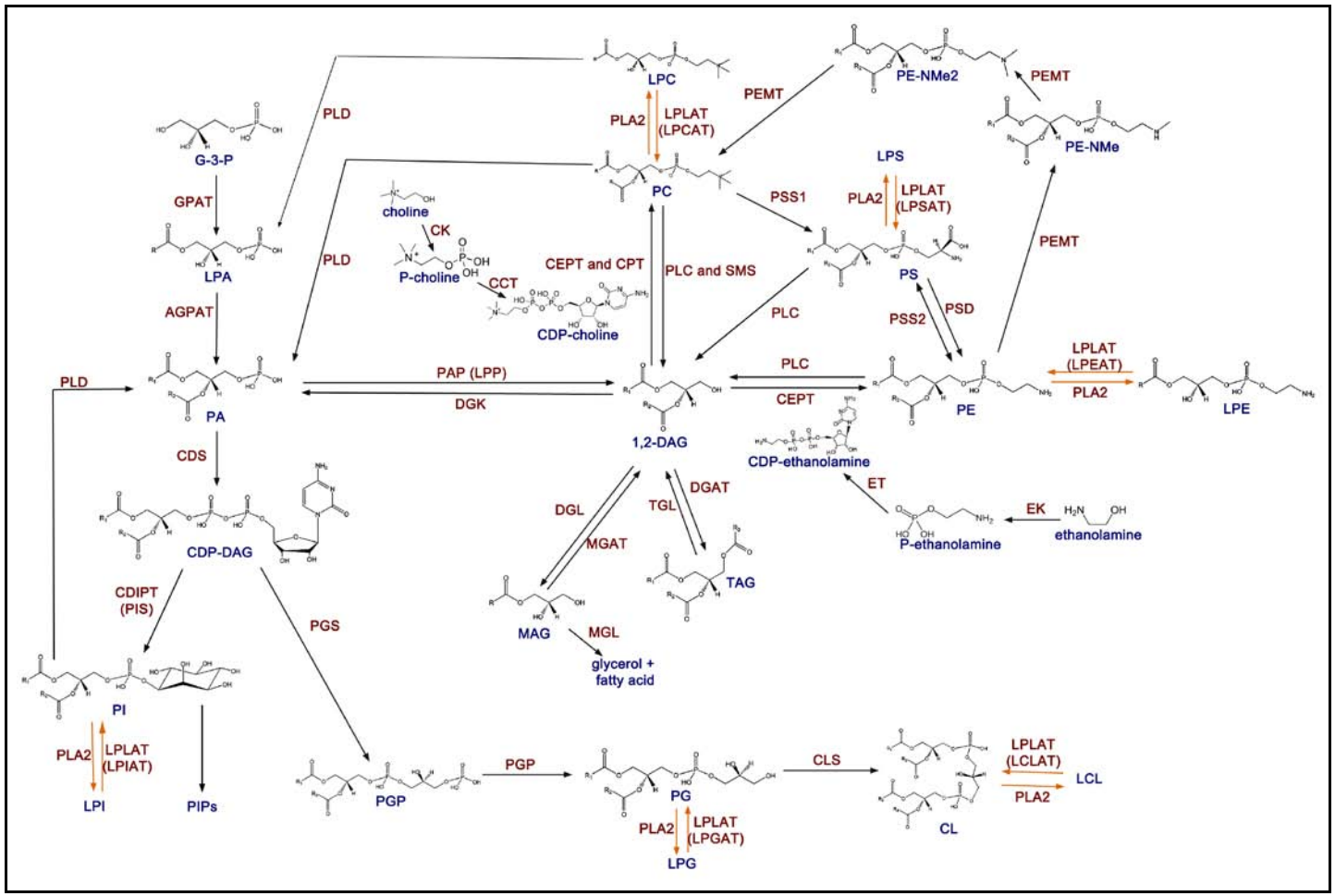


**Figure 1-6. Integrated metabolic pathways of glycerolipids and glycerophospholipids. See footnote on next page[1].**

In addition to the *de novo* synthesis, three alternative pathways can generate DAG through the action of sphingomyelin synthase (SMS), PLC and phospholipase D. In the last two pathways, DAG generation is highly dependent on extracellular stimulation, and DAG generated by these mechanisms is not usually consumed for metabolic purposes (Carrasco & Merida, 2007). The principal effect of DAG on responsive proteins, such as protein kinase C (PKC), is considered to be protein translocation to membranes, mediated by its direct binding to the C1 domain (Yang & Kazanietz, 2003) and regulation of membrane curvature (Goñi & Alonso, 1999). Considering the numerous metabolic pathways in which DAG is implicated, cells must rigorously control the production and clearance of DAG to guarantee a permanent reservoir of this lipid.

The mammalian Golgi also specializes in sphingolipid synthesis, and produces SM, GlcCer, lactosylceramide (LacCer) and higher-order GSLs, all of which are primarily destined for export to the plasma membrane (Futerman & Riezman, 2005). The production of sphingolipids is reviewed in *Chapter 3*. Although the plasma membrane is not involved in autonomous synthesis of its structural lipids, numerous reactions for either synthesizing or degrading lipids that are involved in signaling cascades have been described for this organelle, such as the SM-Cer cycle (Di Paolo & De Camilli, 2006). Plasma membranes are also enriched in sterols (Figure 1-5), which are packed together with sphingolipids at a higher density than glycerophospholipids and confer to the membrane higher resistance to mechanical stress.

[1] **Figure1-6.** The scheme shows the *de novo* synthesis of glycerolipids and glycerophospholipids (Kennedy pathway) and the remodeling pathway (Lands cycle) indicated by orange arrows. The names of the enzymes are in red: GPAT, Glycerol-3-phosphate acyltransferase; AGPAT, 1-acyl-sn-glycerol-3-phosphate acyltransferase; PAP (LPP), Phosphatidic acid phosphatase (Lipid phosphate phosphohydrolase); CEPT, Diacylglycerol choline/ethanolamine phosphotransferase; CPT, Diacylglycerol choline phosphotransferase; MGAT, Acyl-CoA:monoacylglycerol acyltransferase; DGAT, Acyl-CoA:diacylglycerol acyltransferase; MGL, Monoacylglycerol lipase; DGL, Diacylglycerol lipase; TGL, triacylglycerol lipase; PEMT, Phosphatidylethanolamine N-methyltransferase; PSS1/2, Phosphatidylserine synthase; PSD, Phosphatidylserine decarboxylase; CDS, Phosphatidate cytidylyltransferase; CDIPT (PIS), CDP-diacylglycerol--inositol 3-phosphatidyltransferase; CLS, Cardiolipin synthetase; PGS, Phosphatidylglycerophosphate synthase; DGK, Diacylglycerol kinase; PLC, Phospholipase C; PLD, Phospholipase D; CK, Choline kinase; EK, Ethanolamine kinase; CCT, CTP-phosphocholine cytidylyltransferase; PLA2, Phospholipase A2; LPLAT (LPCAT, LPEAT, LPSAT, LPIAT, LPGAT, LCLAT), lysophospholipid acyltransferases. PLC and PLD act on every glycerophospholipid, although in the picture is only shown for some of them. The names of the lipid species are in blue: G3P, glycerol-3-phosphate; LPA, lysophosphatidic acid; PA, phosphatidic acid; CDP-DAG, CDP-diacylglycerol; 1,2-DAG, 1,2-diacylglycerol; MAG, monoacylglycerol; TAG, triacylglycerol; PC, phosphatidylcholine; LPC, lysophosphatidylcholine; PE, phosphatidylethanolamine; LPE, lysophosphatidylethanolamine; PE-NMe, methylphosphoethanolamine; PS, phosphatidylserine, LPS, lysophosphatidylserine; PI, phosphatidylinositol; LPI, lysophosphatidylinositol; PIPs, phosphatidylinositol phosphates; PGP, phosphatidylglycerol phosphate; PG, phosphatidylglycerol; CL, cardiolipin; LCL, lysocardiolipin. Lipid structures were obtained from Sud et al, 2006.

Many aspects of the glycerophospholipid metabolism and function in the cytoplasm are recapitulated in the nucleus (Irvine, 2003). The nuclear envelope contains the large bulk of nuclear lipids, which, in addition to providing structural support and isolation of nuclear functions, are also the source of numerous signaling reactions. Recent studies have shown that endonuclear loci are also the source of numerous phospholipid signaling reactions, in agreement with their detection in chromatin, nucleolus, and nuclear matrix (Ledeen & Wu, 2008). These include metabolic cycles involving SM-Cer, Cer-Sph, glycerophospholipid acylation-deacylation, and PLC-mediated breakdown of phosphoinositides (Ledeen & Wu, 2004). SM, the most represented lipid in chromatin with respect to microsomes and nuclear membranes, is localized near to newly synthesized RNA, and appears to protect RNA from RNase digestion. SM increases during the differentiation process and apoptosis, while an increase of sphingomyelinase, with a concomitant decrease in SM, is observed at the beginning of S-phase of the cell cycle in rat hepatocytes; indicating a possible role in stabilizing the DNA double helix (Albi & Viola Magni, 2004; Cascianelli *et al.*, 2008).

Fatty acid oxidation is the process by which fatty acids are degraded in living organisms. In animal cells, fatty acids are degraded both in mitochondria and peroxisomes. The initial event is the activation of fatty acids by esterification with CoA. The degradation of the resultant fatty acyl-CoA thioesters proceeds by a cyclic process named β-oxidation (Schulz, 2004). Passage through one cycle of β-oxidation produces fatty acids that are shortened by two carbon atoms and yields acetate in the form of acetyl-CoA. Repetitive cycling through β-oxidation results in the complete degradation of fatty acids, releasing energy that drives the formation of ATP by oxidative phosphorylation. α-Oxidation occurs in peroxisomes and is the process that results in the oxidative removal of the first carbon atom, the carboxyl group, of a fatty acid or carboxylic acid to yield $CO_2$ and a fatty acid or carboxylic acid shortened by one carbon atom. Substrates of peroxisomal oxidation are the CoA derivatives of fatty acids and carboxylic acids that are poorly or not at all taken up by mitochondria as, for example very long-chain fatty acids, methyl-branched carboxylic acids like phytanic acid, and α-hydroxylated fatty acids, among others. It is worth to mention that while α-oxidation was extensively studied for phytanic acid (Jansen & Wanders, 2006), very little was done with hydroxylated fatty acids (Foulon *et al.*, 2005). Once they are chain-shortened by one carbon atom they can be degraded by β-oxidation (Schulz, 2004).

## 1.4 Lipid alterations in cancer

There are several signaling pathways that are deregulated in cancer cells and can be summarized by six essential alterations in the cell's physiology, and that collectively dictate malignant growth: self-sufficiency in growth signals, insensitivity to growth-inhibitory (antigrowth) signals, evasion of programmed cell death (apoptosis), limitless replicative potential, sustained angiogenesis, and tissue invasion and metastasis (Hanahan & Weinberg, 2000). Similar to regulation of gene expression, changes in the presence and levels of membrane lipid species have been described in several human pathologies, associated either with adaptive responses or with the aetiology of the disease. In this regard, numerous studies have shown that the lipid composition of tumor cell membranes is altered with respect to non-tumor cells (Table 1-2). This area of study has received little attention in cancer research, mainly because structural and functional concepts of lipid alterations in cancer are more difficult to understand than the functional role of certain proteins and their genes in defining cancer cell phenotypes. Although thus far it has not been shown a common pattern of alterations characteristic for different kinds of tumors, certain cancer-induced lipid profile changes have been described and should possess some diagnostic value (Hendrich & Michalak, 2003).

In this context, a hallmark of cancer cells is the constitutive activation of the fatty acid biosynthetic pathway, which produces SFA and monounsaturated fatty acids (MUFA) to sustain the increasing demand of new membrane phospholipids with appropriate acyl composition (Kuhajda, 2006; Rashid *et al.*, 1997; Swinnen *et al.*, 2000). In this regard, the increased levels of oleic acid, detected in several tumors, are related to the activation of the fatty acid synthesis (Igal, 2010). The enzyme responsible for the oleic acid synthesis is the stearoyl-CoA desaturase (SCD) and its role in cancer is discussed in *chapter 4*.

Gangliosides, which are membrane-bound glycosphingolipid molecules, are frequently aberrantly expressed in tumors (Hettmer *et al.*, 2005). Ganglioside antigens on the cell surface, act as immunosuppressors; and certain gangliosides, such as GD3 or GM2, promote tumor-associated angiogenesis (Birkle *et al.*, 2003). The reduced levels of Cer that were found in some types of cancer could be related to its pro-apoptotic role (Riboni *et al.*, 2002). The role of ceramides in cancer is discussed in *chapter 3*. One lipid alteration highly connected to the genetic alterations found in cancer, is the elevated levels of $PI(3,4,5)P_3$ formed by the activation of phosphatidylinositol 3-kinase (PI3K) that was observed in several tumors and contribute to oncogenesis (see below; Samuels *et al.*, 2004). In the present study, we showed that SM levels are markedly reduced in cancer cells, ranging between one third and one half the levels found in

normal cells (Castagnet *et al.*, 2005; Merchant *et al.*, 1991b), suggesting that this change might be relevant for tumorigenesis.

**Table 1-2. Lipid composition alterations in cancer cells.**

| Tumor type/Cell type | Lipid alteration | Reference |
|---|---|---|
| Human neuroblastoma and small cell lung carcinoma | Aberrant ganglioside (GM1 and GM2) containing high levels of hydroxyl fatty acids | (Ladisch *et al.*, 1989; Nilsson *et al.*, 1986) |
| Human ovarian tumors | Increased sulfated glycolsphingo-lipid expression. | (Kiguchi *et al.*, 1992; Liu *et al.*, 2010) |
| Human neuroblastoma | Aberrant ganglioside glycolsyla-tion: Increased GD2 expression. | (Hettmer *et al.*, 2005) |
| Human glioma | Altered PUFA composition: reduced DHA (22:6n-3) and increased linoleic acid (18:2n-6). | (Martin *et al.*, 1996) |
| Human head and neck squamous cell carcinoma (HNSCC) | Downregulation of C18:0-Cer. | (Koybasi *et al.*, 2004) |
| Human astrocytomas (low grade and high grade malignancy) | Decreased total Cer levels. | (Riboni *et al.*, 2002) |
| Human prostate cancer | Cholesterol accumulation. | (Di Vizio *et al.*, 2008; Freeman & Solomon, 2004) |
| Human breast, colon, esophageal Cancer | Altered phospholipid profile (e.g. reduced SM). | (Merchant *et al.*, 1993; Merchant *et al.*, 1991a; Merchant *et al.*, 1991b) |
| Human ovarian tumors | Activation of choline phospho-lipid metabolism. | (Iorio *et al.*, 2005) |
| Mice brain tumors | Abnormalities in CL content or composition. | (Kiebish *et al.*, 2008) |
| Human ovarian, colon, prostate and lung carcinomas, malignant melanoma and glioblastoma-astrocytoma cell lines compared to different human fibroblast cell lines | Increased oleic acid, reduced stearic acid, DHA. | (Meng *et al.*, 2004c) |
| **Plasma, Red Blood Cells or platelets from cancer patients** | | |
| Pancreatic and non-small lung cancer | Reduced n-3 fatty acid levels. | (Zuijdgeest-van Leeuwen *et al.*, 2002) |
| Non-small lung cancer | Reduced linoleic acid (LA, 18:2n-6). | (de Castro *et al.*, 2009) |
| Breast, prostate, liver, pancreas, colon and lung cancer | Increased oleic acid and decreased stearic acid; reduced DHA in relation to ALA. | (Mikirova *et al.*, 2004; Pala *et al.*, 2001) |
| non-Hodgkin lymphoma | Abnormal fatty acid profile: higher levels of palmitic (16:0), oleic (18:1n-9) and arachidonic acids (20:4n-6); reduced levels of LA (18:2n-6), EPA (20:5n-3) and DHA (22:6n-3). | (Cvetkovic *et al.*, 2010) |
| Colorectal cancer | Reduced n-6 fatty acids. | (Baro *et al.*, 1998) |

Therefore, because the type and/or composition of membrane lipids are altered in several pathologies, and important cellular functions occur within or around membranes, Membrane Lipid Therapy (see below) might have potential use for the treatment of several illnesses.

In the present work, a human glioma cell line was used as the main model system, thus, a brief description of brain tumors and the specific genetic alterations that they contain are indicated below. Brain and other central nervous system tumors represent about 2% of all cancers and they account for about 2% of all cancer-related deaths (Ferlay *et al.*, 2008). Brain tumors have a poor prognosis and poor survival rates, around 20% (Wrensch *et al.*, 2002), indicating the great therapeutic needs for the treatment of this condition (Schwartzbaum *et al.*, 2006). The only established risk factor for glial and meningeal neoplasms is the exposure to therapeutic or high-dose ionizing radiation and is determined by genetic factors (DeAngelis, 2001). The standard treatment for a primary brain tumor is surgery, radiotherapy and chemotherapy, mainly with temozolomide (Temodar;Chandana *et al.*, 2008; Stupp *et al.*, 2005). However the use of temozolomide only provides a modest increase in life span (ca. 10 weeks) to patients with glioma.

There are several types of brain tumors, classified by the World Health Organization based on their cellular origin and histologic appearance (Louis *et al.*, 2007). Neuroglial tumors account for more than 80% of primary brain tumors and derive from astrocytes, oligodendrocytes, or ependymal cells. In addition, gliomas are divided into four grades, according to the malignancy of the tumor. Glioblastoma multiforme is the most common type of glioma, the most aggressive one and is associated with very poor survival (Schwartzbaum *et al.*, 2006). High-grade (malignant) glial neoplasms can arise either alone (primary glioblastoma) or from a preexisting low-grade tumor (secondary glioblastoma; DeAngelis, 2001; Schwartzbaum *et al.*, 2006).

The most frequent genetic alteration found in glioma is the loss of heterozygosity of chromosome 10q, which contains functional copies of tumor suppressor genes (Fujisawa *et al.*, 2000). A key signaling pathway in the development of primary glioblastomas is the EGFR/PTEN/Akt/mTOR pathway. In fact, EGFR amplification has been identified as a genetic hallmark of glioblastomas (Kleihues & Sobin, 2000). Activated EGFR transduces a mitotic signal (Arteaga, 2002), recruiting PI3K to the cell membrane. PI3K phosphorylates $PI(4,5)P_2$ to PI3P, which activates downstream effector molecules such as Akt (protein kinase B) and mTOR; resulting in cell proliferation and increased cell survival by blocking apoptosis (Ohgaki & Kleihues, 2007). Apoptosis can be elicited in cells through two major routes, an extrinsic route initiated through activation of cell surface receptors such as TNF and Fas; and an

intrinsic route that is activated by permeabilization of the outer mitochondrial membrane via pro-apoptotic stimuli (MacFarlane & Williams, 2004). Both pathways converge on caspases, which are responsible for executing subsequent steps in the apoptotic program. PTEN (phosphatase and tensin homology), whose gene is located at 10q23.3, inhibits the PI3P signal, thereby inhibiting cell proliferation (Teng *et al.*, 1997). In addition, the signaling pathway Ras/MAPK is also activated in many gliomas (Tatevossian *et al.*, 2010). Indeed, high levels of active Ras-GTP are found in advanced astrocytomas (Guha *et al.*, 1997). Ras-GTP phosphorylates Raf kinase, which phosphorylates MEK, which phosphorylates ERK, which enters the nucleus and phosphorylates nuclear transcription factors that induce the expression of genes promoting cell cycle progression, such as cyclin D1 (Furnari *et al.*, 2007).

The cell cycle involves a series of events which result in DNA duplication and cell division. The cell cycle is divided into two stages: mitosis (M), the process of nuclear division; and interphase, the interlude between two M phases. Interphase includes the first gap phase ($G_1$), the DNA replication phase (S) and the second gap phase ($G_2$). Cells in $G_1$ can, before commitment to DNA replication, enter a resting (or quiescent) state called $G_0$, which accounts for most of the non-growing, non-proliferating and differentiated (mature) cells in the human body. The progression from one stage to the next is carefully controlled by the sequential formation, activation and subsequent degradation or modification of a series of cyclins and their partners, the cyclin-dependent kinases (CDKs), a family of serine/threonine protein kinases that are activated at specific points of the cell cycle. Transition from one stage to the next is regulated at a number of checkpoints which prevent premature entry into the next phase of the cycle (Macdonald *et al.*, 2004; Vermeulen *et al.*, 2003).

The retinoblastoma protein (pRb) and p53 regulate the cell cycle primarily by governing the $G_1$ to S phase transition, are major targets of inactivating mutations in glioblastomas. The absence of these cell cycle guardians renders tumors particularly susceptible to inappropriate cell division driven by constitutively active mitogenic signaling effectors, such as PI3K and MAPK. In its hypophosphorylated state, pRb blocks proliferation by binding and inhibiting the proliferation inducing transcription factors E2F, which prevents the expression of genes essential for progression from $G_1$ into S phase (Sherr & McCormick, 2002). Upon mitogenic stimulation, the activation of the MAPK cascade leads to the association of the CDK4/cyclin D1 complex that phosphorylates pRB, thereby releasing active E2F. In turn, $p16^{INK4a}$ binds to CDK4, inhibits the CDK4/cyclin D1 complex and, therefore, the G1 to S transition (Sherr & Roberts, 1999). In glioblastomas, disruption of the $p16^{INK4a}$ gene occurs through homozygous deletion (Kleihues & Sobin, 2000). The p53 tumor suppressor is a transcription factor that prevents the propagation of cells with unstable genomes,

predominantly by halting the cell cycle in the $G_1$ phase or instigating a program of apoptosis or proliferative arrest (Vousden & Lu, 2002). Loss of p53, through either point mutations that prevent DNA binding or loss of chromosome 17p, is a frequent and early event in the pathological progression of secondary glioblastomas (Furnari *et al.*, 2007; Ichimura *et al.*, 2004).

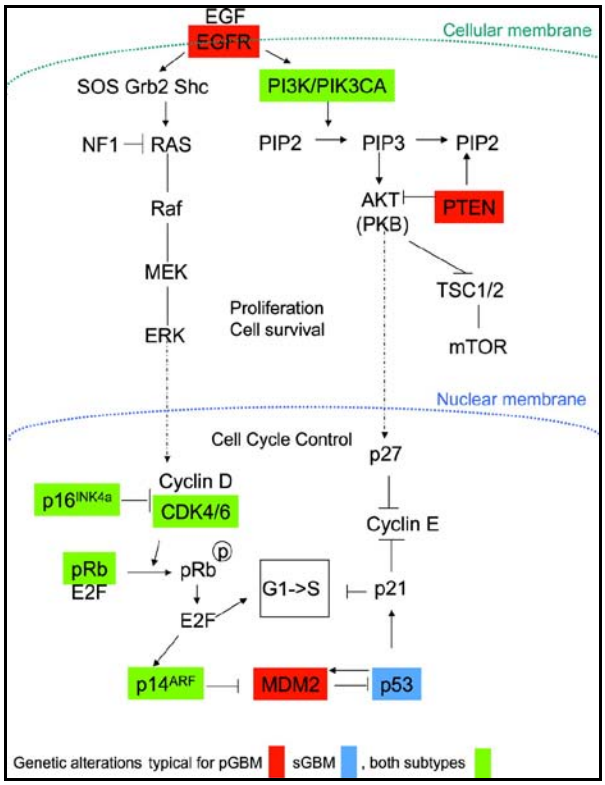


**Figure 1-7. Signaling pathways altered in human gliomas.**
Most of the molecular entities in the Ras/MAPK and PI3K/Akt have been seen mutated in human gliomas. The greater the number of genes mutated, the higher the degree of malignancy of the glioma. This figure shows these signaling pathways, as well as its relation with the cell cycle machinery (cyclin/CDK, Rb/E2F, $p27^{kip1}$, $p16^{INK4b}$, etc). The boxes indicate the genes more frequently mutated in human primary glioblastoma (pGBM, red), secondary glioblastoma (sGBM, blue) or both (green) (Adapted from Ohgaki & Kleihues, 2007).

## 1.5 Membrane Lipid Therapy

Previous works showed that the membrane lipid structure influences cell signaling (Escribá *et al.*, 1997; Escribá *et al.*, 1995; Vogler *et al.*, 2004). Thus, for example, the presence of the nonlamellar-prone lipid PE favors the binding of heterotrimeric $G_i$ proteins and $G_{\beta\gamma}$ dimmers to model membranes, whereas $G_{\alpha i}$ subunit prefers lamellar structures. Consequently, the association of both G protein coupled receptors and G proteins to the plasma membrane makes them susceptible to their lipid environment so that lipid-protein interactions are crucial to their function. Furthermore, the types and relative abundance of lipids in the membrane not only control numerous functions but also regulate the localization and activity of membrane proteins (Vogler *et al.*, 2004). Thus, molecules that interact with membrane lipids and modify the composition and structure of cell membranes can change the localization and/or activity of membrane proteins. The net result of these effects is the modulation of certain signaling pathways that reverse the pathological state.

Due to this participation in cellular activities, membrane lipids might constitute targets for drugs whose pharmacological effects would be associated with the modulation of the composition, structure and physicochemical properties of membranes, as states the Membrane Lipid Therapy (Escribá, 2006). Indeed, G proteins, PKC and heat shock proteins are among the proteins regulated by membrane-lipid therapy and the therapeutic agents used can inhibit cell proliferation or induce apoptosis and cell differentiation (Escribá, 2008).

In this context, it was demonstrated that the antitumor effect of anthracyclines and the ensuing modifications in cell signaling, involved interactions with the plasma membrane without unspecific interactions with other cell targets (Escribá *et al.*, 1995; Triton & Yee, 1982). Based on these results, 2-hydroxy-9-cis-octadecenoic acid (2OHOA), patented and registered as Minerval®, was designed rationally (Figure 1-8). A first approach showed that 2OHOA binds to membranes and modifies the biophysical properties of the lipid bilayer in model membranes (Barceló *et al.*, 2004; Martínez *et al.*, 2005b).

Further studies demonstrated that 2OHOA induces cell cycle arrest in human lung adenocarcinoma cells by causing, both *in vitro* and *in vivo* PKC translocation to the plasma membrane and by downregulating the expression of certain cyclins, CDKs, E2F-1 and dihydrofolate reductase (DHFR), a protein directly involved in DNA synthesis (Lladó *et al.*, 2009; Martínez *et al.*, 2005a; Martínez *et al.*, 2005b). Interestingly, DHFR downregulation is also involved in the effect of 2OHOA on human leukemia cells, where it induces ligand-independent Fas receptor (FasR) capping and apoptosis (Lladó

*et al.*, 2010). In addition, cell cycle arrest was followed by cancer cell differentiation in human glioma cells, as a result of the translocation of Ras to the cytosol and the subsequent inhibition of the ERK (MAPK) pathway. These effects in turn contribute to the inactivation of the cyclin/CDK/RB/E2F-1/DHFR and PI3K/Akt pathways. Moreover, increased expression of the cyclin/CDK inhibitors $p21^{Cip1}$ and $p27^{Kip1}$ caused further reductions in the phosphorylation of Rb and triggered autophagic cell death (Marcilla-Etxenike *et al.*, 2011; Terés *et al.*, 2011).

Despite the potency of 2OHOA against cancer, it is a safe non-toxic compound with $IC_{50}$ values in non-tumor IMR90 fibroblasts cells 30 to 150-fold greater than in tumor cells (Lladó *et al.*, 2010). This lack of toxicity was confirmed by GLP (Good Laboratory Practice) studies showing that the minimum lethal dose is greater than 3,000 mg/kg and that no undesired side effects were observed at therapeutic doses (Martínez *et al.*, 2005a; Terés *et al.*, 2011).

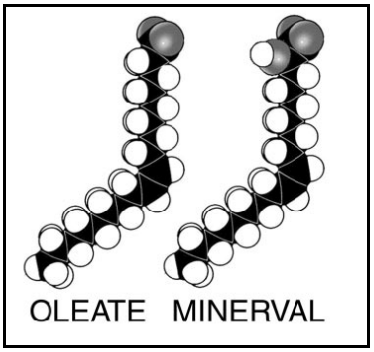


**Figure 1-8. Structure of oleic acid and 2-hydroxyoleic acid (Minerval®).**

Despite all our current knowledge on the importance of the plasma membrane in 2OHOA action against cancer and its impact on membrane associated signaling pathways, the regulatory effects of 2OHOA on the composition of cancer cell membranes are not fully understood. Until now, it has not been determined whether 2OHOA incorporates itself in cell membranes and tissues, as a free fatty acid; or if it is incorporated into other lipids classes, or even if it modulates lipid composition at another level. Therefore, the aim of this study was to investigate the effects of 2OHOA

on the composition and structure of human glioma (and other types of cancer and normal) cells, and related molecular events involved in the biosynthesis and metabolism of membrane lipids.

## 1.6 Aim of the study

Taking into account all the facts exposed above, the **main goal** of the present study was to investigate the molecular lipid alterations induced by 2OHOA and its potential relationship with its mechanism of action. In order to do so, our approach was:

- To analyze the effect of 2OHOA on the phospholipid and sphingolipid composition of human cancer cells;
- To analyze the metabolic fate of 2OHOA and its effect on fatty acid composition of human cancer cells;
- To investigate the molecular bases of the main changes induced by 2OHOA in cancer cell membrane composition;
- To determine the impact of cancer cell membrane alterations induced by 2OHOA on the biophysical properties of model membranes and;
- To analyze the effect of 2OHOA treatments on the lipid composition of mice tissues.

# 2 SM and Sphingomyelin Synthase (SMS) in 2OHOA's effect against cancer

## 2.1 Sphingolipids

Sphingolipids were originally named by J.L.W. Thudichum in 1884 due to their enigmatic nature. Apparently, Thudichum spent much of his spare time thinking about the sphinx of Greek mythology, and so named the compounds that he isolated after the sphinx because of the mystery of their function. Sphingolipids have become the focus of renewed attention because they are an unusually versatile class of membrane lipid that, besides providing mechanical stability, have important roles in molecular signaling and sorting as well as in cell recognition (Tafesse & Holthuis, 2010). As is the case for all membrane lipids, sphingolipids are amphipathic molecules that have both hydrophobic and hydrophilic properties, albeit to varying extents. The hydrophobic region consists of a sphingoid long chain base with a dozen of structural variants, normally sphingosine, dihydrosphingosine (dhSph, also called sphinganine) or phytosphingosine, to which a fatty acid is attached by an amide bond to carbon 2 (Futerman & Riezman, 2005).

The *de novo* biosynthetic pathway for sphingoid bases and complex sphingolipids is depicted in Figure 2-1. The first steps in sphingolipid biosynthesis involve formation of the sphingoid base by the condensation of L-serine and palmitoyl-CoA, a reaction catalyzed by Serine-palmitoyl transferase (SPT), generating 3-ketodihydrosphingosine, which is then reduced to dhSph by 3-ketosphinganine reductase. This is followed by *N*-acylation of dhSph to form dihydroceramide (dhCer), by sphinganine N-acyl transferase, also called ceramide synthase (CerS). At this point, the dhCer undergoes desaturation by dhCer desaturase (the *cis* 4–5 double bond is inserted in mammals) to generate Cer. All these reactions occur on the cytosolic surface of the ER.

A family of six mammalian CerS has been described (Table 2-1), each of them with a high specificity toward the acyl-CoA chain length used for *N*-acylation of the sphingoid base, using either dhSph, derived from the biosynthetic pathway, or Sph, derived from sphingolipid recycling (Levy & Futerman, 2010; Stiban *et al.*, 2010).

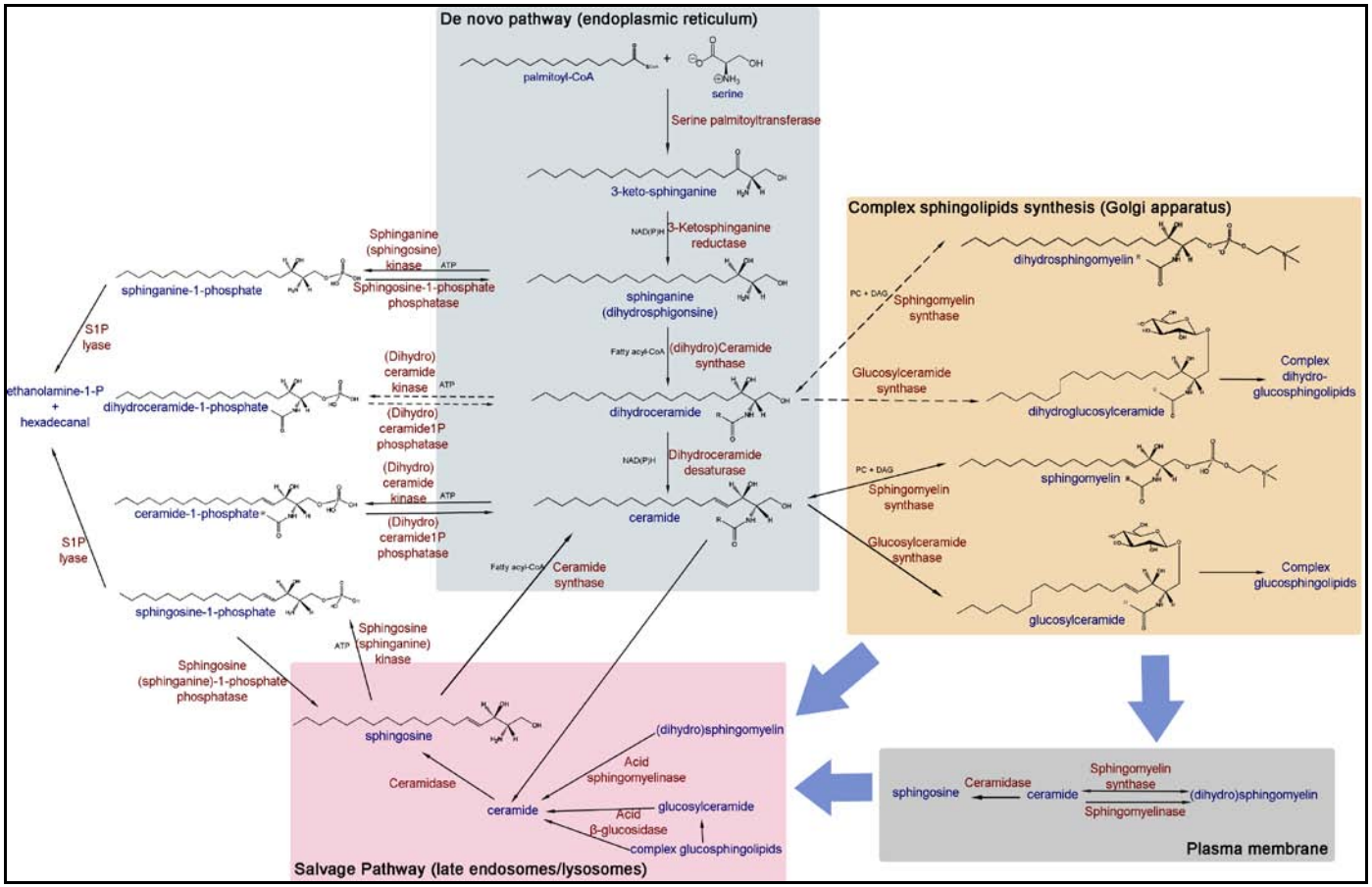


**Figure 2-1. Scheme of sphingolipid metabolism. See footnote on next page[2].**

Thus, CerS are responsible for the fatty acid composition of Cer. Evidence is currently emerging that different CerS, and consequently Cer containing specific fatty acids, play different roles in mediating specific biochemical events and thus specific roles in the cell's physiology (Hannun & Obeid, 2011). In this context, in one of the earliest studies to examine molecular Cer species involved in cell responses, it was observed that triggering of the B-cell receptor in lymphocytes induced a biphasic elevation in Cer (Kroesen *et al.*, 2001). The early phase -minutes/hours- consists primarily of *de novo* synthesis of C16-Cer and preceded the onset of activation-induced cell death. The late phase involves accumulation of C24-Cer after cell death activation. Among the various Cer, only C18-Cer is selectively downregulated in head and neck cancer tissues (Koybasi *et al.*, 2004). In a recent study, CerS5 and CerS6 have been implicated in mediating cytotoxic responses to ionizing radiation whereas CerS2, probably acting in mitochondria, offered partial protection (Mesicek *et al.*, 2010). Similarly, CerS5 and CerS6 are also implicated in the generation of Cer by the salvage pathway, which are necessary for regulating membrane permeability in the programmed cell death execution phase in MCF-7 breast cancer cells in response to UV radiation (Mullen *et al.*, 2011). In addition, the first study to demonstrate biological activities for the dhCer class showed that autophagy was induced in prostate cancer cells treated with C2-dhCer (Zheng *et al.*, 2006). Taken together, these studies on CerSs not only implicate each of these enzymes in the formation of specific Cer and perhaps in specific compartments, but also they clearly suggest Cer-species-specific functions.

**Table 2-1. Comparison of human CerS features.**

| Name | Acyl chain-length Specificity | Tissue mRNA expression profile |
|---|---|---|
| CerS1 | C18 | Brain, skeletal muscle, testis |
| CerS2 | C20-C26 | Widely expressed, acts as housekeeping |
| CerS3 | C22-C26 | Testis, skin |
| CerS4 | C18-C20 | Low expression levels in all tissues |
| CerS5 | C16 | Low expression levels in all tissues |
| CerS6 | C14 and C16 | Low expression levels in all tissues |

(Adapted from Levy & Futerman, 2010; Stiban *et al.*, 2010).

[2] **Figure 2-1.** The scheme shows metabolic pathways for sphingolipids including the *de novo* pathway in the ER, the sphingomyelinase (SMase) pathway at the plasma membrane and the salvage pathway in the lysosomes. The names of the biosynthetic enzymes are in red and the names of the sphingolipid species are in blue. Dash lines represent minor pathways (Adapted from Bartke and Hannun, 2009; Kitatani et al, 2008; Menaldino et al, 2003; and Merrill, 2002).

Subsequently, Cer is delivered to the Golgi apparatus where it is converted to SM or GlcCer, by SM Synthase (SMS) or GlcCer Synthase, respectively. As the hydrophobic nature of Cer prevents its spontaneous transfer through the cytosol, it must travel from the ER to the Golgi apparatus by facilitated mechanisms (Venkataraman & Futerman, 2000). The transport of Cer to the Golgi complex occurs either through vesicular transport, which delivers Cer for the synthesis of GlcCer, or through the action of the transfer protein CERT, which specifically delivers Cer for SM synthesis (Fukasawa *et al.*, 1999). CERT specifically extracts ceramide from the ER and contains a pleckstrin homology (PH) domain to allow its targeting to the Golgi apparatus (Futerman & Hannun, 2004; Hanada *et al.*, 2003; Hannun & Obeid, 2008). GlcCer synthase catalyzes the transfer of glucose from UDP-glucose to Cer. This enzyme resides in the *cis* Golgi and has its active site oriented toward the cytosol (Futerman & Riezman, 2005). After translocation to the Golgi lumen, GlcCer is converted to more complex GSLs. FAPP2 was recently identified as an essential component of the GSLs synthetic machinery, as it mediates non-vesicular transport of GlcCer from its site of synthesis at the early Golgi to distal Golgi compartments, where most of the enzymes involved in complex GSLs assembly are located (D'Angelo *et al.*, 2007).

SM production involves the enzymatic transfer of a phosphocholine head group from PC to the primary hydroxyl of Cer, yielding DAG in the process (Figure 2-2; Huitema *et al.*, 2004). The enzyme catalyzing this reaction, phosphatidylcholine: ceramide choline-phosphotransferase, or SMS, occupies a central position in sphingolipid and glycerolphospholipid metabolism. Since the enzyme is also able to catalyze the reverse reaction, the formation of PC and Cer from SM and DAG (van Helvoort *et al.*, 1994), it has considerable biological potential as a regulator of pro-apoptotic factor Cer and mitogenic factor DAG (Huitema *et al.*, 2004; Tafesse *et al.*, 2006). Two SMS isoforms with close structural similarities and a 57% sequence homology have been described to date, SMS1 and SMS2. SMS1 is mostly associated with the Golgi apparatus, and SMS2 is mainly distributed to the plasma membrane and to a lesser extent to the perinuclear region (Huitema *et al.*, 2004). Both enzymes have the active site facing the exoplasmic leaflet of the membranes and while the Golgi enzyme would be responsible for generating the bulk of cellular SM, the second enzyme may serve a principal role in signal transduction at the plasma membrane. Remarkably, a difference in substrate preference between both isozymes has been described. Thus, SMS1 uses PC as a substrate, whereas SMS2 can use PE and PC (Ternes *et al.*, 2009). SMS1 and SMS2 are uniformly distributed among mammalian tissues, and are encoded by ubiquitously expressed genes (Huitema *et al.*, 2004). In addition to SMS1 and SMS2, there is a third SMS-related (SMSr) protein that synthesizes Cer

phosphoethanolamine, a SM analog. This enzyme is localized to the ER and controls Cer homeostasis in the ER (Vacaru *et al.*, 2009).

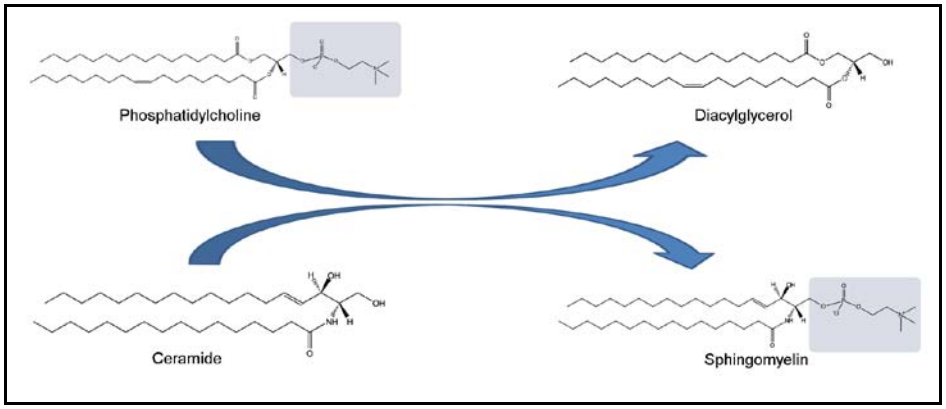


**Figure 2-2. Scheme of the enzymatic reaction regulated by SMS.**
SM synthase catalyzes the transfer of the phosphorylcholine moiety from one molecule of PC to one molecule of Cer. This leads to the formation of one molecule of SM and one of DAG.

Once synthesized, SM and complex GSLs are transported to the plasma membrane via vesicular trafficking. There, SM can be metabolized to Cer either by acidic sphingomyelinase (aSMase), on the outer leaflet of the membrane, or by neutral sphingomyelinase (nSMase), which resides on the inner leaflet of the bilayer (Bartke & Hannun, 2009). Currently, seven distinct SMase have been identified based on their preferred optimal pH for activity, subcellular localization, and dependence on cations (Goñi & Alonso, 2002; López Jiménez, 2008). From the plasma membrane, sphingolipids may be recirculated through the endosomal pathway, also called the salvage or recycling pathway (Kitatani *et al.*, 2008). Thereby, SM and GlcCer are metabolized to Cer in the lysosomal compartment by aSMase and glucosidases, and Cer is then degraded by acid Ceramidase (CDase) to form Sph (Futerman & Hannun, 2004; Futerman & Riezman, 2005). Due to its ionizable positive charge, the salvaged Sph is able to leave the lysosome and shows adequate solubility in the cytosol to move between membranes, including the ER where it would be available for recycling (Kitatani *et al.*, 2008). These bases serve also as substrates for sphingosine kinases that form sphingosine-1-phosphate (S1P; Figure 2-1).

Cer functions both as a key player in cell signaling and as the precursor of more complex sphingolipids (Merrill, 2002). As bioactive molecules, sphingolipid metabolites have been recognized as important modulators of cell survival, cell growth, migration and angiogenesis, and therefore have an important role in cancer progression. Cer and Sph are mostly anti-proliferative or pro-apoptotic, regulating cell responses such as growth arrest, senescence, apoptosis, and recently, it has been shown that they also participate in autophagy; but they can be reversibly converted to ceramide-1-phosphate (C1P) by ceramide kinase and to S1P by sphingosine kinase, respectively (Figure 2-1; Oskouian & Saba, 2010). C1P promotes growth and counteracts apoptotic stimuli, by activating cPLA2 and inhibiting aSMase in a cell-dependent manner (Gómez-Muñoz, 2006; Gómez-Muñoz *et al.*, 2004). S1P also functions as a growth and survival factor, acting as a ligand for a family of G protein-coupled receptors, as well as a second messenger (Cuvillier *et al.*, 1996; Spiegel & Milstien, 2003).

Diverse cellular and environmental stresses such as chemotherapeutics (Bose *et al.*, 1995), heat shock (Jenkins *et al.*, 2002), ischemia-reperfusion (Yu *et al.*, 2007), UV radiation (Rotolo *et al.*, 2005), and ionizing radiation (Truman *et al.*, 2005), stimulate the generation of Cer. This Cer, produced either by the *de novo* biosynthetic (Uchida *et al.*, 2003), the SMase (Haimovitz-Friedman *et al.*, 1994) or recycling metabolic pathways (Jin *et al.*, 2008), triggers activation of signals affecting intrinsic and extrinsic apoptotic pathways and the cell cycle control, while simultaneously inhibiting signaling events that promote cell growth and survival mediated by the AKT pathway (Oskouian & Saba, 2010). In contrast to other sphingolipids, which contain a hydrophilic region such as phosphate in the case of S1P and C1P, phosphorylcholine in SM, and sugar residues in GSLs, Cer has a minimal hydrophilic region comprising two OH groups (Futerman & Hannun, 2004). Because Cer is highly hydrophobic, it tends to reside in the membranes where it is generated unless it is transported, thus Cer can exert their primary actions at the membrane level, acting only on membrane related proteins, either permanently or transiently linked to the membrane. This may occur in two different ways: 1) on proteins lacking specific Cer binding sites, Cer may act by inducing localized changes in the biophysical properties of the membrane bilayer, for example, increase in lipid chain order and the formation of Cer-enriched membrane platforms, which can in turn modify enzyme activities, for example by concentrating and oligomerizing membrane receptors (Cremesti *et al.*, 2001; Gulbins & Kolesnick, 2003; Kolesnick *et al.*, 2000; Stancevic & Kolesnick, 2010). Cer can also induce permeabilization of mitochondria membranes, releasing the cytochrome c, and leading to activation of the caspase-dependent apoptotic pathway (Siskind *et al.*, 2002; Siskind *et al.*, 2006). 2) Cer may bind to specific sites in the target protein, thereby modulating their activity. Among the proteins that contain ceramide-binding sites are proteins that

are transiently bound to membranes, such as Cer-activated protein kinase (Bourbon *et al.*, 2000; Yao *et al.*, 1995); and proteins without known membrane binding capacity, such as Cer-activated protein phosphatase 2 (Dobrowsky & Hannun, 1993).

The fact that sphingolipids are implicated in such important processes for the cell, points towards the need of a fine regulation mechanism. In fact, the balance between the relative levels of the bioactive sphingolipids, Cer, Sph, S1P and C1P, has been proposed to act as a 'rheostat' to determine the fate of the cell with respect to survival (Ruvolo, 2003; Zheng *et al.*, 2006). Recently, Orm proteins were identified as essential components of the sphingolipid rheostat that allows cells to fine-tune sphingolipid synthesis according to their needs. These experiments demonstrated that Orm proteins form a conserved complex with SPT that is regulated by a phosphorylation cycle of Orm proteins relieving their inhibitory activity when sphingolipid production is disrupted (Breslow *et al.*, 2010).

The sphingolipid metabolism rheostat can also be deregulated by defects in enzymes and proteins required for lysosomal catabolism that lead to inherited diseases, the lysosomal storage diseases. Indeed, human diseases caused by alterations in the metabolism of sphingolipids or GSLs are mainly disorders of the degradation of these compounds. Table 2-2 shows some examples of lysosomal storage diseases, which can be classified according to the stored substances, as sphingolipidoses, mucopolysaccharidoses, mucolipidoses, glycoprotein and glycogen storage diseases. However, in most lysosomal diseases more than one compound accumulates and in some disorders for various reasons the stored material can be rather heterogeneous (Ballabio & Gieselmann, 2009; Kolter & Sandhoff, 2006; Kolter & Sandhoff, 2010). As a result of the growing amount of accumulating material, a variety of pathogenic cascades are activated such as altered calcium homeostasis, oxidative stress, inflammation, altered lipid trafficking, autophagy, endoplasmic reticulum stress, and autoimmune responses, and subsequently to cell death (Vitner *et al.*, 2010).

In this chapter, we show that 2OHOA activated SMS isozymes, inducing a rapid increase in the membrane levels of SM. In addition, the use of various 2OHOA analogues showed that this effect was strongly associated with the fatty acid structure. Because the plasma membrane is the first cell structure 2OHOA encounters, SMS activation could be one of the first molecular events associated with its antitumor effects. Significantly, SM accumulation specifically occurred in cancer cells but not in non-cancer cells and SMS pharmacological inhibition reversed the effects of 2OHOA on the cell cycle. These results might explain why 2OHOA acts specifically against cancer cells and therefore, induces no undesired side effects at therapeutic doses. In

addition, the sustained activation of SMS provoked a deregulation of the whole sphingolipid metabolism.

**Table 2-2. Examples of lysosomal storage diseases.**

| Disease | Defective protein | Main storage material | Altered pathways |
|---|---|---|---|
| GM1 gangliosidosis | β-Galactosidase | GM1 | a, b, c, d, e, f. |
| GM2 gangliosidosis (Sandhoff) | β-Hexosaminidase A and B | GM2 | a, c, d, e, f |
| Gaucher | β-Glucosidase or saposin C activator | GlcCer | a, c, e, f |
| Fabry | α-Galactosidase A | Globotriaosyl-Ceramide | a, f |
| Niemann-Pick Type A and B | Sphingomyelinase | SM | c, e, f |
| Niemann-Pick Type C | NPC1 and 2 | Cholesterol and sphingolipids | a, b, c, d, e, f |
| Farber | Ceramidase | Ceramide | e |

a, oxidative stress; b, ER stress and UPR; c, altered calcium homeostasis; d, autophagy; e, inflammation; f, altered lipid trafficking (Adapted from Ballabio & Gieselmann, 2009; Vitner *et al.*, 2010).

## 2.2 Results

### 2.2.1 2OHOA inhibited cell viability and downregulated DHFR levels in human U118 glioma cells.

Previous studies from our group have shown that 2OHOA induces apoptosis in human leukemia cells (Jurkat) or cell cycle arrest in human lung adenocarcinoma (A549) cells. Interestingly, in both cell lines 2OHOA downregulates DHFR, a protein required for DNA synthesis and cell proliferation (Lladó *et al.*, 2009). Here, we evaluated the capacity of 2OHOA to diminish the viability of human U118 glioma cells using the XTT method and evaluating its effect on DHFR levels. In this context, 2OHOA (0-1000 μM; 48 h) reduced the viability of human U118 glioma cells in a concentration dependent manner (Figure 2-3A-B). In addition, 2OHOA (200 μM, 48 h) induced a marked decrease in DHFR protein levels (69.7%) in U118 cells while it had no such effect in non-tumor human lung fibroblast (MRC-5) cells (Figure 2-3C). These results extend previous studies, for the first time showing that 2OHOA has a distinct

effect on DHFR in tumor and non-tumor cells (Lladó *et al.*, 2010; Lladó *et al.*, 2009; Martínez *et al.*, 2005b).

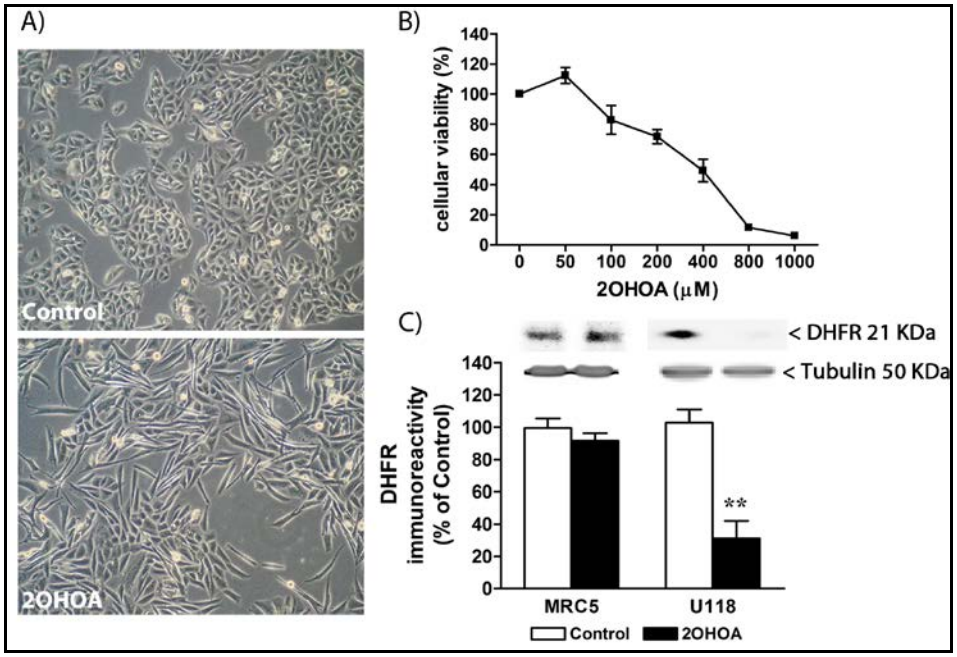


**Figure 2-3. 2OHOA inhibited cell viability and downregulates DHFR levels in U118 cells.**
(A) Representative phase-contrast micrographs (40 × magnification) of U118 cells in the presence (200 μM, 48 h) or absence (control) of 2OHOA. (B) Cell viability assessed by the MTT assay. (C) DHFR protein levels in MRC-5 and U118 cells after treatment with 2OHOA (200 μM, 48 h) were determined by immunoblotting. Results are expressed as percentage of untreated cells and represents mean ± SEM, n=3. The asterisks indicate a significant effect of the treatment as compared with the control (**$P < 0.01$).

### 2.2.2 2OHOA specifically augmented SM mass in cancer cells.

Because lipid composition is usually altered in various human pathologies, including cancer, we investigated the impact of 2OHOA (200 μM, 72 h) on U118 cells phopholipid mass and composition. After extraction, lipids were separated by thin layer chromatography (TLC) and the phospholipid mass was determined by measuring the lipid phosphorus content of the different bands. Treatments with 2OHOA induced a

marked increase in SM mass (4.6-fold) that was accompanied by a decrease in PE and PC mass (57% and 30%, respectively; Table 2-3). In addition, while PS mass decreased 43%, PI mass remained unchanged. Despite these changes, the total phospholipid content was essentially unaffected by 2OHOA.

**Table 2-3. Phospholipid mass changes in control and treated U118 cells.**

| | Control | 2OHOA |
|---|---|---|
| | Mean ± SEM | Mean ± SEM |
| SM | 42 ± 4 | 193 ± 16*** |
| PC | 249 ± 16 | 176 ± 13*** |
| PS | 70 ± 3 | 40 ± 5*** |
| PI | 36 ± 2 | 31 ± 6 |
| PE | 106 ± 8 | 46 ± 3*** |
| Total PL | 463 ± 79 | 486 ± 38 |

U118 cells were treated with 2OHOA (200 µM, 72 h). Total lipid extracts were separated by TLC as described in *Experimental procedures*, Values are expressed as mass (nmol/mg protein) and represent mean ± SEM, $n$ = 4–5. The asterisks indicate a significant effect of the treatment as compared with the control (***$P$ < 0.001).

To determine whether the observed changes in lipid composition were associated with the effects of 2OHOA against cancer, we further analyzed the effect of 2OHOA on the glycerophospholipid composition in human leukemia (Jurkat) cells, non-small cell lung cancer (A549) cells, an additional human glioma cell line (1321N1), and in non-tumor (MRC-5) cells. Exposure to 2OHOA (200 µM, 24 h) significantly increased the SM content of cancer cells (2.4-fold in Jurkat cells, 2.2-fold in 1321N1 cells, 2.7-fold in A549 cells) but not that of MRC-5 cells (Figure 2-4). The complete glycerophospholipid profile of these cell lines is depicted in Figure A 1. Therefore, these data not only revealed the ability of 2OHOA to regulate the glycerophospholipid composition of tumor cells but also, they indicated that this effect was specific to cancer cells. Interestingly, all the cancer cells studied here had approximately half the SM content of the non-tumor MRC-5 cells, suggesting a relevant role for this lipid in tumorigenesis (see below).

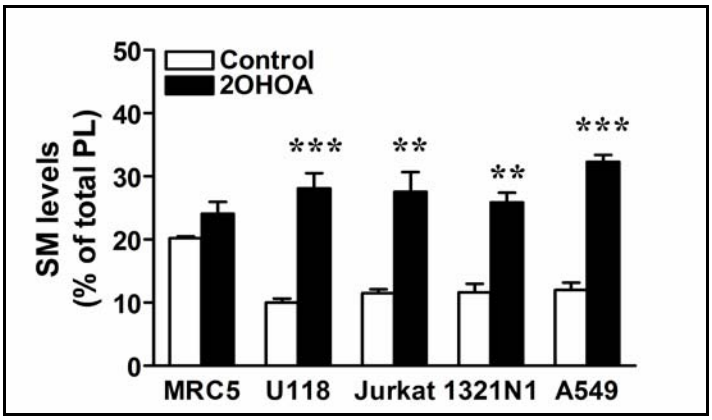


**Figure 2-4. 2OHOA increased SM levels in different cancer cells but not in non-tumor MRC-5 cells.** SM content in different cells lines (MRC-5, U118, Jurkat, 1321N1 and A549 cells) after treatment with 2OHOA (200 μM, 24 h). SM levels were determined by HPTLC analysis and expressed as percentage of total phospholipids. Values represent the mean ± SEM, $n$ = 3–5. The asterisks indicate a significant effect of the treatment as compared with the control (**$P$ < 0.01; ***$P$ < 0.001).

To study the effects of 2OHOA on SM accumulation in depth, we investigated the effect of the duration of treatment and of the 2OHOA concentration on U118 cells. First, cells were treated with 2OHOA (200 μM) for 2, 6, 12, 24, 48 and 72 h (Figure 2-5A) and after 6 h exposure, the increase in SM content was already significant when compared to control cells. Then, we evaluated the effect of different 2OHOA concentrations (25-400 μM, 24 h) on SM content. A concentration as low as 25 μM was sufficient to produce a significant increase in SM content (Figure 2-5C). Thus, the effect of 2OHOA on SM content was concentration-dependent, and it was maximal at 200 μM. Accordingly, the levels of PC and PE decreased with time and concentration in a similar way to the increases in SM content (Figure 2-6).

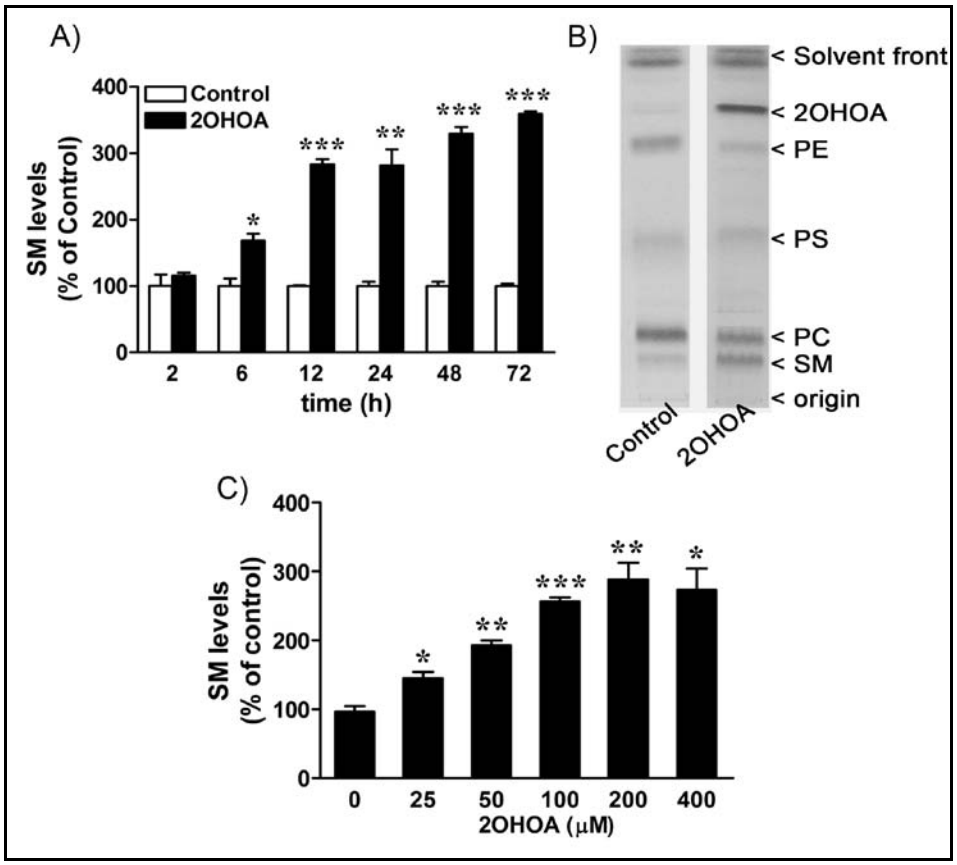


**Figure 2-5. 2OHOA increased SM levels in a time- and concentration-dependent manner in U118 cells.** (A) SM content after treatment with 2OHOA (200 μM) at different times in U118 cells. (B) Representative HPTLC analysis of total lipid extracts from control and treated (200 μM, 72 h) U118 cells. (C) SM content after treatment with 2OHOA (24 h) at different concentrations in U118 cells. In all cases SM levels were determined by HPTLC analysis and expressed as percentage of untreated cells. Values represent the mean ± SEM, $n$ = 3–5. The asterisks indicate a significant effect of the treatment as compared with the control (*$P$ < 0.05; **$P$ < 0.01; ***$P$ < 0.001).

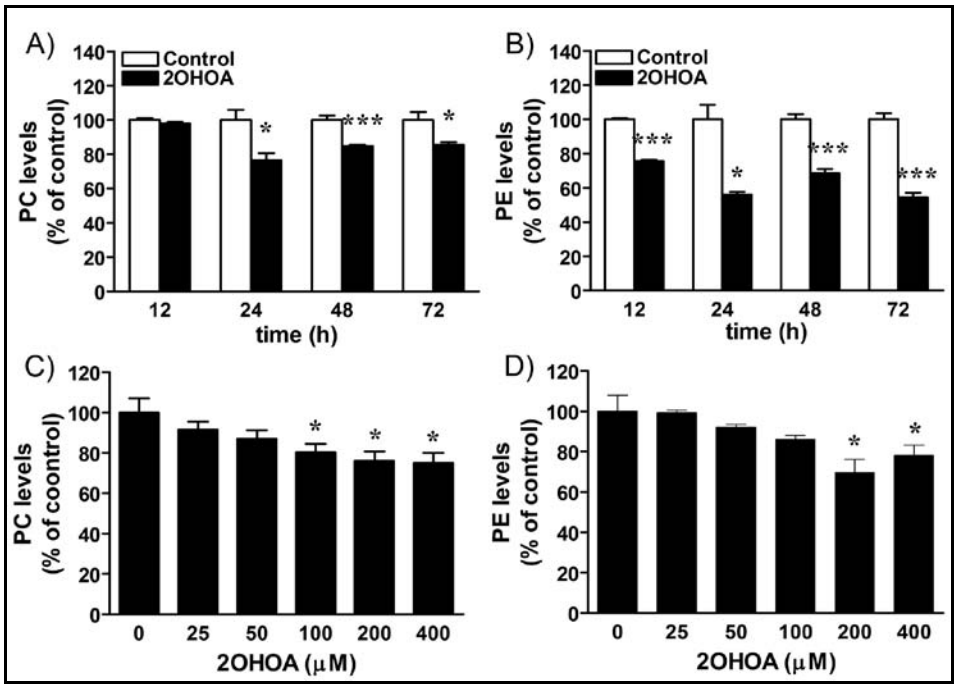


**Figure 2-6. 2OHOA decreased PC and PE in U118 cells.**
(A) PC and (B) PE content after treatment with 2OHOA (200 μM) at different times. (C) PC and (D) PE content after treatment with 2OHOA (24 h) at different concentrations. PC and PE levels were determined by HPTLC analysis and expressed as percentage of untreated cells. Values represent the mean ± SEM, $n$ = 3–5. The asterisks indicate a significant effect of the treatment as compared with the control (*$P$ < 0.05; ***$P$ < 0.001).

We used a number of 2OHOA analogues to investigate the structural bases underlying the regulatory effects of 2OHOA on SM accumulation in U118 glioma cells (200 μM, 24 h). We focused our study on the effect of the fatty acid length, the presence and number of double bonds and the substitution at C-2. The failure of oleic acid (18:1n-9) and 2-methyloleic acid (2Me-18:1n-9) to significantly increase SM levels indicated that the presence of the hydroxyl group at C-2 is crucial for SM accumulation. In addition, we assessed the effects of 2-hydroxystearic acid, (2OH-18:0), 2-hydroxylinoleic acid, (2OH-18:2n-6), 2-hydroxy-α-linolenic acid (2OH-18:3n-3), 2-hydroxy-γ-linolenic acid, (2OH-18:3n-6), 2-hydroxyarachidonic acid (2OH-20:4n-6), 2-hydroxyeicosapentaenoic acid (2OH-20:5n-3) and 2-hydroxydocosahexaenoic acid (2OH-22:6n-3) on U118 cells. SM levels only increased when cells were treated with 18-carbon fatty acids containing a hydroxyl moiety at C-2 and at least one double bound

(Figure 2-7). Therefore, SM accumulation induced by 2OHOA appeared to be a highly structure-related phenomenon.

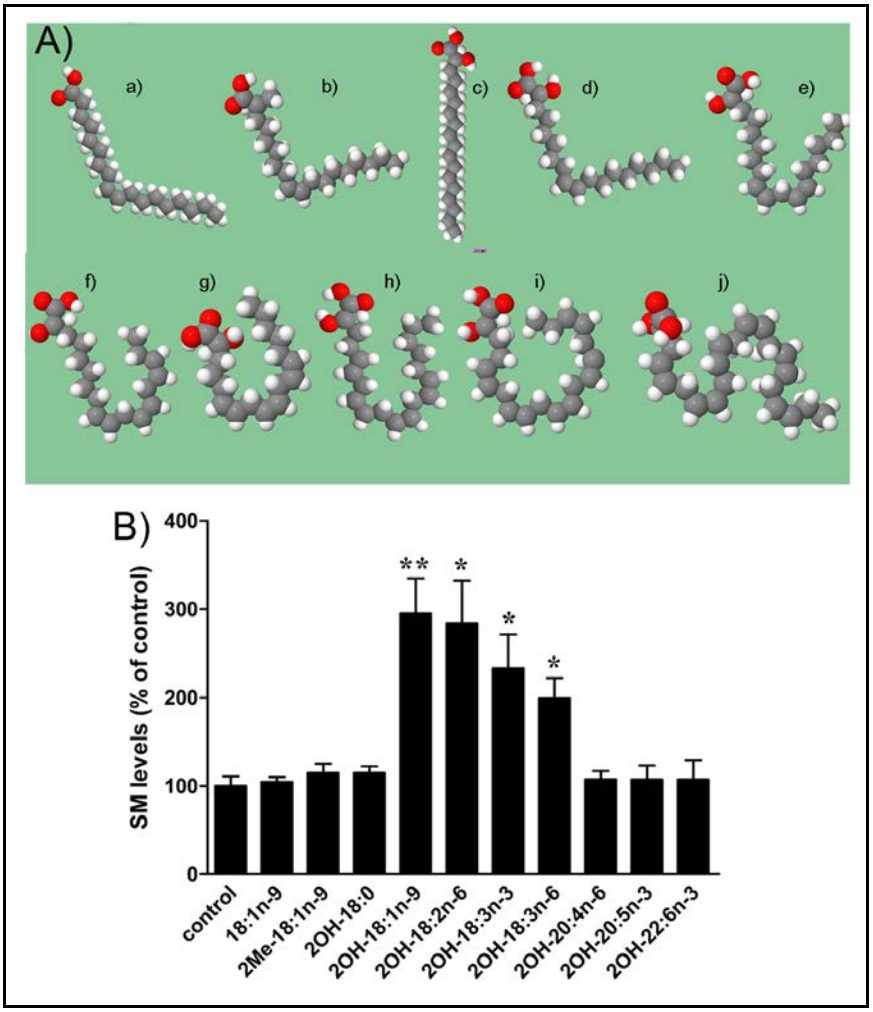


**Figure 2-7. SM accumulation was dependent on the fatty acid structure.**
(A) Structures of the compounds used to study the structural bases underlying the SM accumulation. The fatty acid structure was obtained from the LIPID MAPS database and was drawn as CPK spheres with Jmol, an open-source Java viewer for chemical structures in 3D (http://www.jmol.org/). 18:1n-9, oleic acid (a); 2Me-18:1n-9, 2-methyloleic acid (b); 2OH-18:0, 2-hydroxystearic acid (c); 2OH-18:1n-9, 2-hydroxyoleic acid (d); 2OH-18:2n-6, 2-hydroxylinoleic acid (e); 2OH-18:3n-3, 2-hydroxy-α-linolenic acid (f); 2OH-18:3n-6, 2-hydroxy-γ-linolenic acid (g); 2OH-20:4n-6, 2-hydroxyarachidonic acid (h); 2OH-20:5n-3, 2-hydroxyeicosapentaenoic acid (i); 2OH-22:6n-3, 2- hydroxydocosahexaenoic acid (j). (B) SM content after treatment with different fatty acids (200 μM, 24 h) in U118 cells. SM levels were determined by HPTLC analysis and expressed as percentage of untreated cells. Values represent the mean ± SEM, $n$ = 3–5. The asterisks indicate a significant effect of the treatment as compared with the control (*$P$ < 0.05; **$P$ < 0.01).

Nuclear phospholipids, either in the membrane or associated with chromatin (e.g., SM), regulate DNA synthesis and cell cycle progression (Albi & Magni, 1999; Albi *et al.*, 2003). Thus, an increase in SM, through its direct association with chromatin, would hamper DNA unfolding, which is necessary for its duplication. Given that 2OHOA impairs glioma cell proliferation and induces SM accumulation, we analyzed its influence on nuclear lipid composition. When nuclear lipid extracts were analyzed by high performance TLC (HPTLC), a marked increase in SM (2.0-fold) was also observed in nuclei of treated cells when compared with nuclei of control cells (Figure 2-8), consistent with our results in total cell extracts. Nevertheless, SM accumulation occurred mainly at plasma membrane level as it was demonstrated by incubating cells with lysenin, a SM specific binding protein (Figure 2-9; Yamaji *et al.*, 1998).

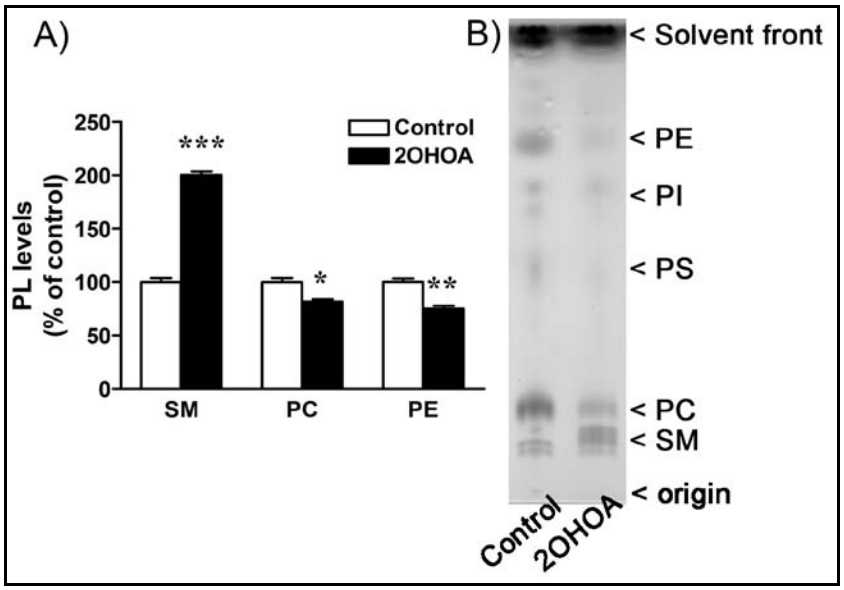


**Figure 2-8. 2OHOA increased nuclear SM levels in U118 human glioma cells.**
(A) Nuclear SM content after treatment with 2OHOA (200 μM, 24 h). (B) Representative HPTLC analysis of nuclear lipid extracts from control and treated (200 μM, 24 h) U118 cells. SM levels were determined by HPTLC analysis and expressed as percentage of untreated cells. Values represent the mean ± SEM, $n = 3–5$. The asterisks indicate a significant effect of the treatment as compared with the control (*$P < 0.05$; **$P < 0.01$; ***$P < 0.001$).

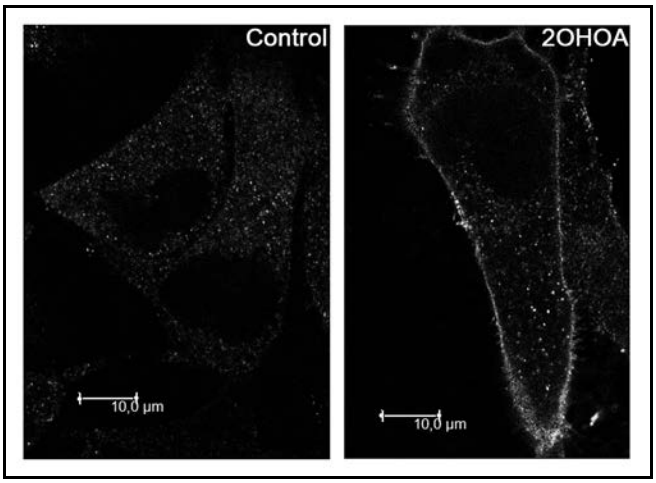


**Figure 2-9. Visualization of 2OHOA-induced plasma membrane SM accumulation by lysenin staining.** Representative confocal microscope micrographs of U118 cells labeled with lysenin in the absence (control) or presence of 2OHOA (200 µM, 72 h). Cells were fixed and incubated with lysenin as is described in the *Experimental procedures* section.

### 2.2.3 2OHOA activated both the SMS1 and SMS2 isozymes.

*De novo* SM synthesis involves numerous reactions that commence with the condensation of palmitic acid and L-serine by SPT and that end with the transfer of the phosphocholine moiety from PC to the primary alcohol of a Cer by SMS isozymes (Figure 2-2; Huitema *et al.*, 2004). Consequently, the accumulation of SM induced by 2OHOA could be due to the regulation of various enzymes (Figure 2-1). However, the rapid increase in SM (Figure 2-5A) in addition to the decrease in PC content observed in our experiments (Table 2-3 and Figure 2-6) suggested that SMS was the molecular target for 2OHOA. Thus, we assessed SMS activity in cultured U118 cells using the fluorescent Cer analogue, NBD-C6-Cer (NBD-Cer, 3 µM, 3 h), in the absence or presence of 2OHOA (200 µM, 24 h). When cell lipids were extracted and separated by HPTLC in order to detect the newly synthesized NBD-C6-SM (NBD-SM), SMS activity in the presence of 2OHOA was 3.6-fold greater than that of control (untreated) cells (Figure 2-10A-B).

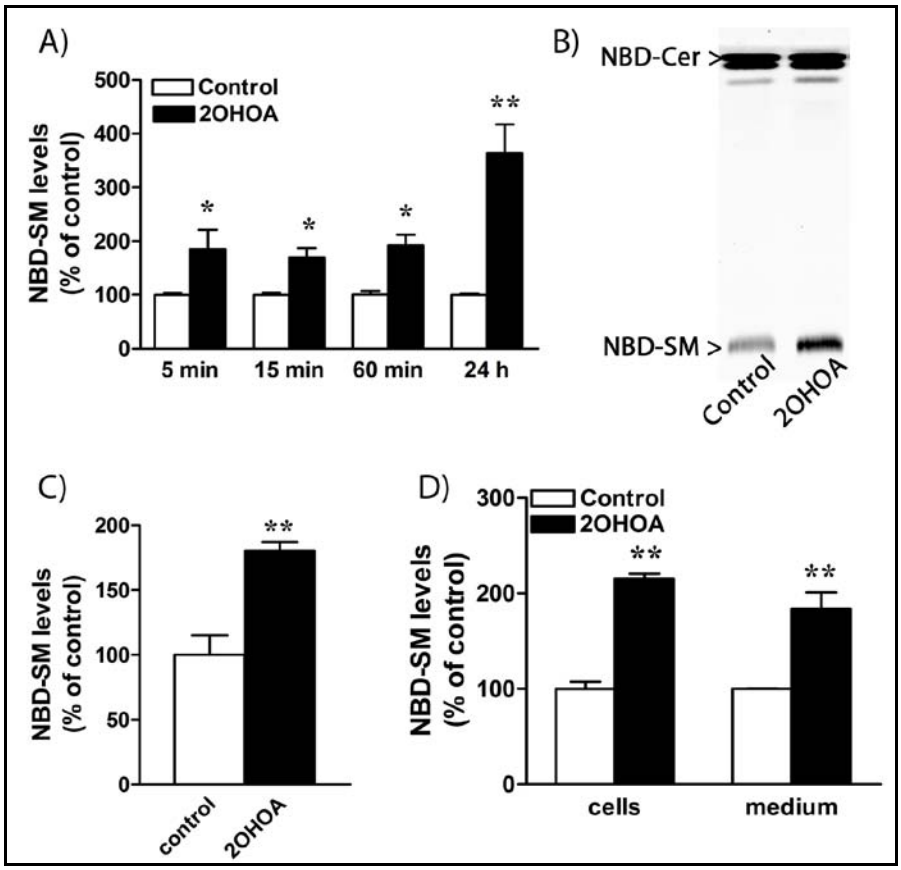


**Figure 2-10. 2OHOA activated SMS isozymes in U118 cells.**
(A) Effect of duration of treatment on NBD-SM levels. Cells were incubated with NBD-Cer (3 μM, 3 h) and treated with 2OHOA (200 μM) for different times. (B) Representative TLC analysis of total lipid extracts from control and treated (200 μM, 72 h) U118 cells incubated with NBD-Cer. (C) *In vitro* SMS activity assay. Cell homogenates (100 μg protein) were incubated with NBD-Cer (0.1 μg/μl) for 2 h at 37ºC in the presence (200 μM) or absence of 2OHOA. (D) SMS1 and SMS2 isoforms activation was determined by a cell surface SMS assay. Control and treated cells (200 μM, 6 h) were incubated for 3 h at 0ºC with NBD-Cer (5 μM) in BSA-containing medium. Then, lipids were extracted from cells and medium. In all cases NBD-SM formation was determined HPTLC. Values represent the mean ± SEM, $n = 3$. The asterisks indicate a significant effect of the treatment as compared with the control (*$P < 0.05$; **$P < 0.01$).

Because 2OHOA can rapidly enter the cells, as it was detected by gas chromatography (Figure 2-11), we investigated the effect of exposing cells incubated with NBC-Cer (3 μM, 3 h) to 2OHOA (200 μM) for 5, 15, and 60 min. SMS activity increased 85.5% after 5 min in the presence of 2OHOA, indicating that it has an extremely rapid effect on SMS. This rapid response and the highly fatty acid structure-dependency described above suggested the possibility that 2OHOA directly interacts

and activates SMS. To address this possibility we carried out an *in vitro* SMS activity experiment. Thus, cells were homogenized with the zwitterionic detergent CHAPS (8% w/v) in order to disrupt cell membranes and the post-nuclear supernatant was incubated with NBD-C6-Cer (0.1 µg/µl) and 2OHOA (200 µM) for 2 h. In these *in vitro* conditions, 2OHOA increased SMS activity 80.5% (Figure 2-10C), indicating altogether a rapid and direct interaction between the drug and the enzyme.

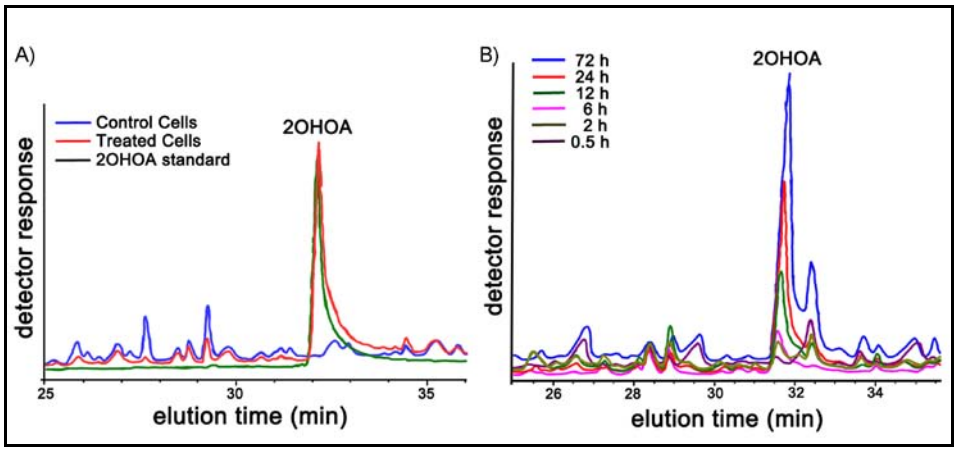


**Figure 2-11. Detection of 2OHOA by gas chromatography in total cell lipid extracts.**
(A) Gas chromatograms showing the detection of 2OHOA in total cell lipids extracts. Green line, 2OHOA standard; blue line, control cells and red lines, 2OHOA treated cells (200 µM, 72 h). (B) Time-dependent accumulation of 2OHOA, each color line corresponds to different times of treatment (200 µM). Total lipids were transmethylated in acidic conditions as described in the *Experimental procedures* section.

Having established that 2OHOA activates SMS, we studied next whether this effect might be selective for one of the SMS isoforms (Huitema *et al.*, 2004). By adapting a procedure published previously (Tafesse *et al.*, 2007), we found that both SMS1 and SMS2 isozymes were activated (2-2-fold and 1.8-fold, respectively), indicating that 2OHOA is a general SMS activator (Figure 2-10C). Moreover, there were no significant differences in SMS1 and SMS2 protein and mRNA expression in control and 2OHOA-treated cells (200 µM, 24 h; Figure 2-12), showing that the increase in SM mass was exclusively due to the specific activation of SMS isozymes by 2OHOA, and not to increased SMS expression.

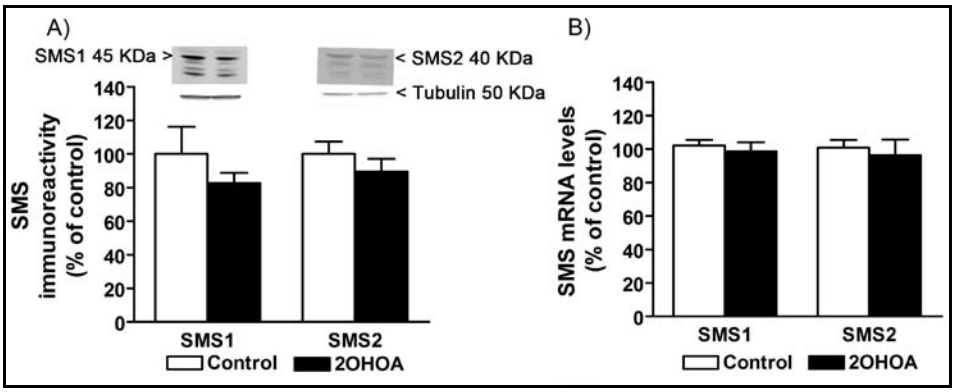


**Figure 2-12. Effect of 2OHOA on SMS protein and mRNA levels in U118 cells.**
(A) Effect of 2OHOA on SMS protein levels as determined by quantitative immunoblotting (a representative immunoblot is also shown). (B) Effect of 2OHOA on SMS mRNA expression. U118 cells were incubated in the presence (200 μM, 24 h) or absence (control) of 2OHOA. Values are expressed as percentage of control and represent the mean ± SEM, $n = 4$.

### 2.2.4 Inhibition of SMS by D609 reversed the effect of 2OHOA on the cell cycle progression in cancer cells

2OHOA induces cell cycle arrest by increasing the proportion of cells in the $G_0/G_1$ phase (Lladó *et al.*, 2010; Martínez *et al.*, 2005a). To demonstrate the importance of SMS activation in the effect of 2OHOA against cancer, we examined how the inhibition of SMS expression, using specific small interference RNA (siRNA), and the inhibition of SMS activity, using the enzyme inhibitor D609, affected the cell cycle progression. Both experiments were initially done on U118 and A549 cells. Since both the silencing and the pharmacological inhibition worked better on A549 cells, the latter were selected to continue with these experiments.

First, A549 cells were treated for 48 h with non-silencing siRNA (Scramble, 75 nM), SMS1 (50 nM), or SMS2 (25 nM) siRNAs or both, in the presence or absence of 2OHOA (200 μM, 24 h). After treatment, SM levels were determined by TLC while the effect of SMS knockdown on the cell cycle was evaluated by flow cytometry. As expected, in the absence of 2OHOA, SMS1 and SMS2 siRNAs, both individually or combined, reduced SM content by 50-60% compared to non-silenced cells (Scramble). However, in all cases, 2OHOA still induced an increase in SM content, probably by activating the remaining SMS (Figure 2-13C). In agreement with the cell surface assay previously shown (Figure 2-10), these results indirectly confirmed that 2OHOA

activated both SMS1 and SM2 enzymes. Because of this remaining SMS activity, 2OHOA was able to induce cell cycle arrest in the double-silenced cells (Figure 2-13A-B), since the distribution of cells in the $G_1$ phase shifted from 54.3 ± 0.1% in the absence to 70.4 ± 1.7% cells in the presence of 2OHOA.

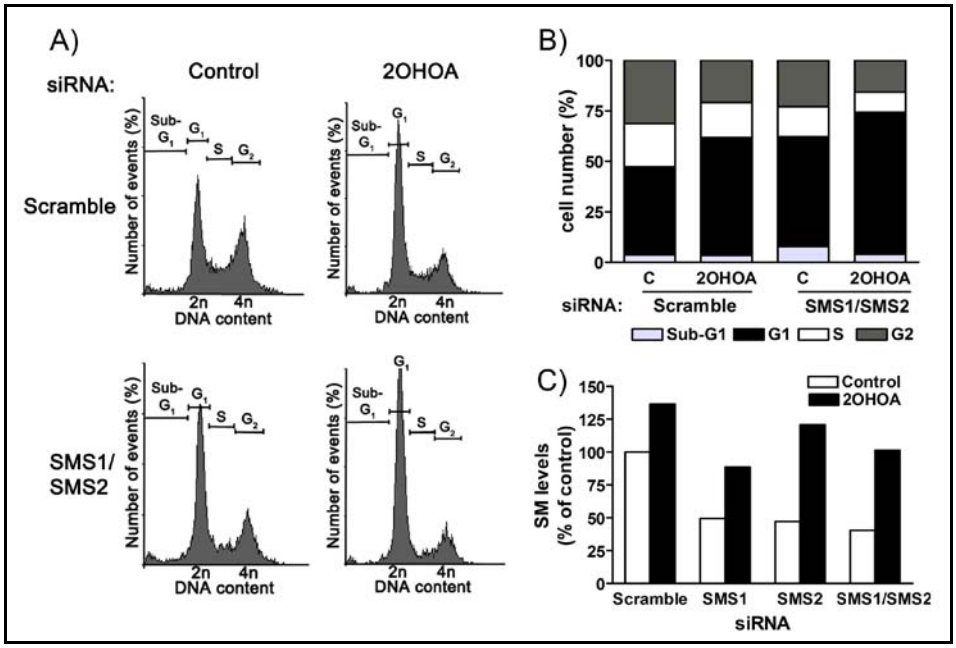


**Figure 2-13. 2OHOA induced SM accumulation and cell cycle arrest despite SMS1 and SMS2 downregulation by siRNA.**
Effect of SMS knockdown by siRNA on cell cycle progression. (A) Representative histograms of control (untreated) and treated cells with 2OHOA (200 µM), exposed to specific SMS1 and SMS2 siRNA and non-specific All Star siRNA sequence (Scramble siRNA). DNA content of A549 cells was measured by flow cytometry after a 48 h exposure to siRNA in the presence or absence of 2OHOA (200 µM, 24 h). (B) Bar graphs show the percentage of A549 cells in Sub-$G_1$, $G_1$, S and $G_2$/M phases with respect to the total cell number; (C) Effect of SMS knockdown on SM content in A549 cells. SM content was determined by TLC as described in the *Experimental Procedures* section. Values represent the mean ± SEM, $n = 2$.

Second, A549 cells were treated with D609 (350 µM, 17 h), the only pharmacological SMS inhibitor known (Gonzalez-Roura *et al.*, 2002; Li *et al.*, 2007; Meng *et al.*, 2004b). When A549 cells were exposed to 2OHOA (200 µM, 16 h) in the presence or absence of D609, the effect of 2OHOA on SM levels was reversed from 172.1 ± 13.1% in the absence to 118.3 ± 20.1% in the presence of D609 compared to

control with D609 (117.8%). These results indicated that 2OHOA was not able to exert its effect on SMS, suggesting that D609 affected the interaction between 2OHOA and SMS. Indeed, the distribution of cells in the $G_1$ phase of the cell cycle shifted from 50.7 ± 5.0% in the absence to 40.5 ± 4.1% cells in the presence of D609 (values compared to control with D609 30.1 ± 1.4%, Figure 2-14), showing that SMS inhibition diminishes 2OHOA capability to induce cell cycle arrest. Therefore, these results indicate that SMS activation, and the subsequent accumulation of SM, plays an important role in the effects of 2OHOA against non-small cell lung adenocarcinoma cells growth.

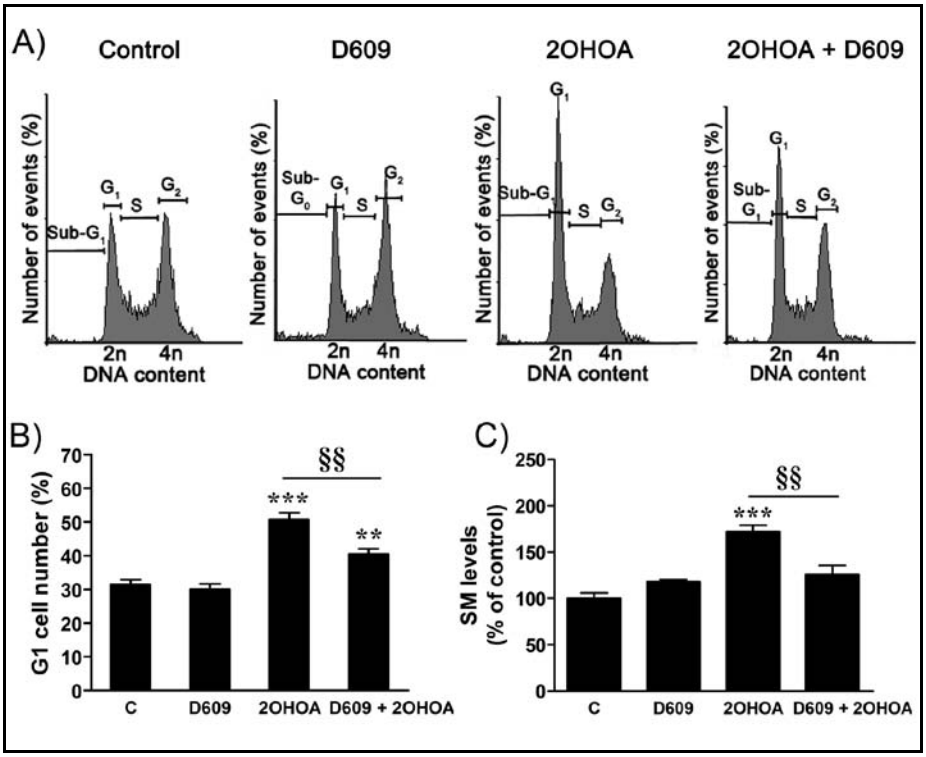


**Figure 2-14. Inhibition of SMS by D609 diminished 2OHOA effect on the cell cycle progression.**
Effect of SMS pharmacological inhibition on cell cycle progression. (A) Representative histograms of control (untreated) and treated cells with 2OHOA (200 μM, 16 h) or with D609+2OHOA (350 μM, 17 h) are shown. DNA content of A549 cells was measured by flow cytometry after a 16 h exposure to 2OHOA (200 μM) in the presence or absence of D609 (350 μM). (B) Bar graphs show the percentage of A549 cells in in Sub-$G_1$, $G_1$, S and $G_2$/M phases with respect to the total cell number. (C) Effect of SMS inhibition on SM content in A549 cells. SM content was determined by TLC as is described in the *Experimental procedures* section. Values represent the mean ± SEM, $n = 3$. The asterisks indicate a significant effect of the treatment as compared with the control (*$P < 0.05$; ***$P < 0.001$). In this case, § indicates a significant effect of the inhibition as compared with the treatment (§§ $P < 0.01$).

### 2.2.5 Impact of SMS activation on the sphingolipid rheostat

In order to sustain the large increase in SM over the time, cells exposed to 2OHOA must have a pool of Cer available. Three pathways individually or coordinately contribute to Cer synthesis, leading to the generation of Cer signaling and subsequent modulation of downstream cell responses: the *de novo* pathway, the salvage pathway, and the SMase pathway (Kitatani *et al.*, 2008).

Considering the rapid effect that 2OHOA had on SMS and the ensuing SM accumulation, we investigated the impact of 2OHOA over a wide range of exposure times (200 μM, 0.5-72 h) on U118 cells sphingolipid mass and composition, by mass spectrometry (MS). Consistently, while at short times (0.5-6 h) there were no significant changes; most of the sphingolipids were significantly affected after a 72 h exposure to 2OHOA. Thus, while Cer and GlcCer increased 1.9-fold and 1.2-fold, respectively; LacCer decreased 28.6% in treated cells when compared to controls (Figure 2-15A-C). Regarding the sphingoid bases, Sph and dhSph increased 1.7-fold and 4.4-fold, respectively, when compared to non-treated cells (Figure 2-15E-F). Sph increase was further confirmed by HPLC (Figure A 3). It should be noted that whereas free dhSph is mostly generated by *de novo* sphingolipid biosynthesis, free Sph appears to derive exclusively from the turnover of complex sphingolipids (Figure 2-1). Thus, all Sph should be considered a product of hydrolysis of complex sphingolipids and then Cer (Kitatani *et al.*, 2008). Therefore, these results indicate the *de novo* synthesis of Cer (through dhSph accumulation) and the salvage pathway (through Sph accumulation) were both activated by 2OHOA. Furthermore, this analysis showed a time-dependent accumulation of dhSM (Figure 2-15D), which derives metabolically from dhSph.

The MS analysis allowed a detailed characterization of the molecular species of every class of lipid analyzed, which showed that indeed, 2OHOA profoundly remodeled the sphingolipid fatty acid profile (Figure 2-16). The most consistent change was the increase in C16- and C22-containing sphingolipid species in all the sphingolipids. Thus, after 72 h of treatment, C16-Cer, C16-GlcCer and C16-dhSM increased 2.2-fold, 3.0-fold and 7.8-fold, respectively. Similarly, C22-Cer, C22-GlcCer and C22-LacCer increased 5.4-fold, 3.2-fold and 2.2-fold, respectively. Interestingly, the most abundant species in U118 control cells, C24 (24:0 and 24:1), were not affected (in Cer) or even reduced (in GlcCer and LacCer).

Even though the accumulation of sphingolipids was consistent after an exposure of 72 h to 2OHOA, some significant changes were already detected after 24 h.

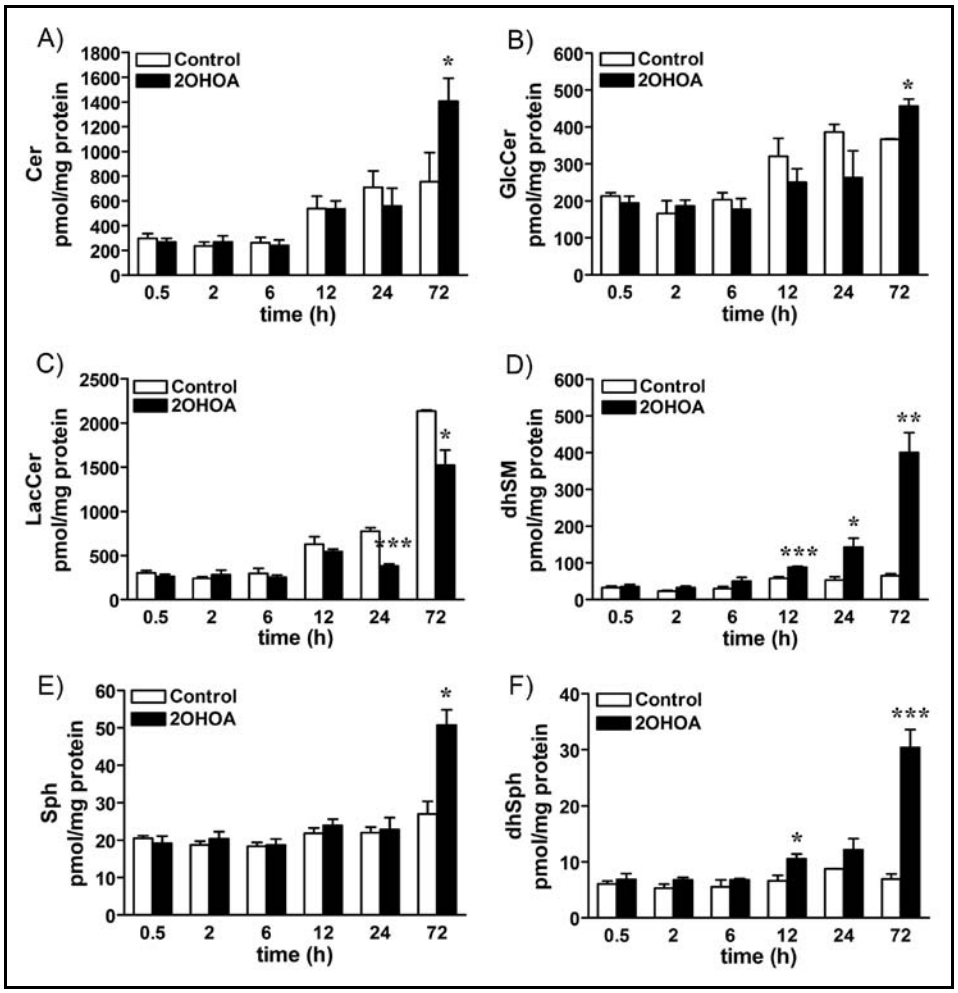


**Figure 2-15. 2OHOA affected U118 cells sphingolipid composition.**
U118 cells were exposed to 2OHOA for different times (200 μM, 0.5-72 h) and then lipids were extracted and analyzed by mass spectrometry. (A) Total Cer mass; (B) Total GlcCer mass; (C) Total LacCer mass; (D) Total dhSM mass; (E) Sph mass; (F) dhSph mass. Values represent the mean ± SEM, $n$ = 3-4. The asterisks indicate a significant effect of the treatment as compared with the control (*$P$ < 0.05; **$P$ < 0.01; ***$P$ < 0.001).

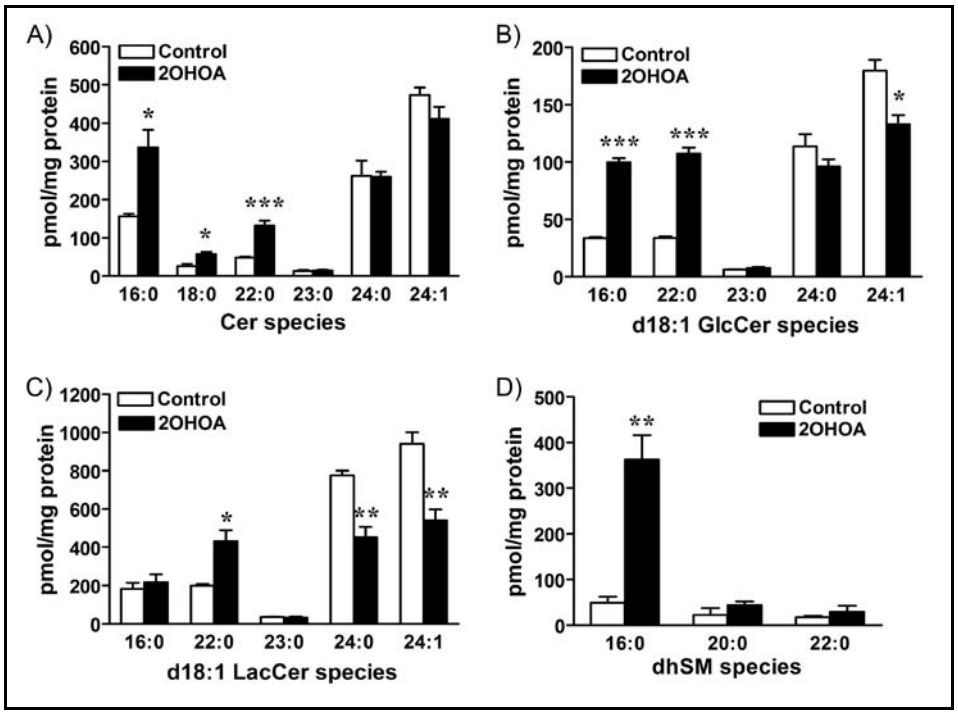


**Figure 2-16. 2OHOA modulated the sphingolipids molecular species profile.**
U118 cells were exposed to 2OHOA (200 μM, 72 h) and then lipids were extracted and analyzed by mass spectrometry. (A) Cer species mass; (B) GlcCer species mass; (C) LacCer species mass; (D) dhSM species mass. Values represent the mean ± SEM, $n = 3$. The asterisks indicate a significant effect of the treatment as compared with the control (*$P < 0.05$; **$P < 0.01$; ***$P < 0.001$).

Each CerS has a high specificity toward the acyl-CoA chain length used for *N*-acylation of the sphingoid base, thus, being responsible for the fatty acid composition of Cer (Table 2-1). For this reason, we determined if there was a correlation between CerS mRNA levels and Cer acyl chain lengths in control cells, comparing the distribution of Cer subspecies with that of the relative levels of CerS mRNA. Indeed, CerS2, which mainly synthesizes C24 species, was the most abundant enzyme, followed by CerS5 and CerS4, which synthesize C16 and C18-C20, respectively (Figure 2-17 A). CerS1 and CerS6 were extremely low and CerS3 was almost undetected, in agreement with its high tissue specificity for testis and skin. Despite the large increase in C16- and C18-containing sphingolipids, no significant differences in CerS5 and CerS1 mRNA expression in 2OHOA-treated cells were observed when compared to control (200 μM, 72 h; Figure 2-17B). The origin for the specific accumulation of C16-containing

sphingolipids is under research and may involve direct or indirect enzyme activation by 2OHOA.

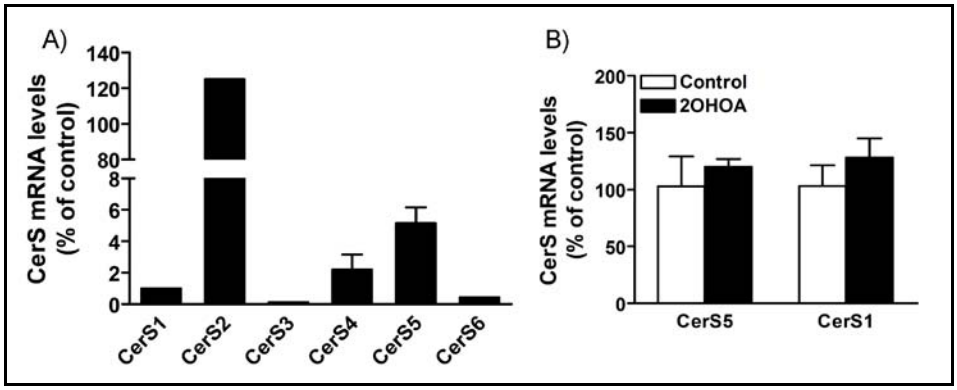


**Figure 2-17. CerS mRNA levels in U118 cells.**
(A) RNA was extracted from U118 control (untreated) cells and the levels of the different CerS were analyzed by qRT-PCR as described in *Experimental Procedures*. (B) Effect of 2OHOA on CerS1 and CerS5 mRNA expression. U118 cells were incubated in the presence (200 μM, 72 h) or absence (control) of 2OHOA. Values are expressed as percentage of control and represent the mean ± SEM, $n = 4$.

Considering the indirect evidence that both the *de novo* synthesis and the salvage pathway were activated by 2OHOA, we further investigated both pathways. Activation of the *de novo* pathway can be detected selectively by pulse labeling with radioactive precursors, such as palmitate or serine, which are the substrates of the SPT, the first enzyme in this pathway (Figure 2-1). Thus, U118 cells exposed to 2OHOA for 6 and 24 h were pulse-labeled with [$H^3$]-palmitic acid for 5 min prior to extraction. Then, lipids were separated by TLC and quantified by liquid scintillation counting. [$H^3$]-Cer content increased upon exposure to 2OHOA for 6 h and 24 h (7.8-fold and 5.6-fold, respectively; Figure 2-18), indicating that indeed the *de novo* synthesis pathway was activated. Interestingly, in agreement with the rapid activation of the SMS shown in the previous sections, [$H^3$]-SM content also increased after 2OHOA treatment (2.7-fold after 6 h and 3.4-fold after 24 h). Finally, the detection of increased levels of [$H^3$]-LacCer and [$H^3$]-cerebrosides provided further evidence for the activation of this pathway.

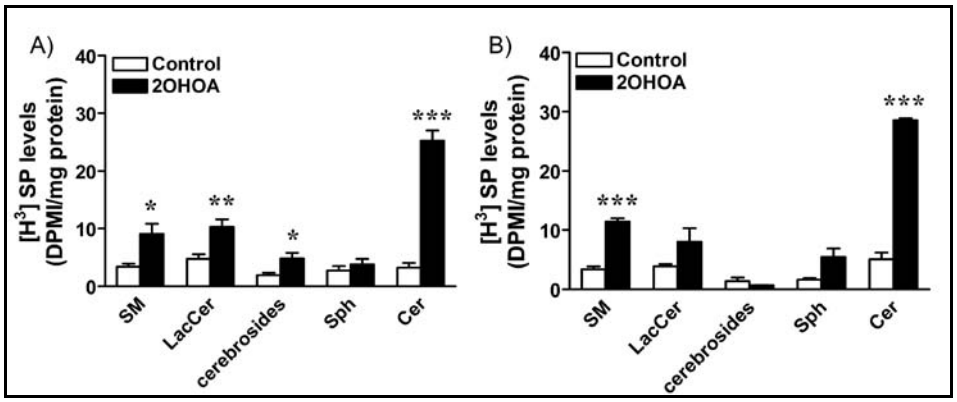


**Figure 2-18. 2OHOA induced *de novo* Cer synthesis.**
U118 cells exposed to 2OHOA for 6 h (A) and 24 h (B) were pulse-labeled with [$H^3$]-palmitic acid for 5 min. Then, the radioactive lipids were separated by TLC and quantified by liquid scintillation counting. Cerebrosides include GlcCer+GalCer; [$H^3$]SP, [$H^3$]sphingolipids. Values represent the mean ± SEM, $n = 3$. The asterisks indicate a significant effect of the treatment as compared with the control (*$P < 0.05$; **$P < 0.01$; ***$P < 0.001$).

We further studied this aspect by incubating control and treated (200 µM, 24 h) cells with different NBD-C6sphingolipid analogs (3 µM, 3 h), NBD-Cer, NBD-SM and NBD-C6-GlcCer (NBD-GlcCer; Figure 2-19). When cell lipids were analyzed in order to detect the synthesized NBD-sphingolipid products, results showed that 2OHOA significantly altered the sphingolipid metabolism. Thus, when cells were incubated with NBD-Cer, in addition to NBD-SM, an increased formation of NBD-GlcCer was observed, 5.9-fold and 11.6-fold, respectively. Similarly, when cells were incubated with NBD-SM, an increased formation of NBD-Cer (2.7-fold) and NBD-GlcCer (3.0-fold) was observed. Finally, after NBD-GlcCer incubation, NBD-Cer and NBD-SM formation increased 4.6-fold and 5.3-fold, respectively (Figure 2-19). Altogether these experiments demonstrated that all enzymes participating in the sphingolipid turnover were activated after 24 h of treatment.

Collectively, the experiment with radioactive- and fluorescent-labeled lipids provided further evidence that both the *de novo* synthesis and the salvage pathway were activated; indicating that 2OHOA completely altered the sphingolipid metabolism.

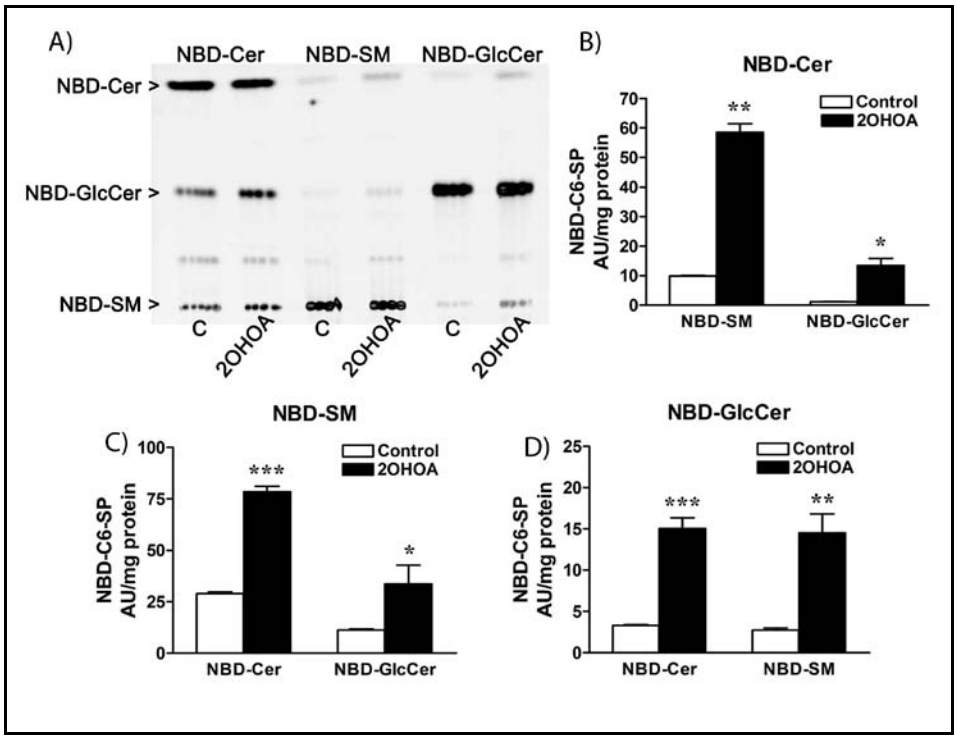


**Figure 2-19. 2OHOA altered the turnover of sphingolipids in U118 cells.**
(A) Representative TLC of lipid extracts from control and 2OHOA treated cells (200 µM, 24 h) incubated with NBD-Cer (B), NBD-SM (C) and NBD-GlcCer (D) (3 µM, 3 h). After incubation, lipids were extracted and analyzed by TLC. NBD-C6-SP, NBD-C6-sphingolipids; AU, arbitrary units of fluorescence intensity. Values represent the mean ± SEM, $n = 3$. The asterisks indicate a significant effect of the treatment as compared with the control (*$P < 0.05$; **$P < 0.01$; ***$P < 0.001$).

The breakdown of sphingolipids for recycling Sph takes place in the acidic compartments of the cells, the late endosomes and lysosomes (Kolter & Sandhoff, 2010; Tettamanti, 2004; Tettamanti *et al.*, 2003). Taking this into account, further evidence supporting the salvage pathway activation was obtained by staining the lysosomes with Lysosensor, a fluorescent probe that labels the acidic organelles. After 72 h of exposure, we observed that 2OHOA (200 µM) induced the accumulation of lysosomes (Figure 2-20), in agreement with the observed increase of sphingolipids at this time. Finally, an ultrastructural study also revealed that exposure to 2OHOA (200 µM, 72 h) induced the appearance of unidentified intracellular membranous, myelin-like bodies (Figure 2-21), probably constituted by the accumulated sphingolipids, such as SM.

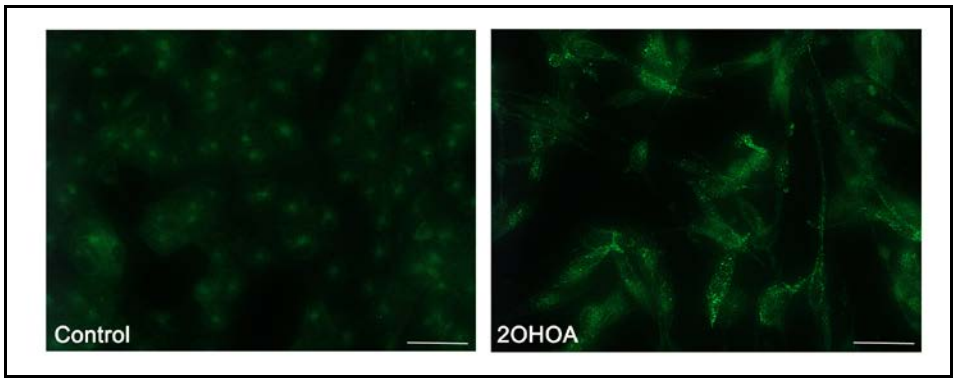


**Figure 2-20. 2OHOA increased the number of lysosomes.**
Representative micrographs of control and 2OHOA treated cells (200 μM, 72 h) labeled with Lysosensor, as explained in the *Experimental procedures* section. Scale bar =100 μM.

## 2.3 SMS activation induced by 2OHOA led to deregulation of the sphingolipid metabolism

Our first aim was to investigate the effects of 2OHOA on the composition of non-cancer and cancer cell membranes and the relationship of the induced changes with its activity against tumors. In the present work, we demonstrated that 2OHOA induces marked changes in the lipid composition of cancer cells that can in part explain its specificity against cancer and its mechanism of action. Thus, treatment of human glioma U118 cells with 2OHOA increased the SM mass 4.6-fold, while it decreased the PC and PE mass by 30 and 57%, respectively (Table 2-3). This effect of 2OHOA on SM accumulation was time- and concentration-dependent (Figure 2-5). Moreover, similar changes were observed in other glioma, leukemia and lung cancer cell lines (Jurkat, 1321N1 and A549 cells), while no such differences in phospholipid composition were observed in non-tumor MRC-5 cell membranes (Figure 2-4). These results reflect 2OHOA's specificity against cancer cells and its failure to produce the toxic effects of other anticancer drugs. The incapacity to produce relevant effects on non-tumor MRC-5 cells could be due to the fact that these cells already contain high levels of SM such that SMS activation cannot further increase the amount of this lipid in membranes. Interestingly, in different normal tissues, higher SM levels have been found when compared to their tumors counterparts (Merchant *et al.*, 1992; Merchant *et al.*, 1993; Merchant *et al.*, 1995; Merchant *et al.*, 1991b). Consequently, these results

highlight the potential role of the plasma membrane in the malignant transformation of many cancer cells and reinforce the importance of regulating its lipid composition.

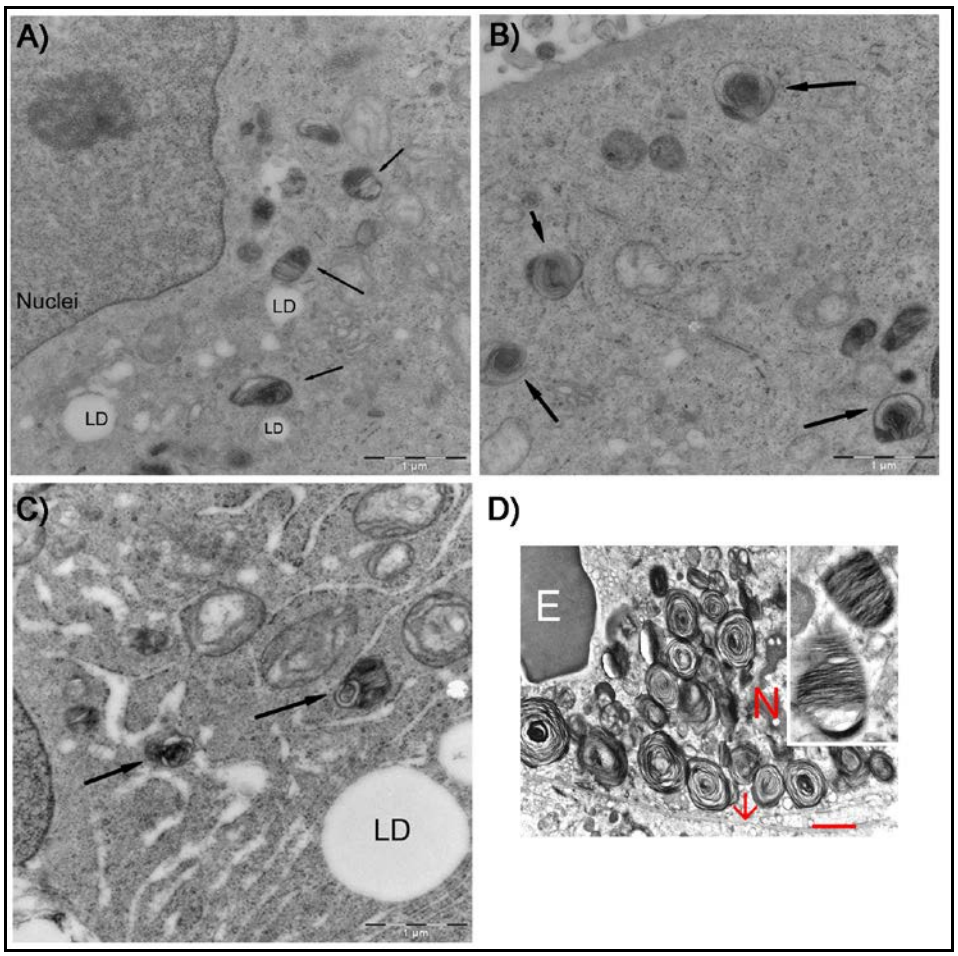


**Figure 2-21. 2OHOA induced the appearance of myelin-like bodies and the formation of lipid droplets.** (A-C) U118 were exposed to 2OHOA for 72 h, fixed and processed for electron microscopy. Magnification: 20500 ×. Arrows, myelin-like bodies; LDs, lipid droplets. (D) Structures formed in *Niemann-Pick disease* caused by SM accumulation due to a deficiency of SMase. Cortical endothelial cell is filled with concentric membranous bodies and parallel palisaded lamellar bodies ("*zebra bodies*" - inset). E, erythrocyte; N, nucleus of endothelium; arrow, basal lamina. Scale bar = 2 μm (Human neocortex; Spacek, 2004).

SM and DAG are products of SMS, while PC and PE are substrates (Huitema *et al.*, 2004; Ternes *et al.*, 2009). Since 2OHOA increased the former and decreased the latter, we investigated the effects of 2OHOA on this enzyme. The effect of 2OHOA on DAG levels and metabolism is described in the next chapter. 2OHOA augments SMS activity (Figure 2-10A) whereas it has no effect on SMS mRNA and protein levels (Figure 2-12). Interestingly, activation of SMS by 2OHOA turned out to be extremely rapid and sustained, probably due to a direct interaction between 2OHOA and SMS. This direct interaction would explain the structural relationship between the fatty acid structure and SMS activation (Figure 2-7). Indeed, we found that the 2-hydroxy moiety, 18 C atoms and at least one double bond in the fatty acid structure, were crucial to induce SM accumulation, 2OHOA being the most efficient molecule. The *in vitro* SMS activation in the presence of 2OHOA offers further evidence of the direct binding of this compound to the enzyme (Figure 2-10C). Considering that the metabolism of PC, PE and PS is interconnected (Figure 1-6), it is worth to mention that the increase in SM content (151 nmoles/mg protein) was similar to the total decrease in PC, PE and PS together (163 nmoles/ mg protein; Table 2-3).

Here, we showed that 2OHOA can activate both SMS1 and SMS2 (Figure 2-10D), probably due to the high structural similarity of these isoforms. Moreover, 2OHOA rapidly enters the cell so that after a few minutes, both SMS1 and SMS2 are exposed equally to the drug (Figure 2-11). SMS2 activation, would be consistent with the rapid activation of the SMS (Figure 2-10A), since the catalytic site of this enzyme is exoplasmic (Huitema *et al.*, 2004). Finally, additional evidence supporting SMS1 and SMS2 activation was obtained by using the specific interference RNA. Upon SMS1 or SMS2 knockdown, 2OHOA was still able to induce SM accumulation indicating that it activated both SMS isozymes. To our knowledge, 2OHOA is the first specific and direct activator of SMS.

Upon SMS activation induced by 2OHOA, newly synthesized SM mainly accumulates in the plasma membrane (Figure 2-9). In addition, 2OHOA may enter the nucleus, which would provoke the increases in SM as a result of the activation of chromatin-associated or perinuclear SMS (Figure 2-8). Interestingly, increased SMS activity has been related to a decrease in DNA synthesis in rat hepatocytes (Albi *et al.*, 2003), which is consistent with previous studies showing that 2OHOA induces cell cycle arrest in cancer cells (Martínez *et al.*, 2005a; Martínez *et al.*, 2005b).

Some studies suggest that SMS inhibition and the ensuing Cer accumulation are associated with the cell cycle arrest (Tafesse *et al.*, 2007) or cell death (Lafont *et al.*, 2010; Separovic *et al.*, 2007) in different tumor cell lines. However, recent studies show that reduced SM synthesis causes resistance to certain apoptosis-inducing drugs, such as

the lipopolysaccharide or the alkyl-lysophospholipid edelfosine (Ding *et al.*, 2008; Van der Luit *et al.*, 2007). On the other hand, increased SM membrane content appears to enhance Fas- and TNF-α induced apoptosis through the efficient clustering of FasR, or by increasing TNF-α receptor exposure at the plasma membrane (Ding *et al.*, 2008; Miyaji *et al.*, 2005). Analogously, decreased SM levels protect THP-1 derived macrophages from LPS-induced apoptosis (Miyaji *et al.*, 2005). For all these reasons, the physiological significance of SMS goes beyond the mere regulation of Cer levels since SM modulates the biophysical properties of lipid rafts and the activity of the proteins they contain (Milhas *et al.*, 2010). In this context, our results demonstrated the important role that SMS activation plays in 2OHOA antitumor mechanism attributing pro-apoptotic properties to the large and sustained SMS activation (Barceló-Coblijn & Martin et al, 2011). All these controversial results clearly point to a complex scenario, where the effect of SMS activation on cell fate would depend on, among other factors, the cell line, the type and intensity of the stimuli (Milhas *et al.*, 2010) and even on the specific pool of regulated Cer (Hannun & Obeid, 2011; Senkal *et al.*, 2010). Our current understanding of the role of SMS activation in the mechanism of 2OHOA against cancer is discussed in *chapter 6*.

In order to sustain the large increase in SM, a pool of Cer must be available to the cells. Cer may be synthesized *de novo* or recycled through the salvage pathway (Kitatani *et al.*, 2008). Our results indicated that indeed both pathways were activated by 2OHOA. In this regard, total Cer and GlcCer mass increased 1.9- and 1.2-fold, respectively, upon 72 h of treatment. In a similar way, Sph and dhSph mass increased 1.7- and 4.4-fold, respectively, providing the first evidence that both pathways were activated because while dhSph is mostly generated by *de novo* sphingolipid biosynthesis, Sph appears to derive exclusively from the turnover of complex sphingolipids (Figure 2-1; Kitatani *et al.*, 2008). It is worth to point out that increased SM was detected before any of the increased sphingolipids, suggesting that the sphingolipid accumulation is driven by the sustained increase in SM. Interestingly, the MS analysis showed that dhSM was particularly affected, increasing its content 4.6-fold after a 72 h exposure to 2OHOA. One possible explanation for this result could be that in order to maintain the large and sustained SMS activation, cells channel dhCer directly into the synthesis of dhSM bypassing the last step in the Cer synthetic pathway. However, the fact that dhCer desaturase could be inhibited by 2OHOA cannot be ruled out. In fact, inhibition of its function with siRNA along with the subsequent accumulation of endogenous dhCer, and possibly more complex dh-sphingolipids, leads to the cell cycle arrest in human neuroblastoma (SMS-KCNR) cells (Kraveka *et al.*, 2007).

Further evidence about the deregulation of the sphingolipid metabolism was the accumulation of C16- and C22-containing sphingolipids (Cer, dhSM and GlcCer; Figure 2-16). Interestingly, C16-Cer is associated with the induction of apoptosis in Ramos B-cells (Kroesen *et al.*, 2001). When the amount of the fatty acyl-species was correlated with the mRNA levels of the CerS in control cells, CerS2, which synthesizes C20‑C26‑Cer (Table 2-1), was the most abundant CerS (Figure 2-17A). This would explain why C24-containing sphingolipids were the most abundant species in U118 cells. Furthermore, previous works established CerS2 as the most ubiquitously expressed of all the CerS isoforms with the broadest tissue distribution (Laviad *et al.*, 2008). Particularly, CerS2 was found to have the highest expression of all CerS isoforms in oligodendrocytes and Schwann cells (Becker *et al.*, 2008). Despite all these results, a differential effect induced by 2OHOA over the expression of CerS that synthesize the C16 and C18 species was not observed (Figure 2-17B). Interestingly, these fatty acid species, 16:0 and 18:0, also increased in glycerophopsholipids, as it will be shown in the next chapter.

Upon activation of SMS, with the ensuing SM accumulation induced by 2OHOA, the turnover of sphingolipids would be stimulated, as it was demonstrated by different means: i) by the metabolic labeling of cells with NBD-sphingolipids, and the consequent formation of different NBD-products induced by 2OHOA (Figure 2-19); ii) by a pulse-labeling experiment that showed the activation of the *de novo* Cer synthesis after 6 and 24 h of exposure to 2OHOA (Figure 2-18); and iii) by staining the lysosomes, where the recycling of sphingolipids occurs, showing that these acidic vesicles accumulated after a 72 h exposure to 2OHOA (Figure 2-20). In addition, the formation of unidentified myelin-like bodies was observed, probably related to the sphingolipid accumulation due to the sustained activation of SMS (Figure 2-21). These bodies reminded of the membranous bodies formed in *Niemann-Pick disease* caused by deficiency of SMase (Figure 2-21D). Finally, this accumulation of sphingolipids may account for the increased number of lysosomes observed after treatment. This result is in agreement with the 2OHOA-induced autophagy demonstrated in glioma cells (Marcilla-Etxenike *et al.*, 2011; Terés *et al.*, 2011), which is a hallmark of several sphingolipid metabolism disorders (Table 2-2). Autophagy is a vacuolar, self-digesting mechanism responsible for removal of long lived proteins and damaged organelles. Autophagosomes fuse with lysosomes for degradation of their cargo by lysosomal hydrolases. Aside from its role in survival during stress conditions, autophagy can also serve as a programmed cell death mechanism, with impairment of autophagosome-lysosome fusion or overinduction of autophagy leading to autophagosome accumulation and cell death (Vitner *et al.*, 2010).

In conclusion, this chapter provides new insights into the antitumor molecular mechanism of action for 2OHOA and demonstrates its specificity against tumor cells via SMS activation that results in a robust increase in SM mass. To sustain this activation, the whole sphingolipid metabolism is altered, both the *de novo* synthesis and the salvage pathway, inducing a kind of sphingolipidoses that would contribute to the effect of 2OHOA against cancer.

# 3 SCD1 inhibition was involved in the 2OHOA's antitumor mechanism

## 3.1 Stearoyl-CoA Desaturases

The processes of cell growth, proliferation and survival require the formation of new membranes, which implies the production of new lipids with an appropriate molecular composition. A basic step in the synthesis of lipids is the formation of saturated (SFA) and monounsaturated (MUFA) fatty acids, the major fatty acid species in mammalian cells (Igal, 2010). *De novo* fatty acid synthesis involves three key enzymes, ATP citrate lyase (ACL), acetyl-CoA carboxylase (ACC) and fatty-acid synthase (FAS). ACL catalyzes the conversion of citrate to acetyl-CoA, thus connecting glycolysis to lipogenesis; ACC carboxylates acetyl-CoA to form malonyl-CoA, which is further converted by FAS to long-chain fatty acids (Mashima *et al.*, 2009). As building blocks of glycerolipids, glycerophospholipids, and cholesteryl esters, these fatty acids are fundamental constituents of membrane structures, vital pools of metabolic energy and important mediators/signals that regulate many cellular activities (Igal, 2010).

Stearoyl-CoA desaturase (SCD) is the rate-limiting enzyme in the biosynthesis of MUFAs. Also known as fatty acyl-CoA delta-9 desaturase, this ER-resident enzyme catalyzes the introduction of the first double bond in the *cis* delta-9 position (between carbons 9 and 10) of several saturated fatty acyl-CoAs, mainly palmitoyl-CoA and stearoyl-CoA, to yield palmitoleoyl- and oleoyl-CoA, respectively (Figure 3-1). This reaction catalyzed by SCD, also requires NADPH, cytochrome $b_5$ reductase, and cytochrome $b_5$ in the presence of molecular oxygen (Enoch *et al.*, 1976). Based on recent isotope kinetic data of the plant desaturase, the current hypothesis for the desaturation reaction is that the enzyme removes hydrogen atoms starting with the one at the C-9 position, followed by the removal of the second hydrogen atom from the C-10 position. Fatty acid desaturation is an oxidation reaction and requires molecular oxygen and two electrons. However, oxygen itself is not incorporated into the fatty acid chain but is released in the form of water (Ntambi & Miyazaki, 2004). The human SCD1 gene is ubiquitously expressed, with highest levels in brain, liver, heart and lung (Zhang *et al.*, 1999).

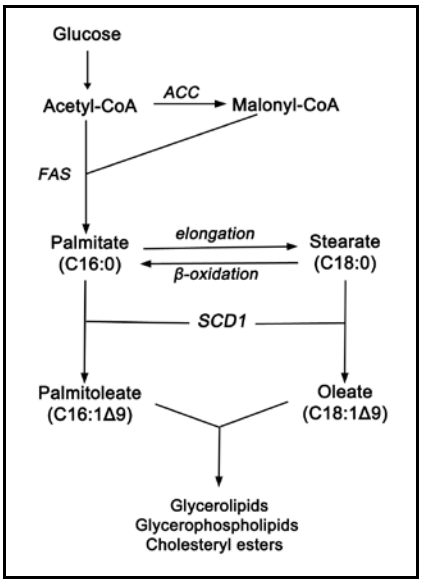


**Figure 3-1. A simplified pathway for the synthesis of monounsaturated fatty acids and their incorporation into glycerolipids and glyerophospholipids.**
Stearate can be reconverted to palmitate by β-oxidation. SCD1, stearoyl-CoA desaturase 1; FAS, fatty acid synthase; ACC, acetyl-CoA carboxylase (Kim & Ntambi, 1999).

Oleic acid is the preferred substrate for acyl-CoA:cholesterol acyltransferase and DGAT, the enzymes responsible for cholesteryl ester and TAG synthesis, respectively. Thus, the regulation of SCD is very diverse and could affect a variety of key physiological variables, including insulin sensitivity, metabolic rate, adiposity, atherosclerosis and cancer. In order to support continuous cell proliferation, cancer cells coordinate the activation of lipid biosynthesis and the signaling networks that stimulate this process. In fact, elevated expression and activity of SCD1 have been detected in several types of cancers and cancer cells. Moreover, the essential role of SCD1 in cancer cell mitogenesis was unambiguously demonstrated by recent work in which suppression of SCD1 by genetic and pharmacological means led to a slower rate of cell proliferation and decreased survival in different types of cancer cells (Fritz *et al.*, 2010; Li *et al.*, 1994; Scaglia *et al.*, 2005; Scaglia *et al.*, 2009).

Excessive content of long chain fatty acids, especially SFA, triggers programmed cell death in a process known as lipid mediated toxicity or lipoapoptosis (Schaffer, 2003). The protective action of SCD1 against SFA-mediated apoptosis was observed in non-transformed mammalian cells in which overexpression of SCD1 blocked the induction of programmed cell death by palmitic acid (Listenberger *et al.*,

2003). TAG accumulation in response to acute lipid overload represents an initial cellular defense against lipotoxicity. Induction of lipid droplets (LDs) with exogenous fatty acids can be regarded as a simple channeling of excess material into neutral lipids that are stored in LDs (Listenberger *et al.*, 2003). However, the fact that different fatty acids induce different types of LDs suggests a more complex scenario.

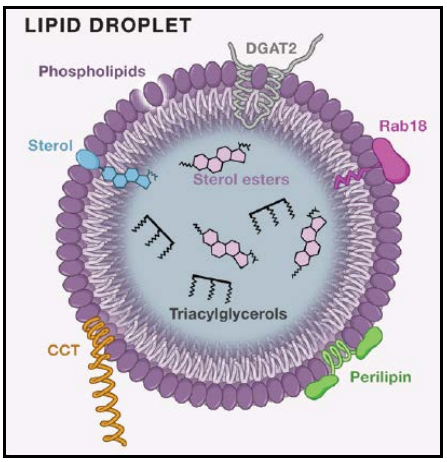


**Figure 3-2. Anatomy of a lipid droplet.**
The structural features of a lipid droplet. The surface is formed by a monolayer of polar lipids (e.g., phospholipids and sterols) and a variety of proteins, whereas the core contains nonpolar lipids (e.g., sterol esters and triacylglycerols). The proteins include DGAT2, Rab18, perilipin, and CTP:phosphocholine cytidylyltransferase (CCT); the rate-limiting enzyme in phosphatidylcholine synthesis. Several hypothetical mechanisms for how proteins interact with the lipid droplet are shown, including amphipathic α helices, embedding of hydrophobic regions directly in the droplet, and lipid anchors (Adapted from Krahmer *et al.*, 2009).

As it was mentioned in the *Introduction* section, LDs are key cellular organelles involved in lipid storage and mobilization (Figure 3-2). Most cells in culture form LDs whenever there is lipid availability from the medium. When maintained in serum-deprived conditions, cells are practically devoid of LDs, which appear upon addition of complete serum, containing lipoproteins and increase in number and size when free fatty acids are supplemented at nontoxic concentrations (Gubern *et al.*, 2008). A number of proteins associated with LDs have been characterized over the years. Among them, the best known is the perilipin-adipophilin-TIP47 family of proteins, termed collectively PAT (Brasaemle, 2007; Kimmel *et al.*, 2010; Miura *et al.*, 2002). Adipophilin, also

called adipose differentiation-related protein (ADRP), is a constitutive PAT protein, which is degraded in the absence of LDs, and therefore expression levels of this protein reflect the mass of stored neutral lipids (Brasaemle *et al.*, 1997). Unlike perilipin, which is specific for adipocytes and steroidogenic cells, ADRP is expressed ubiquitously (Brasaemle *et al.*, 2000).

In addition, exogenously added fatty acids, indeed, can be incorporated into glycerolipids and glycerophospholipids either by acylation of glycerophosphate to phosphatidic acid, through *de novo* synthesis via the Kennedy pathway (Kennedy, 1961), or by remodeling of *de novo* synthesized glycerophospholipids via deacylation-reacylation (Lands, 1958) or the MAG-pathway in the case of glycerolipids (Figure 1-6). Most mammalian cells continually synthesize, remodel, transport and degrade glycerophospholipids and glycerolipids. Whether a fatty acid is incorporated into glycerolipids and glycerophospholipids by the *de novo* or remodeling pathways can depend on its structure (Schmid *et al.*, 1995). In particular, hydroxyl fatty acids have been exclusively found in sphingolipids (Hama, 2010). Thus, part of the metabolic fate of 2OHOA is revealed in this chapter.

In this chapter we show that 2OHOA remodeled the fatty acid profile of tumor cells, being the most notorious changes the decrease in oleic acid, the increase in stearic acid and the incorporation of 2OHOA into different lipid classes. In addition, the decrease in oleic acid and the increase in stearic acid were linked to the SCD1 inhibition induced by 2OHOA. Finally, the analysis of the neutral lipid fraction showed an increase in the formation of DAG, free fatty acids (FFA) and TAG levels, with the ensuing formation of LDs.

## 3.2 Results

### 3.2.1 2OHOA induced reduction of oleic acid content in cancer cells

In the previous chapter we have demonstrated how 2OHOA affects glycerophospholipid composition of tumor cells. In this chapter, we analyzed the effects of 2OHOA on tumor cell fatty acid composition. Thus, human glioma (U118) cells were first treated with 2OHOA at 200 µM for 72 h. After extraction, lipids were separated by TLC, and PE and PC fractions were collected, transesterified in basic conditions and analyzed by gas chromatography.

**Table 3-1. Effect of 2OHOA on fatty acid composition of individual phospholipid of human glioma U118 cells.**

| | PC | | PE | |
|---|---|---|---|---|
| **FAME** | Control | 2OHOA | Control | 2OHOA |
| | Mean ± SD | Mean ± SD | Mean ± SD | Mean ± SD |
| 16:0 | 32.3 ± 1.4 | 44.4 ± 2.8*** | 4.4 ± 0.9 | 1.7 ± 0.3*** |
| 18:0 | 7.2 ± 0.2 | 11.2 ± 0.5*** | 15.5 ± 0.5 | 30.2 ± 0.6*** |
| 18:1n-9 | 42.1 ± 0.6 | 23.7 ± 1.1*** | 33.2 ± 1.9 | 14.8 ± 0.4*** |
| 18:1n-7 | 13.0 ± 0.5 | 9.8 ± 0.6*** | 9.5 ± 0.4 | 6.4 ± 0.2*** |
| 20:3n-6 | 0.5 ± 0.2 | 1.1 ± 0.1*** | 2.7 ± 0.6 | 2.7 ± 0.2 |
| 22:0 | 0.8 ± 0.1 | 1.7 ± 0.3*** | 3.5 ± 0.9 | 7.0 ± 1.0*** |
| 20:4n-6 | 0.8 ± 0.2 | 1.6 ± 0.2*** | 12.6 ± 0.3 | 9.7 ± 0.3*** |
| 20:5n-3 | 0.3 ± 0.2 | 0.4 ± 0.1 | 3.0 ± 0.4 | 1.4 ± 0.2*** |
| 22:5n-3 | 0.5 ± 0.2 | 1.9 ± 0.4** | 8.5 ± 0.7 | 12.9 ± 0.3*** |
| 22:6n-3 | 0.6 ± 0.2 | 2.2 ± 1.0* | 7.2 ± 1.9 | 13.1 ± 0.5*** |
| SFA | 40.3 ± 1.2 | 57.3 ± 2.1*** | 23.4 ± 0.7 | 38.9 ± 1.1*** |
| MUFA | 56.2 ± 0.6 | 34.1 ± 1.8*** | 42.7 ± 2.3 | 21.4 ± 0.6*** |
| PUFA | 3.5 ± 0.9 | 8.6 ± 1.4*** | 33.9 ± 2.7 | 39.7 ± 1.4*** |
| n-3 | 1.4 ± 0.5 | 4.4 ± 1.2*** | 18.6 ± 2.5 | 27.4 ± 1.0** |
| n-6 | 2.1 ± 0.4 | 4.2 ± 0.4*** | 15.3 ± 0.8 | 12.3 ± 0.4*** |
| n-3/n-6 | 0.6 ± 0.16 | 1.1 ± 0.28* | 1.2 ± 0.17 | 2.2 ± 0.02*** |

U118 cells were treated with 2OHOA (200 µM, 72 h). After treatment, lipids were extracted and analyzed by TLC. The PC and PE fractions were converted to FAME and analyzed by gas chromatography. Values are expressed as mole% and represent mean ± SD, n = 4-5. The asterisks indicate a significant effect of the treatment as compared with the control (*$P < 0.05$; **$P < 0.001$; ***$P < 0.001$).

We observed a profound effect on the PE and PC fatty acid composition upon 2OHOA treatment (Table 3-1). Particularly, oleic acid (18:1n-9), which is structurally related to 2OHOA, was reduced 44% in PC and 55% in PE. This decrease accounted for most of the reduction in MUFA, 39% and 49%, in PC and PE, respectively, together with *cis*-vaccenic acid (18:1n-7), reduced by 24% in PC and 32% in PE. In contrast, SFA increased 42% in PC and 66% in PE. PC SFA included primarily palmitic acid (16:0) and stearic acid (18:0), which increased 37% and 55%, respectively; while PE SFA increase was mainly due to 18:0 (94%). In addition, total PUFA levels increased 2.5-fold in PC, but only 17% in PE. Within total PUFA, n-3 increased 3.1-fold while n-6 increased 2.0-fold in PC. These changes affected, in both phospholipids, the n-3 to n-6

ratio, which increased 66% in PC and 82% in PE. In a similar way, oleic acid level decreased and palmitic acid increased in total lipid extracts (Table A 3).

To further study the fatty acid profile remodeling induced by 2OHOA, U118 cells were treated for 12, 24, 48 and 72 h at 200 µM and the PC and PE the fatty acid composition was analyzed (Figure 3-3). In this context, oleic acid was significantly reduced in treated cells at all times in both glycerophospholipids, with a concomitant increase in stearic acid. Interestingly, oleic acid levels in control (untreated) cells increased with time (ca. 31% at 12 h to 42% at 72 h in PC and ca. 20% at 12 h to 33% at 72 h in PE) while remained constant in treated cells (ca. 24% in PC and ca. 14% in PE). On the contrary, stearic acid content followed the opposite pattern. While it did not change in control cells (ca. 7% in PC and ca. 14% in PE), it increased in treated cells (ca. 9% at 12 h to 11% at 72 h in PC and ca. 19% at 12 h to 30% at 72 h in PE).

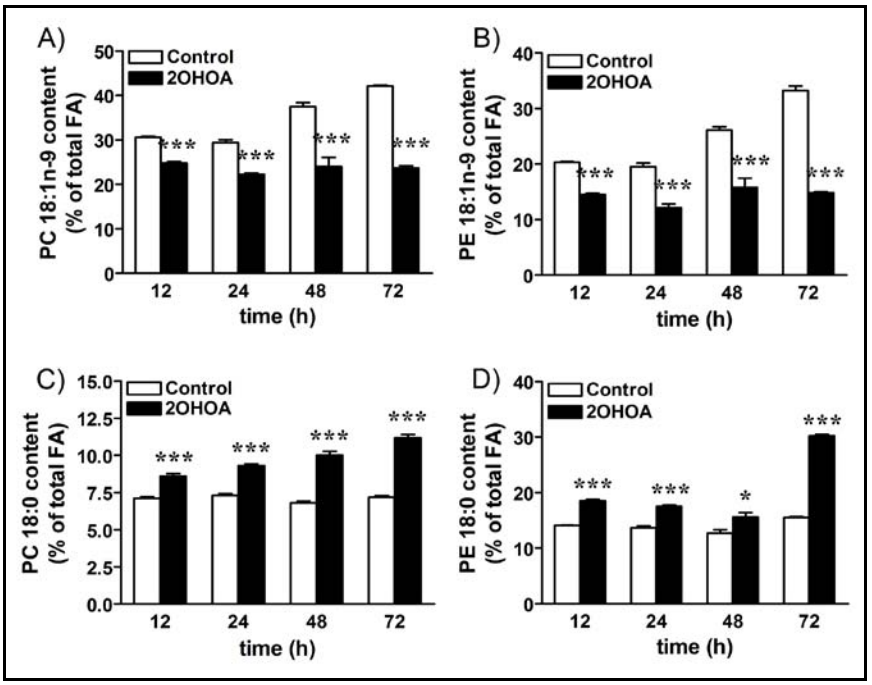


**Figure 3-3. Time dependent changes in fatty acids induced by 2OHOA in U118 cells.**
U118 cells were treated in the presence or absence of 2OHOA (200 µM, 12-72 h). After treatment lipids were extracted and analyzed by TLC. PC (A and C) and PE (B and D) fractions were converted to FAME in basic conditions and analyzed by gas chromatography. The bar graphs show the oleic acid content (A, B); and the stearic acid content (C, D). Values are expressed as mole% and represent mean ± SD, n= 4-5. The asterisks indicate a significant effect of the treatment as compared with the control (*$P < 0.05$; ***$P < 0.001$).

To determine whether the observed changes in fatty acid composition occurred in other tumor cells, we analyzed the effect of 2OHOA on the fatty acid composition in human non-small cell lung cancer (A549) cells and an additional line of human glioma (SF767) cells (Figure 3-4). After 2OHOA treatment (200 µM, 72 h), Oleic acid decreased 52% in PC and 41% in PE, while stearic acid increased 2.7-fold in PC and 62% in PE, in A549 cells. Likewise, oleic acid was reduced 17% in PC and 40% in PE, while stearic acid increased 19.2% only significantly in PE, in SF767 cells. Altogether, these results indicated that the effect on fatty acid composition was not dependent on the particular type of tumor. The complete fatty acid profile of SF767 and A549 cells is shown in the appendix (Table A 1 and Table A 2, respectively).

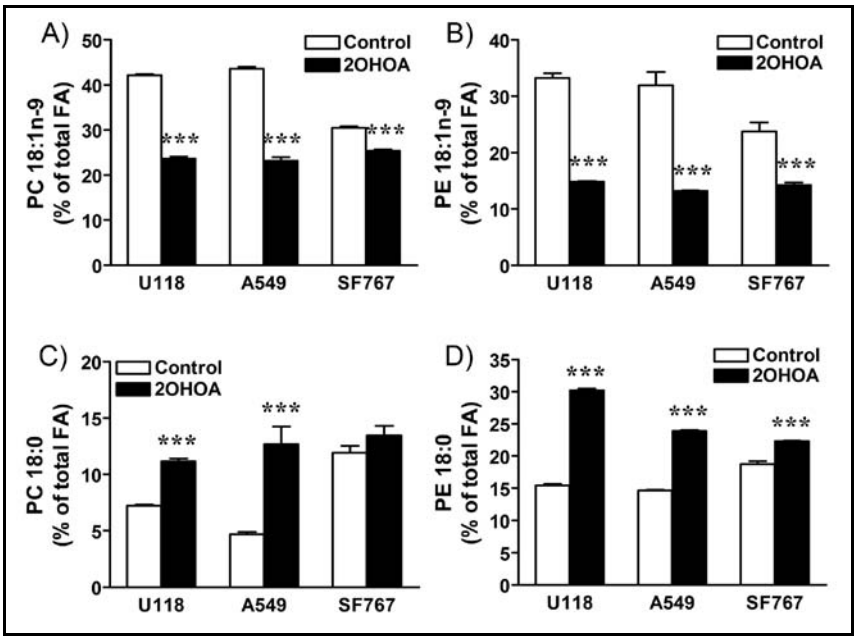


**Figure 3-4. 2OHOA reduced oleic acid content in different cancer cells.**
Different cancer cells (U118, SF767 and A549) were treated with 2OHOA (200 µM, 72 h). Lipids were extracted and separated by TLC. PC (A and C) and PE (B and D) fractions were converted to FAME in basic conditions and analyzed by gas chromatography. The bar graphs show the oleic acid content (A, B), and the stearic acid content (C, D). Values are expressed as mole% and represent mean ± SD, n= 4-5. The asterisks indicate a significant effect of the treatment as compared with the control (***$P < 0.001$).

### 3.2.2 2OHOA was incorporated into different lipid classes

The presence of 2OHOA in total lipid extracts has been already shown (Figure 2-11), but it remained to be determined if it stayed as a FFA or if it was incorporated into any lipid fraction. TLC analysis of control and 2OHOA treated U118 cells (200 µM, 24 h) allowed the detection of free 2OHOA. Interestingly, 2OHOA's RF (Ratio of Front) was considerably different than the RF of FFA (Figure 3-6). Despite these results, part of 2OHOA could still be incorporated into lipids. In order to detect 2OHOA, lipid extracts were analyzed by mass spectrometry (MS), as hydroxyl fatty acids are not transesterified in the basic conditions used in the previous fatty acid analysis (Barceló-Coblijn *et al.*, 2010). Thus, U118 cells were treated with 200 µM 2OHOA for a wide range of incubation times (0.5 – 72 h) and it was observed that at least part of the 2OHOA was primarily incorporated into glycerophospholipids and glycerolipids TAG and DAG (Figure 3-5 and Figure 3-7).

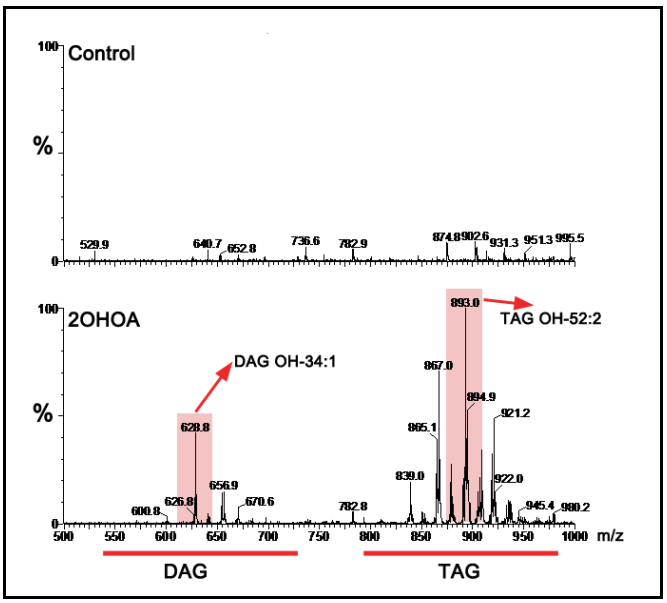


**Figure 3-5. Mass spectra from glycerolipids containing 2OHOA.**
U118 cells were treated in the presence or absence of 2OHOA (200 µM, 24 h). After treatment lipids were extracted and analyzed by LC/MS. The peak corresponding to 893.0 represents TAG containing OH-52:2 and the peak corresponding to 628.8 represents DAG containing OH 34:1. The spectra are normalized to the highest peak in both control and treated sample.

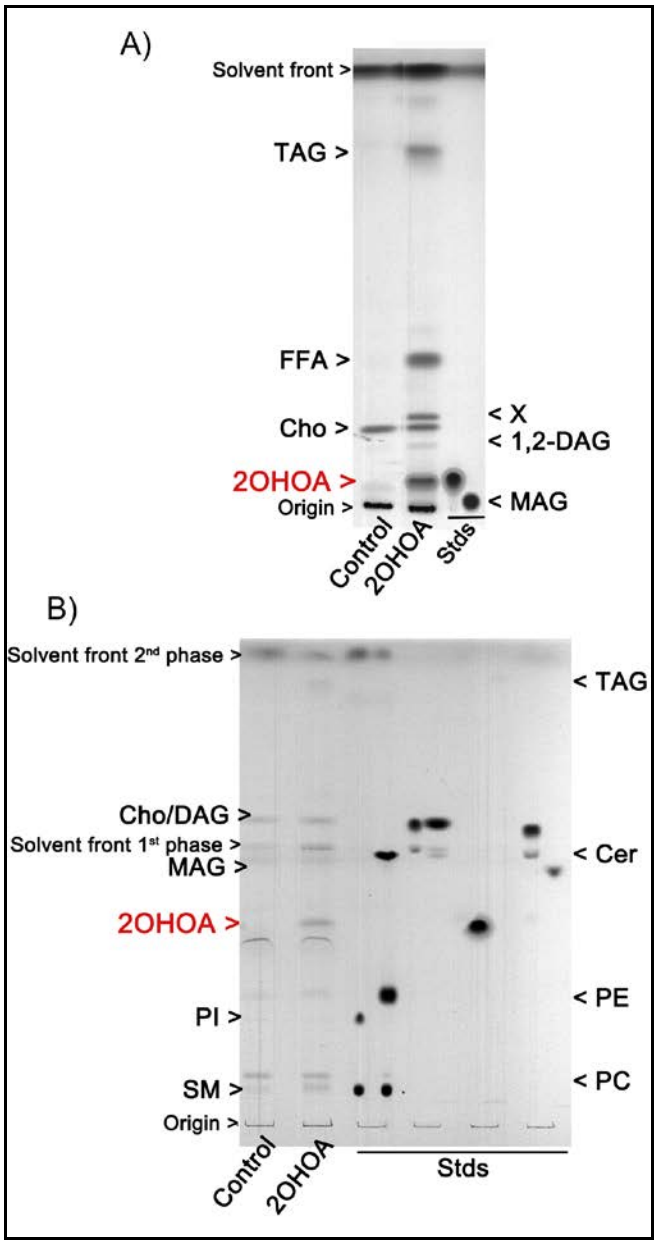


**Figure 3-6. 2OHOA remained in part as a free fatty acid.**
U118 cells were exposed to 2OHOA (200µM) for 24 h. Then, lipids were extracted and analyzed by TLC. (A) Representative HPTLC for neutral lipids, separated in petroleum ether/diethyl ether/acetic acid (75:25:1.3 by vol) (Marcheselli, 1988). (B) Representative separation by TLC (Kuerschner *et al*., 2005). After running two-thirds of the separation distance in chloroform/ethanol/water/triethylamine (35:40:9:35, by vol.), the plates were dried and subsequently separated in isohexane/ethylacetate (5:1, by vol) for the full distance.

Figure 3-7 clearly shows the time-dependent accumulation of 2OHOA into the glycerophospholipid fraction with the highest incorporation into PC (30.1% ± 0.3%) and PE (29.0% ± 0.7%) after 72 h. 2OHOA was also incorporated, although to a lesser extent, into PS (11.7% ± 0.47%) and PI (13.4% ± 1.3%). Interestingly, 0.5 h of treatment was sufficient to observe a significant incorporation of 2OHOA into PC, while for PE, 6 h of treatment were needed. In the case of PS and PI, its incorporation was significant after 24 h of treatment. These results not only indicate that 2OHOA was replacing its analogue oleic acid but they can also support that the kinetics of fatty acid incorporation depends on the particular glycerophospholipid.

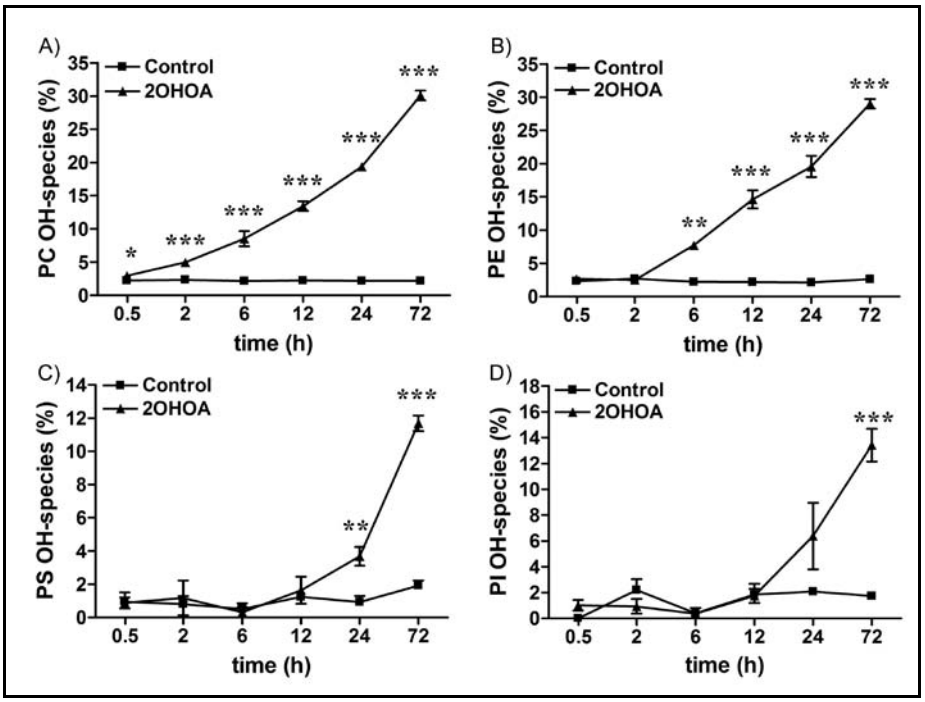


**Figure 3-7. 2OHOA was incorporated into the glycerophospholipid fraction.**
U118 cells were treated in the presence or absence of 2OHOA (200 µM, 0.5-72 h). After treatment lipids were extracted and analyzed by LC/MS. Values are expressed as % of total fatty acids and represent mean ± SEM, n= 3-4. Line plots show PC (A), PE (B), PS (C) and PI (D) OH-species content. The asterisks indicate a significant effect of the treatment as compared with the control (*$P < 0.05$; **$P < 0.01$; ***$P < 0.001$).

### 3.2.3 2OHOA inhibited SCD1

The severe decrease in oleic acid in addition to the increase in stearic acid (Figure 3-4 and Figure 3-3), not only in the glycerophospholipid fraction but also in the total lipid extract (Table A 3), clearly suggested that the rate of Δ9-desaturation could be affected. For this reason, we evaluated the effect of 2OHOA on SCD1 activity, by measuring the conversion of exogenous [$H^3$]-palmitic acid (16:0) into MUFA. Thus, control and treated cells (200 µM, 48 h) were incubated with [$H^3$]-palmitic acid for 6 h. After incubation, lipids were extracted; transesterified in basic conditions, and FAME were then separated by argentation TLC. The MUFA spot was scraped and radioactivity was measured by scintillation counting. Figure 3-8 shows that [$H^3$]-MUFA levels were reduced 48% in treated cells compared to control cells, indicating that SCD1 was significantly inhibited by 2OHOA.

These results indicate that the SCD1 inhibition, in addition to the incorporation of 2OHOA into the glycerophospholipid fraction, are the main processes driving the profound fatty acid remodeling induced by 2OHOA.

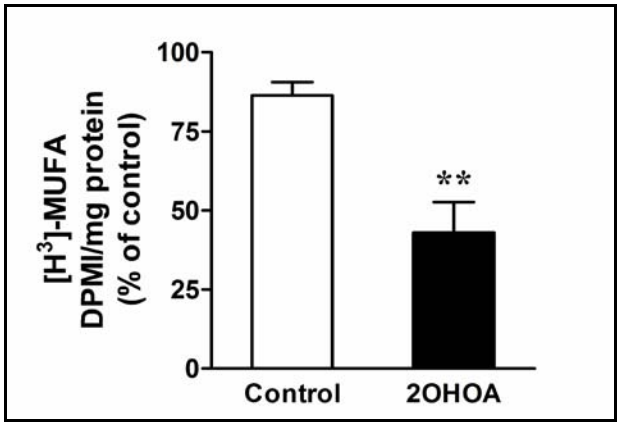


**Figure 3-8. 2OHOA inhibited SCD1.**
Control and treated (200 µM, 48 h) U118 cells were labeled with [$H^3$]-palmitic acid (0.25 µCi/ 60 mm petri dish) for 6 h. Conversion of [$H^3$]-palmitic acid to [$H^3$]-MUFA was measured following the separation of FAME on TLC plates impregnated with silver nitrate and determination of radioactivity as indicated in the *Experimental procedures* section. Values represent the mean ± SEM, n= 3-4. The asterisks indicate a significant effect of the treatment as compared with the control (**$P < 0.01$).

### 3.2.4 2OHOA affected neutral lipid composition

Because 2OHOA was also incorporated into the glycerolipids TAG and DAG, we next studied the effect of 2OHOA on these lipids. Lipid extracts from control and 2OHOA treated U118 cells (200 µM) at different times were analyzed by HPTLC. Results showed that although TAG levels increased at all times they followed a cyclic pattern (Figure 3-9). Thus, the increases in TAG peaked after 12 h and 48 h of treatment (6.7-fold and 8.5-fold, respectively), while after 24 h and 72 h the increases were more modest (2.6-fold and 2.4-fold, respectively). This increase in TAG after treatment was further confirmed by mass spectrometry (Figure A 4). In addition, similar increases in TAG levels were observed in A549 and SF767 cells (Figure A 5).

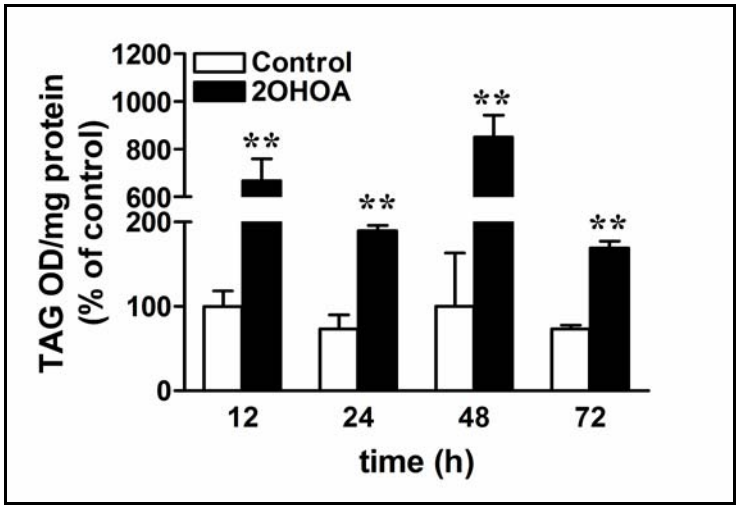


**Figure 3-9. 2OHOA induced TAG accumulation in U118 cells.**
U118 cells were exposed to 2OHOA (200 µM) for different times. Lipids were extracted and neutral lipids were analyzed by HPTLC as explained in the *Experimental procedures* section. Results are means ± SEM, n=3. The asterisks indicate a significant effect of the treatment as compared with the control (**$P$ < 0.01).

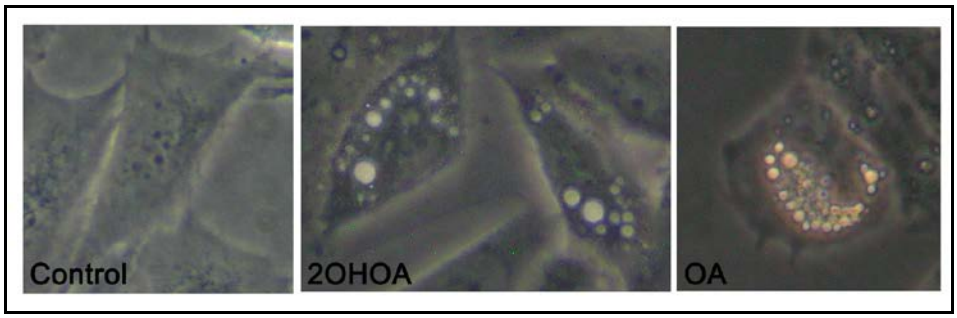


**Figure 3-10. Representative phase-contrast micrographs (100 × magnification) of U118 cells exposed to 2OHOA or OA (200 µM, 24 h).**

The observation of treated cells by phase contrast microscopy showed the presence of white round vesicles of unknown nature (Figure 3-10). Taking into account that 2OHOA induced increases in TAG levels, we explored the possibility that these vesicles could be LDs. Exposure to oleic acid (OA, 100 µM, 2 h) was used as a positive control, as it is well established that OA induces the formation of LDs (Gubern *et al.*, 2008). As it can be observed in Figure 3-11, after the exposure to 2OHOA (200 µM, 24 h), there was an increased number of LDs with an increased total area and particle average size in comparison to control cells. Interestingly, when compared to cells exposed to OA, the number of particles and the total area were smaller, while the particle average size was bigger (Figure 3-11A-D). These results suggested that 2OHOA was metabolized differently than OA, inducing, after a longer period of exposure, less but larger LDs. Finally, the formation of LDs was confirmed by the presence of ADRP analyzed by western blot (Figure 3-12) and by electron microscopy (Figure 2-21).

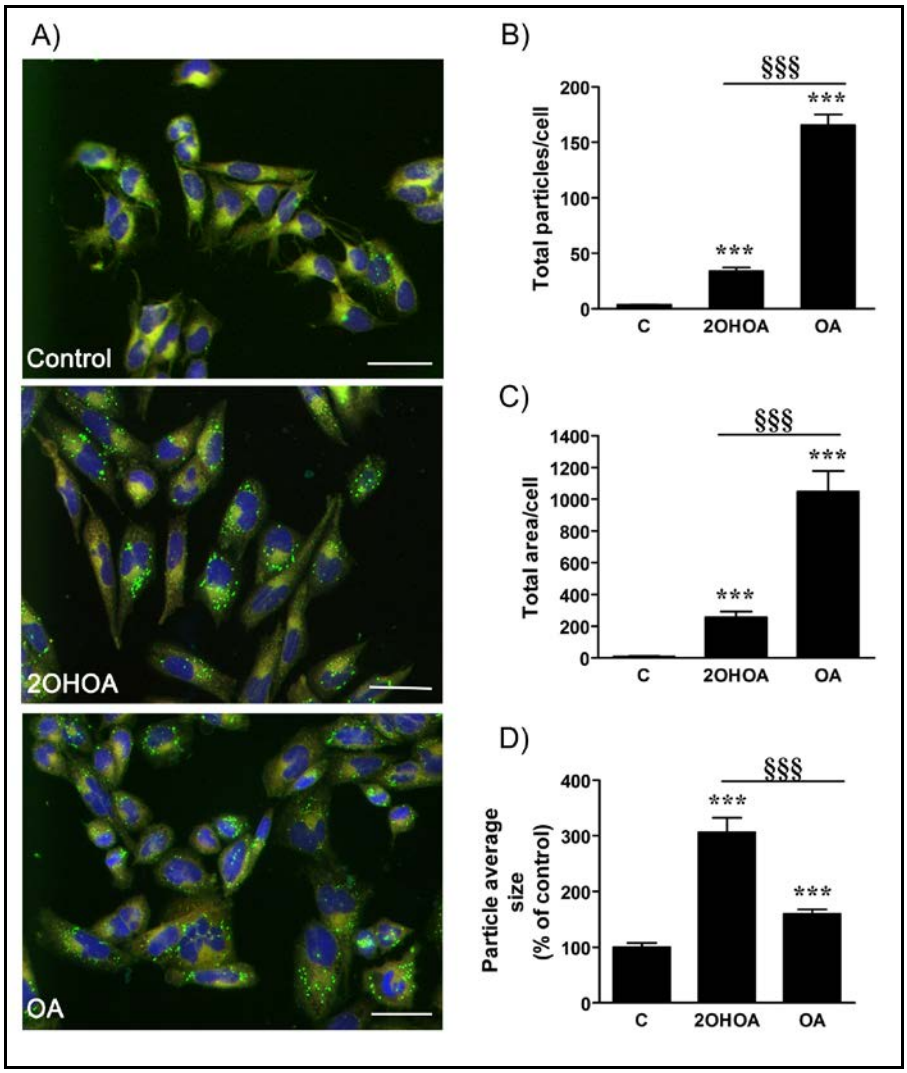


**Figure 3-11. 2OHOA induced lipid droplet formation.**
U118 cells were treated in the absence (Control) or presence of 2OHOA (200 μM, 24 h) or OA (100 μM, 2 h). (A) After treatment cells were fixed and stained with Nile Red (green for LDs) and Hoescht (blue for nuclei). The presence of LDs was quantified by fluoresce microscopy with ImageJ analysis of total particle/cell (B), total LDs area/cell (C) and average size (D) in 9 micrographs from each experimental condition. Bar scale = 100 μM. Results are means ± SEM of three experiments, each carried out with triplicate determinations. The asterisks indicate a significant effect of the treatment as compared with the control (***$P$ < 0.001). In this case, § indicates a significant effect of OA compared with 2OHOA treatment (§§§ $P$ < 0.001).

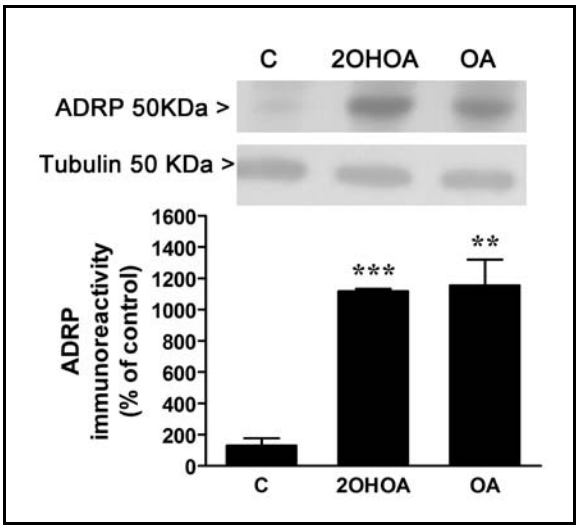


**Figure 3-12. 2OHOA induced ADRP formation.**
Western blot of ADRP in total cell extracts under the three experimental conditions. U118 cells were treated in the absence (Control) or presence of 2OHOA (200 μM, 24 h) or OA (100 μM, 2 h). Results are means ± SEM of three independent experiments carried out by triplicate. The asterisks indicate a significant effect of the treatment as compared with the control (***P* < 0.01; ****P* < 0.001).

Hitherto, we have described the effect of 2OHOA on TAG levels. In addition, the analysis of the neutral lipid separation led to additional information. Thus, cholesterol mass increased 1.3-fold after 72 h of treatment and FFA levels (which did not include 2OHOA, Figure 3-6) increased 3.1-fold and 2.3-fold, after 24 h and 48 h of treatment, respectively. The 1,2-DAG levels increased 2.5-fold only after 24 h of treatment. Finally, the TLC analysis showed the presence of a band of unknown nature. Consistently, similar changes were found in A549 and SF767 glycerolipid composition (Figure A 5).

As it was previously indicated, PC is the donor of the phosphocholine group, which is transferred by SMS onto the primary hydroxyl group of Cer, generating DAG as an additional product of the reaction (Huitema *et al.*, 2004; Ternes *et al.*, 2009). Interestingly, DAG levels did not follow the same increase pattern as SM (Figure 2-5), probably because, as a crucial signaling lipid, the increased DAG production is compensated by channeling it into TAG formation or into its degradation to MAG. To address this issue, control and 2OHOA treated cells (200 μM, 24 h) were incubated with the fluorescent phospholipid analogues NBD-C6-PC (NBD-PC) or NBD-C6-PE (NBD-PE; 3 μM, 4 h), which contain the NBD-fluorescent moiety at the *sn*-2 position of the

glycerol backbone. The analysis of lipids by TLC revealed new insights on the effect of 2OHOA on lipid metabolism (Figure 3-14). First, it was demonstrated that 2OHOA increased the formation of NBD-DAG. Interestingly, the increase was larger when cells had been incubated with NBD-PE than with NBD-PC. In addition, the TLC analysis showed that 2OHOA activated the conversion of NDB-PE to NBD-PC, which confirmed the interconnection between PE and PC metabolism, suggested in the previous chapter (Figure 2-6). Second, the TLC analysis showed that NBD-DAG was probably being degraded to NBD-MAG, since no NBD-TAG could be detected.

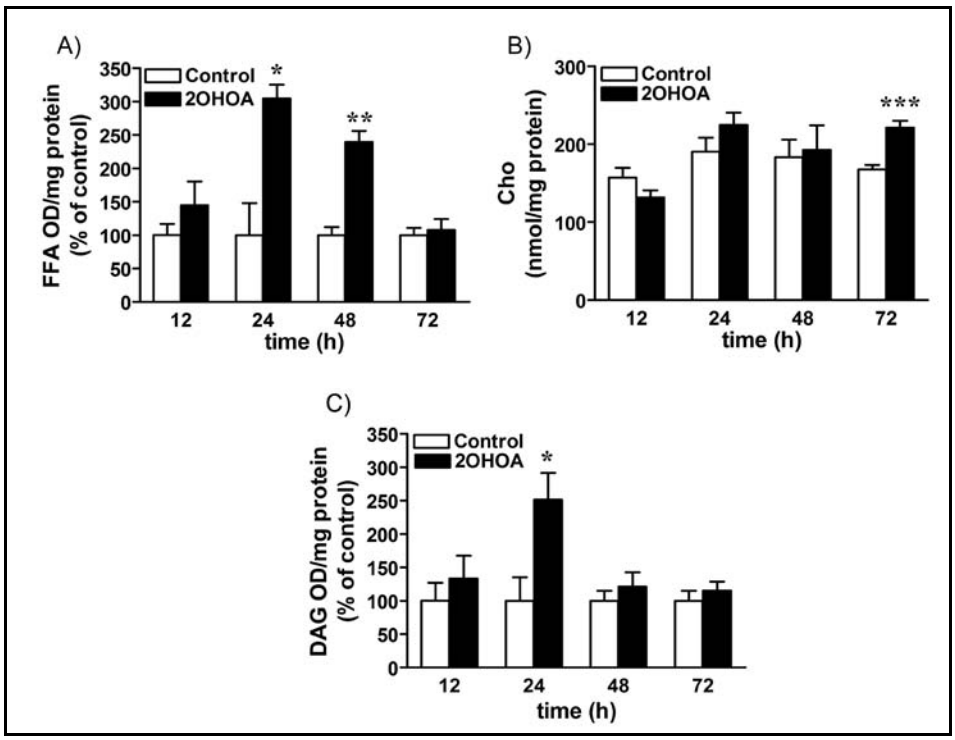


**Figure 3-13. 2OHOA affected U118 neutral lipid composition.**
U118 cells were treated in the presence or absence of 2OHOA (200 µM, 12-72 h). After treatment lipids were extracted and analyzed by TLC. (A) Free fatty acids (FFA); (B) Cholesterol (Cho); (C) DAG. Values are OD/mg protein and are expressed as % of control and represent mean ± SD, n= 4-5. The asterisks indicate a significant effect of the treatment as compared with the control (*$P < 0.05$; **$P < 0.01$; ***$P < 0.001$).

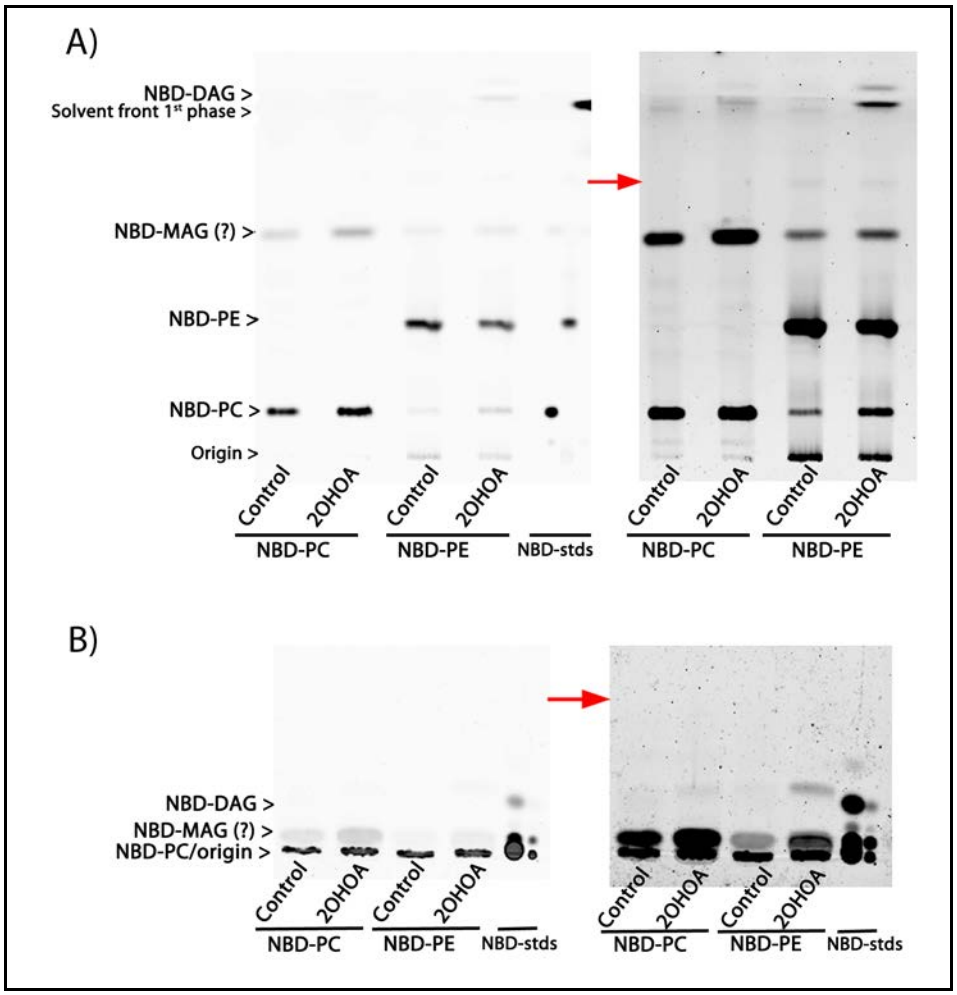


**Figure 3-14. DAG from PC was converted into MAG.**
Control and treated cells (2OHOA, 200µ, 24 h) were incubated with NBD-C6-PC or NBD-C6-PE for 3 h. After incubation, lipids were extracted and analyzed by TLC. (A) Separation was achieved by using two solvent system (Kuerschner *et al.*, 2005). Thus, after running two-thirds of the separation distance in chloroform/ethanol/water/triethylamine (35:40:9:35, by vol.), plates were dried and subsequently separated in isohexane/ethylacetate (5:1, by vol) for the full distance. (B) Neutral lipids were separated in petroleum ether/diethyl ether/acetic acid (75:25:1.3 by vol) (Marcheselli, 1988). The image contrast was saturated for a better visualization of minor bands (image on right side of the panel indicated by an arrow).

## 3.3 2OHOA incorporation into glycerolipids and glycerophospholipids provoked a profound fatty acid remodeling

In the previous chapter it was demonstrated that 2OHOA affects the glycerophospholipid composition of different cancer cells (U118, A549, 1321N1, Jurkat and SF767), but it does not affect the non-tumor MRC-5 cells. Specifically, 2OHOA treatment strongly augmented SM mass, while a loss of PE and PC was observed. In this chapter, based on the fatty acid nature of 2OHOA, we demonstrated that 2OHOA profoundly remodeled the fatty acid profile of cancer cells. Among the fatty acids, oleic acid, a structural analogue to 2OHOA, was the most affected by the treatment, decreasing significantly in the main membrane lipids PC and PE in the cell lines studied (U118, SF767 and A549 cells). While in PC the reduction in oleic acid was between 20-50%, in PE it was between 40-60%, depending on the cell line (Table 3-1 and Figure 3-4). This is a very significant reduction, considering that oleic acid is the most abundant fatty acid in these cell lines. In order to explain this reduction two possibilities were explored: its substitution by 2OHOA and the potential inhibition of SCD1, which would consequently inhibit the synthesis of oleic acid.

MS analysis of the glycerophospholipid fraction revealed that 2OHOA was mainly incorporated into the major glycerophospholipids fractions PC and PE, and to a lesser extent into PS and PI, indicating that indeed 2OHOA could be replacing oleic acid. In fact, taking into account the glycerophospholipid composition (Table 2-3), 2OHOA would account for ca. 15% of the total fatty acids composition, becoming one of the most abundant fatty acids in membranes from glioma treated cells. It is worth mentioning that 2OHOA was also incorporated into the glycerolipid fraction, mainly into TAG and DAG, while no incorporation into sphingolipids was detected. The latter was somehow unexpected since endogenous hydroxyl fatty acids have been found almost exclusively as N-acyl chains within the Cer moiety of a variety of sphingolipids while there is no evidence in the literature supporting the incorporation of hydroxyl fatty acids into glycerophospholipids in mammals (Hama, 2010). This difference may rely on the exogenous nature of 2OHOA. Thus, upon activation of 2OHOA by its conversion to 2OHOA-CoA (Foulon *et al.*, 2005), 2OHOA would be incorporated into the DAG-pathway and consecutively into the Kennedy-pathway (Kennedy, 1961). Moreover, it could also be subjected to a rapid turnover of the acyl moiety (probably the *sn*-2) of glycerophospholipids (Hishikawa *et al.*, 2008; Lands, 1958). Therefore, these results would be the first evidence of the incorporation of hydroxyl fatty acids into glycerolipids and glycerophospholipids.

It is well documented that various tumors undergo exacerbated endogenous fatty acid biosynthesis irrespective of the levels of extracellular lipids (Kuhajda, 2006; Rashid *et al.*, 1997; Swinnen *et al.*, 2000). In contrast, most adult normal tissues, even those with high cellular turnover, preferentially use circulating fatty acids for the synthesis of new structural and signaling lipids (Mashima *et al.*, 2009). That is why noncancer cells do not have relevant requirements of *de novo* lipid synthesis, and therefore, normal cells are not sensitive to inhibition of this pathway (Fritz *et al.*, 2010). In addition, it is known that cancer cells and tumors usually have elevated oleic acid and lower stearic acid content than their normal non-tumor counterparts (Mikirova *et al.*, 2004), leading to the possibility of considering the oleic acid/stearic acid ratio as a tumor marker (Cvetkovic *et al.*, 2010; Meng *et al.*, 2004c).

In this context, previous studies show a strong functional association of SCD1 activity with membrane lipid synthesis in neoplastic cells (Scaglia *et al.*, 2005; Scaglia & Igal, 2008). Accordingly, the induction of apoptosis with etoposide and Cer led to the downregulation of SCD1 activity and expression, accompanied by a decrease in oleic acid and an increase in stearic acid (Ariyama *et al.*, 2010; Fritz *et al.*, 2010; Scaglia & Igal, 2005). This chapter showed that SCD1 activity decreased by ca. 50% upon 2OHOA treatment, suggesting that the SCD1 inhibition could be an additional factor contributing to the effect of 2OHOA on the cell cycle. At least two possibilities, may explain the observed SCD1 inhibition. First, SCD1 could be inhibited by oleic acid released induced by substitution for 2OHOA, as oleyl-CoA is a good competitive inhibitor of the desaturase enzyme (Enoch *et al.*, 1976). Second, because of the Δ9 insaturation present in 2OHOA, and their high structural similarity, SCD1 could recognize it as an end product, inhibiting consequently its activity.

Although it requires further investigation, SCD1 could be a therapeutic target for 2OHOA as this enzyme was identified as a target for inducing cytotoxicity and cell death in a recent study, where a siRNA library against 3,700 genes was screened in several cancer cells (Morgan-Lappe *et al.*, 2007). Remarkably, SCD1 was one of the three main targets identified in this screening, confirming that this enzyme is a crucial factor for cancer cell survival. Potent and specific small molecule inhibitors of SCD1 activity have been recently discovered and if, as observed in *in vitro* studies, the anti-growth effect of SCD1 inhibition proves to be selective for cancer cells, this may open an interventional window for SCD1 inhibitors in cancer treatment (Koltun *et al.*, 2009).

The analysis of neutral lipid showed that 2OHOA induced increases in TAG and FFA levels while DAG levels remained constant (except at 24 h). It is known that TAG accumulation may be a general metabolic phenomenon in response to increased cellular levels of unsaturated fatty acids. Thus, exogenous OA supplied in the media leads to

TAG synthesis in CHO cells and mouse embryonic fibroblasts (Gubern *et al.*, 2008; Listenberger *et al.*, 2003). Therefore, 2OHOA-induced accumulation of TAG may have a similar explanation, because part of 2OHOA was channeled to TAG synthesis, which could also be influenced by the oleic acid hydrolyzed from the glycerophospholipids. In any case, the increase in TAG levels would contribute to the formation of LDs. The difference between OA and 2OHOA in their capacity to stimulate LDs formation indicated that despite their high structural similarity, 2OHOA is differentially metabolized when compared to OA.

The robust increase in SM was not accompanied by a similar effect on DAG levels, despite that the latter is the second product of the reaction catalyzed by SMS. This result was not completely unexpected because, considering the important role of DAG in cell signaling, its metabolism is very active in cells. However, the increased formation of DAG was demonstrated by incubating cells with NBD-PC and NBD-PE (Figure 3-14). In addition, these experiments suggested that part of the newly synthesized DAG may be converted into MAG, allowing glioma cells to maintain DAG within appropriate levels. In this context, alternative pathways that lead to DAG metabolization to promptly compensate for its accumulation may be expected.

To sum up, the results of this chapter not only helped to elucidate part of 2OHOA fate but also revealed what would be an additional aspect of its molecular mechanism of action, which would involve a profound fatty acid remodeling and SCD1 inhibition. Finally, we have shown that 2OHOA, oleic acid released from the glycerophospholipids, or both, induced TAG accumulation with the consequent formation of LDs.

# 4 2OHOA affected the biophysical properties of membranes

## 4.1 Membrane biophysics and fluorescence spectroscopy

As it was previously mentioned in the *Introduction*, cellular membranes are complex and dynamic systems, defined by specific lipid-lipid and lipid-proteins interactions that can induce the formation of lipid microdomains. There are many different types of membrane domains in the plasma membrane, and perhaps the entire membrane should be viewed as a mosaic of microdomains (Maxfield, 2002). The most actively studied type of lipid domains are lipid rafts, which are thought to consist of sphingolipid–cholesterol-enriched and (unsaturated) PC-depleted domains (de Almeida *et al.*, 2009). One approach to study such a complex system with different phases, properties and proportion is fluorescence spectroscopy.

This technique allows obtaining dynamical information of biological systems due to its intrinsic sensitivity and the time-scale of fluorescence emission together with the time-resolution of detection. Fluorescence measurements can be classified into two types: steady-state and time-resolved (Lakowicz, 2006).

Steady-state measurements are those performed with constant excitation and emission. The sample is illuminated with a continuous beam of light, and the fluorescence intensity is measured. When fluorescence intensity is obtained as a function of the emission wavelength, an emission spectrum is recorded. When using polarized light, steady-state fluorescence anisotropy, a widely used steady-state parameter, can be obtained (see below).

For time-resolved measurements the sample is exposed to a pulse of light, whose width is typically shorter than the decay time of the sample. This intensity decay is recorded with a high-speed detection system that allows the intensity or anisotropy to be measured on the nanosecond timescale. In this case, several types of parameters can be used, such as fluorescence lifetimes, anisotropy decays and time-resolved emission spectra, the two latter out of the scope of this thesis. Because these parameters depend on different characteristics of the probe environment, like polarity or microviscosity, they can report the appearance of new phases which otherwise would not be detected. By combining these parameters with the direct observation of heterogeneities through imaging techniques, fluorescence methods with time resolution are one of the potentially most useful tools to study lipid domains and rafts (de Almeida *et al.*, 2009).

Anisotropy measurements are based on the principle of photoselective excitation of fluorophores by polarized light (Figure 4-1). Fluorophores preferentially absorb photons whose electric vectors are aligned parallel to the transition moment of the fluorophore. The transition moment has a defined orientation with respect to the molecular axis. In an isotropic solution, the fluorophores are oriented randomly. Upon excitation with polarized light, the probability of excitation is maximal for fluorophore molecules whose absorption transition dipole is parallel to the electric vector of the excitation, and is zero for those molecules which have the transition moment perpendicular to the polarization of the excitation light. This selective excitation results in a partially oriented population of fluorophores (photoselection), and in partially polarized fluorescence emission, which also occurs with the light polarized along a fixed axis in the fluorophore. Thus, the fluorescence anisotropy is defined by ($r$),

$$r = \frac{I_{II} - I_{\perp}}{I_{II} + 2I_{\perp}}, \qquad \text{(Equation 3)}$$

where $I_{\parallel}$ and $I_{\perp}$ are the fluorescence intensities of the vertically ($\parallel$) and horizontally ($\perp$) polarized emission, when the sample is excited with vertically polarized light. The anisotropy is a dimensionless quantity that is independent of the total intensity of the sample, because the difference ($I_{\parallel} - I_{\perp}$) is normalized by the total intensity, which is defined as $I_T = I_{\parallel} + 2I_{\perp}$. Rotational diffusion, limited by the viscosity and fluidity of the membranes, changes the direction of the transition moments and is one common cause of depolarization (Figure 4-2). Anisotropy measurements reveal the average angular displacement of the fluorophore that occurs between absorption and subsequent emission of a photon. This angular displacement is dependent upon the rate and extent of rotational diffusion during the lifetime of the excited state. In addition, the rate of rotational diffusion depends not only on the size and shape of the rotating molecule, but also on viscosity and temperature. Therefore, the same probe, i.e., with the same size and shape, will display very different average angular displacements whether it is incorporated in a highly packed environment with high viscosity, or in a less restrictive towards rotation and more fluid one. Thus, the anisotropy of a membrane probe reflects the fluidity and order of the membrane.

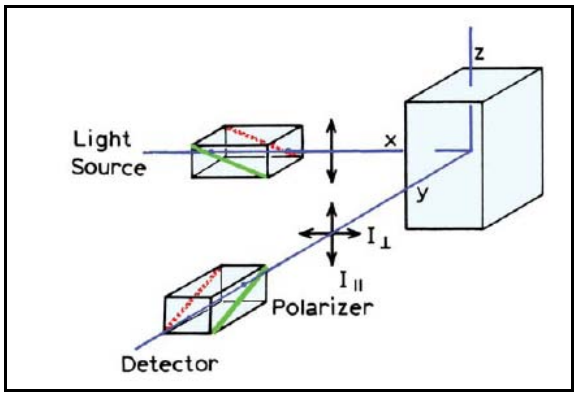


**Figure 4-1. Schematic diagram for measurements of fluorescence anisotropies (Lakowicz, 2006).**

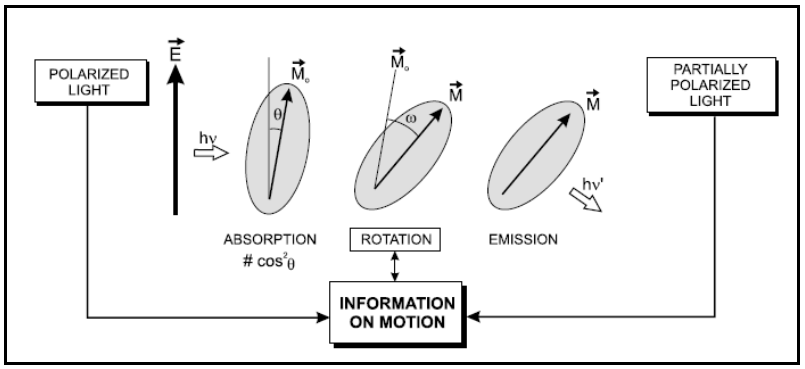


**Figure 4-2. Rotational motions inducing depolarization of fluorescence.**
The Θ angle between $\mathbf{M}_o$, the absorption transition moment and **E**, the electric vector of the excitation light, accounts for the photoselection effect. The absorption and emission (**M**) transition moments are assumed to be parallel and the angular displacement between them (ω) is due to molecular rotation (Valeur, 2001).

Time-resolved experiments are often performed through direct measurements in the time domain, in which a short pulse of light excites the sample, and the subsequent fluorescence emission is recorded as a function of time. This is generally achieved using time-correlated single photon counting, which uses electronics to detect single-photon events at a detector. By repeating many start-stop signals, a histogram of single-photon counts in discrete time channels is obtained (Figure 4-3). In a microheterogeneous

medium the decay of a fluorophore is not usually described by a single exponential function but by a complex decay with several components:

$$I(t) = \sum_{i=1}^{n} \alpha_i^{-t/\tau i}$$

(Equation 4)

Where $\alpha_i$ and $\tau_i$ are the normalized amplitude and lifetime of component *i*, respectively. Then, it is useful to describe the fluorescence kinetics through a parameter named mean or average lifetime, given by

$$<\tau>= \frac{\sum \alpha_i \tau_i^2}{\sum \alpha_i \tau_i}$$

(Equation 5)

For a decay described by a sum of exponentials, where $\alpha_i$ is the normalized pre-exponential and $\tau_i$ the lifetime of the decay component i. Thus, the mean lifetime is the average amount of time a fluorophore remains in the excited state following excitation. As exemplified below, fluorescence lifetime is in certain cases highly dependent on the environment of the probe and potentially very useful in membrane biophysical studies. It should also be highlighted that time resolved techniques have the advantage of not evaluating the total intensity, so they are much less biased by the known problems associated to steady-state data such as light scattering, or error in probe concentration.

Most lipids do not display intrinsic fluorescence, thus the application of fluorescence spectroscopy to this kind of studies requires the labeling of the bilayer with an extrinsic fluorophore (membrane probe). Membrane probes include fluorescent molecules similar to natural lipids, such as 1,6-diphenyl-1,3,5-hexatriene (DPH) and their derivatives having the same chromophore, for example the cationic trimethylamino-DPH (TMA-DPH), which are the most widely used. Important information about the membrane can be also obtained using linear conjugated polyene fluorescent fatty acids such as all-*trans*-9,11,13,15-octadecatetraenoic acid, known as *trans*-parinaric acid (*t*-PnA) and all-*trans*-8,10,12,14,16-octadecapentaenoic acid (de Almeida *et al.*, 2009).

In this work, two probes that have different phase partitioning behavior were used, DPH and *t*-PnA (Figure 4-4). DPH incorporates parallel to the acyl chains of the phospholipids and it distributes indistinctly between $l_d$ and $l_o$ phases, but is excluded from Cer-rich gel phase (de Almeida *et al.*, 2003; Lentz, 1993; Silva *et al.*, 2006; Silva *et al.*, 2007).

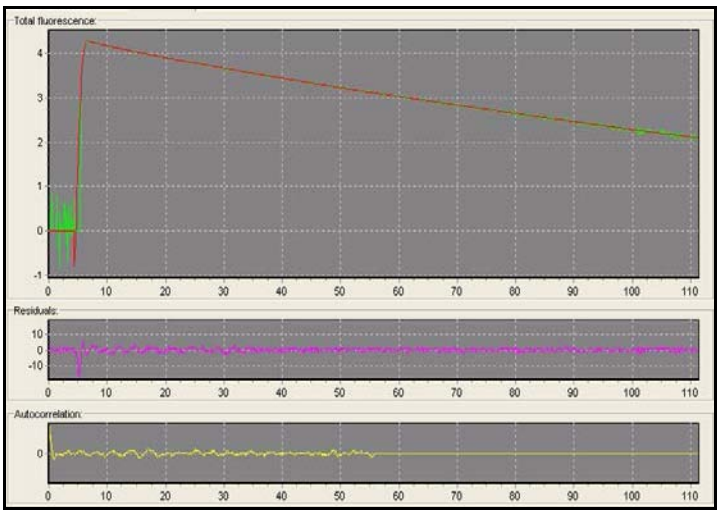


**Figure 4-3. Data obtained by the single-photon timing technique with TRFA data processor.**
Sample: solution of POPC:POPE:PSM:Cholesterol with *t*-Pna at 24°C. Excitation wavelength: 320 nm; observation wavelength: 404 nm. Reference: scattering solution (Ludox). Number of channels: 1024; $\chi^2$=1.4.

On the other hand, *t*-PnA presents a high preference for $l_o$ and Cer-rich gel phase, where it displays an increased fluorescence quantum yield and therefore is an exceptional reporter of these phases (de Almeida *et al.*, 2009). Due to the *trans*-configuration of its double bonds, *t*-Pna is not only one of the few probes that has a preference for $l_o$ phases, but in addition it is the only probe that displays a strong preference for the gel phase. Moreover, *t*-Pna does not have a tendency to aggregate and consequently, does not affect significantly the organization of the lipid bilayer. Thus, the fluorescence properties of this probe are particularly sensitive to the changes undergone in the $l_o$ domains or the lipid rafts. Consequently, by combining these two membrane probes complementary information is obtained. In addition, the quantum yield of the probes, i.e. the number of emitted photons relative to the number of absorbed photons, behaves differently. Thus, whereas the DPH quantum yield is not strongly sensitive to the presence of either type of phase, *t*-PnA presents quantum yield values and fluorescence lifetime components that are typical of each phase. The fluorescence intensity decay of *t*-PnA (Equation 4) is usually described by the sum of several exponentials, each one with a certain fluorescence lifetime component. As the mean fluorescence lifetime depends on the squares of the lifetime components, it is very sensitive to changes undergone in the long lifetime component ($\tau_{long}$). In addition, the

$\tau_{long}$ of this probe is specifically due to the ordered domains, such as the $l_o$ (lipid rafts) or the $s_o$ (gel) phases, directly reflecting the composition and acyl chain packing of those domains (Aresta-Branco *et al.*, 2011). The fact that for both probes the fluorescence anisotropy is high in the gel and low in the fluid state, together with the previously mentioned differences, allows for a detailed characterization of the lipid phases that are formed in the system under investigation (Castro *et al.*, 2007). In addition, for both probes, the chromophore is buried in the hydrophobic core of the lipid bilayer, providing direct information on acyl chain packing. Thus, the results can be interpreted without taking into consideration biophysical complexities on the lipid-water interface/lipid headgroup region or interactions with extra membrane molecules or domains of membrane proteins (Aresta-Branco *et al.*, 2011).

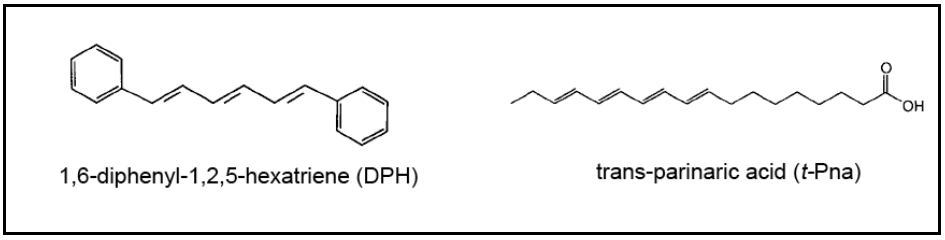


**Figure 4-4. Probes used in this study for fluorescence spectroscopy (Valeur, 2001).**

## 4.2 Results

### 4.2.1 Effect of the SM increase on the biophysical properties of model membranes

As a first approach to understand the consequences that the dramatic changes in phospholipid composition observed after treatment of U118 cells with 2OHOA (200 µM) would have on membrane biophysical properties, we prepared membrane model systems with compositions mimicking the major alterations observed in SM, PC, PE and cholesterol levels (Table 4-1). The mixtures used in this study met the criteria for formation of raft-like domains (Marsh, 2009). By using this set of lipids, the changes in

artificial membrane lipid composition reflected the alterations induced by the treatment on the different lipid headgroups content, rather than in the acyl chain, which are analyzed in the next section. These liposomes were then labeled with either *t*-PnA or DPH.

**Table 4-1. Mole fractions of the lipids used to mimic 2OHOA action on membrane lipid composition.**

| | 12 h | | 24 h | | 48 h | | 72 h | |
|---|---|---|---|---|---|---|---|---|
| | Control | 2OHOA | Control | 2OHOA | Control | 2OHOA | Control | 2OHOA |
| PSM | 5.3 | 15.0 | 6.8 | 20.3 | 8.4 | 26.8 | 10.1 | 30.9 |
| POPC | 40.6 | 39.9 | 36.2 | 29.4 | 39.7 | 32.3 | 42.4 | 32.5 |
| POPE | 22.6 | 17.1 | 23.6 | 19.0 | 22.9 | 15.0 | 23.2 | 10.7 |
| Cho | 31.5 | 28.0 | 33.4 | 31.3 | 28.9 | 25.9 | 24.3 | 25.9 |

Values were calculated according to the experimental values for phospholipid and cholesterol composition obtained during the time-dependent incubation of U118 cells in the presence or absence of 2OHOA (200 µM;Figure 2-5 and Figure 2-6) and are expressed as mole%. Cho, Cholesterol.

As mentioned above, the steady-state fluorescence anisotropy of DPH (DPH <r>; Equation 3) is a parameter that reflects the global order of the acyl chains of the lipid bilayer membrane (de Almeida *et al.*, 2003). For liposomes resembling 48 and 72 h treated cell membranes, DPH <r> was higher than that of liposomes mimicking control (untreated) cell membranes (Figure 4-5A), indicating an increase in the general lipid order. Figure 4-5B shows that changes in phospholipid composition clearly induced an increase in *t*-PnA $\tau_{long}$ values indicating that the $l_o$ domains became more ordered and more compact. The mean fluorescence lifetime (Equation 5) of *t*-PnA ($\tau$) paralleled the long lifetime component (Figure 4-5C). This suggests that the major changes in phospholipid composition occurred at the $l_o$ domains, and not in the disordered ones. Because the cholesterol mole fraction did not change severely (Table 4-1), it is reasonable to explain this increase in the lipid bilayer order through a SM-enrichment of the $l_o$ domains, which was expected taking into account the changes observed in lipid composition.

To interpret quantitatively the results obtained we mapped the compositions studied in a phase diagram, which are available for ternary lipid mixtures (Marsh,

2009). The best diagram to represent the liposomes used in the present study is the ternary lipid system POPC/PSM/Cholesterol at 23ºC (de Almeida *et al.*, 2003). It was considered that POPE is equally distributed between PC and SM and the mole fractions were thus recalculated (Table 4-2).

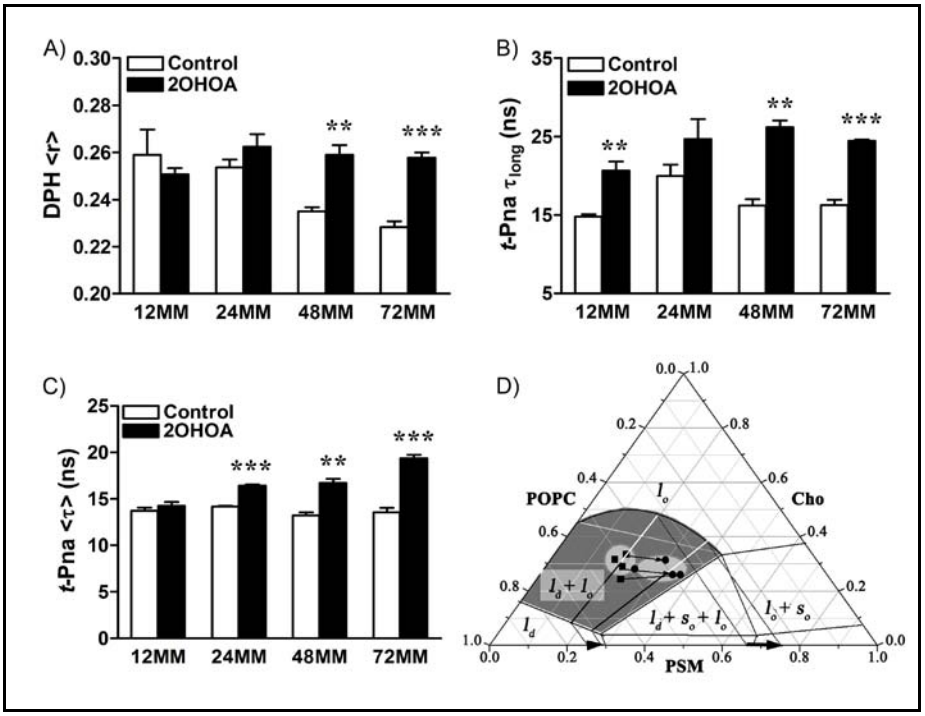


**Figure 4-5. 2OHOA-induced phospholipid composition changes lead to significant biophysical alterations in model membranes.**
(A) Steady state fluorescence anisotropy, <r>, of DPH; (B) Long lifetime component of the mean fluorescent lifetime, $<\tau>_{long}$, of *t*-Pna. (C) The mean fluorescence lifetime <τ> (Eq. 5) of *t*-PnA. All these measurements were done on PC:PE:SM:Cholesterol MLVs at 24ºC; (D) Ternary phase diagram of POPC/PSM/Cholesterol at 23ºC including the compositions of liposomes mimicking control (squares) or treated (balls) cells recalculated in Table 4-2. The fraction of $l_d$ and lo domains were calculated using the diagram tie-line and the lever rule (Marsh, 2009). The gray region represents the raft region ($l_d$+$l_o$). All the experimental points are within this region which is the physiologically relevant of the phase diagram. The region around them is shaded to stress out the average behavior. The black to white lines represent the $l_o$ to $l_d$ molar ratios in each case. The black arrows on the PSM axis show the increase in SM content of the non-raft (small arrow) and of the raft fraction of the membrane (large arrow). It can be clearly seen that the raft fraction is much more SM-enriched upon 2OHOA treatment. MM: model membrane mimicking the lipid composition of control and 2OHOA treated cells (200 µM, 12-72 h). Values represent the mean ± SD, n=3. The asterisks indicate a significant effect of the treatment as compared with the control (***P* < 0.01; ****P* < 0.001).

Then, these compositions were mapped in the ternary phase diagram (Figure 4-5D), and the fraction of $l_d$ and $l_o$ domains was calculated using the diagram tie-line and the lever rule (Marsh, 2009). From the calculations, it was concluded that the $l_o$ phase fraction may increase ca. 5-10 mole% upon 2OHOA treatment, but the SM content of the $l_o$ domains can increase by more than 15 mole%, i.e., virtually all of the SM induced by the treatment is incorporated into $l_o$ domains, from where POPC and even cholesterol could be depleted. This is in agreement with the preceding results, where the observed increase in the global order of the bilayer membrane (Figure 4-5A) could be mainly explained by a much higher order and packing of the $l_o$ domains (Figure 4-5B), rather than by a marked increase in their relative abundance.

**Table 4-2. Recalculated lipid mole fractions mapped in the phase diagram.**

| | 12 h | | 24 h | | 48 h | | 72 h | |
|---|---|---|---|---|---|---|---|---|
| | Control | 2OHOA | Control | 2OHOA | Control | 2OHOA | Control | 2OHOA |
| SM | 16.6 | 23.5 | 18.6 | 29.8 | 19.9 | 34.3 | 21.7 | 36.3 |
| PC | 51.9 | 48.4 | 48.0 | 38.9 | 51.2 | 39.8 | 54.0 | 37.8 |
| Cho | 31.5 | 28.0 | 33.4 | 31.3 | 28.9 | 25.9 | 24.3 | 25.9 |

The lipid mole fractions were calculated considering the system a ternary mixture of PC/SM/Cholesterol in order to compare with the published phase diagram. Values are expressed as mole%. Cho: Cholesterol.

### 4.2.2 Effect of 2OHOA on the biophysical properties of cell membranes

In this section we focused not only on the changes induced by 2OHOA in the phospholipid headgroups but also in the acyl-chain remodeling described in *chapter 3*, as well as in the changes in sphingolipids described in *chapter 2*. To do this, we analyzed the biophysical properties of liposomes reconstituted from total lipid extracts obtained from control and treated U118 cells, labeled with either *t*-PnA or DPH. For simplification, from now on and within this chapter, “liposomes reconstituted from total lipid extracts” will be referred to as “lipid extracts”.

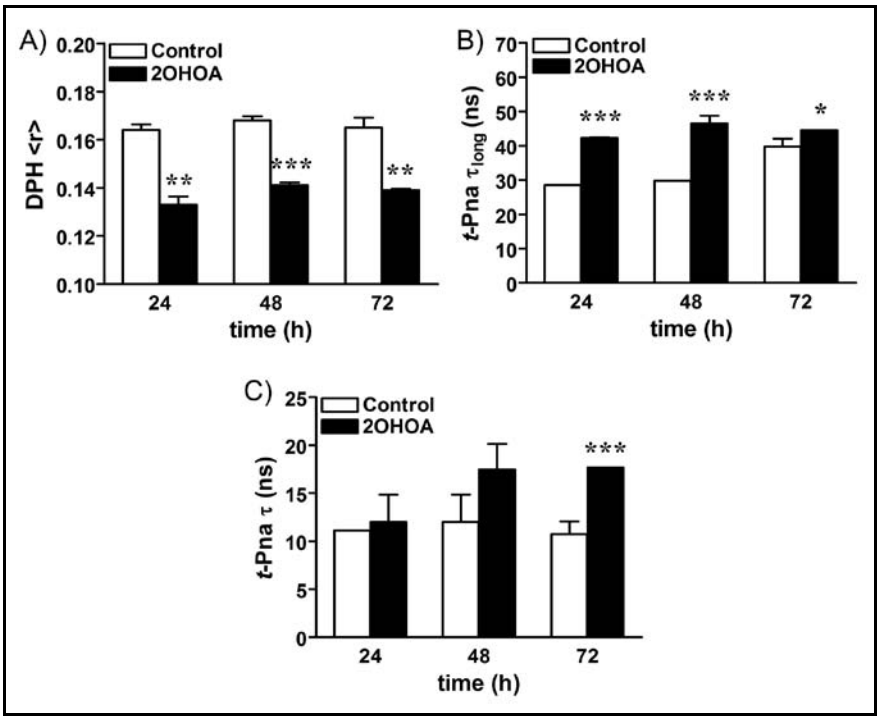


**Figure 4-6. 2OHOA induced a decrease of the global membrane order while the $l_o$ domains became more ordered in reconstituted liposomes.**
DPH anisotropy, <r> (A), *t*-Pna long lifetime component, $<\tau>_{long}$ (B) and *t*-Pna mean fluorescence lifetime, <τ> (C) of lipid extracts from control and treated cells (200 μM, 24, 48 and 72 h) reconstituted into liposomes. Values represent the mean ± SEM, n= 3. The asterisks indicate a significant effect of the treatment as compared with the control (*$P < 0.05$; **$P < 0.01$; ***$P < 0.001$).

Contrary to what it was observed with artificial membranes in the previous section, DPH <r> decreased when compared to control lipid extracts at all times of treatment, indicating a general decrease of the membrane global order (Figure 4-6A). As shown in Figure 4-6 B, changes in lipid composition induced an increase in *t*-PnA $\tau_{long}$ indicating that the $l_o$ domains became more ordered and more compact, in agreement with the observations in artificial membranes. It is usually considered that, at room temperature, the lipid phase is $l_o$ if its *t*-PnA $\tau_{long}$ value is below 30 ns, and it is a gel phase when this value is over 30 ns (de Almeida *et al.*, 2009). In these experiments, *t*-PnA $\tau_{long}$ value was generally below 30 ns for the controls, indicating the presence of sphingolipid-cholesterol enriched domains (lipid rafts). However, the value was always much longer than 30 ns in the treated samples, indicative of a possible sphingolipid-

enriched gel-like phase. In addition, the mean fluorescence lifetime (Equation 5) of *t*-PnA (τ) showed a trend that paralleled the long lifetime component (Figure 4-6 C), indicating that the increased lipid packing of the $l_o$ domains is the major factor affecting *t*-PnA fluorescence lifetime. The opposite behavior of *t*-PnA (τ) compared to the DPH <r>, also indicated that the $l_o$ and $l_d$ domains of the membrane were differently affected by 2OHOA.

### 4.2.3 Partition of free 2OHOA partially explained the changes in the biophysical properties of membranes

Considering the results of the previous sections, the next question raised was whether the partition of free 2OHOA into membranes could explain the differences observed between artificial membranes and lipid extracts DPH <r> values. To address this issue, large unilamellar vesicles (LUVs) mimicking the composition of control and treated cells after a 24 h treatment (Table 4-1), were prepared and incubated with or without 2OHOA (5 or 20 mole%) for 1 h before the measurements. As it was explained in the *Experimental procedures* section, 5 mole% would represent the concentration of 2OHOA most commonly used in this study, i.e., 200 μM. Here, model membranes (MM) mimicking the composition of control cells incubated with 2OHOA (C + 5/20 mole% 2OHOA) would reflect the initial situation of a treatment, i.e., when 2OHOA first encounters cells, while MM mimicking the composition of treated cells incubated with 2OHOA (T+ 5/20 mole% 2OHOA) would represent the composition of lipid extracts at the end of the 24 h treatment.

In agreement with the results obtained with artificial liposomes, DPH <r> of MM mimicking treated cells (T) was higher than that of control cells (C; Figure 4-7A-B). When 5 mole% of 2OHOA was added, DPH <r> decreased only in MM mimicking treated cells (T + 5 mole% 2OHOA), although this value was still higher than that of MM mimicking control cells. These results indicated that the partition of free 2OHOA decreased the global order of the acyl chains of glycerophospholipids. Consistently, the reduction in DPH <r> was more pronounced when 20 mole% of 2OHOA was added to the MM (T + 20 mole% 2OHOA; Figure 4-7 B). Nevertheless, the addition of 2OHOA to MM did not reduce DPH <r> to the extent observed for lipid extracts (Figure 4-6 A). Therefore, the partition of free 2OHOA into membranes may only partially explain the decrease in DPH <r> observed for lipid extracts. This discrepancy may be due to: i) the changes in other fatty acids; ii) the differences in lipid composition between MM and lipid extracts; and iii) the difference between 2OHOA as free fatty acid or incorporated into glycerophospholipids.

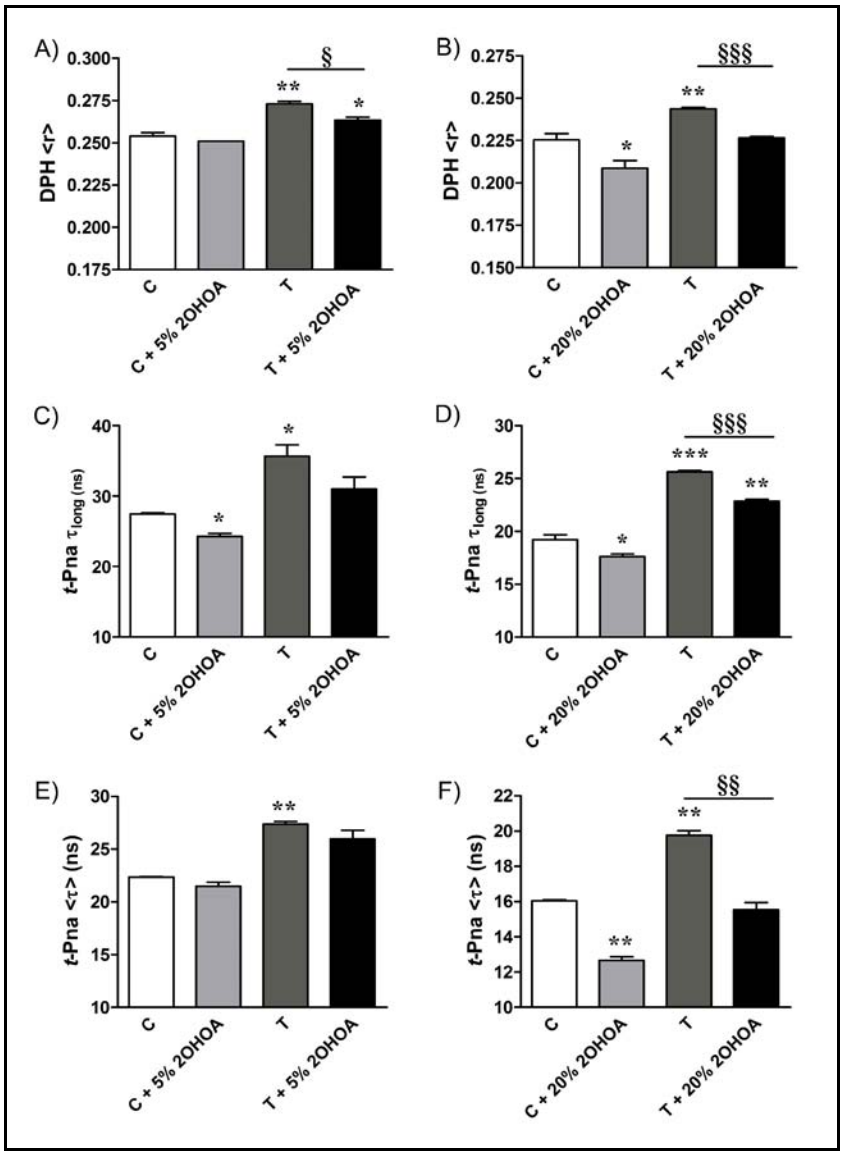


**Figure 4-7. Partition of free 2OHOA explained in part the effects on the biophysical properties of the membranes.**

(A-B) Steady state fluorescence anisotropy, <r>, of DPH; (C-D) Long lifetime component of the mean fluorescent lifetime, $<\tau>_{long}$, of *t*-Pna. (E-F) The mean fluorescence lifetime <τ> (Eq. 5) of *t*-PnA. All these measurements were done on PC:PE:SM:Cholesterol mixtures at 24ºC with or without the addition of 2OHOA (5 mole%, A, C, E; and 20 mole%, B, D, F); All the experiments were performed with LUVs mimicking the 24 h lipid composition of Control (C) and Treated (T) cells. The asterisks indicate a significant effect as compared with the control (**P* < 0.05; ***P* < 0.01; ****P* < 0.001). In this case, § indicates a significant effect of the addition of 2OHOA (T + 2OHOA) as compared with the composition of treated cells (T) (§*P* < 0.05; §§*P* < 0.01; §§§*P* < 0.001).

As expected from the results with artificial liposomes (Figure 4-5B), MM mimicking treated cells showed increased *t*-Pna $\tau_{long}$ when compared to control ones (T vs. C; Figure 4-7C-D). In this case, the presence of 5 mole% of 2OHOA induced a slight decrease of *t*-Pna $\tau_{long}$ only in MM mimicking control cells (Figure 4-7C), an indication that 2OHOA partitions in both $l_d$ and $l_o$ domains. In addition, higher amounts of 2OHOA (20 mole%) did not counteract the ordering effect of the increase in SM because, despite the decrease in *t*-Pna $\tau_{long}$ in MM mimicking treated cells, this value still remained higher than in the MM mimicking control cells. In addition, the mean fluorescence lifetime (Equation 5) of *t*-Pna ($\tau$) showed a trend that parallels the long lifetime component (Figure 4-7 E-F).

Since the alterations in lipid headgroup composition explained the increased order of the $l_o$ domains, and neither that nor the partition of free 2OHOA explain the increased disorder of $l_d$ domains, this latter effect must be due to the alterations in lipid acyl chain composition of the $l_d$ domains.

## 4.3 Lipid raft became more ordered and more compact

In this chapter, we used a biophysical approach to understand the effects that changes in both phospholipid and fatty acid composition would have on cell membrane biophysical properties.

In model membranes mimicking the lipid composition of U118 cell membranes before and after treatment with 2OHOA, we observed a slight increase in the fraction of $l_o$ domains, but a rather marked rise in the membrane hydrophobic core packing, probably associated with an increase in the size of these domains (Figure 4-5). Consequently, the global membrane order was enhanced. These biophysical effects were due to the substantial increase in SM content, as the amount of cholesterol was only modestly modified. In this context, previous studies in membrane model systems have shown that both an increase in SM content and an increase of the $l_o$ phase fraction lead to the formation of larger size domains (Figure 4-8; de Almeida *et al.*, 2005). Therefore, the alterations in phospholipid composition observed in treated cells significantly modified the biophysical properties of the cell membrane, particularly the packing of SM/cholesterol-enriched $l_o$ domains, and consequently, the membrane's lateral reorganization. Because SM plays a relevant role in the formation and regulation of lipid rafts, which in turn influence signal transduction and membrane trafficking (Escribá *et al.*, 2008; Simons & Toomre, 2000), this change in the structure of

membrane microdomains might alter the interaction of relevant peripheral signaling proteins with the membrane and the subsequent propagation of messages into the cell.

Increased compactness of the $l_o$ domains was also observed in lipid extracts from treated cells reconstituted into liposomes when compared to control (untreated) cells (Figure 4-6). However, in this case, the global order of the membranes decreased in lipid extracts from treated cells. These results indicated that not only the changes in the phospholipid headgroup but also in the fatty acid composition, such as the incorporation of 2OHOA, were strongly affecting membrane domains. Thus, while the increase in $l_o$ domains order/packing would be mainly due to the strong increase in SM content, the profound changes in fatty acid composition would account for the decrease in global order. Nevertheless, it cannot be ruled out that the presence of TAG in the artificial membranes could influence the decrease in the global order, although the solubility of TAG in cholesterol-containing liposomes is extremely low (Khandelia *et al.*, 2010).

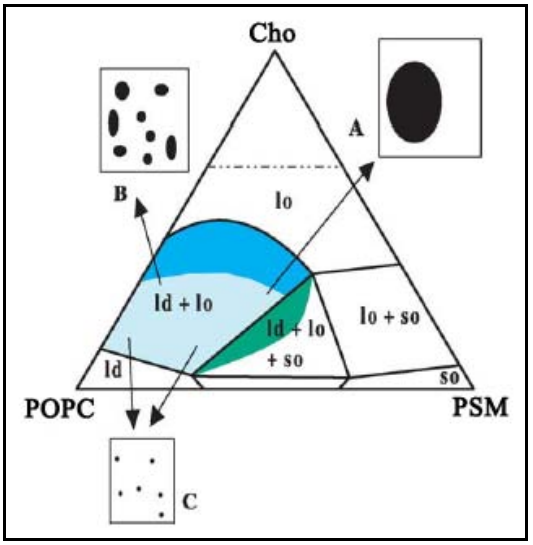


**Figure 4-8. PSM/POPC/Cho phase diagram at 23°C, showing also the boundaries and schematic illustrations of the size of lipid rafts.**
Rafts are present in the blue-shaded area ($l_d/l_o$, coexistence). In the darker area, $l_o$ predominates over $l_d$, and the opposite situation occurs for the light-shaded area. Rafts can also exist in the green-shaded area, where there is coexistence of three phases, but the $s_o$ phase is present only in very low amounts. Insets: (a) region of large rafts; detected by microscopy and FRET (>75–100 nm); (b) region of intermediate size rafts: detected by FRET but not by microscopy (between ~20 nm and ~75–100 nm); (c) region of small rafts: not detected by FRET nor microscopy (< 20 nm; de Almeida *et al.*, 2005).

The $l_o$ domains in artificial membranes maintained the properties of such lipid structures, as *t*-Pna $\tau_{long}$ was below 30 ns in artificial liposomes. However, in lipid extracts, where all lipid changes are represented, results pointed to the appearance of a different type of domain, instead of the appearance of additional very disordered domains. Because of the high value of the long lifetime component of *t*-Pna (*t*-Pna $\tau_{long}$>>30 ns), it cannot be ruled out that part of the $l_o$ domains become so ordered and rigid that they can exclude DPH. The opposite would happen to $l_d$ domains that would thus become even more disordered. If this composition alteration would lead to a coalescence of $l_o$ domains, decreasing the ordered/disordered interfacial regions, or would be accompanied by a small decrease of total $l_o$ domain fraction, the anisotropy of DPH would decrease because in fact the global order of the membrane would be smaller, but the mean fluorescence lifetime of *t*-PnA would increase, because its fluorescence stems primarily from the $l_o$ domains. This would explain the opposite behavior observed for both probes in total lipid extracts. The presence of gel-like or solid-ordered phase has been implicated in situations of cellular stress, apoptotic or pathological conditions.

A more rigid gel-like domain formation could also be explained by the increase in Cer, the accumulation of Sph, or even by the accumulation of dhSM, as determined by MS analysis in membranes from 2OHOA-treated cells. In a ternary model system of palmitoyl-ceramide (PCer), PSM and POPC characterized by the same two fluorescent membrane probes that were used in this study; PCer recruits POPC and PSM in the fluid phase to form extremely ordered and compact gel domains. Gel domain formation by low PCer mole fraction (up to 12 mole%) is enhanced by physiological PSM levels (20–30 mole% total lipid). For higher PSM content, it was shown that a three phase situation, consisting of fluid (POPC-rich)/gel (PSM-rich)/gel (PCer-rich) coexistence is possible (Castro *et al.*, 2007). Sphingosine, at 5–15 mole% total lipids, was shown to rigidify gel domains in liposomal and erythrocyte ghost membranes, raising their melting temperatures and increasing the transition cooperativity. Structural defects originating during the lateral phase separation of the “more rigid” and “less rigid” domains caused the leakage of aqueous solutes to the extravesicular medium (Contreras *et al.*, 2006). DhSM rigidifies $l_o$ domains in giant unilamellar vesicles of PC:PE:dhSM:Cholesterol (1:1:1:1 mole ratio), inducing the formation of $s_o$ phases interspersed in the $l_o$ domains. In cells, increasing amounts of dhSM, induced by cell treatment with two desaturase inhibitors or by knockdown of desaturase expression, correlated with lower cell susceptibility to HIV-1 infection (Vieira *et al.*, 2010).

In addition, the results obtained from the present study indicated that partition of free 2OHOA does not counteract the effects of the changes in lipid composition (Figure 4-7). In general it was observed that at a high concentration of 2OHOA (20 mole%, far

above the ones used to treat the cells) slightly reduced the global order of the membrane as well as the order of the $l_o$ domains. At low concentrations (5 mole%, similar to those used to treat the cells), 2OHOA did not have any effect or this was rather small when compared to the effect of the changes in lipid composition. Therefore, a plausible explanation for the strong decrease in the global order may be the incorporation of 2OHOA in the glycerophospholipids PC and PE. Although the effect of such hydroxylated glycerophospholipids in the biophysical properties of fluid domains is yet to be studied, it was found that the presence of 2-hydroxylation in the fatty acyl chain of sphingolipids in *S. cervisiae* cells significantly reduces acyl chain packing of their sphingolipid-enriched domains (Aresta-Branco *et al.*, 2011). In this way, both effects would be explained: reduced global order caused by the incorporation of 2OHOA into the phospholipids (and possibly increased PUFA content) and increased compactness of the ordered domains due to accumulation of SM. Finally, the fact that the variation in *t*-PnA average lifetime parallels that of its long component indicates that there are no significant alterations in the fraction of $l_o$ and $l_d$ domains.

It is worth to point out that the changes in the biophysical properties observed in this study were due to changes in total cell lipid composition. Therefore, a more accurate study focused on the plasma membrane would be necessary. In fact, this aspect was addressed without successful results. On the one hand, the induction and isolation of plasma membrane blebs was tested, but the protocol provoked cellular stress, affecting the lipid composition of the plasma membrane and consequently, biasing the biophysical properties of membranes (data not shown). On the other hand, we tried to obtain plasma membrane after cell fractionation, but the purity of the fractions was not as expected in order to carry out this type of study.

In summary, 2OHOA affected the properties of both $l_o$ and $l_d$ domains and induced the formation of membrane microdomains with biophysical properties different from the existing ones. Because many proliferative signals start at the plasma membrane, the changes found here could influence signaling in cancer cells. Thus, 2OHOA induced complex changes in the glioma cell membranes lipid composition that would lead to significant changes on the biophysical properties of cell membranes, and thus to a membrane lateral reorganization, which may in part explain 2OHOA biological action.

# 5 Effect of 2OHOA on the lipid composition of tissues

In order to study whether 2OHOA affects the lipid composition of tissues, we determined the individual glycerophospholipid classes, cholesterol levels and phospholipids fatty acid composition of the liver, heart, and brain of untreated and 2OHOA-treated CD-1 mice (600 mg $kg^{-1}$ $day^{-1}$, 10 days).

The effect of 2OHOA on mice tissues glycerophospholipid composition is shown in Figure 5-2 (A-C). Thus, tissue glycerophospholipid composition was not significantly altered by 2OHOA neither had changed cholesterol content in treated mice (Figure 5-1). Likewise, fatty acid composition, analyzed by gas chromatography in basic conditions, was not affected in treated mice compared to control (Table 5-1). Only 18:1n-9 decreased 23% in liver PE.

Hence, 2OHOA did not significantly affect either glycerophospholipid or fatty acid composition of brain, liver and heart of healthy mice. Nevertheless, it remains to be determined whether 2OHOA is incorporated in tissue lipids.

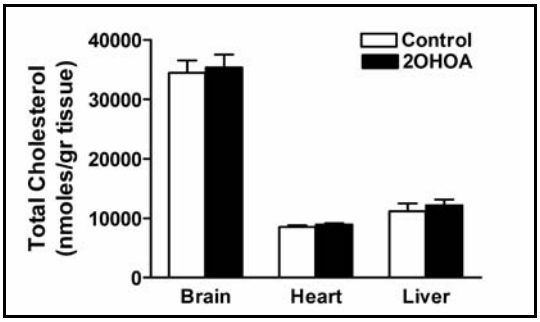


**Figure 5-1. Effect of 2OHOA treatment on brain, heart and liver total cholesterol content.**
Total cholesterol mass from brain, heart, and liver of mice treated with 2OHOA (600 mg $kg^{-1}$ $day^{-1}$, 10 days). After treatment, lipids were extracted and the total cholesterol mass was determined by an iron binding assay according to the *Experimental procedures* section. Values represent mean ± SD, n = 4-5.

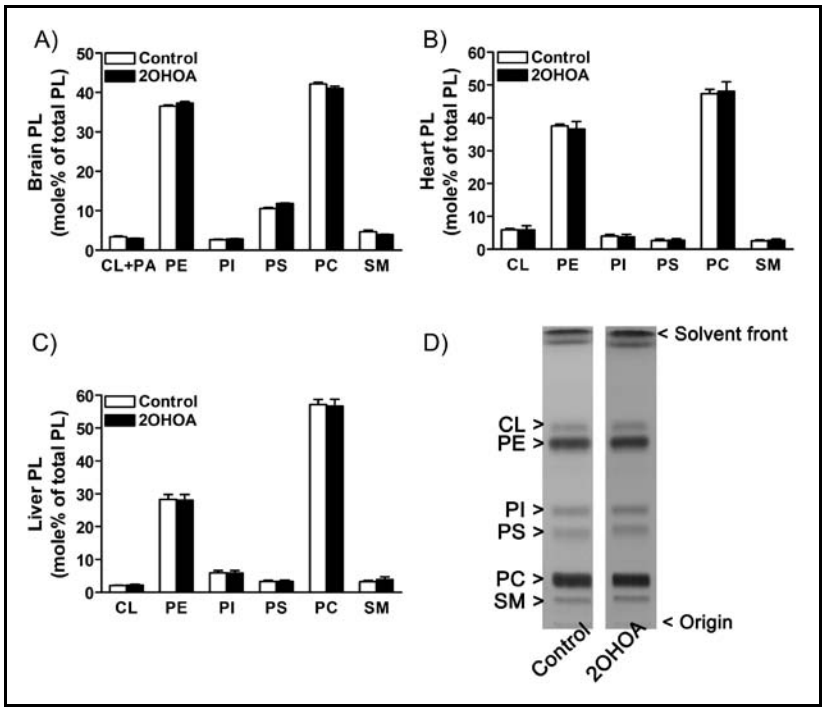


**Figure 5-2. Effect of 2OHOA treatment on brain, heart and liver phospholipid composition.**
(A) Brain, (B) Heart, and (C) Liver glycerophospholipid composition of mice treated with 2OHOA (600 mg $kg^{-1}$ $day^{-1}$, 10 days). After treatment, lipids were extracted and analyzed by TLC. The glycerophospholipids mass was determined by assaying for the lipid phosphorus content of individual lipid classes separated by TLC, according to the *Experimental procedures section*. Values are expressed as mole% and represent mean ± SD, n = 4-5. (D) Representative TLC plate stained with iodide.

Thus, the lack of changes in tissues lipid composition might be related to the low toxicity shown in other studies and complements the previous findings of this work, where it was shown that non-tumor MRC-5 cells were not significantly affected by 2OHOA. The low toxicity of the compound is an important feature of the lipid therapy with 2OHOA (Martínez *et al.*, 2005b). In this study, the authors were unable to determine the maximally tolerated dose of this drug because after treatments up to 3 g $kg^{-1}$ per day for 2 weeks, the animals were still alive. Histological analyses of several rat organs showed that high doses of 2OHOA (1.2 g $kg^{-1}$ $day^{-1}$ p.o.) did not induce observable toxicity. In this context, the tissues analyzed here (brain, liver and heart) might have regulatory controls of lipid metabolism capable of maintaining a relatively normal lipid pattern facing 2OHOA treatment (Thompson, 1992).

**Table 5-1. Effect of 2OHOA on PE fatty acid composition from brain, heart and liver.**

| | Brain | | Heart | | Liver | |
|---|---|---|---|---|---|---|
| | Control | 2OHOA | Control | 2OHOA | Control | 2OHOA |
| FAME | Mean ± SD | Mean ± SD | Mean ± SD | Mean ± SD | Mean ± SD | Mean ± SD |
| 16:0 | 7.3 ± 0.4 | 7.5 ± 0.2 | 8.3 ± 0.5 | 7.9 ± 0.6 | 23.2 ± 1.5 | 22.9 ± 2.5 |
| 18:0 | 25.0 ± 0.6 | 25.1 ± 0.6 | 26.2 ± 1.5 | 27.7 ± 1.7 | 16.6 ± 1.7 | 19.2 ± 2.3 |
| 18:1n-9 | 11.9 ± 0.7 | 11.7 ± 0.7 | 7.4 ± 1.3 | 6.4 ± 1.1 | 7.8 ± 1.2 | 6.0 ± 0.6* |
| 18:1n-7 | 3.2 ± 0.3 | 3.2 ± 0.2 | 3.7 ± 0.4 | 3.9 ± 0.3 | 3.1 ± 1.0 | 3.2 ± 0.6 |
| 22:0 | 0.9 ± 0.1 | 1.1 ± 0.8 | 0.9 ± 0.2 | 1.2 ± 0.2 | 1.1 ± 0.2 | 0.9 ± 0.1 |
| 20:4n-6 | 15.2 ± 0.4 | 15.5 ± 0.6 | 9.4 ± 1.4 | 9.5 ± 1.0 | 19.4 ± 1.2 | 18.9 ± 2,0 |
| 24:0 | 5.7 ± 0.2 | 6.0 ± 0.5 | 1.2 ± 0.4 | 1.3 ± 0.2 | 0.7 ± 0.1 | 0.1 ± 0.3 |
| 22:6n-3 | 26.5 ± 0.2 | 25.6 ± 1.0 | 33.6 ± 1.7 | 33.4 ± 1.4 | 17.4 ± 0.8 | 21.0 ±1.5** |

Mice were treated with 2OHOA (600 mg $kg^{-1}$ $day^{-1}$) for 10 days. After each treatment, lipids were extracted and analyzed by TLC. Then PE acyl chains were converted to FAME in basic conditions and analyzed by gas chromatography. Values are expressed as mole% and represent mean ± SD, n = 4-5. The asterisk (*) indicates a significant effect of the 2OHOA treatment as compared with the control (*$P < 0.05$).

# 6 DISCUSSION

Lipid alterations are often associated with the etiology of important human diseases, such as atherosclerosis, infectious diseases, Alzheimer's disease and cancer. In cancer, although it has not been described a common feature among the different types of tumors, a number of lipid changes have been described. Among all of them, two were of special interest for this study. Thus, altered phospholipid levels were described in different human tumor tissues compared to their normal non-tumors counterparts (Reviewed by Hendrich & Michalak, 2003). Moreover, increased oleic acid content and reduced stearic acid content have been usually found in tumors, in comparison to the non-tumor tissues (Meng *et al.*, 2004c; Mikirova *et al.*, 2004). Therefore, it is clear that a molecular understanding of the lipid contribution to the disease process would allow the development of novel approaches to prevention, diagnosis and cure of cancer and other diseases (van Meer *et al.*, 2008).

The participation of membrane lipids in cellular activities indicates that they might constitute targets for drugs whose pharmacological effects would be associated with the modulation of the physicochemical properties of membranes (Escribá, 2006). These are the foundations of the novel pharmacological approach called Membrane Lipid Therapy, which consists in the modulation of the structural and functional properties of cell membranes, by external means (Martínez *et al.*, 2005b). Thus, 2-hydroxyoleic acid (2OHOA) was designed based on this principle. From the molecular point of view, 2OHOA is a first-in-class anticancer drug because its mechanism of action is not shared by other drugs used for the treatment of cancer. In addition, within the heterogeneous family of the drugs used in the treatment of human glioma, 2OHOA is a best-in-class molecule, because it has greater efficacy and lesser toxicity than temozolomide and other drugs used to treat this condition (Terés *et al.*, 2011).

Although some of the mechanisms of action induced by 2OHOA have been elucidated, the way this molecule exerts its anticancer action without killing normal cells is not fully understood. Neither the regulatory effects of 2OHOA on membrane lipids were known. To address this point we analyzed whether 2OHOA modified the lipid composition of tissues and cells. This study describes for the first time not only the effects of 2OHOA on the lipid composition of membranes but also elucidates part of its metabolism, i.e., its entrance into the cells, its accumulation and incorporation into different lipid classes. The results of this study indicate that the lipid composition of human cancer cells was greatly altered. According to our analyses a large number of changes occurred, affecting the levels of glycerolipids, glycerophospholipids, and sphingolipids as well as the fatty acyl composition. Among these changes, the present study focused mainly on two. First, the net increase in SM mass via direct and specific

activation of SMS; and second, the decrease in oleic acid, via SCD1 inhibition and its substitution by 2OHOA. Consequently, these changes had an impact on the structure of membrane microdomains.

The rapid SMS activation by 2OHOA indicated that this could be one of the first critical events in its effect against tumors. The striking increase in plasma membrane SM, an important component of 'lipid rafts', led to modifications of the lipid bilayer properties (Futerman & Hannun, 2004). Hence, if lipid rafts containing a given set of proteins can change their size and composition in response to intra- or extracellular stimuli; this will modulate specific protein–protein interactions, resulting in the activation or inhibition of signaling cascades (Simons & Toomre, 2000). These effects could include FasR capping or Ras translocation from the membrane to the cytosol, which have been associated with the induction of apoptosis and autophagy, respectively (Lladó *et al.*, 2010; Terés *et al.*, 2011). It is worth mentioning that the markedly lower levels of SM in cancer cells suggested that the malignant transformation of glioma and other cancer cells not only requires the activation of certain oncoproteins (e.g., Ras) but also, the modification of the membrane structure to permit their membrane docking and proliferative signal propagation. Therefore, the alterations found in the lipid composition of cancer cell membranes appeared to be crucial in the activation of tumorigenesis. Figure 6-1 and Figure 6-2 depict the model where the results presented in this study are related with the antitumor effect of 2OHOA.

Two different molecular mechanisms are known to be activated by 2OHOA in cancer cells. In leukemia cells, 2OHOA induces FasR capping and activates extrinsic apoptosis pathway (Lladó *et al.*, 2010) while in human glioma and lung cancer cells, 2OHOA induces translocation of Ras from the membrane to the cytosol and cell cycle arrest, which is followed by cell differentiation and autophagy (Lladó *et al.*, 2010; Terés *et al.*, 2011). Both these mechanisms may be triggered by the significant alterations that 2OHOA induced, increases in membrane SM and changes in the fatty acid profiles, on the properties of both $l_d$ and $l_o$ domains. Indeed, Ras has a bulky isoprenyl lipid anchor and requires $l_{\mathrm{d}}$ microdomains with loose surface packing (e.g., PE-rich domains) to permit its insertion into the membrane, which is necessary for subsequent interactions of Ras with upstream (e.g., EGFR) and downstream (e.g., Raf) proteins in the MAPK pathway (Figure 6-2). The alteration of both $l_d$ and $l_o$ domains could also result in the inactivation of the MAPK pathway. Through cross-talk, this inhibition can impair the PI3K/Akt pathway and the cell cycle machinery (cyclin/cdk complexes). Additionally, SCD1 inhibition by 2OHOA could contribute to the inactivation of the Akt pathway since knockdown of SCD1 reduces Akt phosphorylation and activity in cancer cells (Fritz *et al.*, 2010; Scaglia & Igal, 2008). In turn, as a feedback mechanism, Akt and MAPK pathways regulate the process of lipogenesis in mammalian cells (Plas &

Thompson, 2005; Porstmann *et al.*, 2005). The sustained activation of SMS increases 1,2-DAG synthesis, which together with the presence of 2OHOA in membranes, would be involved in the relatively sustained and mild activation of PKC (ca. 3-fold; Cerbon & del Carmen Lopez-Sanchez, 2003; Martínez *et al.*, 2005b). This activation could lead to the overexpression of the CDK inhibitors, $p21^{Cip1}$ and $p27^{Kip1}$, which are associated with the hypophosphorylation of the pRb, and the ensuing inhibition of E2F-1 and β-catenin (Martínez *et al.*, 2005a; Martínez *et al.*, 2005b; Terés *et al.*, 2011). The cellular outcome of these molecular processes is the inhibition of cell growth, and the induction of cell differentiation and autophagy (Gwak *et al.*, 2006; Gwak *et al.*, 2009; Jiang *et al.*, 2010; Lladó *et al.*, 2009; Terés *et al.*, 2011). In addition, the accumulation of sphingolipids in lysosomes could also contribute to the induction of autophagy.

On the other hand, the FasR oligomerizes in the presence of the Fas ligand, which initiates the formation of the death-inducing signaling complex (DISC) that activates the "extrinsic" caspase-8-mediated apoptosis pathway. In this context, 2OHOA provokes the clustering (capping) of FasR to defined cell membrane areas, favoring spontaneous interactions of FasR subunits and ligand-free induction of apoptosis in human leukemia cells (Lladó *et al.*, 2010). Previous studies have shown that alteration of lipid rafts by lipid-interacting molecules (including anticancer drugs) induces apoptosis in a ligand-free manner (Beneteau *et al.*, 2008; Gajate & Mollinedo, 2007). Moreover, FasR capping has been linked to SM synthesis (Miyaji *et al.*, 2005), such that the changes in the composition and structure of membranes induced by 2OHOA also explain the induction of apoptosis observed in Jurkat cells (Lladó *et al.*, 2010). Thus, a common molecular mechanism that activates SMS and increases the amount of SM in the membrane can induce either autophagy (glioma) or apoptosis (leukemia) in different cancer cells. Interestingly, a similar mechanism is described for edelfosine, a synthetic ether lipid with a high apoptotic activity which also induces reorganization of membrane rafts, FasR capping and cell apoptosis (Busto *et al.*, 2007; Conesa-Zamora *et al.*, 2005; Escribá, 2006; Gajate & Mollinedo, 2007; Jendrossek & Handrick, 2003). Thus, SM levels not only appear to be relevant in tumorigenesis but also in the molecular mechanism of action of 2OHOA against cancer.

Because 2OHOA is a potent and specific drug to combat tumors, with no side effects at therapeutic doses, the data presented in this study not only introduce the first known activator of SMS but also, define a novel molecular target for the design of new drugs against cancer. Considering the scarce information available on SMS proteins, we consider that this study may be helpful to future studies focused on understanding the regulation and role of these enzymes in the cell biology.

Figura 6-1. See next page

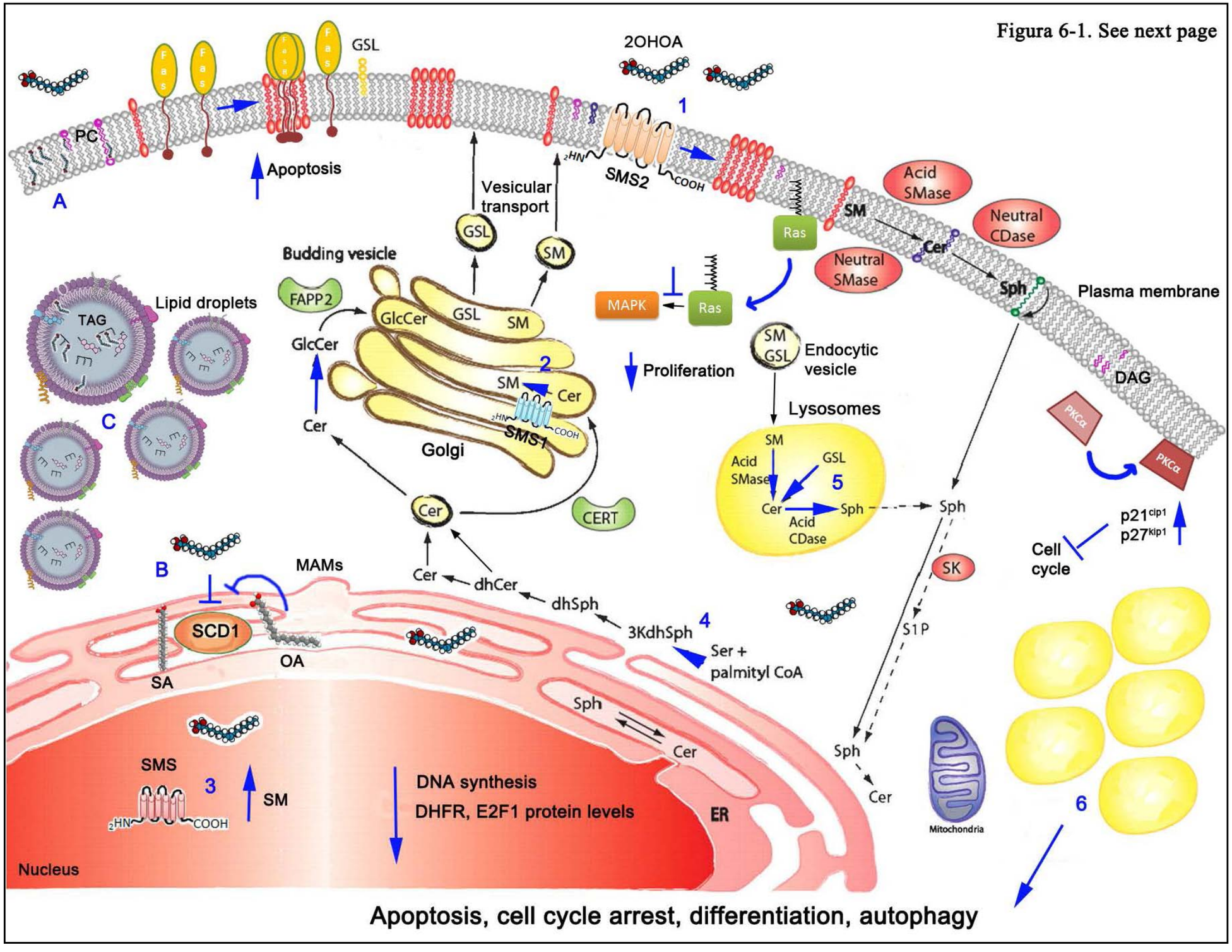

**Figure 6-1. Role of the lipid changes induced by 2OHOA in its antitumor mechanism.**
The model depicts our current view of the lipid changes in the effects of 2OHOA against tumors. The model includes new and reported data from our group, as well as data from the literature (see text). The activated lipid pathways are indicated by blue arrows. The sustained SMS activation by 2OHOA (1 and 2) increases the SM content at the plasma membrane leading to the deregulation of the sphingolipid metabolism evidenced by the activation of both the *de novo* synthesis (4) and the salvage pathway (5-6). In addition, 2OHOA provokes a profound remodeling of the cell fatty acid composition mainly caused by the incorporation of 2OHOA into the glycerolipids and glycerophospholipids (A and C) fractions and the inhibition of SCD1 (B). All together, these lipid changes affect the lipid raft properties as well as raft dependent signaling pathways, such as the Fas- and Ras-regulated (see Figure 6-2) pathways (Lladó *et al*., 2010; Miyaji *et al*., 2005; Terés *et al*., 2011). In addition, an increase in nuclear SM (3) may compromise DNA duplication (Albi & Magni, 1999; Albi *et al*., 2003), an effect that is reflected by the decrease in DHFR and E2F1, and that leads to cell cycle arrest, apoptosis or differentiation, all effects that can be observed after treatment with 2OHOA (Lladó *et al*., 2009; Martínez *et al*., 2005a).

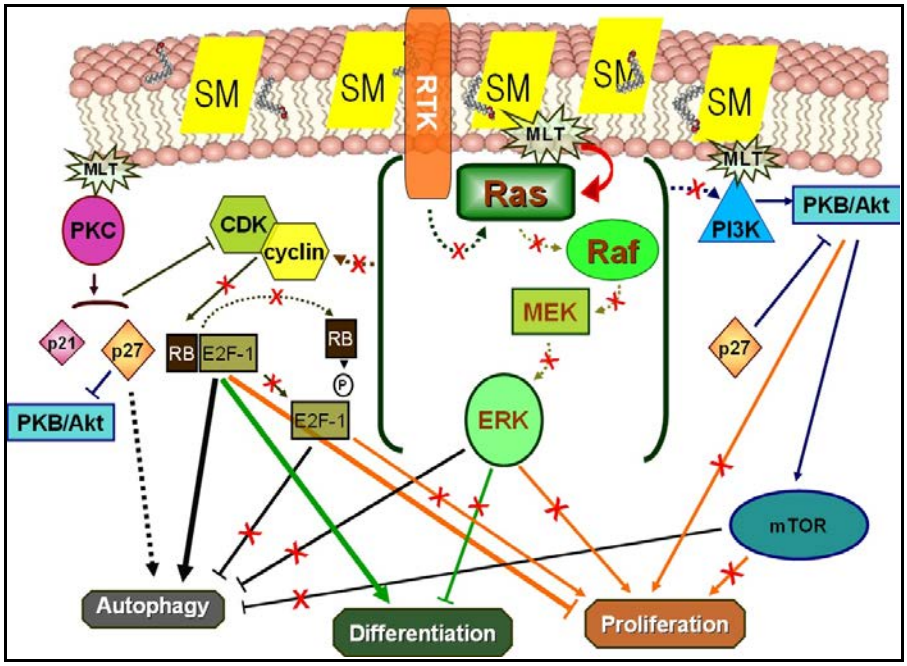


**Figure 6-2. 2OHOA mechanism of action in glioma.**
Scheme of 2OHOA molecular mechanism of action in human glioma cells. Signals that induce cell proliferation, loss of differentiation and survival, are often propagated through Receptor Tyrosine Kinases (RTK, e.g., EGFR) that activate Ras, which in turn activates Raf. Then, Raf activates MEK (MAPKK), which finally phosphorylates and activates ERK (MAPK). The Ras/MAPK signaling cassette regulates positively the PI3K/Akt and Cyclin/CDK pathways. The alterations of both $l_o$ and $l_d$ domains induced by 2OHOA, caused Ras translocation to the cytosol, preventing RTK-Ras and Ras-Raf interactions (which only occur at the plasma membrane) and impairing the signaling and cross-talk events mentioned above. MLT, membrane lipid therapy.

# 7 CONCLUDING REMARKS

Collectively, these results indicated that,

1. 2OHOA induced a profound effect on cell membrane lipid composition:
    a. 2OHOA induced an increase of SM mass and a decrease in PC and PE mass in several human cancer cells but not in the non-tumor cells MRC-5;
    b. These changes were time- and concentration- dependent and specifically related to the synthetic structure of the fatty acids used to treat cells;
    c. The increase in SM was due to a rapid and specific activation of SMS, which could be the first event triggered in the 2OHOA antitumor mechanism;
    d. The sustained activation of SMS and the ensuing SM accumulation provoked the deregulation of the sphingolipid metabolism, activating both the d*e novo* synthesis and the salvage pathway;
    e. 2OHOA dramatically affected fatty acid composition of lipids; mainly replacing oleic acid in phospholipids by 2OHOA and inhibiting SCD1.
2. The changes induced by 2OHOA on glioma cell lipid composition altered the biophysical properties of the membranes by inducing a complex reorganization of membrane lipid domains:
    a. The $l_d$ domains became more disordered, probably because of the changes in fatty acid composition;
    b. The $l_o$ domains became more rigid and compact, due to the robust SM enrichment;
3. Altogether these results support the idea that 2OHOA effects on membrane structure and composition would lead to its antitumor action. Specifically, the present results showing that cancer cells had lower SM content than non-tumor cells, indicate that SM levels in membranes are
        a. Relevant in the induction of tumorigenesis and
        b. Critical in the pharmacological mechanism of action of 2OHOA against glioma and possibly other types of cancer.

4. Mice tissue glycerophospholipid composition, glycerophospholipids fatty acids and cholesterol content were not significantly altered by 2OHOA, constituting a new evidence on the lack of toxicity of the drug.

# 8 Experimental procedures

## 8.1 Lipids

2OHOA was kindly provided by Lipopharma Therapeutics (Palma de Mallorca, Spain) and analyzed for its purity as it was described previously (Lladó *et al.*, 2009). 2-hydroxystearic acid (2OH-18:0) and 2-methyloleic acid (2Me-18:1n-9) were kindly provided by Dr. Oliver Vögler (Dpt. of Biology, University of the Balearic Islands, Palma). The rest of 2-hydroxy fatty acids were synthesized by Medalchemy, SL (Alicante, Spain). NBD-C6-PE, NBD-C6-PC, 1-palmitoyl-2-oleoyl-*sn*-glycero-3-phosphocholine (POPC), N-palmitoyl-sphingomyelin (PSM), and 1-palmitoyl-2-oleoyl-*sn*-glycero-3-phosphoethanolamine (POPE) were also purchased from Avanti Polar lipids (Alabaster, AL). Oleic acid and cholesterol were purchased from Sigma Chemicals Co (Madrid, Spain). NBD-C6-Cer, NBD-C6-SM and the probes *trans*-parinaric acid (*t*-PnA) and 1,6-diphenyl-1,3,5-hexatriene (DPH) were purchased from Invitrogen, Molecular Probes (Barcelona, Spain). NBD-C6-GlcCer was purchased from Larodan (Sweden). LUDOX (diluted 50 wt% colloidal silica in water) and cholesterol were from Sigma-Aldrich (Steinheim, Germany). [$H^3$]-palmitic acid was purchased from Amersham biosciences (Now GE Healthcare, England). Organic solvents for lipid and probe solutions were spectroscopic grade from Merck (Darmstadt, Germany).

## 8.2 Animals

The protocols used in this study were revised and approved by the Ethics Committee of the University of the Balearic Islands. CD-1 male mice (International Genetic Standard) were treated with 600 mg $kg^{-1}day^{-1}$ of 2OHOA during 10 days. After treatment they were killed by decapitation, and brains, hearts, and livers were snap frozen in liquid nitrogen and stored at -80ºC till processing.

## 8.3 Cell culture

The cell lines used in this work, human glioma (U118 and 1321N1), human non-small lung adenocarcinoma (A549), Jurkat-T lymphoblastic human leukemia cells, and non-tumor human fibroblast MRC-5 cells were obtained from the European Collection of Cell Cultures (ECCAC) through Sigma Aldrich Co (St Lous, MO). The human glioma SF767 cell line was obtained from the Brain Tumor Research Center Tissue Bank (San Francisco, CA). Cells were maintained at 37°C in a fully humidified atmosphere of 5% $CO_2$ in air. U118, A549, SF767, 13221N1 monolayer cultures and Jurkat suspension cultures were maintained in exponential growth using 2 mM glutamine-supplemented RPMI 1640 medium, containing 10% fetal bovine serum, 100 units/ml penicillin, 100 µg/ml streptomycin, and 0.25 µg/ml amphotericin B. In addition, the complete RPMI medium used for MRC-5 monolayers contained 1% non-essential aminoacids. Tissue culture medium and supplements were all purchased from Sigma (Madrid, Spain).

Monitoring and observation of morphological changes induced by 2OHOA were performed using an optical inverted microscope Leica DMIL (100 × or 400 ×, Leica Microsystems, Wetzlar, Germany). Pictures of control and treated cells were taken at different times of treatment, using a digital camera Coolpix 4500 (Nikon Corp., Tokyo, Japan) coupled to the inverted microscope.

## 8.4 Lipid extraction

Frozen tissues were homogenized with a tissue blender (Ultra-Turrax, Janke & Kunkel). Lipids were extracted using *n*-hexane/2-propanol (3:2 vol/vol, 1.8 ml/100 mg tissue). Tissue extracts were centrifuged at 1,000 *g* to pellet debris. The lipid-containing the organic phase was decanted and stored under nitrogen at −80°C until analysis.

Cellular lipids were extracted directly from the frozen monolayer of cells using a modified *n*-hexane/2-propanol (3:2, by volume) extraction method (Hara & Radin, 1978). After washing cells with phosphate-buffered saline (PBS; 137 mM NaCl, 2.7 mM KCl, 12 mM $Na_2HPO_4$, 1.38 mM $KH_2PO_4$, pH 7.4), lipids were extracted by addition of 2.2 ml of 2-propanol and the frozen cells were removed from the plate by scraping with a Teflon cell scraper. The 2-propanol was added to 6 ml of hexane and the cell dish was rinsed with 2.2 ml of 2-propanol, which was then combined with the hexane containing the first wash (Murphy *et al.*, 1997; Murphy *et al.*, 2000). Cell extracts were centrifuged at 1,000 *g* for 5 min at room temperature, to pellet the

denatured protein and other cellular debris. The lipid-containing organic phase was decanted and stored under a $N_2$ (g) atmosphere at -80ºC until analysis. The residual protein pellet was dried under a $N_2$ (g) atmosphere, and stored at -20ºC for protein analysis.

Alternatively, lipids were extracted by the method of Bligh and Dyer (Bligh & Dyer, 1959). Briefly, for each 1 ml of sample, 3.75 ml of 1:2 (v/v) $CHCl_3$:MeOH was added and vortexed thoroughly for 1 min. Then 1.25 ml of $CHCl_3$ was added and also vortexed thoroughly for 1 min. Finally 1.25 ml of 1 M NaCl was added and again vortexed thoroughly for 30 sec. Samples were centrifuge at 1,000 *g* for 5 min at room temperature to give a two-phase system (aqueous top, organic bottom) and the bottom phase was recovered and stored under a $N_2$ atmosphere at -80ºC until analysis. In order to measure the protein a 10 µl aliquot was taken from the sample before the extraction procedure and stored at -20ºC for protein analysis.

## 8.5 Protein analysis

Protein concentration in the pellet was measured using the bicinchoninic acid assay, according to manufacturer's instructions (Pierce Biotechnologies, Thermo Fisher Scientific, Rockford, USA). Briefly, this assay is based on the reduction of $Cu^{+2}$ to $Cu^{+1}$ by proteins in an alkaline medium, followed by colorimetric detection of the cuprous cation using bicinchoninic acid. Absorbance was then measured at 560 nm (Smith *et al.*, 1985).

Alternatively, the *RC DC* protein assay was used (Bio-Rad, Barcelona, Spain). It is a colorimetric assay for determining protein concentration in the presence of both reducing agents and detergents. This assay is based on a modification of the Lowry protocol, which involves the reduction of the Folin phenol reagent, and the absorbance is measured at 750 nm (Lowry *et al.*, 1951).

In both cases, the protein concentration was calculated interpolating absorbance values into a standard curve with known amount of bovine serum albumin (BSA; Pierce, part of Thermo Fisher Scientific, Rockford, USA).

## 8.6 Thin Layer Chromatography

Individual phospholipids classes and neutral lipids were separated by thin layer chromatography (TLC) or HPTLC. Advancement in TLC is termed high-performance

TLC (HPTLC; Sherma, 2000). HPTLC utilizes gel grades that are finer, allowing plates to be thinner and smaller. This allows for faster separation times and better separation efficiency. HPTLC has improved resolution and lowered detection limits (Peterson & Cummings, 2006). Whatman silica gel-60 plates (20 × 20 cm, 250 μm, GE Healthcare, England) or (10 × 10 cm, Merck, Darmstadt, Germany) were heat-activated at 110°C for 1 h, and samples were streaked onto the plates. On the 10 × 10 Silica gel 60 HPTLC plates, lipids were spotted using a Camag Linomat III auto-TLC spotter (Camag Scientific Inc., Wilmington, NC, USA). Phospholipids were separated using chloroform/methanol/acetic acid/water (55:37.5:3:2 by vol; Jolly *et al.*, 1997), which separates all major glycerophospholipids. Neutral lipids were separated in petroleum ether/diethyl ether/acetic acid (75:25:1.3 by vol; Marcheselli V. L., 1988). Lipids were identified using commercially available standards (Larodan, Sweden). In some cases, plates were air-dried after development, sprayed with 8% (w/v) $H_3PO_4$ containing 10% (w/v) $CuSO_4$, and charred at 180°C for 10 min (Gellermann *et al.*, 2005). Then, lipids were quantified by photodensitometry.

## 8.7 Phosphorus and cholesterol assay

The phospholipids mass was determined by quantitation of the lipid phosphorus content of individual lipid classes separated by TLC (Rouser *et al.*, 1966). Briefly, 0.5 ml of water was added to the scrapped TLC bands containing the phospholipids, then 0.65 ml of perchloric acid (70%) was added and the tubes were heated at 185ºC for 1 h. Following digestion, the tubes were cooled to room temperature and 0.5 ml of ascorbic acid (10% w/v), 0.5 ml of ammonium molybdate (2.5% w/v) and 3.3 ml of water were added and mixed by vortexing. Color was developed by boiling the mixture for 6 min and, after cooling, the absorbance was measured at 797 nm. The phospholipid mass was calculated interpolating absorbance values into a standard curve with known amounts of $K_2HPO_4$.

Cholesterol mass of the neutral lipid fraction was determined by an iron binding assay after separation by TLC (Bowman & Wolf, 1962). Briefly, the lipids were dissolved in 3 ml of ethanol. Then 3 ml of a 0.2% solution of ferric chloride hexahydrate ($FeCl_3$-$6H_2O$) in phosphoric acid (85%) and concentrated sulfuric acid ($H_2SO_4$) were added. Color was developed by mixing and the absorbance was measured at 550 nm. The cholesterol mass was calculated interpolating absorbance values into a standard curve with known amounts of cholesterol.

## 8.8 Fatty acid transesterification and gas liquid chromatography

The PC and PE fractions were subjected to base-catalyzed transesterification, converting the glycerophospholipids acyl chains to fatty acid methyl esters (FAME). To each fraction, 2 ml of 0.5 M KOH dissolved in anhydrous methanol was added (Brockerhoff, 1975). They were incubated at 37°C for 30 min and the reaction was stopped by adding 200 µl of methylformate. Heptadecanoic acid (17:0) was used as the internal standard.

For 2OHOA identification, total lipid extract was subjected to acid-catalyzed transesterification. To each fraction, 1.5 ml of 5% HCl was added and the reaction occurred at 80ºC for 2 h. Water was added to stop the reaction.

In both cases, FAMEs were extracted using 3 ml of *n*-hexane. The lower phase was reextracted two more times with 3 ml of *n*-hexane, and these washes were combined with the original aliquot. Individual FAMEs were separated by gas liquid chromatography using a SP-2330 column (0.32 mm ID, 30 m length, Supelco, Bellefonte, PA, USA) and a gas chromatograph (GC5890 Agilent, USA) equipped with dual autosamplers and dual flame ionization detectors.

## 8.9 Cell viability assay

Viability was evaluated by measuring the mitochondrial dehydrogenase activity of living cells with the MTT (3-(4,5-dimethylthiazol-2-yl)-2,5-diphenyltetrazolium bromide) method according to the manufacturer's instructions. Briefly, cells were seeded in flat-bottom 96-well plates ($2 \cdot 10^4$ cells per ml, 200 µl per well) for the times indicated in the corresponding figure, at 37ºC. MTT (0.2 mg/ml in PBS; Sigma-Aldrich) was added during the last hour. The mitochondrial dehydrogenases of viable cells reduce the tetrazolium salt yielding water insoluble colored formazan crystals. Then, these formazan crystals were solubilized by adding 100 µl of DMSO. The absorbance of the resulting purple solution was measured spectrophotometrically at 590 nm. The absorbance was also measured at 650 nm as a background measurement and substracted from the 590 nm value.

## 8.10 Electrophoresis (SDS/PAGE), Immunoblotting, and Protein Quantification

Cells were incubated in the presence or absence of 2OHOA, in 6-well culture plates under the experimental conditions indicated above. The cells were then washed twice with PBS and harvested by using a Teflon cell scraper in 100 µl 10 mM Tris-HCl buffer, pH 7.4, containing 50 mM NaCl, 1 mM $MgCl_2$, 2 mM EDTA, 1% SDS, 5 mM iodoacetamide, 1 mM phenylmethylsulfonylfluoride, 1 µM sodium orthovanadate, and 1 µM cantharidin. Then the cells were homogenized by ultrasounds (3 cycles of 10 s at 50 W) in a Braun Labsonic U sonicator (10% cycle), and 10-µl aliquots were removed for total protein quantification by the Bradford method (Bio-Rad). Then, 10 µl of 10× electrophoresis loading buffer (120 mM Tris-HCl, pH 6.8, 4% SDS, 50% glycerol, 0.1% bromphenol blue, and 10% mM β-mercaptoethanol) was added to the remaining suspension, which was then boiled for 3 min. For immunoblotting, 25 µg total protein were resolved on the same SDS-polyacrylamide gel (9% polyacrylamide) and transferred to nitrocellulose membranes (Whatman, Schleicher, and Schuell). After protein transference, membranes were incubated with blocking solution (PBS containing 5% nonfat dry milk and 0.1% Tween) for 1 h at room temperature. Then, membranes were incubated overnight at 4°C in fresh blocking solution containing the specific primary antibodies: rabbit anti-SMS1 (diluted 1:1,000, Santa Cruz); mouse anti-SMS2 (diluted 1:1,000, Abcam); mouse anti-DHFR (diluted 1:250, Abcam); chicken anti-ADRP (1:1,000, Sigma Aldrich); mouse anti-α-tubulin (1:10,000, Sigma). After removing the primary antibody, membranes were washed three times for 10 min with PBS containing Tween 0.1%, and all membranes (except for ADRP) were incubated with fluorescent-labeled secondary antibody at 1:5,000 dilution with 3% BSA in PBS for 60 min at room temperature protected from light and after washing with PBS containing 0.1 % Tween, the proteins were visualized and quantified by near infrared fluorescence spectroscopy (Odyssey Infrared Imaging System, LI-COR, Inc., Lincoln, NE, USA). In the case of ADRP, the membrane was incubated with the horseradish peroxidase-linked goat anti-chicken secondary antibody (1:5,000, Sigma Aldrich) for 1 h at room temperature in blocking solution and immunoreactivity was detected with the enhanced chemiluminescence Western blot detection system (Amersham Biosciences UK, Ltd.) followed by exposure to ECL hyperfilm (Amersham Biosciences UK, Ltd). Films were scanned with a resolution of 63.5 µm (400 dpi). The protein content measured for a given protein was normalized by the α-tubulin content.

## 8.11 Quantitative Reverse Transcription-Polymerase Chain Reaction (qRT-PCR)

Cells were incubated in the presence or absence of 2OHOA for 24 h and then, total RNA was extracted from U118 cells using the RNeasy Mini kit in combination with the RNase-free DNase kit (Qiagen) according to the manufacturer's instructions. Total amount and purity of RNA was determined using a Nanodrop 1000 spectrophotometer (Thermofisher Scientific, Waltham, MA), by optical density at 260 and 280 nm. Product quality was assessed by electrophoresis on 1% agarose gel and ethidium bromide staining. Reverse transcription of RNA was carried out in a thermal cycler Eppendorf Master Cycler Gradient using the Transcriptor First Strand cDNA Synthesis Kit (Roche Diagnostics) according to the manufacturer's instructions. Briefly, 1 µg of RNA was mixed with oligonucleotides (random hexamers and Poly-A hexamer, 1 µl from stock 500 µg/ml) and incubated at 65°C for 10 min, and then immediately transferred to ice. Then, a reaction mix was added containing, first-strand buffer (4 µl from 5× stock), dNTP mix (2.5 µl, 10 nM), protector RNase inhibitor (0.5 µl, 40 units/µl) and the transcriptor reverse transcriptase (0.5 µl, 20 units/µl). The reaction tubes were then incubated at 25°C for 10 min, followed by 55°C for 30 min and finally 85°C for 5 min. The cDNA samples obtained were stored at -20°C before use. For PCR amplification, the primers were designed with a SDSC Biology Workbench Program (http://workbench.sdsc.edu) based on the gene sequences in the GenBank. To differentiate between cDNA and genomic DNA, primers were designed at distinct sites of the exon-exon boundaries (Table 8-1).

Real-time PCR amplifications were carried out in 96-well plates in a StepOne Plus thermal cycler (Applied Biosystems) using the SYBR Premix Ex Taq 2× (Perfect Real Time, Takara). The reaction also contained an internal probe ROX 1 and 0.1 µM of each primer. An initial denaturation step at 95°C for 30 s preceded thermal cycling. DNA amplification and fluorescence quantification was determined over 35 cycles with a denaturation step at 95°C for 5 s, followed by an annealing/extension step at 60°C for 34 s. Fluorescence detection and quantification was carried out after each DNA extension step, and the data were analyzed using the StepOne software (v2.0). As endogenous control, the expression of β-actin was determined, as it is not modulated by 2OHOA.

**Table 8-1. Primers used in this study.**

| Gene | Orientation | Sequence (5'-3') |
|---|---|---|
| SMS1 | Forward | GAG CCT CTG GAG CAT TTC AC |
| | Reverse | TGC TCC ATT TTC AGG GTT TC |
| SMS2 | Forward | CAA CAC TGT TTT GGT GG |
| | Reverse | GGA GAA GCA GCA AGG AAT TG |
| CerS1 | Forward | GGC CAC TCC ATC TAC GCT AC |
| | Reverse | ACT CAA GCT GCA CGT CAC TG |
| CerS2 | Forward | TCT CTA TAT CAC GCT GCC CC |
| | Reverse | GCT TGC CAC TGG TCA GGT AG |
| CerS3 | Forward | ATC AAG AGA GGC CTT CCA GG |
| | Reverse | ATA GCC ATT CCA AAC CTC CC |
| CerS4 | Forward | ATC AGA CCA GGA GGC AAG TG |
| | Reverse | GAA CTT CTT GGT CAG CTG GG |
| CerS5 | Forward | CCA ATG CCA TCC TTG AAA AG |
| | Reverse | AAC CAG CAT TGG ATT TTT CG |
| CerS6 | Forward | TTC GAC AAA GAC GCA ATC AG |
| | Reverse | AGC AAT GCC TCG TAT TCC AC |
| β-actin | Forward | GCG GGA AATCGT GCG TGA CAT |
| | Reverse | CTA CCT CAACTT CCA TCA AAG CAC |

The ratio between the expression of the genes of interest and β-actin was determined by means of the equation described by Pfaffl *et al.* (Pfaffl, 2001):

$$\Delta\Delta Ct = \frac{Ex^{(Ctcontrolx - Ct2OHOAx)}}{Eend^{(Ctcontrolend - Ct2OHOAend)}}, \qquad \text{Equation 1}$$

Where $E_x$ is the efficiency of the gene of interest and $E_{end}$ is the efficiency of the endogenous. This value was used to calculate the relative expression in 2OHOA-treated cells with respect to untreated cells (control = 1). The efficiency of the reaction was estimated via increase in absolute fluorescence according to Pfaffl, 2002 (unpublished, from http://www.gene-quantification.de/efficiency01.html#e-fluoro-2):

$$E = \left(\frac{RnB}{RnA}\right)^{\left[\frac{1}{(CpB - CpA)}\right]}, \qquad \text{Equation 2}$$

Where Rn is the fluorescence measured at two treasholds and CP is the cycle at that threshold. Melting curve analysis and agarose gel electrophoresis were used to further characterize the PCR products.

## 8.12 SMS activity assay in cell culture

SMS activity assay in cell culture was carried out similarly as described elsewhere (Tafesse *et al.*, 2007). Briefly, control and treated U118 cells were incubated with 3 μM NDB-C6-Cer for 4 h prior to lipid extraction with hexane:2-propanol (3:2 vol/vol). Lipids were separated by HPTLC as described above and the NBD-lipids were visualized on a Bio-Rad Molecular Imager FX and quantified using Quantity One software (Bio-Rad, Barcelona, Spain). The SMS activity was associated with the newly synthesized NBD-C6-SM.

## 8.13 In vitro SMS activity assay

The *in vitro* SMS synthase activity protocol was adapted from Ding *et al.* and Villani *et al*. (Ding *et al.*, 2008; Villani *et al.*, 2008). Thus, U118 cells were collected and homogenized in ice-cold lysis buffer (50 mM Tris/HCl, 1 mM EDTA, 1 mM PMSF, 8% (w/v) CHAPS, pH 7.4) by passing 20 times through a 28.5 gauge needle. The cell lysate was centrifuged at 500 *g* for 5 min at 4ºC, and the enzymatic activity was measured in the post-nuclear supernatant. Protein concentrations were determined using the Bio-Rad assay and the SMS assay was performed using 100 μg of protein. The substrate was prepared as a mixture of 0.1 μg/μl of NBD-C6-Cer, 0.01 μg/μl of synthetic PC and PE resuspended by sonication and vortexing until clear in 50 mM Tris/HCl, 25 mM KCl, 1 mM EDTA, pH 7.4. The substrate was diluted 1:1 with the proteins resuspended in reaction buffer (final incubation volume of 200 μl) and the incubation was carried out for 2 h at 37ºC in the dark. The reaction was stopped on ice by adding 2 vol. of chloroform/methanol (1:2, v/v). Lipids were extracted using the Bligh and Dyer method and analyzed as described above.

## 8.14 Cell surface SMS activity assay

Cell surface SMS activity assay was adapted from Tafesse *et al*. (Tafesse *et al.*, 2007). Briefly, subconfluent U118 cells pretreated with 2OHOA (200 μM) for 6 h were washed with ice-cold Hanks' Balanced Salt Solution (HBSS, Gibco, Invitrogen, Barcelona, Spain) and incubated for 3 h at 0°C in HBSS containing 3 μM NBD-C6-Cer and 1% (w/v) fatty acid-free BSA followed by a 30-min incubation in HBSS containing only 1% (w/v) fatty acid free BSA. Under these conditions, any vesicular transport from the Golgi apparatus to the plasma membrane is impaired. All HBSS media were

collected and lipids from medium and from cells were extracted by the Bligh and Dyer method (Bligh & Dyer, 1959) and analyzed as described above.

## 8.15 Nuclei lipid composition analysis

Nuclei of control and treated cells were isolated using the Nuclear Extract Kit (Active Motive, Belgium) following the manufacturer's instructions. Then, lipids were extracted with hexane:2-propanol (3:2 vol/vol) and analyzed as described above.

## 8.16 RNA interference assay

RNA interference assay was performed on A549 and U118 cells transfected with small interfering RNA duplexes (siRNAs; Qiagen, Germantown, MD) using HiPerfect Transfection Reagent (Qiagen), according to the manufacturer's instructions. A number of different SMS1- and SMS2-directed siRNAs were initially tested on U118 and A549 cells. Because results showed that the silencing worked better on A549 cells, this cell line was selected to continue with these experiments. The tests yielded one custom made SMS1 siRNA (target sequence, 5'-AACTACACTCCCAGTACCTGG-3') that reduced the expression of the SMS1 60-80% (50 nM, 48 h) and two different commercially available SMS2 siRNA (Hs_MGC26963_1 target sequence, 5'-AACGCTGTAACCAAAGGTATA-3' and Hs_MGC26963_8, target sequence, 5'-AACGATTAGAAAGATGAACAA-3') that strongly reduced the expression of SMS2 80-90% (25 nM, 24 h or 48 h) (Figure A 2). As the Hs_MGC26963_8 siRNA had been already validated, all the experiments were carried out with this sequence. The non-specific All Star siRNA sequence (SCR; scrambled siRNA) was used as non-silencing control and All Star Hs Cell Death Control siRNA was used as a transfection positive control (Qiagen). Briefly, the day before transfection cells were seeded at 1.5 cells/$cm^2$ in 24-well plates with 0.5 ml per well of complete RPMI medium as indicated above. The day of transfection, the corresponding siRNA (50 nM for SMS1 and 25nM for SMS2, stocks at 20 μM) were mixed with the transfection reagent (7 μl for SMS1 and 5 μl for SMS2) in 100 μl of serum- and antibiotic-deprived RPMI medium. These mixtures were incubated 10 min at room temperature to allow the formation of the transfection complexes and then dropped-wise onto the cells. After 24 h, the medium was changed with fresh medium and cells were incubated for 24 h more. For cell treatments 2OHOA (200 μM, 24 h) was added with the fresh medium (after 24 h of silencing, i.e.; 48 h of silencing and 24 h of 2OHOA treatment). When double silencing

was done, the total concentration of silencing siRNA was 75 nM and 12 µl of transfection reagent were added. Thus, scramble and mock controls were done with the same amounts. As a validation method for the silencing, a qRT-PCR was performed as indicated above. After the 48 h, cells were subjected to either lipid extraction as detailed above or to DNA content analysis by flow cytometry as explained below.

## 8.17 D609 Inhibition experiments

A549 cells were incubated with D609 (potassium tricyclodecan-9-yl xanthate, Figure 8-1) for 16 h (350 µM, a gift from Dr Amadeu Llebaria, Dept. of Biomedicinal Chemistry IQAC-CSIC, Barcelona) and 2OHOA (200 µM) was added 1 h after the addition of D609. Among different biological effects, D609 is a potent inhibitor of PC-PLC (Muller-Decker, 1989). In addition, a few reports show that D609 can also inhibit the enzymes of the sphingomyelin cycle, namely sphingomyelin synthase (Luberto & Hannun, 1998; Luberto *et al.*, 2000; Meng *et al.*, 2004a). SM levels were established as described above while the effect of SMS inhibition on the cell cycle was evaluated by flow cytometry. Thus, after treatment, A549 cells were washed with PBS and harvested using trypsin. Cells were then fixed with ice-cold 70% ethanol for 1 h at 4°C, centrifuged for 5 min at 1,260 *g*, and then resuspended in sodium citrate (38 mM, pH 7.4). Finally, cells were incubated for 20 min at 37°C with buffer A (sodium citrate (38 mM, pH 7.4), 50 µg/ml propidium iodide and 5 µg/ml RNase A; Sigma-Aldrich) and analyzed on a Beckman Coulter Epics XL flow cytometer. Cell populations in the different phases of cell cycle (sub$G_1$, $G_0$ /$G_1$, S, and $G_2$/M) were determined on the basis of their DNA content.

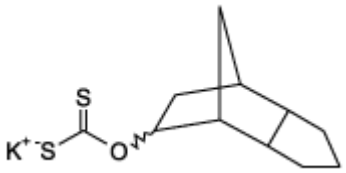


**Figure 8-1. Chemical structure of D609.**
From Enzo Life Sciences data sheet (catalog number ST-330).

## 8.18 Measurement of S1P and sphingosine

S1P was extracted by a modified two-step lipid extraction previously described (Ruwisch *et al.*, 2001; Yatomi *et al.*, 1995). Briefly, the cell monolayers were washed with PBS and then removed from the 6 cm petri dishes in 1 ml of methanol containing 0.25% hydrochloric acid by scraping with a Teflon cell scraper into a siliconized glass tube. An aliquot of 100 µl of the sample was transferred into another siliconized glass tube and 200 pmol dihydro-S1P as internal standard was added. After alkalization with 100 µl of a 3N NaOH solution, lipids were extracted by addition of 1 ml of chloroform and 1 ml of 1N NaCl. The mixture was centrifuged (300 *g*, 5 min) for an effective separation of the alkaline aqueous phase containing S1P. The organic phase was reextracted with 0.5 ml of methanol, 0.5 ml of 1N NaCl and 50 µl of 3N NaOH. The collected aqueous phases were acidified with 100 µl of concentrated HCl and extracted twice with 1.5 ml of chloroform each. The combined organic phases were evaporated using a Centrivac vacuum system and the dried lipids were resolved in 325 µl methanol/0.07 M $K_2HPO_4$ (8:2) by thorough vortexing and sonication on ice for 5 min.

A derivatization mixture of 7 mg of o-phthaldialdehyde, 7 µl of mercaptoethanol, 100 µl of ethanol and 4.9 ml of boric acid solution adjusted to pH 10.5 with potassium hydroxide was prepared and 25 µl of this mixture was added to the resolved lipid fraction. After 15 min at room temperature the derivatives were analyzed on a Merck Hitachi LaChrom HPLC system (Merck Hitachi, Darmstadt, Germany). Fluorescence was measured at an emission wavelength of 455 nm after separation on a RP 18 Kromasil column (Chromatographie Service, Langerwehe, Germany) kept at 35°C. The flow rate was adjusted to 1.3 ml/min and a gradient program with methanol and 0.07 M $K_2HPO_4$ solution as solvents was used (Table 8-2). Resulting profiles were evaluated using the Merck system manager software.

**Table 8-2. Gradient program for S1P and dihydro-S1P separation utilized for the HPLC analysis of S1P.**

| Time (min) | 0.07 M $K_2PO_4$ (%) | Methanol (%) |
|---|---|---|
| 0 | 24 | 76 |
| 10 | 24 | 76 |
| 30 | 16 | 84 |
| 40 | 8 | 92 |
| 46 | 0 | 100 |
| 56 | 0 | 100 |
| 58 | 24 | 76 |

(Prakash *et al.*, 2010).

## 8.19 Mass Spectometry

Lipid extraction and mass spectrometry based targeted lipid analysis in the presence of isotopic labeled or not naturally occurring lipid species as internal standards was performed essentially as described previously (Liebisch *et al.*, 1999; Liebisch *et al.*, 2004; Scherer *et al.*, 2010a; Scherer *et al.*, 2009; Scherer *et al.*, 2010b). In brief, cells were washed with PBS and lysed in 0.1% sodium dodecyl sulfate SDS by scrapping, sonicated and aliquots corresponding to 100 µg total protein were used for lipid extraction and analysis. Direct flow injection utilized a 1200 series binary pump (Agilent, Waldbronn, Germany) coupled via electrospray ionization (ESI) to a Quattro Ultima tandem mass spectrometer (Micromass, Manchester, UK). Reversed phase and hydrophilic interaction chromatography ESI tandem mass spectrometry (HILIC LC-ESI-MS/MS) was conducted using a 1,200 series binary pump and a hybrid triple quadrupole linear ion trap mass spectrometer API 4,000 Q-Trap equipped with a Turbo V source ion spray operating in positive ESI mode was used for detection (Applied Biosystems, Dasrmstadt, Germany). Analysis of fatty acid species was performed after FAME derivatisation using a Shimadzu 2,010 GC-MS. Quantification was performed by standard addition calibration to cell homogenates using a number of naturally occurring lipid species for each lipid class.

## 8.20 Metabolic labeling of cells to measure *de novo* [$H^3$]-Cer synthesis

Control and treated (200 µM, 6 and 24 h) U118 cells were pulse labeled with 0.30 µCi/ml of [$H^3$]-palmitic acid (stock at 1 mCi) for 5 min. After incubation, total cell lipids were extracted and separated by TLC. After running two-thirds of the separation distance in chloroform/ethanol/water/triethylamine (35:40:9:35, by vol.), the plates were dried at room temperature and subsequently separated in isohexane/ethylacetate (5:1, by vol) for the full distance (Kuerschner *et al.*, 2005). The plates were dried at room temperature and the side with the standards was sprayed with 8% (w/v) $H_3PO_4$ containing 10% (w/v) $CuSO_4$, air-dried and charred at 180°C for 10 min to develop the non-radioactive standard bands. The area corresponding to each lipid was scraped off, and the radioactivity was measured by liquid scintillation counting. The level of [$H^3$]-Cer produced was normalized to cellular protein content.

## 8.21 Electron microscopy

Cells were seeded at $1.1 \cdot 10^4$ cell/cm$^2$ in 4-well Lab-Tek chamber slides (Nalge Nunc International, Naperville, IL) as indicated above in the presence or absence of 2OHOA (200 µM, 48 h or 72 h). After washing twice with 0.1 M phosphate buffer (PB; $NaH_2PO_4$ 20 mM, $Na_2HPO_4$ 80 mM, pH 7.4) for 5 min, cells were fixed in 3.5% glutaraldehyde for 1 h at 37°C. After washing four times with 0.1 M PB for 10 min, cells were postfixed in 2% $OsO_4$ for 1 h at room temperature protected from light. Then, cells were washed with distilled $H_2O$ three times for 5 min and were sequentially washed with ethanol 30°, then ethanol 50° and ethanol 70°, each for 5 min. Afterwards, cells were stained in 2% uranyl acetate (in ethanol 70°) in the dark for 2 h at 4°C and again sequentially dehydrated in ethanol 70° (2 × 5 min), ethanol 96° (2 × 5 min), ethanol 100° (2 × 7 min and 1 × 10 min). Finally, cells were infiltrated overnight in Araldite (in ethanol 100°; Durcupan, Fluka, Buchs SG, Switzerland). Following polymerization at 70°C during 3 days, embedded cultures were detached from the chamber slide and glued to Araldite blocks. Serial semi-thin (1.5 µm) sections were cut with an Ultracut UC-6 (Leica, Heidelberg, Germany) and mounted onto slides and stained with 1% toluidine blue. Selected semi-thin sections were glued (Super Glue, Loctite) to araldite blocks and detached from the glass slide by repeated freezing (in liquid nitrogen) and thawing. Ultrathin (0.06 – 0.09 µm) sections were prepared with the Ultracut and stained with lead citrate. Finally, photomicrographs were obtained under a transmission electron microscope (FEI Tecnai G2 Spirit Biotwin) using a digital camera (Morada, Soft Imaging System, Olympus).

## 8.22 Immunofluorescence labeling of SM by lysenin

Cells were plated at a density of $1.1 \cdot 10^4$ cell/cm$^2$ on Chambered Coverglass (Lab-Tek$^{TM}$ II, Thermo Fisher Scientific Inc.) as indicated above in the presence or absence of 2OHOA (200 µM, 72 h). SM was labeled with lysenin as previously described by Yamaji *et al* with minor modifications (Yamaji *et al.*, 1998). Lysenin is a natural sphingomyelin-specific binding protein without any cross reactions with other sphingolipids that was isolated from the coelomic fluid of earthworm (Sekizawa *et al.*, 1997). All steps were carried out at room temperature. After washing twice with phosphate buffer 0.1 M PB for 5 min, cells were fixed with 4% paraformaldehyde in PB for 20 min and washed again with PB. To quench any excess of reactive groups of paraformaldehyde, cells were incubated with 0.1 M $NH_4Cl$ in PB for 15 min and washed again twice with PB. After blocking with 2% BSA in PB for 30 min, cells were

incubated with lysenin (1 µg/ml in blocking solution; PeptaNova GmbH, Sandhausen, Germany) for 2 h and washed twice with PB for 5 min. Next, cells were incubated with rabbit anti-lysenin antiserum (1:500 in blocking solution; PeptaNova GmbH, Sandhausen, Germany) for 1 h, followed by incubation with a fluorescent secondary antibody (conjugated to Alexa Fluor 488-labelled goat anti-rabbit at 1:200 dilution, Molecular Probes; excitation at 488 nm and detection at 510–550 nm) for 1 h. After washing cells twice with PB for 5 min images were acquired using a Leica TCS SP2 spectral confocal microscope with 630 × optical magnification and 3 × digital magnification (approximately 1,800 × total magnification), and analyzed with the software provided by the manufacturer.

## 8.23 Metabolic labeling of cells with NBD-lipids

Similar to the SMS activity assay, U118 cells were incubated with 3 µM NDB-C6-SM, NBD-C6-GlcCer, NBD-C6-PC or NBD-C6-PE for 4 h prior to lipid extraction. Lipids were separated by HPTLC as described above and fluorescent lipids were visualized on a Bio-Rad Molecular Imager FX and quantified using Quantity One software (Bio-Rad, Barcelona, Spain).

## 8.24 Determination of SCD activity

Control and treated (200 µM, 48 h) U118 cells were steady-state labeled with trace amounts of [$H^3$]-palmitic acid (0.25 µCi/ 60 mm petri dish, stock at 1 mCi) for 6 h. At the end of the incubation, total cell lipids were extracted and transesterified as indicated above. The derivatives methyl esters were separated by argentation TLC following the procedure of Wilson and Sargent (Wilson & Sargent, 2001). Briefly, silica gel 60 HPTLC (10 × 10 cm) plates were sprayed uniformly with 20 ml of acetonitrile containing 2 g of silver nitrate until the plates were saturated. The plates were air-dried in subdued light, heated at 110°C for 30 min to achieve activation and used within 1 h. FAME mixtures were applied to the silver nitrate impregnated plates and were separated in hexane: ethyl ether (90:10, by vol), which allows to separate SFA from MUFA. Lipid fractions were identified using pure methyl stearic acid and methyl oleic acid as standards (Larodan, Sweden) The plates were air-dried and the side with the standards was sprayed with 8% (w/v) $H_3PO_4$ containing 10% (w/v) $CuSO_4$, air-dried and charred at 180°C for 10 min to develop the non-radioactive standard bands. SFA

and MUFA spots were scraped from the TLC plate and quantified by liquid scintillation counting. The level of [$H^3$]-MUFA produced was normalized to cellular protein content.

## 8.25 Nile red staining of lipid droplets for fluorescence microscopy

U118 cells were plated at a density of 1.5 · $10^4$ cells/ml on Chambered Coverglass (Lab-Tek™ II, Thermo Fisher Scientific Inc.) as indicated above in the presence or absence of 2OHOA (200 µM, 24 h). After treatment, cells were washed with 0.1 M PB, fixed with 4% paraformaldehyde for 10 min, and washed twice with PB. Cells were overlaid with 0.5 ml PB, to which 2.5 µl of a stock solution of Nile red (Sigma Aldrich) in acetone (0.2 mg/ml) were added, so that the final concentrations of Nile red and acetone were 1 µg/ml and 0.5%, respectively. Samples were kept in the dark until photographed on a Nikon Eclipse TE2000-S Fluorescence microscope at 40 × magnification. Analysis of the vesicles in photomicrographs was performed with Image J 1.38× public software (Wayne Rasband, National Institutes of Health; rsb.info.nih.gov). Briefly, the image was split into the blue, green and red channels. To maximize the signal to noise ratio, analysis was carried out with the blue component, as Nile red emission shifts to shorter wavelengths when incorporated into LDs. After thresholding the blue component at a value of 40, particles were counted, recording total amount, total area, and average size.

## 8.26 Immunofluorescence labeling of lysosomes with Lysonsensor

U118 cells were plated at a density of 1.1 · $10^4$ cell/$cm^2$ on Chambered Coverglass (Lab-Tek™ II, Thermo Fisher Scientific Inc.) as indicated above in the presence or absence of 2OHOA (200 µM, 48 h). After treatment, cells were incubated 1 h with 1 µM LysoSensor Green DND-189 probe pH Indicator (pH 4.5 - 6) (Invitrogen™) and in the last 5 min with Hoechst stain (trihydrochloride trihidrate, 40 µg/ml, Invitrogen molecular probes™). Samples were observed on a Nikon Eclipse TE2000-S Fluorescence microscope at 40 × magnification. The LysoSensor™ dyes are acidotropic probes that appear to accumulate in acidic organelles, such as lysosomes, as the result of protonation.

## 8.27 Liposome preparation

The glycerophospholipids used to prepare multilamellar vesicles (MLV) and large unilamellar vesicles (LUV) were POPC, POPE and PSM as this combination of acyl chains is one of the most common in the plasma membrane of mammalian cells (Marsh, 1990). Likewise, PSM was used as it is a very common acyl chain in sphingolipids (Estep *et al.*, 1979) and it reflects the properties of natural SM (Barenholz *et al.*, 1976). POPC has a main transition temperature ($T_m$) of -3ºC (Koynova & Caffrey, 1998) well below the temperature of this study (24ºC), whereas PSM has a $T_m$ of 41ºC (Marsh, 1990). Therefore, the mixtures used in this study met the criteria for formation of raft-like domains, i.e., $l_o$ domains in coexistence with a $l_d$ phase (Marsh, 1990). In general, $l_d$ domains are enriched in low $T_m$ lipids, particularly POPC, whereas $l_o$ domains are high $T_m$ lipid- (in this case PSM) and cholesterol-enriched. POPE has a $T_m$ that is approximately the average between the $T_m$ of POPC and PSM, i.e., 24.5ºC (Polozov & Gawrisch, 2004). In addition, in the range of concentrations used POPE is able to mix with both POPC (Epand & Bottega, 1988) or SM/cholesterol (Shaikh *et al.*, 2002). Thus, POPE is expected to have a fairly homogeneous distribution between ordered and disordered domains in the mixtures used.

MLV of quaternary mixtures of POPC, POPE, PSM and cholesterol were prepared with either *t*-PnA, or DPH, or no probe (blank; de Almeida *et al.*, 2007; de Almeida *et al.*, 2005). Briefly, lipid stock solutions were made in chloroform except for POPE which was dissolved in chloroform:methanol (2:1, v/v). Appropriate volumes of lipids and probe stock solutions were added to a tube to have the desired lipid mole fractions and lipid/probe ratio. Then, the solvent was dried under a $N_2$ stream, and the residue was dried for at least 3 h under vacuum. The molar proportions of each lipid are given in Table 4-1. Total lipid concentration in MLV suspensions was always 0.2 mM. The suspension medium used was sodium phosphate 10 mM, NaCl 150 mM, EDTA 0.1 mM buffer (pH 7.4). The samples were then progressively vortexed and submitted to 10 freeze/thaw cycles (liquid nitrogen/water bath at 60°C). Afterwards, they were slowly cooled and kept in the dark at 4°C. Before measurements, they were slowly brought to room temperature.

To analyze the effect of the partition of free 2OHOA into membranes, measurements were carried out in LUV suspension for effective 2OHOA incorporation, mimicking the 24 h composition of control and treated U118 cells. First, MLVs were prepared as described above, without probe, and with final lipid concentration of 0.5 mM to ensure that an efficient incorporation of 2OHOA in the lipid bilayer is achieved. To obtain LUVs, the MLV suspensions were extruded (21 times) using an Avanti Mini-Extruder and polycarbonate filters with a pore diameter of 100 nm (Nuclepore,

Whatman). The suspension was slowly brought to room temperature and allowed to equilibrate. 2OHOA was then added in water to the suspension to a final concentration of 25 µM (5 mole%) or 100 µM (20 mole%) at least 1 h before the fluorescence measurements. The samples were kept in the dark until the measurements. The 2OHOA/lipid ratio in the 25 µM 2OHOA samples is similar to the estimated 2OHOA/lipid ratio in cells treated with 200 µM of the drug.

In order to prepare liposomes from lipid extracts, these were dissolved in chloroform/methanol (2:1, v/v) to obtain a concentration of 1 µmol Pi/ml. Three aliquots of 150 µl were taken from each sample (for DPH, *t*-Pna and blank), and for the following calculations the cholesterol/phospholipid ratios calculated from the lipid analysis were also taken into consideration. Here, the lipids and probe were suspended in a volume of previously warmed (50°C) HEPES buffer (pH 7.4) for a total final lipid concentration of 0.2 mM and MLV were prepared as indicated above.

In all cases, the probe: lipid ratios used were 1:200 for DPH and 1:500 for *t*-PnA, that were added from the stock ethanol solutions followed by 1 h incubation at 50ºC. The volume of ethanol was below 1% ensuring no alterations of the lipid bilayers (Marques *et al.*, 2011). They were allowed to equilibrate overnight protected from light. The concentration of lipids was determined by phosphorous content (McClare, 1971). Probe concentrations in stock solutions were determined by absorption spectrophotometry as it was previously described (de Almeida *et al.*, 2005). Absorption spectrophotometry was carried out with a Jasco V-560 UV/Vis spectrophotometer.

## 8.28 Spectrofluorescence measurements and data analysis

Fluorescence measurements were carried out at 24ºC on a Horiba Jobin Yvon FL-1057 Tau 3 spectrofluorometer.

For steady-state measurements (450 W Xe arc lamp light source), the samples were under constant magnetic stirring, and the excitation/emission wavelengths were 358 nm/430 nm for DPH and 303nm/404 nm for *t*-PnA, respectively. The steady-state anisotropy (<*r*>) was calculated according to:

$$< r >= \frac{\left(I_{vv} - G \times I_{vh}\right)}{\left(I_{vv} + 2G \times I_{vh}\right)}, \qquad \text{Equation 3}$$

Where *G* is the instrumental correction factor and “V” and “H” in the subscripts represent the vertical and horizontal orientations of the polarizers and the order of the

subscripts corresponds to excitation and emission. An adequate blank was subtracted from each intensity reading.

For time-resolved measurements by the single photon counting technique, nanoLED N-320 (Horiba Jobin Yvon) was used for the excitation of *t*-PnA, and emission wavelength was 404 nm. Diluted LUDOX was used as the scatterer to obtain the instrumental response function. The program TRFA Data Processor v.1.4 (Scientific Software Technologies Center, Minsk, Belarus) was used for analysis of the experimental fluorescence decays. An adequate blank decay was acquired and subtracted to the respective sample. The decays were analyzed by fitting a sum of exponentials,

$$I(t) = \sum_{i=1}^{n} \alpha_i^{-t/\tau i} \qquad \text{Equation 4}$$

Where $\alpha_i$ and $\tau_i$ are the normalized amplitude and lifetime of component *i*, respectively. The mean fluorescence lifetime is obtained through:

$$<\tau>= \frac{\sum \alpha_i \tau_i^2}{\sum \alpha_i \tau_i}, \qquad \text{Equation 5}$$

The quality of fit was judged by non-linear least squares (NLLS) with a reduced-$\chi^2$ value close to 1 and random distribution of weighted residuals and residuals autocorrelation. The goal of least squares is to test whether a given mathematical model is consistent with the data, and to determine the parameter values for that model which have the highest probability of being correct (Lakowicz, 2006).

## 8.29 Statistics

Statistical analysis was done using GraphPad Prism 4.01 (GraphPad Software Inc., San Diego, CA). Unless indicated, data are expressed as mean ± SEM, from at least three independent experiments (*n*). The statistical significance of the mean difference was determined by Student's *t* test. The asterisks indicate a significant effect of the treatment as compared with the control: **P* < 0.05; ***P* < 0.01; ****P* < 0.001.

# 9 Appendix

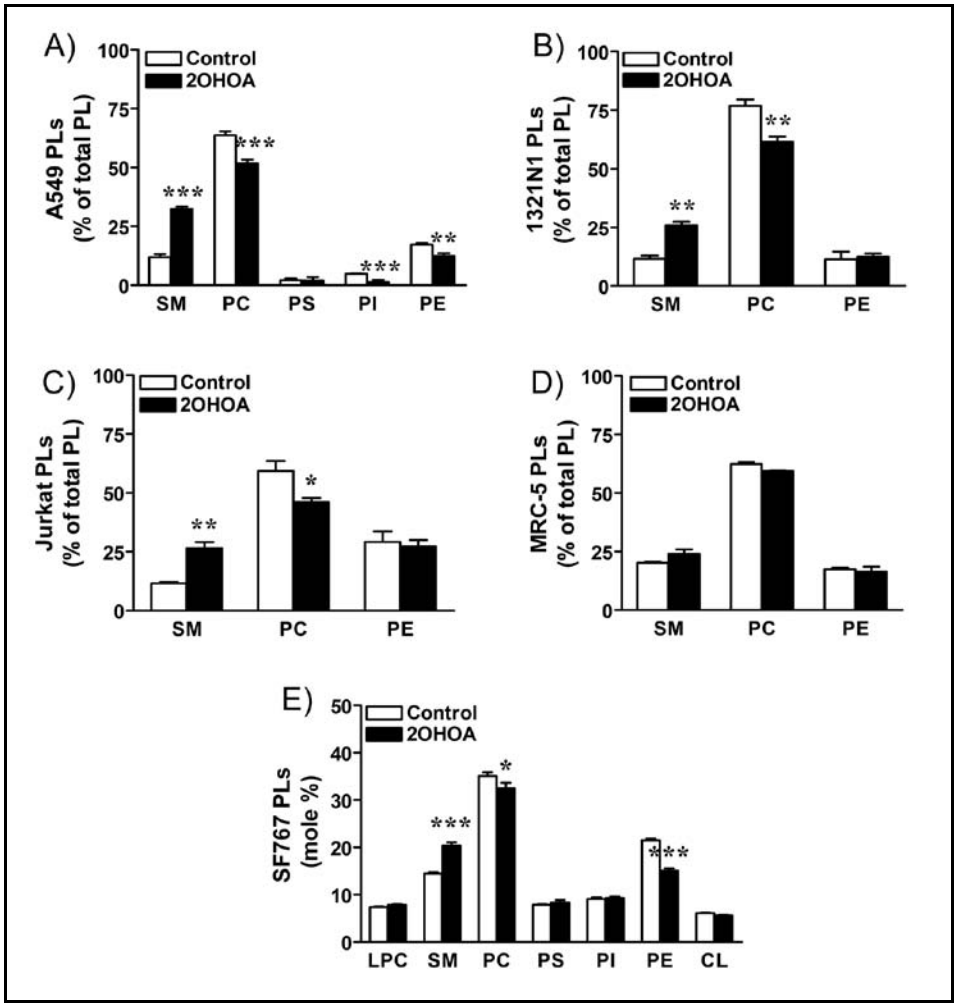


**Figure A 1. Effect of 2OHOA on the glycerophospholipid composition of different cell lines.**
Cells were treated in the absence (Control) or presence (200 μM, 24 h) of 2OHOA. After treatment, lipids were extracted and analyzed by HPTLC and quantified by densitometry. Non-small cell lung cancer (A549) cells (A), human glioma 1321N1 cells (B), human leukemia Jurkat cells (C), non-tumor human fetal fibroblast MRC-5 cells (D). Human glioma SF767 cells (E) were treated for 72 h and the phospholipid mass was determined by assaying the lipid phosphorous content of individual lipid classes separated by TLC, according to the *Experimental procedures* section. Values represent the mean ± SEM, $n = 3–5$. The asterisks indicate a significant effect as compared with the control (*$P < 0.05$; **$P < 0.01$; ***$P < 0.001$).

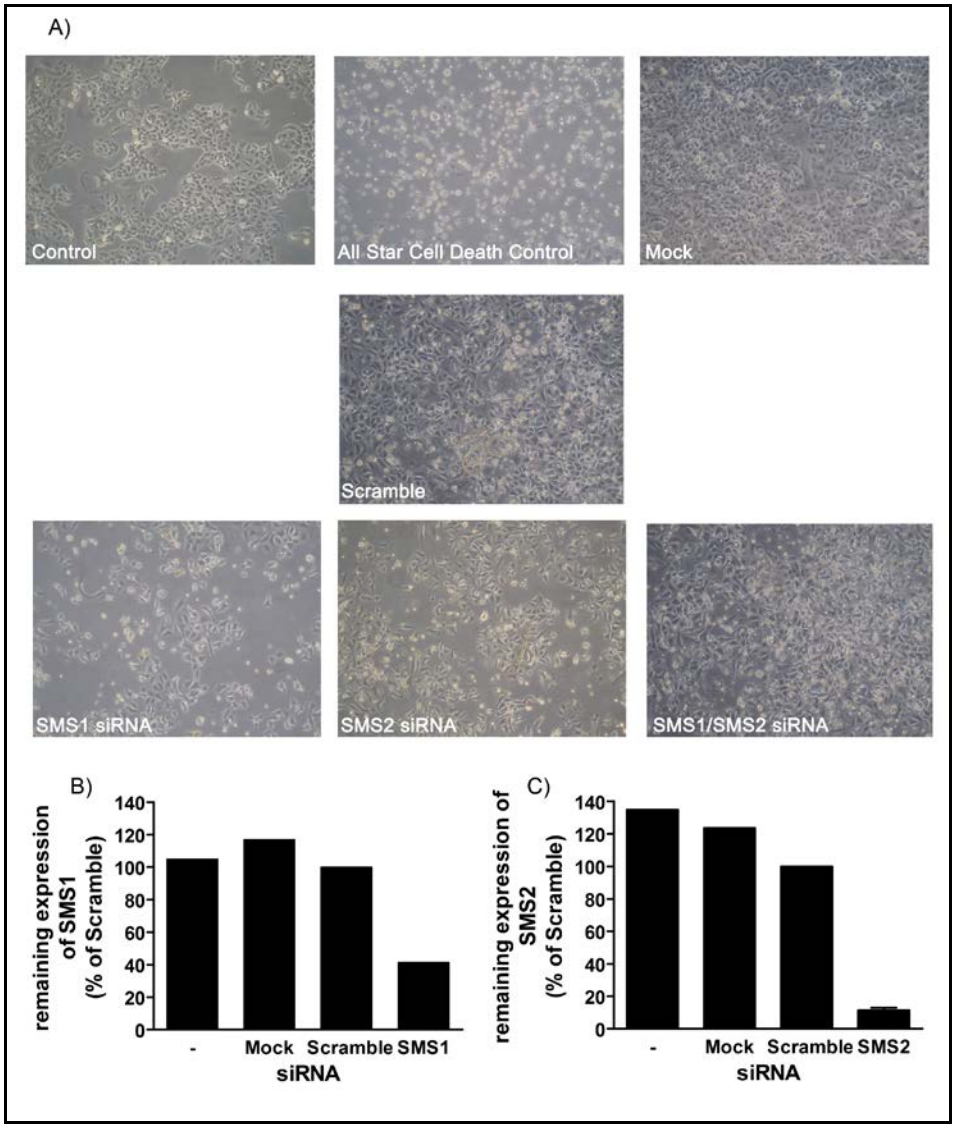


**Figure A 2. RNA interference experiment on A549 cells.**
A549 cells exposed to different siRNA treatments. (A) Representative pictures of the cells. Validation of the method by qRT-PCR for SMS1 (B) and SMS2 (C).

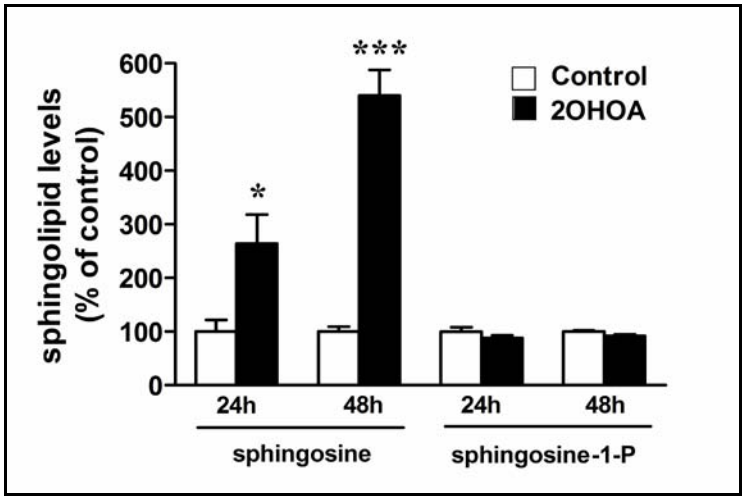


**Figure A 3. 2OHOA increased the sphingosine mass content in U118 cells.**
U118 cells were exposed to 2OHOA (200 μM) for 24 h and 48 h, and the lipids were then extracted and analyzed by HPLC as described in Experimental procedures. Values represent the mean ± SEM, n = 4. The asterisks indicate a significant effect of 2OHOA as compared with the control (*$P < 0.05$;***$P < 0.001$).

**Table A 1. Effect of 2OHOA on SF767 fatty acid composition of individual phospholipid.**

| FAME | PC | | PE | |
|---|---|---|---|---|
| | Control | 2OHOA | Control | 2OHOA |
| | Mean ± SD | Mean ± SD | Mean ± SD | Mean ± SD |
| 16:0 | 27.7 ± 1.2 | 25.4 ± 0.7** | 8.1 ± 0.6 | 8.9 ± 0.8 |
| 16:1 | 2.0 ± 0.2 | 1.6 ± 0.2** | 1.1 ± 0.1 | 0.7 ± 0.2 |
| 18:0 | 11.9 ± 1.3 | 13.5 ± 1.9 | 18.7 ± 0.9 | 22.3 ± 0.2*** |
| 18:1n-9 | 30.5 ± 0.7 | 25.4 ± 0.6*** | 23.8 ± 3.5 | 14.3 ± 0.9*** |
| 18:1n-7 | 4.4 ± 0.5 | 4.4 ± 0.6 | 4.8 ± 0.7 | 5.4 ± 0.3 |
| 18:2n-6 | 13.5 ± 1.7 | 14.4 ± 1.2 | 6.1 ± 0.4 | 7.6 ± 0.4*** |
| 20:3n-6 | 1.9 ± 0.1 | 2.1 ± 0.8 | 2.1 ± 0.1 | 2.1 ± 0.1 |
| 20:4n-6 | 4.2 ± 0.4 | 7.1 ± 0.7*** | 20.0 ± 1.5 | 18.2 ± 0.8* |
| 20:3n-3 | 1.2 ± 0.1 | 2.5 ± 0.3*** | 4.4 ± 0.2 | 4.7 ± 0.1* |
| 22:5n-3 | 1.0 ± 0.2 | 1.3 ± 0.1 | 4.0 ± 0.3 | 6.3 ± 0.4*** |
| 22:6n-3 | 0.8 ± 0.1 | 1.7 ± 0.2*** | 4.8 ± 0.3 | 7.4 ± 0.7*** |
| | | | | |
| SFA | 39.5 ± 0.6 | 38.8 ± 2.5 | 26.8 ± 1.3 | 31.2 ± 0.7*** |
| MUFA | 37.5 ± 0.8 | 31.7 ± 0.8*** | 30.5 ± 3.0 | 21.0 ± 0.9*** |
| PUFA | 22.9 ± 1.3 | 29.4 ± 1.9*** | 42.7 ± 2.5 | 47.8 ± 1.5** |
| n-3 | 3.0 ± 0.4 | 5.5 ± 0.6*** | 13.2 ± 0.7 | 18.4 ± 1.1*** |
| n-6 | 20.0 ± 1.4 | 24.0 ± 1.5** | 29.5 ± 2.0 | 29.4 ± 0.5 |
| n-3/n-6 | 0.2 ± 0.0 | 0.2 ± 0.0*** | 0.5 ± 0.0 | 0.6 ± 0.0*** |

SF767 cells were treated with 2OHOA (200 µM) for 72 h. After treatment, lipids were extracted and analyzed by TLC. The PC and PE fractions were converted to FAME in basic conditions and analyzed by gas chromatography. Values are expressed as mole% and represent mean ± SD, n = 4-5. The asterisk indicate a significant effect of 2OHOA compared to the control (*$P < 0.05$; **$P < 0.01$; ***$P < 0.001$).

**Table A 2. Effect of 2OHOA on A549 fatty acid composition of individual glycerophospholipids.**

| FAME | PC | | PE | |
|---|---|---|---|---|
| | Control | 2OHOA | Control | 2OHOA |
| | Mean ± SD | Mean ± SD | Mean ± SD | Mean ± SD |
| 16:0 | 37.3 ± 0.6 | 36.3 ± 1.6 | 8.2 ± 0.3 | 9.1 ± 1.3 |
| 18:0 | 4.7 ± 0.5 | 12.7 ± 3.5*** | 14.7 ± 0.4 | 23.9 ± 0.4*** |
| 18:1n-9 | 43.6 ± 0.9 | 23.1 ± 1.8*** | 32.0 ± 5.3 | 13.2 ± 0.1*** |
| 18:1n-7 | 6.5 ± 0.3 | 9.9 ± 0.5*** | 10.8 ± 0.5 | 10.8 ± 0.8 |
| 18:2n-6 | 1.8 ± 0.0 | 3.7 ± 1.0** | 3.3 ± 0.2 | 3.5 ± 0.2 |
| 20:3n-6 | 0.5 ± 0.0 | 1.3 ± 0.1*** | 1.6 ± 0.1 | 2.0 ± 0.1*** |
| 22:0 | 0.9 ± 0.1 | 3.0 ± 0.2*** | 2.6 ± 0.2 | 6.7 ± 0.5*** |
| 20:4n-6 | 1.0 ± 0.0 | 3.1 ± 0.1*** | 17.7 ± 0.3 | 18.0 ± 0.7 |
| 20:5n-3 | 0.4 ± 0.0 | 0.4 ± 0.0 | 4.8 ± 0.1 | 1.9 ± 0.1*** |
| 22:5n-3 | 0.2 ± 0.0 | 1.3 ± 0.0*** | 0.7 ± 0.1 | 4.0 ± 0.2*** |
| 22:6n-3 | 0.6 ± 0.0 | 1.8 ± 0.1*** | 5.9 ± 0.4 | 6.9 ± 0.4** |
| SFA | 42.9 ± 0.7 | 52.0 ± 2.1*** | 25.4 ± 0.6 | 39.7 ± 0.7*** |
| MUFA | 52.6 ± 0.6 | 36.6 ± 2.6*** | 40.6 ± 0.6 | 24.0 ± 0.8*** |
| PUFA | 4.4 ± 0.1 | 11.5 ± 0.7*** | 34.0 ± 0.8 | 36.2 ± 1.2** |
| n-3 | 1.1 ± 0.0 | 3.5 ± 0.3*** | 11.3 ± 0.6 | 12.7 ± 0.6** |
| n-6 | 3.3 ± 0.0 | 8.0 ± 0.9*** | 22.7 ± 0.3 | 23.5 ± 0.6* |
| n-3/n-6 | 0.3 ± 0.0 | 0.4 ± 0.1* | 0.5 ± 0.0 | 0.5 ± 0.0** |

A549 cells were treated with 2OHOA (150 µM) for 72 h. After treatment, lipids were extracted and analyzed by TLC. The PC and PE fractions were converted to FAME in basic conditions and analyzed by gas chromatography. Values are expressed as mole% and represent mean ± SD, n = 4-5. The asterisk indicate a significant effect of 2OHOA compared to control (*$P < 0.05$; **$P < 0.01$; ***$P < 0.001$).

**Table A 3. Effect of 2OHOA on U118 total lipids fatty acid composition.**

| FAME | Control | 2OHOA |
|---|---|---|
| | Mean ± SD | Mean ± SD |
| 16:0 | 3.0 ± 0.2 | 30.4 ± 2.8*** |
| 18:0 | 16.6 ± 5.1 | 18.2 ± 5.0 |
| 18:1n-9 | 34.7 ± 2.8 | 13.0 ± 5.5*** |
| 18:1n-7 | 9.7 ± 1.4 | 6.7 ± 1.4* |
| 18:2n-6 | 5.4 ± 1.4 | 4.2 ± 2.8 |
| 20:4n-6 | 10.2 ± 1.2 | 9.0 ± 2.1 |
| 20:5n-3 | 7.5 ± 2.6 | 8.1 ± 2.2 |
| 22:5n-3 | 3.2 ± 0.5 | 3.3 ± 1.4 |
| 22:6n-3 | 9.7 ± 4.6 | 7.0 ± 4.2 |
| | | |
| MUFA | 44.4 ± 3.4 | 19.7 ± 5.6*** |
| PUFA | 36.0 ± 7.4 | 31.6 ± 7.6 |
| n-3 | 20.4 ± 7.1 | 18.4 ± 6.7 |
| n-6 | 15.5 ± 2.6 | 13.3 ± 3.1 |
| n-3/n-6 | 1.5 ± 0.6 | 1.4 ± 0.6 |

U118 cells were treated with 2OHOA (200 µM, 72 h). After treatment, lipids were extracted and an aliquot was converted to FAME in basic conditions and analyzed by gas chromatography. Values are expressed as mole% and represent mean ± SD, n = 4-5. The asterisks indicate a significant effect of the treatment as compared with the control (*$P < 0.05$; **$P < 0.001$; ***$P < 0.0001$).

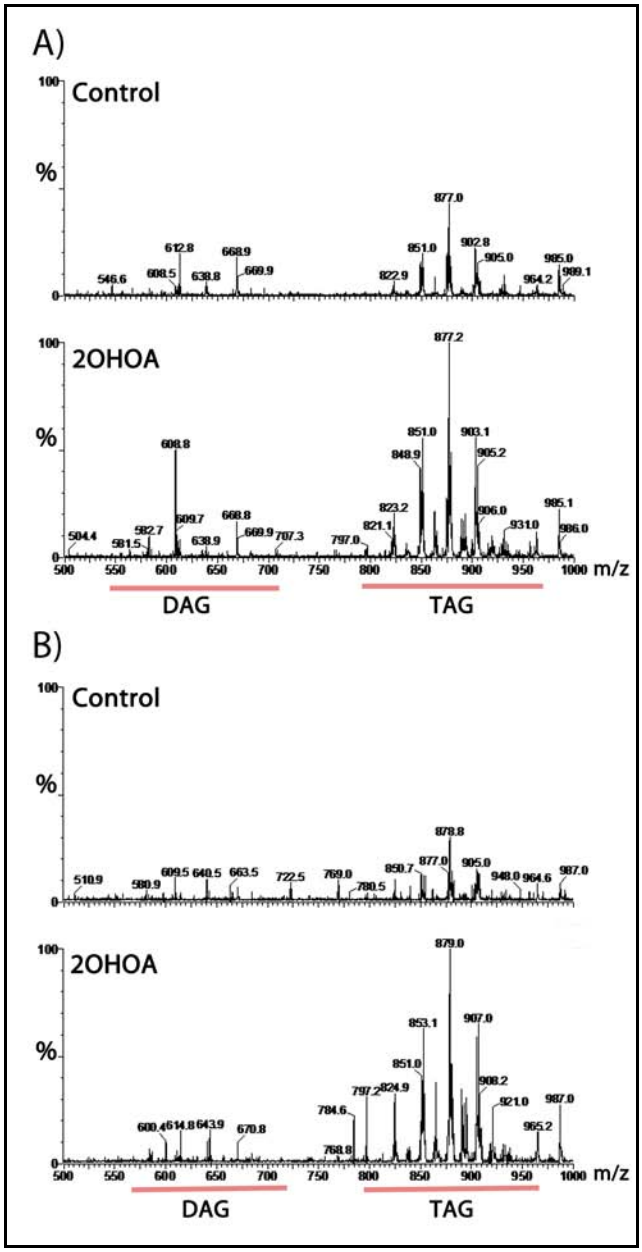


**Figure A 4. Mass spectra from glycerolipids lipids containing oleic acid (A) and stearic acid (B).**
U118 cells were treated in the presence or absence of 2OHOA (200 µM, 24 h). After treatment lipids were extracted and analyzed by LC/MS. The spectra are normalized to the highest peak in both control and treated samples.

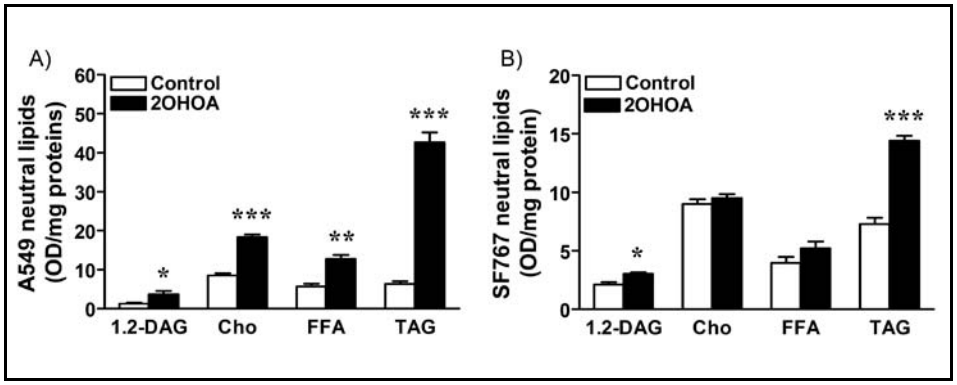


**Figure A 5. 2OHOA affected neutral lipids in A549 and SF767 cells.**
Human lung adenocarcinoma (A549, A) cells and human glioma (SF767, B) were treated in the presence or absence of 2OHOA (200 µM, 72 h). After treatment, lipids were extracted and analyzed by TLC. FFA, free fatty acids; Cho, cholesterol. Values are OD/mg protein and are expressed as % of control and represent mean ± SD, n= 4-5. The asterisks indicate a significant effect of the treatment as compared with the control (*P < 0.05; ***P* < 0.01; ****P* < 0.001).

# Table of Figures

Table of Figures

# Related publications

## Publications related with the thesis:

- Barceló-Coblijn G*, **Martin ML***, de Almeida R, Noguera-Salvà MA, Marcilla-Etxenike A, Guardiola-Serrano F, Lüth A, Kleuser B, Halver, JE, Escribá PV. *Sphingomyelin and Sphingomyelin Synthase (SMS) in the malignant transformation of glioma cells and in 2-hydroxyoleic acid therapy*. Submitted. (*Both authors contributed equally to this work).
- **Martin ML***, Barceló-Coblijn G*, de Almeida R, Noguera-Salvà MA, Higuera M, Terés S, Schmitz G, Liebisch G, Escribá PV. *Stearoyl-CoA desaturase inhibition is involved in 2-hydroxyoleic acid antitumor mechanism*. In preparation. (*Both authors contributed equally to this work).

## Other publications:

- Marcilla-Etxenike A, **Martin ML**, Noguera-Salva MA, Escriba PV, Busquets X. *2-Hydroxyoleic acid selectively induces ER stress and autophagy in astrocytoma but not in non-cancer cells*. Submitted.
- Terés S, Lladó V, Higuera M, Barceló-Coblijn G, **Martin ML**, Noguera MA, García-Verdugo JM, Saus C, Busquets X, Escribá PV. *2-Hydroxyoleate defines a new class of membrane lipid-binding non-toxic anticancer drug with Ras inhibitor-like effect that induces glioma cell differentiation and autophagy*. Submitted.

## Patents:

- Escribá PV, Busquets X, Terés S, Barceló-Coblijn G, Barceló J, Lladó V, Marcilla-Etxenike A, **Martin ML**, Higuera M, Álvarez R, López DH. *Use of 2-hydroxy-poliunsaturated fatty acids as drugs*. P200900725. 09/03/2009.
- Escribá PV, Barceló-Coblijn G, **Martin ML**, Noguera-Salvá MA, Busquets X. Efecto regulador del α-hidroxi-9-cis-octadecenoato sobre la actividad fosfocolina fosfotransferasa: aplicación en investigación básica, clínica y usos terapéuticos.

## Conference presentations:

- 2010. 51th International Conference on the Bioscience of Lipids held in Bilbao, Spain. Poster presentation: *2-Hydroxyoleic acid, a potent antitumor drug, induces disorder of cell membranes by altering cell lipid composition*.
- 2010. 8th International Sphingolipid Club Meeting at the Glasgow Marriott, UK on 30th June-2nd July. Short talk: *Specific activation of sphingomyelin synthase by 2-hydroxyoleic acid (Minerval), a potent antitumour drug*. **Best PhD student short talk award winner**.
- 2009**.** Gordon Research Conference on Lipids, Molecular and Cellular Biology of. Held in Waterville Valley Resort in Waterville Valley, New Hampshire, United States. Poster Presentation: "*Critical Role of Sphingomyelin Synthase in the antitumoral effect of Minerval (2-hydroxyoleic acid) in U118 human glioma cells"*.
- 2008**.** 49th International Conference on the Bioscience of Lipids held in Maastricht, Netherlands. Poster presentation: "*Minerval (2-hydroxyoleic acid) may replace oleic acid in human tumor cell lines*".
- 2008**.** FEBS Workshop: Lipids as regulators of cell function, held in Spetses Islands, Greece. Poster presentation: "*Effects of Minerval on fatty acid and phospholipid composition in mice tissues and human tumor cell lines*".
- 2007. 48th International Conference on the Bioscience of Lipids held in Turku, Finland. Poster presentation: "*Effects of Minerval on fatty acid and phospholipid composition in mice tissues and human glioma cells*"

# References


Alberts B (1994) *Molecular biology of the cell*, 3rd ed edn. New York: Garland Pub.

Albi E, Magni MV (1999) Sphingomyelin synthase in rat liver nuclear membrane and chromatin. *FEBS letters* **460:** 369-372

Albi E, Rossi G, Maraldi NM, Magni MV, Cataldi S, Solimando L, Zini N (2003) Involvement of nuclear phosphatidylinositol-dependent phospholipases C in cell cycle progression during rat liver regeneration. *Journal of cellular physiology* **197:** 181-188

Albi E, Viola Magni MP (2004) The role of intranuclear lipids. *Biology of the cell / under the auspices of the European Cell Biology Organization* **96:** 657-667

Antonsson B (1997) Phosphatidylinositol synthase from mammalian tissues. *Biochimica et biophysica acta* **1348:** 179-186

Aresta-Branco F, Cordeiro AM, Marinho HS, Cyrne L, Antunes F, de Almeida RF (2011) Gel domains in the plasma membrane of Saccharomyces cerevisiae: highly ordered, ergosterol-free, and sphingolipid-enriched lipid rafts. *The Journal of biological chemistry* **286:** 5043-5054

Ariyama H, Kono N, Matsuda S, Inoue T, Arai H (2010) Decrease in membrane phospholipid unsaturation induces unfolded protein response. *The Journal of biological chemistry* **285:** 22027-22035

Arteaga CL (2002) Epidermal growth factor receptor dependence in human tumors: more than just expression? *The oncologist* **7 Suppl 4:** 31-39

Athenstaedt K, Daum G (1999) Phosphatidic acid, a key intermediate in lipid metabolism. *European journal of biochemistry / FEBS* **266:** 1-16

Ballabio A, Gieselmann V (2009) Lysosomal disorders: from storage to cellular damage. *Biochimica et biophysica acta* **1793:** 684-696

Barceló-Coblijn G, Martin ML, de Almeida RFM, Noguera-Salvá MA, Marcilla-Etxenike A, Guardiola F, Lüth A, Kleuser B, Halver JE, Escribá PV (2011) Sphingomyelin and Sphingomyelin Synthase (SMS) in the malignant transformation of glioma cells and in 2-hydroxyoleic acid therapy *Proceedings of the National Academy of Sciences of the United States of America* **Submitted**

Barceló-Coblijn G, Murphy CC, Murphy EJ (2010) Methods for Measuring Fatty Acids Using Chromatographic Techniques. In *Lipid-Mediated Signaling* Murphy EJ, Rosenberger TA (eds). CRC press

Barceló F, Prades J, Funari SS, Frau J, Alemany R, Escribá PV (2004) The hypotensive drug 2-hydroxyoleic acid modifies the structural properties of model membranes. *Molecular membrane biology* **21:** 261-268

Barenholz Y, Suurkuusk J, Mountcastle D, Thompson TE, Biltonen RL (1976) A calorimetric study of the thermotropic behavior of aqueous dispersions of natural and synthetic sphingomyelins. *Biochemistry* **15:** 2441-2447

Baro L, Hermoso JC, Nunez MC, Jimenez-Rios JA, Gil A (1998) Abnormalities in plasma and red blood cell fatty acid profiles of patients with colorectal cancer. *British journal of cancer* **77:** 1978-1983

Bartke N, Hannun YA (2009) Bioactive sphingolipids: metabolism and function. *Journal of lipid research* **50 Suppl:** S91-96

Becker I, Wang-Eckhardt L, Yaghootfam A, Gieselmann V, Eckhardt M (2008) Differential expression of (dihydro)ceramide synthases in mouse brain: oligodendrocyte-specific expression of CerS2/Lass2. *Histochemistry and cell biology* **129:** 233-241

Beneteau M, Pizon M, Chaigne-Delalande B, Daburon S, Moreau P, De Giorgi F, Ichas F, Rebillard A, Dimanche-Boitrel MT, Taupin JL, Moreau JF, Legembre P (2008) Localization of Fas/CD95 into the lipid rafts on down-modulation of the phosphatidylinositol 3-kinase signaling pathway. *Mol Cancer Res* **6:** 604-613

Birkle S, Zeng G, Gao L, Yu RK, Aubry J (2003) Role of tumor-associated gangliosides in cancer progression. *Biochimie* **85:** 455-463

Bligh EG, Dyer WJ (1959) A rapid method of total lipid extraction and purification. *Can J Biochem Physiol* **37:** 911-917

Bose R, Verheij M, Haimovitz-Friedman A, Scotto K, Fuks Z, Kolesnick R (1995) Ceramide synthase mediates daunorubicin-induced apoptosis: an alternative mechanism for generating death signals. *Cell* **82:** 405-414

Bourbon NA, Yun J, Kester M (2000) Ceramide directly activates protein kinase C zeta to regulate a stress-activated protein kinase signaling complex. *The Journal of biological chemistry* **275:** 35617-35623

Bowman RE, Wolf RC (1962) A rapid and specific ultramicro method for total serum cholesterol. *Clin Chem* **8:** 302-309

Brasaemle DL (2007) Thematic review series: adipocyte biology. The perilipin family of structural lipid droplet proteins: stabilization of lipid droplets and control of lipolysis. *Journal of lipid research* **48:** 2547-2559

Brasaemle DL, Barber T, Wolins NE, Serrero G, Blanchette-Mackie EJ, Londos C (1997) Adipose differentiation-related protein is an ubiquitously expressed lipid storage droplet-associated protein. *Journal of lipid research* **38:** 2249-2263

Brasaemle DL, Rubin B, Harten IA, Gruia-Gray J, Kimmel AR, Londos C (2000) Perilipin A increases triacylglycerol storage by decreasing the rate of triacylglycerol hydrolysis. *The Journal of biological chemistry* **275:** 38486-38493

Breslow DK, Collins SR, Bodenmiller B, Aebersold R, Simons K, Shevchenko A, Ejsing CS, Weissman JS (2010) Orm family proteins mediate sphingolipid homeostasis. *Nature* **463:** 1048-1053

Brockerhoff H (1975) Determination of the positional distribution of fatty acids in glycerolipids. *Methods Enzymol* **35:** 315-325

Busto JV, Sot J, Goni FM, Mollinedo F, Alonso A (2007) Surface-active properties of the antitumour ether lipid 1-O-octadecyl-2-O-methyl-rac-glycero-3-phosphocholine (edelfosine). *Biochimica et biophysica acta* **1768:** 1855-1860

Carrasco S, Merida I (2007) Diacylglycerol, when simplicity becomes complex. *Trends in biochemical sciences* **32:** 27-36

Cascianelli G, Villani M, Tosti M, Marini F, Bartoccini E, Magni MV, Albi E (2008) Lipid microdomains in cell nucleus. *Molecular biology of the cell* **19:** 5289-5295

Castagnet PI, Golovko MY, Barcelo-Coblijn GC, Nussbaum RL, Murphy EJ (2005) Fatty acid incorporation is decreased in astrocytes cultured from alpha-synuclein gene-ablated mice. *J Neurochem* **94:** 839-849

Castro BM, de Almeida RF, Silva LC, Fedorov A, Prieto M (2007) Formation of ceramide/sphingomyelin gel domains in the presence of an unsaturated phospholipid: a quantitative multiprobe approach. *Biophysical journal* **93:** 1639-1650

Castro BM, Silva LC, Fedorov A, de Almeida RF, Prieto M (2009) Cholesterol-rich fluid membranes solubilize ceramide domains: implications for the structure and dynamics of mammalian intracellular and plasma membranes. *The Journal of biological chemistry* **284:** 22978-22987

Cerbon J, del Carmen Lopez-Sanchez R (2003) Diacylglycerol generated during sphingomyelin synthesis is involved in protein kinase C activation and cell proliferation in Madin-Darby canine kidney cells. *The Biochemical journal* **373:** 917-924

Coleman RA, Lee DP (2004) Enzymes of triacylglycerol synthesis and their regulation. *Progress in lipid research* **43:** 134-176

Coleman RA, Lewin TM, Van Horn CG, Gonzalez-Baro MR (2002) Do long-chain acyl-CoA synthetases regulate fatty acid entry into synthetic versus degradative pathways? *The Journal of nutrition* **132:** 2123-2126

Conesa-Zamora P, Mollinedo F, Corbalan-Garcia S, Gomez-Fernandez JC (2005) A comparative study of the effect of the antineoplastic ether lipid 1-O-octadecyl-2-O-methyl-glycero-3-phosphocholine and some homologous compounds on PKC alpha and PKC epsilon. *Biochimica et biophysica acta* **1687:** 110-119

Contreras FX, Sot J, Alonso A, Goni FM (2006) Sphingosine increases the permeability of model and cell membranes. *Biophysical journal* **90:** 4085-4092

Coskun U, Grzybek M, Drechsel D, Simons K (2011) Regulation of human EGF receptor by lipids. *Proceedings of the National Academy of Sciences of the United States of America* **108:** 9044-9048

Cremesti A, Paris F, Grassme H, Holler N, Tschopp J, Fuks Z, Gulbins E, Kolesnick R (2001) Ceramide enables fas to cap and kill. *The Journal of biological chemistry* **276:** 23954-23961

Cuvillier O, Pirianov G, Kleuser B, Vanek PG, Coso OA, Gutkind S, Spiegel S (1996) Suppression of ceramide-mediated programmed cell death by sphingosine-1-phosphate. *Nature* **381:** 800-803

Cvetkovic Z, Vucic V, Cvetkovic B, Petrovic M, Ristic-Medic D, Tepsic J, Glibetic M (2010) Abnormal fatty acid distribution of the serum phospholipids of patients with non-Hodgkin lymphoma. *Annals of hematology* **89:** 775-782

Chandana SR, Movva S, Arora M, Singh T (2008) Primary brain tumors in adults. *American family physician* **77:** 1423-1430

D'Angelo G, Polishchuk E, Di Tullio G, Santoro M, Di Campli A, Godi A, West G, Bielawski J, Chuang CC, van der Spoel AC, Platt FM, Hannun YA, Polishchuk R, Mattjus P, De Matteis MA (2007) Glycosphingolipid synthesis requires FAPP2 transfer of glucosylceramide. *Nature* **449:** 62-67

de Almeida RF, Borst J, Fedorov A, Prieto M, Visser AJ (2007) Complexity of lipid domains and rafts in giant unilamellar vesicles revealed by combining imaging and microscopic and macroscopic time-resolved fluorescence. *Biophysical journal* **93:** 539-553

de Almeida RF, Fedorov A, Prieto M (2003) Sphingomyelin/phosphatidylcholine/cholesterol phase diagram: boundaries and composition of lipid rafts. *Biophysical journal* **85:** 2406-2416

de Almeida RF, Loura LM, Fedorov A, Prieto M (2005) Lipid rafts have different sizes depending on membrane composition: a time-resolved fluorescence resonance energy transfer study. *J Mol Biol* **346:** 1109-1120

de Almeida RF, Loura LM, Prieto M (2009) Membrane lipid domains and rafts: current applications of fluorescence lifetime spectroscopy and imaging. *Chemistry and physics of lipids* **157:** 61-77

de Castro J, Rodriguez MC, Martinez-Zorzano VS, Llanillo M, Sanchez-Yague J (2009) Platelet linoleic acid is a potential biomarker of advanced non-small cell lung cancer. *Experimental and molecular pathology* **87:** 226-233

DeAngelis LM (2001) Brain tumors. *The New England journal of medicine* **344:** 114-123

Dennis EA (2009) Lipidomics joins the omics evolution. *Proceedings of the National Academy of Sciences of the United States of America* **106:** 2089-2090

Devaux PF, Morris R (2004) Transmembrane asymmetry and lateral domains in biological membranes. *Traffic* **5:** 241-246

Di Paolo G, De Camilli P (2006) Phosphoinositides in cell regulation and membrane dynamics. *Nature* **443:** 651-657

Di Vizio D, Solomon KR, Freeman MR (2008) Cholesterol and cholesterol-rich membranes in prostate cancer: an update. *Tumori* **94:** 633-639

Digel M, Ehehalt R, Fullekrug J (2010) Lipid droplets lighting up: insights from live microscopy. *FEBS letters* **584:** 2168-2175

Ding T, Li Z, Hailemariam T, Mukherjee S, Maxfield FR, Wu MP, Jiang XC (2008) SMS overexpression and knockdown: impact on cellular sphingomyelin and diacylglycerol metabolism, and cell apoptosis. *Journal of lipid research* **49:** 376-385

Dobrowsky RT, Hannun YA (1993) Ceramide-activated protein phosphatase: partial purification and relationship to protein phosphatase 2A. *Advances in lipid research* **25:** 91-104

Eisenberg S, Henis YI (2008) Interactions of Ras proteins with the plasma membrane and their roles in signaling. *Cellular signalling* **20:** 31-39

Enoch HG, Catala A, Strittmatter P (1976) Mechanism of rat liver microsomal stearyl-CoA desaturase. Studies of the substrate specificity, enzyme-substrate interactions, and the function of lipid. *The Journal of biological chemistry* **251:** 5095-5103

Epand RM, Bottega R (1988) Determination of the phase behaviour of phosphatidylethanolamine admixed with other lipids and the effects of calcium chloride: implications for protein kinase C regulation. *Biochimica et biophysica acta* **944:** 144-154

Escribá PV (2006) Membrane-lipid therapy: a new approach in molecular medicine. *Trends Mol Med* **12:** 34-43

Escribá PV. (2008) Membrane-Lipid Therapy. *Encyclopedia of Cancer*, Vol. 3.

Escribá PV, González-Ros JM, Goñi FM, Kinnunen PK, Vigh L, Sánchez-Magraner L, Fernández AM, Busquets X, Horváth I, Barceló-Coblijn G (2008) Membranes: a meeting point for lipids, proteins and therapies. *Journal of cellular and molecular medicine* **12:** 829-875

Escribá PV, Ozaita A, Ribas C, Miralles A, Fodor E, Farkas T, García-Sevilla JA (1997) Role of lipid polymorphism in G protein-membrane interactions: nonlamellar-prone phospholipids and peripheral protein binding to membranes. *Proc Natl Acad Sci U S A* **94:** 11375-11380

Escribá PV, Sastre M, Garcia-Sevilla JA (1995) Disruption of cellular signaling pathways by daunomycin through destabilization of nonlamellar membrane structures. *Proceedings of the National Academy of Sciences of the United States of America* **92:** 7595-7599

Estep TN, Mountcastle DB, Barenholz Y, Biltonen RL, Thompson TE (1979) Thermal behavior of synthetic sphingomyelin-cholesterol dispersions. *Biochemistry* **18:** 2112-2117

Fadok VA, Voelker DR, Campbell PA, Cohen JJ, Bratton DL, Henson PM (1992) Exposure of phosphatidylserine on the surface of apoptotic lymphocytes triggers specific recognition and removal by macrophages. *J Immunol* **148:** 2207-2216

Fagone PJ, S. (2009) Membrane phospholipid synthesis and endoplasmic reticulum function. *Journal of Lipid Research*

Fahy E, Subramaniam S, Brown HA, Glass CK, Merrill AH, Jr., Murphy RC, Raetz CR, Russell DW, Seyama Y, Shaw W, Shimizu T, Spener F, van Meer G, VanNieuwenhze MS, White SH, Witztum JL, Dennis EA (2005) A comprehensive classification system for lipids. *Journal of lipid research* **46:** 839-861

Fahy E, Subramaniam S, Murphy RC, Nishijima M, Raetz CR, Shimizu T, Spener F, van Meer G, Wakelam MJ, Dennis EA (2009) Update of the LIPID MAPS comprehensive classification system for lipids. *Journal of lipid research* **50 Suppl:** S9-14

Ferlay J, Shin H, Bray F, Forman D, Mathers C, Parkin DM. (2008) GLOBOCAN 2008 v1.2, Cancer Incidence and Mortality Worldwide: IARC CancerBase No. 10 [Internet]. In http://globocan.iarc.fr. IAfRoCAf (ed.).

Foulon V, Sniekers M, Huysmans E, Asselberghs S, Mahieu V, Mannaerts GP, Van Veldhoven PP, Casteels M (2005) Breakdown of 2-hydroxylated straight chain fatty acids via peroxisomal 2-hydroxyphytanoyl-CoA lyase: a revised pathway for the alpha-oxidation of straight chain fatty acids. *The Journal of biological chemistry* **280:** 9802-9812

Freeman MR, Solomon KR (2004) Cholesterol and prostate cancer. *Journal of cellular biochemistry* **91:** 54-69

Fritz V, Benfodda Z, Rodier G, Henriquet C, Iborra F, Avances C, Allory Y, de la Taille A, Culine S, Blancou H, Cristol JP, Michel F, Sardet C, Fajas L (2010) Abrogation of de novo lipogenesis by stearoyl-CoA desaturase 1 inhibition interferes with oncogenic signaling and blocks prostate cancer progression in mice. *Molecular cancer therapeutics* **9:** 1740-1754

Fujisawa H, Reis RM, Nakamura M, Colella S, Yonekawa Y, Kleihues P, Ohgaki H (2000) Loss of heterozygosity on chromosome 10 is more extensive in primary (de novo) than in secondary glioblastomas. *Laboratory investigation; a journal of technical methods and pathology* **80:** 65-72

Fukasawa M, Nishijima M, Hanada K (1999) Genetic evidence for ATP-dependent endoplasmic reticulum-to-Golgi apparatus trafficking of ceramide for sphingomyelin synthesis in Chinese hamster ovary cells. *J Cell Biol* **144:** 673-685

Furnari FB, Fenton T, Bachoo RM, Mukasa A, Stommel JM, Stegh A, Hahn WC, Ligon KL, Louis DN, Brennan C, Chin L, DePinho RA, Cavenee WK (2007) Malignant astrocytic glioma: genetics, biology, and paths to treatment. *Genes & development* **21:** 2683-2710

Futerman AH, Hannun YA (2004) The complex life of simple sphingolipids. *EMBO Rep* **5:** 777-782

Futerman AH, Riezman H (2005) The ins and outs of sphingolipid synthesis. *Trends Cell Biol* **15:** 312-318

Gajate C, Mollinedo F (2007) Edelfosine and perifosine induce selective apoptosis in multiple myeloma by recruitment of death receptors and downstream signaling molecules into lipid rafts. *Blood* **109:** 711-719

Gellermann GP, Appel TR, Tannert A, Radestock A, Hortschansky P, Schroeckh V, Leisner C, Lutkepohl T, Shtrasburg S, Rocken C, Pras M, Linke RP, Diekmann S, Fandrich M (2005) Raft lipids as common components of human extracellular amyloid fibrils. *Proc Natl Acad Sci U S A* **102:** 6297-6302

Gómez-Muñoz A (2006) Ceramide 1-phosphate/ceramide, a switch between life and death. *Biochimica et biophysica acta* **1758:** 2049-2056

Gómez-Muñoz A, Kong JY, Salh B, Steinbrecher UP (2004) Ceramide-1-phosphate blocks apoptosis through inhibition of acid sphingomyelinase in macrophages. *Journal of lipid research* **45:** 99-105

Gonzalez-Roura A, Casas J, Llebaria A (2002) Synthesis and phospholipase C inhibitory activity of D609 diastereomers. *Lipids* **37:** 401-406

Goñi FM (2002) Non-permanent proteins in membranes: when proteins come as visitors (Review). *Molecular membrane biology* **19:** 237-245

Goñi FM, Alonso A (1999) Structure and functional properties of diacylglycerols in membranes. *Progress in lipid research* **38:** 1-48

Goñi FM, Alonso A (2002) Sphingomyelinases: enzymology and membrane activity. *FEBS letters* **531:** 38-46

Gubern A, Casas J, Barcelo-Torns M, Barneda D, de la Rosa X, Masgrau R, Picatoste F, Balsinde J, Balboa MA, Claro E (2008) Group IVA phospholipase A2 is necessary for the biogenesis of lipid droplets. *The Journal of biological chemistry* **283:** 27369-27382

Guha A, Feldkamp MM, Lau N, Boss G, Pawson A (1997) Proliferation of human malignant astrocytomas is dependent on Ras activation. *Oncogene* **15:** 2755-2765

Gulbins E, Kolesnick R (2003) Raft ceramide in molecular medicine. *Oncogene* **22:** 7070-7077

Gwak J, Cho M, Gong SJ, Won J, Kim DE, Kim EY, Lee SS, Kim M, Kim TK, Shin JG, Oh S (2006) Protein-kinase-C-mediated beta-catenin phosphorylation negatively regulates the Wnt/beta-catenin pathway. *J Cell Sci* **119:** 4702-4709

Gwak J, Jung SJ, Kang DI, Kim EY, Kim DE, Chung YH, Shin JG, Oh S (2009) Stimulation of protein kinase C-alpha suppresses colon cancer cell proliferation by down-regulation of beta-catenin. *J Cell Mol Med* **13:** 2171-2180

Haimovitz-Friedman A, Kan CC, Ehleiter D, Persaud RS, McLoughlin M, Fuks Z, Kolesnick RN (1994) Ionizing radiation acts on cellular membranes to generate ceramide and initiate apoptosis. *The Journal of experimental medicine* **180:** 525-535

Hama H (2010) Fatty acid 2-Hydroxylation in mammalian sphingolipid biology. *Biochimica et biophysica acta* **1801:** 405-414

Han MS, Park SY, Shinzawa K, Kim S, Chung KW, Lee JH, Kwon CH, Lee KW, Park CK, Chung WJ, Hwang JS, Yan JJ, Song DK, Tsujimoto Y, Lee MS (2008) Lysophosphatidylcholine as a death effector in the lipoapoptosis of hepatocytes. *Journal of lipid research* **49:** 84-97

Han X (2007) Neurolipidomics: challenges and developments. *Frontiers in bioscience : a journal and virtual library* **12:** 2601-2615

Hanada K, Kumagai K, Yasuda S, Miura Y, Kawano M, Fukasawa M, Nishijima M (2003) Molecular machinery for non-vesicular trafficking of ceramide. *Nature* **426:** 803-809

Hanahan D, Weinberg RA (2000) The hallmarks of cancer. *Cell* **100:** 57-70

Hannun YA, Obeid LM (2008) Principles of bioactive lipid signalling: lessons from sphingolipids. *Nature reviews. Molecular cell biology* **9:** 139-150

Hannun YA, Obeid LM (2011) Many Ceramides. *The Journal of biological chemistry*

Hara A, Radin NS (1978) Lipid extraction of tissues with a low-toxicity solvent. *Anal Biochem* **90:** 420-426

Heacock AM, Agranoff BW (1997) CDP-diacylglycerol synthase from mammalian tissues. *Biochimica et biophysica acta* **1348:** 166-172

Hendrich AB, Michalak K (2003) Lipids as a target for drugs modulating multidrug resistance of cancer cells. *Current drug targets* **4:** 23-30

Henneberry AL, Wright MM, McMaster CR (2002) The major sites of cellular phospholipid synthesis and molecular determinants of Fatty Acid and lipid head group specificity. *Molecular biology of the cell* **13:** 3148-3161

Hettmer S, Ladisch S, Kaucic K (2005) Low complex ganglioside expression characterizes human neuroblastoma cell lines. *Cancer letters* **225:** 141-149

Hishikawa D, Shindou H, Kobayashi S, Nakanishi H, Taguchi R, Shimizu T (2008) Discovery of a lysophospholipid acyltransferase family essential for membrane asymmetry and diversity. *Proceedings of the National Academy of Sciences of the United States of America* **105:** 2830-2835

Holthuis JC, Levine TP (2005) Lipid traffic: floppy drives and a superhighway. *Nat Rev Mol Cell Biol* **6:** 209-220

Hubbard SR, Till JH (2000) Protein tyrosine kinase structure and function. *Annual review of biochemistry* **69:** 373-398

Huitema K, van den Dikkenberg J, Brouwers JF, Holthuis JC (2004) Identification of a family of animal sphingomyelin synthases. *Embo J* **23:** 33-44

Ichimura K, Ohgaki H, Kleihues P, Collins VP (2004) Molecular pathogenesis of astrocytic tumours. *Journal of neuro-oncology* **70:** 137-160

Igal RA (2010) Stearoyl-CoA desaturase-1: a novel key player in the mechanisms of cell proliferation, programmed cell death and transformation to cancer. *Carcinogenesis* **31:** 1509-1515

Iorio E, Mezzanzanica D, Alberti P, Spadaro F, Ramoni C, D'Ascenzo S, Millimaggi D, Pavan A, Dolo V, Canevari S, Podo F (2005) Alterations of choline phospholipid metabolism in ovarian tumor progression. *Cancer research* **65:** 9369-9376

Irvine RF (2003) Nuclear lipid signalling. *Nature reviews. Molecular cell biology* **4:** 349-360

Jansen GA, Wanders RJ (2006) Alpha-oxidation. *Biochimica et biophysica acta* **1763:** 1403-1412

Jendrossek V, Handrick R (2003) Membrane targeted anticancer drugs: potent inducers of apoptosis and putative radiosensitisers. *Current medicinal chemistry. Anti-cancer agents* **3:** 343-353

Jenkins GM, Cowart LA, Signorelli P, Pettus BJ, Chalfant CE, Hannun YA (2002) Acute activation of de novo sphingolipid biosynthesis upon heat shock causes an accumulation of ceramide and subsequent dephosphorylation of SR proteins. *The Journal of biological chemistry* **277:** 42572-42578

Jiang H, Martin V, Gomez-Manzano C, Johnson DG, Alonso M, White E, Xu J, McDonnell TJ, Shinojima N, Fueyo J (2010) The RB-E2F1 pathway regulates autophagy. *Cancer Res* **70:** 7882-7893

Jin J, Hou Q, Mullen TD, Zeidan YH, Bielawski J, Kraveka JM, Bielawska A, Obeid LM, Hannun YA, Hsu YT (2008) Ceramide generated by sphingomyelin hydrolysis and the salvage pathway is involved in hypoxia/reoxygenation-induced Bax redistribution to mitochondria in NT-2 cells. *The Journal of biological chemistry* **283:** 26509-26517

Jolly CA, Hubbell T, Behnke WD, Schroeder F (1997) Fatty acid binding protein: stimulation of microsomal phosphatidic acid formation. *Arch Biochem Biophys* **341:** 112-121

Kennedy EP (1961) Biosynthesis of complex lipids. *Federation proceedings* **20:** 934-940

Khandelia H, Duelund L, Pakkanen KI, Ipsen JH (2010) Triglyceride blisters in lipid bilayers: implications for lipid droplet biogenesis and the mobile lipid signal in cancer cell membranes. *PloS one* **5:** e12811

Kiebish MA, Han X, Cheng H, Chuang JH, Seyfried TN (2008) Cardiolipin and electron transport chain abnormalities in mouse brain tumor mitochondria: lipidomic evidence supporting the Warburg theory of cancer. *Journal of lipid research* **49:** 2545-2556

Kiguchi K, Takamatsu K, Tanaka J, Nozawa S, Iwamori M, Nagai Y (1992) Glycosphingolipids of various human ovarian tumors: a significantly high expression of I3SO3GalCer and Lewis antigen in mucinous cystadenocarcinoma. *Cancer research* **52:** 416-421

Kim YC, Ntambi JM (1999) Regulation of stearoyl-CoA desaturase genes: role in cellular metabolism and preadipocyte differentiation. *Biochemical and biophysical research communications* **266:** 1-4

Kimmel AR, Brasaemle DL, McAndrews-Hill M, Sztalryd C, Londos C (2010) Adoption of PERILIPIN as a unifying nomenclature for the mammalian PAT-family of intracellular lipid storage droplet proteins. *Journal of lipid research* **51:** 468-471

Kitatani K, Idkowiak-Baldys J, Hannun YA (2008) The sphingolipid salvage pathway in ceramide metabolism and signaling. *Cellular signalling* **20:** 1010-1018

Kleihues P, Sobin LH (2000) World Health Organization classification of tumors. *Cancer* **88:** 2887

Kolesnick RN, Goni FM, Alonso A (2000) Compartmentalization of ceramide signaling: physical foundations and biological effects. *Journal of cellular physiology* **184:** 285-300

Kolter T, Sandhoff K (2006) Sphingolipid metabolism diseases. *Biochimica et biophysica acta* **1758:** 2057-2079

Kolter T, Sandhoff K (2010) Lysosomal degradation of membrane lipids. *FEBS letters* **584:** 1700-1712

Koltun DO, Parkhill EQ, Vasilevich NI, Glushkov AI, Zilbershtein TM, Ivanov AV, Cole AG, Henderson I, Zautke NA, Brunn SA, Mollova N, Leung K, Chisholm JW, Zablocki J (2009) Novel, potent, selective, and metabolically stable stearoyl-CoA desaturase (SCD) inhibitors. *Bioorganic & medicinal chemistry letters* **19:** 2048-2052

Kornberg A, Pricer WE, Jr. (1953) Enzymatic synthesis of the coenzyme A derivatives of long chain fatty acids. *The Journal of biological chemistry* **204:** 329-343

Koybasi S, Senkal CE, Sundararaj K, Spassieva S, Bielawski J, Osta W, Day TA, Jiang JC, Jazwinski SM, Hannun YA, Obeid LM, Ogretmen B (2004) Defects in cell growth regulation by C18:0-ceramide and longevity assurance gene 1 in human head and neck squamous cell carcinomas. *The Journal of biological chemistry* **279:** 44311-44319

Koynova R, Caffrey M (1998) Phases and phase transitions of the phosphatidylcholines. *Biochim Biophys Acta* **1376:** 91-145

Krahmer N, Guo Y, Farese RV, Jr., Walther TC (2009) SnapShot: Lipid Droplets. *Cell* **139:** 1024-1024 e1021

Kraveka JM, Li L, Szulc ZM, Bielawski J, Ogretmen B, Hannun YA, Obeid LM, Bielawska A (2007) Involvement of dihydroceramide desaturase in cell cycle progression in human neuroblastoma cells. *The Journal of biological chemistry* **282:** 16718-16728

Kroesen BJ, Pettus B, Luberto C, Busman M, Sietsma H, de Leij L, Hannun YA (2001) Induction of apoptosis through B-cell receptor cross-linking occurs via de novo generated C16-ceramide and involves mitochondria. *The Journal of biological chemistry* **276:** 13606-13614

Kuerschner L, Ejsing CS, Ekroos K, Shevchenko A, Anderson KI, Thiele C (2005) Polyene-lipids: a new tool to image lipids. *Nature methods* **2:** 39-45

Kuhajda FP (2006) Fatty acid synthase and cancer: new application of an old pathway. *Cancer research* **66:** 5977-5980

Ladisch S, Sweeley CC, Becker H, Gage D (1989) Aberrant fatty acyl alpha-hydroxylation in human neuroblastoma tumor gangliosides. *The Journal of biological chemistry* **264:** 12097-12105

Lafont E, Milhas D, Carpentier S, García V, Jin ZX, Umehara H, Okazaki T, Schulze-Osthoff K, Levade T, Benoist H, Segui B (2010) Caspase-mediated inhibition of sphingomyelin synthesis is involved in FasL-triggered cell death. *Cell Death Differ* **17:** 642-654

Lakowicz JR (2006) *Principles of fluorescence spectroscopy*, 3rd edn. New York: Springer.

Lands WE (1958) Metabolism of glycerolipides; a comparison of lecithin and triglyceride synthesis. *The Journal of biological chemistry* **231:** 883-888

Lands WE (2000) Stories about acyl chains. *Biochimica et biophysica acta* **1483:** 1-14

Laviad EL, Albee L, Pankova-Kholmyansky I, Epstein S, Park H, Merrill AH, Jr., Futerman AH (2008) Characterization of ceramide synthase 2: tissue distribution, substrate specificity, and inhibition by sphingosine 1-phosphate. *The Journal of biological chemistry* **283:** 5677-5684

Ledeen RW, Wu G (2004) Nuclear lipids: key signaling effectors in the nervous system and other tissues. *Journal of lipid research* **45:** 1-8

Ledeen RW, Wu G (2008) Nuclear sphingolipids: metabolism and signaling. *Journal of Lipid Research* **49:** 1176-1186

Lehninger AL, Nelson DL, Cox MM (2005) *Principles of biochemistry*, 4th ed edn. New York: W.H. Freeman and Company.

Lentz BR (1993) Use of fluorescent probes to monitor molecular order and motions within liposome bilayers. *Chemistry and physics of lipids* **64:** 99-116

Levy M, Futerman AH (2010) Mammalian ceramide synthases. *IUBMB life* **62:** 347-356

Li J, Ding SF, Habib NA, Fermor BF, Wood CB, Gilmour RS (1994) Partial characterization of a cDNA for human stearoyl-CoA desaturase and changes in its mRNA expression in some normal and malignant tissues. *International journal of cancer. Journal international du cancer* **57:** 348-352

Li Z, Hailemariam TK, Zhou H, Li Y, Duckworth DC, Peake DA, Zhang Y, Kuo MS, Cao G, Jiang XC (2007) Inhibition of sphingomyelin synthase (SMS) affects intracellular sphingomyelin accumulation and plasma membrane lipid organization. *Biochim Biophys Acta* **1771:** 1186-1194

Liebisch G, Drobnik W, Reil M, Trumbach B, Arnecke R, Olgemoller B, Roscher A, Schmitz G (1999) Quantitative measurement of different ceramide species from crude cellular extracts by electrospray ionization tandem mass spectrometry (ESI-MS/MS). *Journal of lipid research* **40:** 1539-1546

Liebisch G, Lieser B, Rathenberg J, Drobnik W, Schmitz G (2004) High-throughput quantification of phosphatidylcholine and sphingomyelin by electrospray ionization tandem mass spectrometry coupled with isotope correction algorithm. *Biochimica et biophysica acta* **1686:** 108-117

Lingwood D, Simons K (2010) Lipid rafts as a membrane-organizing principle. *Science* **327:** 46-50

Listenberger LL, Han X, Lewis SE, Cases S, Farese RV, Jr., Ory DS, Schaffer JE (2003) Triglyceride accumulation protects against fatty acid-induced lipotoxicity. *Proceedings of the National Academy of Sciences of the United States of America* **100:** 3077-3082

Liu Y, Chen Y, Momin A, Shaner R, Wang E, Bowen NJ, Matyunina LV, Walker LD, McDonald JF, Sullards MC, Merrill AH, Jr. (2010) Elevation of sulfatides in ovarian cancer: an integrated transcriptomic and lipidomic analysis including tissue-imaging mass spectrometry. *Molecular cancer* **9:** 186

Lodish H (2008) *Molecular cell biology*, 6th ed edn. New York: W. H. Freeman.

López Jiménez D (2008) Actividades esfingomielinasa bacterianas y de mamíferos. Caracterización y efectos estructurales en membranas. PhD Thesis, Bioquímica y Biología Molecular, Universidad del Pais Vasco, Bilbao

Louis DN, Ohgaki H, Wiestler OD, Cavenee WK, Burger PC, Jouvet A, Scheithauer BW, Kleihues P (2007) The 2007 WHO classification of tumours of the central nervous system. *Acta neuropathologica* **114:** 97-109

Lowry OH, Rosebrough NJ, Farr AL, Randall RJ (1951) Protein measurement with the Folin phenol reagent. *The Journal of biological chemistry* **193:** 265-275

Luberto C, Hannun YA (1998) Sphingomyelin synthase, a potential regulator of intracellular levels of ceramide and diacylglycerol during SV40 transformation. Does sphingomyelin synthase account for the putative phosphatidylcholine-specific phospholipase C? *The Journal of biological chemistry* **273:** 14550-14559

Luberto C, Yoo DS, Suidan HS, Bartoli GM, Hannun YA (2000) Differential effects of sphingomyelin hydrolysis and resynthesis on the activation of NF-kappa B in normal and SV40-transformed human fibroblasts. *The Journal of biological chemistry* **275:** 14760-14766

Lladó V, Gutierrez A, Martínez J, Casas J, Terés S, Higuera M, Galmes A, Saus C, Besalduch J, Busquets X, Escribá PV (2010) Minerval induces apoptosis in Jurkat and other cancer cells. *Journal of cellular and molecular medicine* **14:** 659-670

Lladó V, Terés S, Higuera M, Álvarez R, Noguera-Salvá MA, Halver JE, Escribá PV, Busquets X (2009) Pivotal role of dihydrofolate reductase knockdown in the anticancer activity of 2-hydroxyoleic acid. *Proceedings of the National Academy of Sciences of the United States of America* **106:** 13754-13758

Macdonald FD, Ford CHJ, Casson AG (2004) *Molecular biology of cancer*, 2nd ed / F. Macdonald, C.H.J. Ford, A.G. Casson. edn. London: BIOS Scientific.

MacFarlane M, Williams AC (2004) Apoptosis and disease: a life or death decision. *EMBO reports* **5:** 674-678

Marcilla-Etxenike A, Martin ML, Noguera-Salvá MA, Escribá PV, Busquets X (2011) 2-Hydroxyoleic acid selectively induces ER stress and autophagy in astrocytoma but not in non-cancer cells. **Submitted**

Marcheselli V. L. SBL, Reddy T. S. and Bazan N. G. (1988) *Quantitative analysis of acyl group composition of brain phospholipids, neutral lipids, and free fatty acids, in Neuromethods 7 Lipids and Related Compounds* Clifton, NJ.: Humana Press.

Marques JT, Viana AS, De Almeida RF (2011) Ethanol effects on binary and ternary supported lipid bilayers with gel/fluid domains and lipid rafts. *Biochimica et biophysica acta* **1808:** 405-414

Marsh D (1990) *Handbook of Lipid Bilayers*, Boca Raton, FL CRC.

Marsh D (2009) Cholesterol-induced fluid membrane domains: a compendium of lipid-raft ternary phase diagrams. *Biochimica et biophysica acta* **1788:** 2114-2123

Martelli AM, Bortul R, Tabellini G, Bareggi R, Manzoli L, Narducci P, Cocco L (2002) Diacylglycerol kinases in nuclear lipid-dependent signal transduction pathways. *Cellular and molecular life sciences : CMLS* **59:** 1129-1137

Martin DD, Robbins ME, Spector AA, Wen BC, Hussey DH (1996) The fatty acid composition of human gliomas differs from that found in nonmalignant brain tissue. *Lipids* **31:** 1283-1288

Martínez J, Gutierrez A, Casas J, Lladó V, López-Bellan A, Besalduch J, Dopazo A, Escribá PV (2005a) The repression of E2F-1 is critical for the activity of Minerval against cancer. *J Pharmacol Exp Ther* **315:** 466-474

Martínez J, Vogler O, Casas J, Barceló F, Alemany R, Prades J, Nagy T, Baamonde C, Kasprzyk PG, Terés S, Saus C, Escribá PV (2005b) Membrane structure modulation, protein kinase C alpha activation, and anticancer activity of minerval. *Mol Pharmacol* **67:** 531-540

Mashima T, Seimiya H, Tsuruo T (2009) De novo fatty-acid synthesis and related pathways as molecular targets for cancer therapy. *British journal of cancer* **100:** 1369-1372

Maxfield FR (2002) Plasma membrane microdomains. *Current opinion in cell biology* **14:** 483-487

McClare CW (1971) An accurate and convenient organic phosphorus assay. *Anal Biochem* **39:** 527-530

Megha, Bakht O, London E (2006) Cholesterol precursors stabilize ordinary and ceramide-rich ordered lipid domains (lipid rafts) to different degrees. Implications for the Bloch hypothesis and sterol biosynthesis disorders. *The Journal of biological chemistry* **281:** 21903-21913

Menaldino DS, Bushnev A, Sun A, Liotta DC, Symolon H, Desai K, Dillehay DL, Peng Q, Wang E, Allegood J, Trotman-Pruett S, Sullards MC, Merrill AH, Jr. (2003) Sphingoid bases and de novo ceramide synthesis: enzymes involved, pharmacology and mechanisms of action. *Pharmacological research : the official journal of the Italian Pharmacological Society* **47:** 373-381

Meng A, Luberto C, Meier P, Bai A, Yang X, Hannun YA, Zhou D (2004a) Sphingomyelin synthase as a potential target for D609-induced apoptosis in U937 human monocytic leukemia cells. *Experimental cell research* **292:** 385-392

Meng A, Luberto C, Meier P, Bai A, Yang X, Hannun YA, Zhou D (2004b) Sphingomyelin synthase as a potential target for D609-induced apoptosis in U937 human monocytic leukemia cells. *Exp Cell Res* **292:** 385-392

Meng X, Riordan NH, Riordan HD, Mikirova N, Jackson J, Gonzalez MJ, Miranda-Massari JR, Mora E, Trinidad Castillo W (2004c) Cell membrane fatty acid composition differs between normal and malignant cell lines. *Puerto Rico health sciences journal* **23:** 103-106

Merchant TE, Characiejus D, Kasimos JN, Den Otter W, Gierke LW, Glonek T (1992) Phosphodiesters in saponified extracts of human breast and colon tumors using 31P magnetic resonance spectroscopy. *Magnetic resonance in medicine : official journal of the Society of Magnetic Resonance in Medicine / Society of Magnetic Resonance in Medicine* **26:** 132-140

Merchant TE, de Graaf PW, Minsky BD, Obertop H, Glonek T (1993) Esophageal cancer phospholipid characterization by 31P NMR. *NMR in biomedicine* **6:** 187-193

Merchant TE, Diamantis PM, Lauwers G, Haida T, Kasimos JN, Guillem J, Glonek T, Minsky BD (1995) Characterization of malignant colon tumors with 31P nuclear magnetic resonance phospholipid and phosphatic metabolite profiles. *Cancer* **76:** 1715-1723

Merchant TE, Kasimos JN, de Graaf PW, Minsky BD, Gierke LW, Glonek T (1991a) Phospholipid profiles of human colon cancer using 31P magnetic resonance spectroscopy. *International journal of colorectal disease* **6:** 121-126

Merchant TE, Meneses P, Gierke LW, Den Otter W, Glonek T (1991b) 31P magnetic resonance phospholipid profiles of neoplastic human breast tissues. *British journal of cancer* **63:** 693-698

Merrill AH, Jr. (2002) De novo sphingolipid biosynthesis: a necessary, but dangerous, pathway. *J Biol Chem* **277:** 25843-25846

Mesicek J, Lee H, Feldman T, Jiang X, Skobeleva A, Berdyshev EV, Haimovitz-Friedman A, Fuks Z, Kolesnick R (2010) Ceramide synthases 2, 5, and 6 confer distinct roles in radiation-induced apoptosis in HeLa cells. *Cellular signalling* **22:** 1300-1307

Mikirova N, Riordan HD, Jackson JA, Wong K, Miranda-Massari JR, Gonzalez MJ (2004) Erythrocyte membrane fatty acid composition in cancer patients. *Puerto Rico health sciences journal* **23:** 107-113

Milhas D, Clarke CJ, Hannun YA (2010) Sphingomyelin metabolism at the plasma membrane: implications for bioactive sphingolipids. *FEBS letters* **584:** 1887-1894

Miura S, Gan JW, Brzostowski J, Parisi MJ, Schultz CJ, Londos C, Oliver B, Kimmel AR (2002) Functional conservation for lipid storage droplet association among Perilipin, ADRP, and TIP47 (PAT)-related proteins in mammals, Drosophila, and Dictyostelium. *The Journal of biological chemistry* **277:** 32253-32257

Miyaji M, Jin ZX, Yamaoka S, Amakawa R, Fukuhara S, Sato SB, Kobayashi T, Domae N, Mimori T, Bloom ET, Okazaki T, Umehara H (2005) Role of membrane sphingomyelin and ceramide in platform formation for Fas-mediated apoptosis. *The Journal of experimental medicine* **202:** 249-259

Morgan-Lappe SE, Tucker LA, Huang X, Zhang Q, Sarthy AV, Zakula D, Vernetti L, Schurdak M, Wang J, Fesik SW (2007) Identification of Ras-related nuclear protein, targeting protein for xenopus kinesin-like protein 2, and stearoyl-CoA desaturase 1 as promising cancer targets from an RNAi-based screen. *Cancer research* **67:** 4390-4398

Mullen TD, Jenkins RW, Clarke CJ, Bielawski J, Hannun YA, Obeid LM (2011) Ceramide synthase-dependent ceramide generation and programmed cell death: involvement of salvage pathway in regulating postmitochondrial events. *The Journal of biological chemistry* **286:** 15929-15942

Muller-Decker K (1989) Interruption of TPA-induced signals by an antiviral and antitumoral xanthate compound: inhibition of a phospholipase C-type reaction. *Biochemical and biophysical research communications* **162:** 198-205

Murphy EJ, Rosenberger TA, Horrocks LA (1997) Effects of maturation on the phospholipid and phospholipid fatty acid compositions in primary rat cortical astrocyte cell cultures. *Neurochem Res* **22:** 1205-1213

Murphy EJ, Stiles T, Schroeder F (2000) Sterol carrier protein-2 expression alters phospholipid content and fatty acyl composition in L-cell fibroblasts. *J Lipid Res* **41:** 788-796

Nilsson O, Brezicka FT, Holmgren J, Sorenson S, Svennerholm L, Yngvason F, Lindholm L (1986) Detection of a ganglioside antigen associated with small cell lung carcinomas using monoclonal antibodies directed against fucosyl-GM1. *Cancer research* **46:** 1403-1407

Niv H, Gutman O, Kloog Y, Henis YI (2002) Activated K-Ras and H-Ras display different interactions with saturable nonraft sites at the surface of live cells. *The Journal of cell biology* **157:** 865-872

Ntambi JM, Miyazaki M (2004) Regulation of stearoyl-CoA desaturases and role in metabolism. *Progress in lipid research* **43:** 91-104

Ohgaki H, Kleihues P (2007) Genetic pathways to primary and secondary glioblastoma. *The American journal of pathology* **170:** 1445-1453

Oskouian B, Saba JD (2010) Cancer treatment strategies targeting sphingolipid metabolism. *Advances in experimental medicine and biology* **688:** 185-205

Pala V, Krogh V, Muti P, Chajes V, Riboli E, Micheli A, Saadatian M, Sieri S, Berrino F (2001) Erythrocyte membrane fatty acids and subsequent breast cancer: a prospective Italian study. *Journal of the National Cancer Institute* **93:** 1088-1095

Pearson Education I. (2008) Membranes. Pearson Benjamin Cummings.

Pereto J, Lopez-Garcia P, Moreira D (2004) Ancestral lipid biosynthesis and early membrane evolution. *Trends in biochemical sciences* **29:** 469-477

Peterson BL, Cummings BS (2006) A review of chromatographic methods for the assessment of phospholipids in biological samples. *Biomed Chromatogr* **20:** 227-243

Pfaffl MW (2001) A new mathematical model for relative quantification in real-time RT-PCR. *Nucleic acids research* **29:** e45

Pike LJ (2006) Rafts defined: a report on the Keystone Symposium on Lipid Rafts and Cell Function. *Journal of Lipid Research* **47:** 1597-1598

Piomelli D, Astarita G, Rapaka R (2007) A neuroscientist's guide to lipidomics. *Nat Rev Neurosci* **8:** 743-754

Plas DR, Thompson CB (2005) Akt-dependent transformation: there is more to growth than just surviving. *Oncogene* **24:** 7435-7442

Polozov IV, Gawrisch K (2004) Domains in binary SOPC/POPE lipid mixtures studied by pulsed field gradient 1H MAS NMR. *Biophysical journal* **87:** 1741-1751

Porstmann T, Griffiths B, Chung YL, Delpuech O, Griffiths JR, Downward J, Schulze A (2005) PKB/Akt induces transcription of enzymes involved in cholesterol and fatty acid biosynthesis via activation of SREBP. *Oncogene* **24:** 6465-6481

Prakash H, Luth A, Grinkina N, Holzer D, Wadgaonkar R, Gonzalez AP, Anes E, Kleuser B (2010) Sphingosine kinase-1 (SphK-1) regulates Mycobacterium smegmatis infection in macrophages. *PLoS One* **5:** e10657

Prasad R (1996) *Manual on menbrane lipids*, Berlin: Springer.

Prior IA, Muncke C, Parton RG, Hancock JF (2003) Direct visualization of Ras proteins in spatially distinct cell surface microdomains. *The Journal of cell biology* **160:** 165-170

Rashid A, Pizer ES, Moga M, Milgraum LZ, Zahurak M, Pasternack GR, Kuhajda FP, Hamilton SR (1997) Elevated expression of fatty acid synthase and fatty acid synthetic activity in colorectal neoplasia. *The American journal of pathology* **150:** 201-208

Riboni L, Campanella R, Bassi R, Villani R, Gaini SM, Martinelli-Boneschi F, Viani P, Tettamanti G (2002) Ceramide levels are inversely associated with malignant progression of human glial tumors. *Glia* **39:** 105-113

Rotolo JA, Zhang J, Donepudi M, Lee H, Fuks Z, Kolesnick R (2005) Caspase-dependent and -independent activation of acid sphingomyelinase signaling. *The Journal of biological chemistry* **280:** 26425-26434

Rouser G, Siakotos AN, Fleischer S (1966) Quantitative analysis of phospholipids by thin-layer chromatography and phosphorus analysis of spots. *Lipids* **1:** 85-86

Ruvolo PP (2003) Intracellular signal transduction pathways activated by ceramide and its metabolites. *Pharmacological research : the official journal of the Italian Pharmacological Society* **47:** 383-392

Ruwisch L, Schafer-Korting M, Kleuser B (2001) An improved high-performance liquid chromatographic method for the determination of sphingosine-1-phosphate in complex biological materials. *Naunyn Schmiedebergs Arch Pharmacol* **363:** 358-363

Samuels Y, Wang Z, Bardelli A, Silliman N, Ptak J, Szabo S, Yan H, Gazdar A, Powell SM, Riggins GJ, Willson JK, Markowitz S, Kinzler KW, Vogelstein B, Velculescu VE (2004) High frequency of mutations of the PIK3CA gene in human cancers. *Science* **304:** 554

Scaglia N, Caviglia JM, Igal RA (2005) High stearoyl-CoA desaturase protein and activity levels in simian virus 40 transformed-human lung fibroblasts. *Biochimica et biophysica acta* **1687:** 141-151

Scaglia N, Chisholm JW, Igal RA (2009) Inhibition of stearoylCoA desaturase-1 inactivates acetyl-CoA carboxylase and impairs proliferation in cancer cells: role of AMPK. *PloS one* **4:** e6812

Scaglia N, Igal RA (2005) Stearoyl-CoA desaturase is involved in the control of proliferation, anchorage-independent growth, and survival in human transformed cells. *The Journal of biological chemistry* **280:** 25339-25349

Scaglia N, Igal RA (2008) Inhibition of Stearoyl-CoA Desaturase 1 expression in human lung adenocarcinoma cells impairs tumorigenesis. *Int J Oncol* **33:** 839-850

Schaffer JE (2003) Lipotoxicity: when tissues overeat. *Current opinion in lipidology* **14:** 281-287

Scherer M, Leuthauser-Jaschinski K, Ecker J, Schmitz G, Liebisch G (2010a) A rapid and quantitative LC-MS/MS method to profile sphingolipids. *Journal of lipid research* **51:** 2001-2011

Scherer M, Schmitz G, Liebisch G (2009) High-throughput analysis of sphingosine 1-phosphate, sphinganine 1-phosphate, and lysophosphatidic acid in plasma samples by liquid chromatography-tandem mass spectrometry. *Clinical chemistry* **55:** 1218-1222

Scherer M, Schmitz G, Liebisch G (2010b) Simultaneous Quantification of Cardiolipin, Bis(monoacylglycero)phosphate and their Precursors by Hydrophilic Interaction LC-MS/MS Including Correction of Isotopic Overlap. *Analytical chemistry*

Schlame M, Rua D, Greenberg ML (2000) The biosynthesis and functional role of cardiolipin. *Progress in lipid research* **39:** 257-288

Schmid PC, Spimrova I, Schmid HH (1995) Incorporation of exogenous fatty acids into molecular species of rat hepatocyte phosphatidylcholine. *Archives of biochemistry and biophysics* **322:** 306-312

Schulz H. (2004) Fatty acid oxidation. In Lennarz WJ, Lane MD (eds.), *Encyclopedia of Biological Chemistry* Vol. 2, pp. 90-94.

Schwartzbaum JA, Fisher JL, Aldape KD, Wrensch M (2006) Epidemiology and molecular pathology of glioma. *Nature clinical practice. Neurology* **2:** 494-503; quiz 491 p following 516

Sekizawa Y, Kubo T, Kobayashi H, Nakajima T, Natori S (1997) Molecular cloning of cDNA for lysenin, a novel protein in the earthworm Eisenia foetida that causes contraction of rat vascular smooth muscle. *Gene* **191:** 97-102

Senkal CE, Ponnusamy S, Bielawski J, Hannun YA, Ogretmen B (2010) Antiapoptotic roles of ceramide-synthase-6-generated C16-ceramide via selective regulation of the ATF6/CHOP arm of ER-stress-response pathways. *The FASEB journal : official publication of the Federation of American Societies for Experimental Biology* **24:** 296-308

Separovic D, Hanada K, Maitah MY, Nagy B, Hang I, Tainsky MA, Kraniak JM, Bielawski J (2007) Sphingomyelin synthase 1 suppresses ceramide production and apoptosis post-photodamage. *Biochemical and biophysical research communications* **358:** 196-202

Shaikh SR, Brzustowicz MR, Gustafson N, Stillwell W, Wassall SR (2002) Monounsaturated PE does not phase-separate from the lipid raft molecules sphingomyelin and cholesterol: role for polyunsaturation? *Biochemistry* **41:** 10593-10602

Sherma J (2000) Thin-layer chromatography in food and agricultural analysis. *Journal of chromatography. A* **880:** 129-147

Sherr CJ, McCormick F (2002) The RB and p53 pathways in cancer. *Cancer cell* **2:** 103-112

Sherr CJ, Roberts JM (1999) CDK inhibitors: positive and negative regulators of G1-phase progression. *Genes & development* **13:** 1501-1512

Shimizu T, Ohto T, Kita Y (2006) Cytosolic phospholipase A2: biochemical properties and physiological roles. *IUBMB life* **58:** 328-333

Shindou H, Shimizu T (2009) Acyl-CoA:lysophospholipid acyltransferases. *The Journal of biological chemistry* **284:** 1-5

Silva L, de Almeida RF, Fedorov A, Matos AP, Prieto M (2006) Ceramide-platform formation and -induced biophysical changes in a fluid phospholipid membrane. *Molecular membrane biology* **23:** 137-148

Silva LC, de Almeida RF, Castro BM, Fedorov A, Prieto M (2007) Ceramide-domain formation and collapse in lipid rafts: membrane reorganization by an apoptotic lipid. *Biophysical journal* **92:** 502-516

Simons K, Toomre D (2000) Lipid rafts and signal transduction. *Nature reviews. Molecular cell biology* **1:** 31-39

Singer SJ, Nicolson GL (1972) The fluid mosaic model of the structure of cell membranes. *Science* **175:** 720-731

Siskind LJ, Kolesnick RN, Colombini M (2002) Ceramide channels increase the permeability of the mitochondrial outer membrane to small proteins. *The Journal of biological chemistry* **277:** 26796-26803

Siskind LJ, Kolesnick RN, Colombini M (2006) Ceramide forms channels in mitochondrial outer membranes at physiologically relevant concentrations. *Mitochondrion* **6:** 118-125

Smith PK, Krohn RI, Hermanson GT, Mallia AK, Gartner FH, Provenzano MD, Fujimoto EK, Goeke NM, Olson BJ, Klenk DC (1985) Measurement of protein using bicinchoninic acid. *Anal Biochem* **150:** 76-85

Smith WL, Marnett LJ, DeWitt DL (1991) Prostaglandin and thromboxane biosynthesis. *Pharmacology & therapeutics* **49:** 153-179

Spacek J. (2004) Atlas of Ultrastructural Neurocytology, http://synapses.clm.utexas.edu/atlas/.

Spiegel S, Milstien S (2003) Sphingosine-1-phosphate: an enigmatic signalling lipid. *Nature reviews. Molecular cell biology* **4:** 397-407

Stancevic B, Kolesnick R (2010) Ceramide-rich platforms in transmembrane signaling. *FEBS letters* **584:** 1728-1740

Stiban J, Tidhar R, Futerman AH (2010) Ceramide synthases: roles in cell physiology and signaling. *Advances in experimental medicine and biology* **688:** 60-71

Stupp R, Mason WP, van den Bent MJ, Weller M, Fisher B, Taphoorn MJ, Belanger K, Brandes AA, Marosi C, Bogdahn U, Curschmann J, Janzer RC, Ludwin SK, Gorlia T, Allgeier A, Lacombe D, Cairncross JG, Eisenhauer E, Mirimanoff RO (2005) Radiotherapy plus concomitant and adjuvant temozolomide for glioblastoma. *The New England journal of medicine* **352:** 987-996

Sud M, Fahy E, Cotter D, Brown A, Dennis E, Glass C, Murphy R, Raetz C, Russell D, Subramaniam S (2006) LMSD: LIPID MAPS structure database. . *Nucleic Acids Research* **35:** D527-532

Swinnen JV, Vanderhoydonc F, Elgamal AA, Eelen M, Vercaeren I, Joniau S, Van Poppel H, Baert L, Goossens K, Heyns W, Verhoeven G (2000) Selective activation of the fatty acid synthesis pathway in human prostate cancer. *International journal of cancer. Journal international du cancer* **88:** 176-179

Tafesse FG, Holthuis JC (2010) Cell biology: A brake on lipid synthesis. *Nature* **463:** 1028-1029

Tafesse FG, Huitema K, Hermansson M, van der Poel S, van den Dikkenberg J, Uphoff A, Somerharju P, Holthuis JC (2007) Both sphingomyelin synthases SMS1 and SMS2 are required for sphingomyelin homeostasis and growth in human HeLa cells. *The Journal of biological chemistry* **282:** 17537-17547

Tafesse FG, Ternes P, Holthuis JC (2006) The multigenic sphingomyelin synthase family. *The Journal of biological chemistry* **281:** 29421-29425

Tamm LK (2005) *Protein-lipid interactions : from membrane domains to cellular networks*, Weinheim: Wiley-VCH ; [Chichester : John Wiley, distributor].

Tatevossian RG, Lawson AR, Forshew T, Hindley GF, Ellison DW, Sheer D (2010) MAPK pathway activation and the origins of pediatric low-grade astrocytomas. *Journal of cellular physiology* **222:** 509-514

Teng DH, Hu R, Lin H, Davis T, Iliev D, Frye C, Swedlund B, Hansen KL, Vinson VL, Gumpper KL, Ellis L, El-Naggar A, Frazier M, Jasser S, Langford LA, Lee J, Mills GB, Pershouse MA, Pollack RE, Tornos C, Troncoso P, Yung WK, Fujii G, Berson A, Steck PA, et al. (1997) MMAC1/PTEN mutations in primary tumor specimens and tumor cell lines. *Cancer research* **57:** 5221-5225

Terés S, Lladó V, Higuera M, Barceló-Coblijn G, Martin ML, Noguera-Salvá MA, Busquets X, Escribá PV (2011) 2-Hydroxyoleate defines a new class of membrane lipid-binding non-toxic anticancer drug with Ras inhibitor-like effect that induces glioma cell differentiation and autophagy. **Submitted**

Ternes P, Brouwers JF, van den Dikkenberg J, Holthuis JC (2009) Sphingomyelin synthase SMS2 displays dual activity as ceramide phosphoethanolamine synthase. *Journal of lipid research* **50:** 2270-2277

Tettamanti G (2004) Ganglioside/glycosphingolipid turnover: new concepts. *Glycoconjugate journal* **20:** 301-317

Tettamanti G, Bassi R, Viani P, Riboni L (2003) Salvage pathways in glycosphingolipid metabolism. *Biochimie* **85:** 423-437

Thompson JGA (1992) *The Regulation of Membrane Lipid Metabolism*, 2nd edn.: CRC Press.

Thudichum JLW (1884) *A Treatise on the Chemical Constitution of Brain*, London: Bailliere, Tindall, and Cox.

Triton TR, Yee G (1982) The anticancer agent adriamycin can be actively cytotoxic without entering cells. *Science* **217:** 248-250

Truman JP, Gueven N, Lavin M, Leibel S, Kolesnick R, Fuks Z, Haimovitz-Friedman A (2005) Down-regulation of ATM protein sensitizes human prostate cancer cells to radiation-induced apoptosis. *The Journal of biological chemistry* **280:** 23262-23272

Uchida Y, Nardo AD, Collins V, Elias PM, Holleran WM (2003) De novo ceramide synthesis participates in the ultraviolet B irradiation-induced apoptosis in undifferentiated cultured human keratinocytes. *The Journal of investigative dermatology* **120:** 662-669

Vacaru AM, Tafesse FG, Ternes P, Kondylis V, Hermansson M, Brouwers JF, Somerharju P, Rabouille C, Holthuis JC (2009) Sphingomyelin synthase-related protein SMSr controls ceramide homeostasis in the ER. *The Journal of cell biology* **185:** 1013-1027

Valeur B (2001) *Molecular Fluorescence: Principles and Applications*, Meinheim: Wiley-VCH,.

Van der Luit AH, Budde M, Zerp S, Caan W, Klarenbeek JB, Verheij M, Van Blitterswijk WJ (2007) Resistance to alkyl-lysophospholipid-induced apoptosis due to downregulated sphingomyelin synthase 1 expression with consequent sphingomyelin- and cholesterol-deficiency in lipid rafts. *The Biochemical journal* **401:** 541-549

van Helvoort A, van't Hof W, Ritsema T, Sandra A, van Meer G (1994) Conversion of diacylglycerol to phosphatidylcholine on the basolateral surface of epithelial (Madin-Darby canine kidney) cells. Evidence for the reverse action of a sphingomyelin synthase. *The Journal of biological chemistry* **269:** 1763-1769

van Meer G, Voelker DR, Feigenson GW (2008) Membrane lipids: where they are and how they behave. *Nat Rev Mol Cell Biol* **9:** 112-124

Vance DE, Ridgway ND (1988) The methylation of phosphatidylethanolamine. *Progress in lipid research* **27:** 61-79

Vance DE, Vance JE (1996) *Biochemistry of lipids, lipoproteins and membranes*, Amsterdam ; New York: Elsevier.

Vance DE, Walkey CJ, Cui Z (1997) Phosphatidylethanolamine N-methyltransferase from liver. *Biochimica et biophysica acta* **1348:** 142-150

Vance JE (2008) Phosphatidylserine and phosphatidylethanolamine in mammalian cells: two metabolically related aminophospholipids. *Journal of Lipid Research* **49:** 1377-1387

Venkataraman K, Futerman AH (2000) Ceramide as a second messenger: sticky solutions to sticky problems. *Trends Cell Biol* **10:** 408-412

Vereb G, Szollosi J, Matko J, Nagy P, Farkas T, Vigh L, Matyus L, Waldmann TA, Damjanovich S (2003) Dynamic, yet structured: The cell membrane three decades after the Singer-Nicolson model. *Proc Natl Acad Sci U S A* **100:** 8053-8058

Vermeulen K, Van Bockstaele DR, Berneman ZN (2003) The cell cycle: a review of regulation, deregulation and therapeutic targets in cancer. *Cell proliferation* **36:** 131-149

Vieira CR, Munoz-Olaya JM, Sot J, Jimenez-Baranda S, Izquierdo-Useros N, Abad JL, Apellaniz B, Delgado R, Martinez-Picado J, Alonso A, Casas J, Nieva JL, Fabrias G, Manes S, Goni FM (2010) Dihydrosphingomyelin impairs HIV-1 infection by rigidifying liquid-ordered membrane domains. *Chemistry & biology* **17:** 766-775

Villani M, Subathra M, Im YB, Choi Y, Signorelli P, Del Poeta M, Luberto C (2008) Sphingomyelin synthases regulate production of diacylglycerol at the Golgi. *The Biochemical journal* **414:** 31-41

Vitner EB, Platt FM, Futerman AH (2010) Common and uncommon pathogenic cascades in lysosomal storage diseases. *The Journal of biological chemistry* **285:** 20423-20427

Vogler O, Casas J, Capo D, Nagy T, Borchert G, Martorell G, Escriba PV (2004) The Gbetagamma dimer drives the interaction of heterotrimeric Gi proteins with nonlamellar membrane structures. *J Biol Chem* **279:** 36540-36545

Vousden KH, Lu X (2002) Live or let die: the cell's response to p53. *Nature reviews. Cancer* **2:** 594-604

Walther TC, Farese RV, Jr. (2009) The life of lipid droplets. *Biochimica et biophysica acta* **1791:** 459-466

Watson AD (2006) Thematic review series: systems biology approaches to metabolic and cardiovascular disorders. Lipidomics: a global approach to lipid analysis in biological systems. *Journal of lipid research* **47:** 2101-2111

Weiss SB, Kennedy EP, Kiyasu JY (1960) The enzymatic synthesis of triglycerides. *The Journal of biological chemistry* **235:** 40-44

Welte MA (2007) Proteins under new management: lipid droplets deliver. *Trends in cell biology* **17:** 363-369

Wilson R, Sargent JR (2001) Chain separation of monounsaturated fatty acid methyl esters by argentation thin-layer chromatography. *Journal of chromatography. A* **905:** 251-257

Wrensch M, Minn Y, Chew T, Bondy M, Berger MS (2002) Epidemiology of primary brain tumors: current concepts and review of the literature. *Neuro-oncology* **4:** 278-299

Yamaji A, Sekizawa Y, Emoto K, Sakuraba H, Inoue K, Kobayashi H, Umeda M (1998) Lysenin, a novel sphingomyelin-specific binding protein. *J Biol Chem* **273:** 5300-5306

Yang C, Kazanietz MG (2003) Divergence and complexities in DAG signaling: looking beyond PKC. *Trends in pharmacological sciences* **24:** 602-608

Yao B, Zhang Y, Delikat S, Mathias S, Basu S, Kolesnick R (1995) Phosphorylation of Raf by ceramide-activated protein kinase. *Nature* **378:** 307-310

Yatomi Y, Ruan F, Ohta J, Welch RJ, Hakomori S, Igarashi Y (1995) Quantitative measurement of sphingosine 1-phosphate in biological samples by acylation with radioactive acetic anhydride. *Anal Biochem* **230:** 315-320

Yen CL, Stone SJ, Koliwad S, Harris C, Farese RV, Jr. (2008) Thematic review series: glycerolipids. DGAT enzymes and triacylglycerol biosynthesis. *Journal of Lipid Research* **49:** 2283-2301

Yu J, Novgorodov SA, Chudakova D, Zhu H, Bielawska A, Bielawski J, Obeid LM, Kindy MS, Gudz TI (2007) JNK3 signaling pathway activates ceramide synthase leading to mitochondrial dysfunction. *The Journal of biological chemistry* **282:** 25940-25949

Zhang L, Ge L, Parimoo S, Stenn K, Prouty SM (1999) Human stearoyl-CoA desaturase: alternative transcripts generated from a single gene by usage of tandem polyadenylation sites. *The Biochemical journal* **340 ( Pt 1):** 255-264

Zheng W, Kollmeyer J, Symolon H, Momin A, Munter E, Wang E, Kelly S, Allegood JC, Liu Y, Peng Q, Ramaraju H, Sullards MC, Cabot M, Merrill AH, Jr. (2006) Ceramides and other bioactive sphingolipid backbones in health and disease: lipidomic analysis, metabolism and roles in membrane structure, dynamics, signaling and autophagy. *Biochimica et biophysica acta* **1758:** 1864-1884

Zuijdgeest-van Leeuwen SD, van der Heijden MS, Rietveld T, van den Berg JW, Tilanus HW, Burgers JA, Wilson JH, Dagnelie PC (2002) Fatty acid composition of plasma lipids in patients with pancreatic, lung and oesophageal cancer in comparison with healthy subjects. *Clinical nutrition* **21:** 225-230

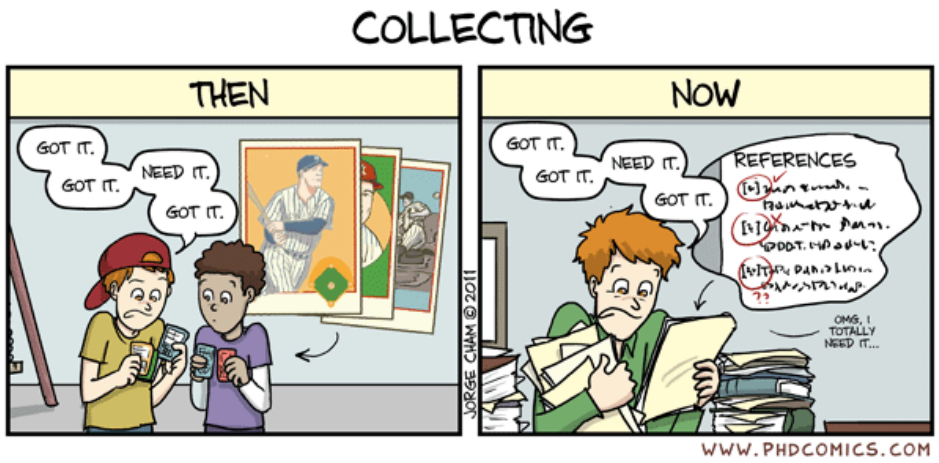
COLLECTING
THEN
GOT IT.
GOT IT.
NEED IT.
GOT IT.
NOW
GOT IT.
GOT IT.
NEED IT.
GOT IT.
REFERENCES
OMG, I TOTALLY NEED IT...
JORGE CHAM © 2011
WWW.PHDCOMICS.COM